

U N I K A S S E L  
V E R S I T Ä T

Efficient Characterisation and Optimal Control of  
Open Quantum Systems -  
Mathematical Foundations and Physical Applications

DISSERTATION

zur Erlangung des akademischen Grades

DOKTOR DER NATURWISSENSCHAFTEN

(Dr. rer. nat.)

im Fach Physik

eingereicht am

Fachbereich Mathematik und Naturwissenschaften

Universität Kassel

von

Daniel Maximilian Reich

Betreuerin: Prof. Dr. Christiane Koch

Zweitgutachter: Prof. Dr. Steffen Glaser

Eingereicht am: 18. Dezember 2014

Disputation am: 30. April 2015



## Zusammenfassung

Kein physikalisches System kann komplett von seiner Umgebung isoliert werden. Daher ist die Untersuchung offener Quantensysteme von enormer Wichtigkeit um eine verlässliche und akkurate Kontrolle komplexer Quantensysteme zu gewährleisten. In der Praxis muss die Zuverlässigkeit eines Kontrollfeldes durch Zertifizierung der gewünschten Zeitentwicklung des Systems überprüft werden, während eine hohe Genauigkeit durch präzise Kontrollstrategien in der Gegenwart von Dekohärenzeffekten garantiert werden muss.

Der erste Teil dieser Arbeit präsentiert einen algebraischen Rahmen zur Bestimmung der minimalen Voraussetzungen zur eindeutigen Charakterisierung beliebiger unitärer Gatter in offenen Quantensystemen, unabhängig von der speziellen physikalischen Implementierung eines Quantenelements. In diesem Rahmen werden Theoreme hergeleitet, mit Hilfe derer entschieden werden kann, ob ein gegebener Satz an Eingangszuständen für solch ein Quantenelement hinreichend zur Beurteilung der erfolgreichen Implementation ist. Dies ermöglicht insbesondere die Herleitung der minimalen Zahl an notwendigen Eingangszuständen mit dem Ergebnis, dass drei solcher Zustände genügen - unabhängig von der Größe des physikalischen Systems. Diese Resultate ermöglichen es, die fundamentalen Grenzen in Bezug auf Zertifizierung und Tomographie offener Quantensysteme herauszustellen. Eine Kombination dieser Ergebnisse mit modernen Monte Carlo Zertifizierungstechniken erlaubt desweiteren eine signifikante Verbesserung der Skalierung in Bezug auf die Systemgröße bei der Zertifizierung allgemeiner unitärer Quantengatter. Diese Verbesserung ist nicht nur auf Quanteninformationsträger mit zwei Zuständen, genannt Qubits, beschränkt sondern kann auch für elementare Informationsträger beliebiger Dimension, den sogenannten Qudits, verallgemeinert werden.

Der zweite Teil dieser Arbeit beschäftigt sich zunächst mit der Anwendung dieser neuen Erkenntnisse auf die Theorie der optimalen Kontrolle (OCT). OCT für Quantensysteme verwendet Konzepte aus den Ingenieurwissenschaften wie Rückkopplung und Optimierung, um konstruktive und destruktive Interferenzen auf solch eine Art und Weise zu erzeugen, dass man mit ihnen physikalische Prozesse in eine bestimmte Richtung steuern kann. Es zeigt sich, dass die obigen mathematischen Resultate es ermöglichen, neue Optimierungsfunktionale aufzustellen, welche signifikante Einsparungen für numerische Kontrollalgorithmen mit sich bringen. Dies gilt sowohl in Bezug auf Prozessorlaufzeit als auch in Bezug auf den notwendigen Speicher.

Zum Abschluss dieser Arbeit werden zwei zentrale Probleme der Quanteninformationsverarbeitung aus der Perspektive der optimalen Kontrolle diskutiert - die Erzeugung reiner Zustände sowie die Implementierung unitärer Gatter in offenen Quantensystemen. In beiden Fällen werden dabei spezifische physikalische Beispiele behandelt: Im ersten Fall handelt es sich um das Kühlen der Vibrationsfreiheitsgrade eines Moleküls mit Hilfe optischen Pumpens, während im zweiten Fall ein supraleitendes Phasenqudit betrachtet wird. Dabei wird insbesondere demonstriert, wie spezielle Eigenschaften der Umgebung dazu verwendet werden können, gewisse Kontrollziele zu erreichen.



## Abstract

Since no physical system can ever be completely isolated from its environment, the study of open quantum systems is pivotal to reliably and accurately control complex quantum systems. In practice, reliability of the control field needs to be confirmed via certification of the target evolution while accuracy requires the derivation of high-fidelity control schemes in the presence of decoherence.

In the first part of this thesis an algebraic framework is presented that allows to determine the minimal requirements on the unique characterisation of arbitrary unitary gates in open quantum systems, independent on the particular physical implementation of the employed quantum device. To this end, a set of theorems is devised that can be used to assess whether a given set of input states on a quantum channel is sufficient to judge whether a desired unitary gate is realised. This allows to determine the minimal input for such a task, which proves to be, quite remarkably, independent of system size. These results allow to elucidate the fundamental limits regarding certification and tomography of open quantum systems. The combination of these insights with state-of-the-art Monte Carlo process certification techniques permits a significant improvement of the scaling when certifying arbitrary unitary gates. This improvement is not only restricted to quantum information devices where the basic information carrier is the qubit but it also extends to systems where the fundamental informational entities can be of arbitrary dimensionality, the so-called qudits.

The second part of this thesis concerns the impact of these findings from the point of view of Optimal Control Theory (OCT). OCT for quantum systems utilises concepts from engineering such as feedback and optimisation to engineer constructive and destructive interferences in order to steer a physical process in a desired direction. It turns out that the aforementioned mathematical findings allow to deduce novel optimisation functionals that significantly reduce not only the required memory for numerical control algorithms but also the total CPU time required to obtain a certain fidelity for the optimised process.

The thesis concludes by discussing two problems of fundamental interest in quantum information processing from the point of view of optimal control - the preparation of pure states and the implementation of unitary gates in open quantum systems. For both cases specific physical examples are considered: for the former the vibrational cooling of molecules via optical pumping and for the latter a superconducting phase qudit implementation. In particular, it is illustrated how features of the environment can be exploited to reach the desired targets.



## Acknowledgements

First of all I would like to thank Prof. Christiane Koch for the supervision of this thesis. It was her encouragement, commitment and patience that allowed me to obtain the results that enabled this work in the first place.

I am also grateful to all the people I had the chance to work with. In particular I would like to thank Michael Goerz for teaching me almost everything I know about programming and Giulia Gualdi for the many engaging discussions and for making our office a small beacon of mathematical physics during her stay. My thanks also go to all present and past group members, Martin Berglund, Michal Tomza, Esteban Goetz, and Wojciech Skomorowski, for creating a very pleasant and friendly working atmosphere.

My thanks also go to Anne Müller who helped to ensure that I did not try to only survive by theorems, formulas, and Fortran code.

Finally, I would like to thank my parents and the rest of my family for their unconditional and limitless support.



*The popular stereotype of the researcher  
Is that of a skeptic and a pessimist.  
Nothing could be further from the truth!  
Scientists must be optimists at heart,  
In order to block out the incessant chorus of those who say  
'It cannot be done.'*

Academician Prokhor Zakharov, University Commencement  
*(from "Sid Meier's Alpha Centauri")*



# Contents

<b>1</b>	<b>Introduction</b>	<b>1</b>
<b>2</b>	<b>Quantum States, Observables and Dynamical Maps</b>	<b>3</b>
2.1	Breakdown of Local Realism and the Copenhagen Interpretation . . . . .	4
2.2	Hilbert Space . . . . .	5
2.3	Observables and Measurements . . . . .	7
2.4	Liouville Space . . . . .	10
2.5	Open Quantum Systems . . . . .	11
2.6	Dynamical Maps . . . . .	13
2.7	The Choi-Jamiołkowski Isomorphism . . . . .	15
2.8	Unitary Dynamical Maps (UDMs) . . . . .	16
<b>3</b>	<b>Minimal Characterisation and Identification of UDMs</b>	<b>19</b>
3.1	Exponential Scaling . . . . .	20
3.2	Unitary Characterisation in Liouville Space . . . . .	21
3.3	Minimal Characterisation of UDMs . . . . .	24
3.4	Efficient Identification of Unitarity for Dynamical Maps . . . . .	27
<b>4</b>	<b>Tomography and Process Certification</b>	<b>29</b>
4.1	Process Tomography of General Dynamical Maps . . . . .	30
4.2	State Tomography of General Density Matrices . . . . .	31
4.3	Qubit Systems and Pauli Matrices - Stabilisers and the Clifford Group . . . . .	33
4.4	Distance Measures and Fidelities . . . . .	35
4.5	Minimal Fidelities involving Pure States for Certification of UDMs . . . . .	39
4.6	Classical Fidelities . . . . .	43
4.7	Statistical Approaches to Tomography and Certification . . . . .	44
4.8	Monte Carlo Process Certification with State Fidelities . . . . .	47
4.9	Qupit Systems and Generalised Pauli Operators . . . . .	52
4.10	Optimal Choice of Measurement Basis . . . . .	53
<b>5</b>	<b>Dynamics and Control of Open Quantum System</b>	<b>55</b>
5.1	Isolated Quantum System Dynamics . . . . .	57
5.2	Open Quantum System Dynamics . . . . .	58
5.3	Optimal Control . . . . .	61
5.4	Optimisation Functionals for Open Quantum Systems . . . . .	64
5.5	Unitary Transformations on Subspaces . . . . .	67
5.6	Numerical Analysis of Reduced Optimisation Functionals . . . . .	70
<b>6</b>	<b>A Quantum Control Perspective on Cooling</b>	<b>75</b>
6.1	Cooling, Markovian Evolutions and Quantum Control . . . . .	76
6.2	Laser Cooling . . . . .	77
6.3	Model for Optical Pumping Utilising Timescale Separation . . . . .	79
6.4	Symmetric Cooling . . . . .	81

6.5	Assembly-Line Cooling . . . . .	83
6.6	Optimisation Results for Vibrational Cooling . . . . .	83
6.7	Perspectives for Quantum Reservoir Engineering . . . . .	88
<b>7</b>	<b>A Quantum Control Perspective on a Non-Markovian Evolution</b>	<b>95</b>
7.1	Superconducting Qudits . . . . .	96
7.2	Control Strategies for Phase Qudits . . . . .	99
7.3	The Two-Level System Model . . . . .	101
7.4	Noise Models for a Harmonic Oscillator . . . . .	103
7.5	Controllability Gain via Environmental Degrees of Freedom . . . . .	106
<b>8</b>	<b>Summary and Outlook</b>	<b>117</b>
<b>A</b>	<b>Proofs</b>	<b>119</b>
A.1	Kraus Operators for UDMs . . . . .	119
A.2	Commutant Spaces . . . . .	121
A.3	Reconstruction Matrices . . . . .	123
A.4	A Unitary Differentiating Matrix . . . . .	127
A.5	Proofs for Minimal Unitary Characterisation . . . . .	128
A.6	Analytical Bounds for Two Classical Fidelities Utilising MUBs . . . . .	137
A.7	Monte Carlo Certification for General Operator Bases . . . . .	141
A.8	Proper Normalisation of the Relevance Distribution for Reduced Fidelities . . . . .	147
A.9	Bounded Variance for the Random Variables Involved in Reduced Fidelities . . . . .	149
<b>B</b>	<b>Optimal Measurement Bases for MC Certification</b>	<b>151</b>
B.1	Spectrum of the Basis Operators . . . . .	153
B.2	Eigenbases of the Basis Operators . . . . .	154
B.3	Optimal Measurement Bases and Efficiently Characterisable Unitaries . . . . .	159
<b>C</b>	<b>Controllability for High-Frequency Amplitude Control on a Phase Qudit</b>	<b>160</b>
	<b>References</b>	<b>163</b>
	<b>List of Publications</b>	<b>177</b>

# 1 Introduction

*“Spukhafte Fernwirkung”*, or as it is commonly translated *“spooky action at a distance”*, this is the slightly derogatory term that Albert Einstein used in a letter to Max Born [1] to describe one of the peculiar aspects of quantum theory we nowadays call “entanglement”. In 1935 Einstein, Podolsky and Rosen wrote their famous paper about one of the most intricate implications of quantum theory, the fact that a measurement on a part of a system can have an instantaneous effect on observable quantities on other parts of the system, no matter how far these parts are spatially separated [2]. This contradicts either the locality of the physical theory, i.e. that a local perturbation on a system only has an immediate effect on this very spatial region of the system, or its realism, i.e. the fact that to any observable property or measurement outcome there needs to be a well-defined variable. Einstein, Podolsky and Rosen proposed that there is a more general theory to which quantum mechanics serves only as an approximation such that this more general theory will uphold both the concepts of locality and realism. This more general theory is commonly termed “local hidden variable theory”. Bell showed in 1964 that if such a theory was underlying quantum mechanics, then certain inequalities, the so-called Bell inequalities, could never be violated [3]. However, the experiments by Aspect et al. in 1982 showed that a statistically significant violation of those inequalities could in fact be observed [4]. Very recently, Yin et al. showed even *“[...] a 12 h continuous violation of the Bell inequality and concluded that the lower bound speed of spooky action was 4 orders of magnitude of the speed of light [...]”* [5].

Entanglement and its striking consequences are a central part of quantum physics. One might even go so far as to say that entanglement is the main ingredient that separates the theory of quantum mechanics from that of classical mechanics. As soon as quantum systems interact, their respective states become entangled. The consequences of this effect are numerous. Most notably, entanglement represents a resource that can be used to extend the computational power of a machine beyond that of classical computation with remarkable consequences for communication and message encryption [6]. However, there are forms of undesired entanglement. For example, the entanglement of a system with environmental degrees of freedom usually leads to a loss of fidelity in practical realisations of quantum information devices. Furthermore, the fact that quantum systems can exhibit entanglement leads to a strongly exponential scaling in the number of basic information carriers when the task is to characterise or certify a quantum state or a quantum operation.

To reach the ultimate goal of harvesting quantumness in practical applications, one needs to answer the question of how to best exploit the beneficial effects of entanglement while minimising its detrimental consequences. In the first place this requires efficient schemes for tomography and certification of quantum systems in the presence of environmental effects in order to determine whether high-fidelity quantum processes can be experimentally realised for complex open quantum systems. Moreover, the question arises how to practically exploit features of quantum theory for specific tasks in the face of experimental limitations and noise effects. Answering the question of how to most efficiently utilise these limited resources from the perspective of characterisation and control of open quantum systems will be the central focus of this work.

In this thesis, we derive a set of fundamental mathematical theorems outlining the lower bounds on the required information to characterise and certify a unitary gate implementation in an open quantum system. This is achieved by finding the mathematical conditions that determine which sets of physical states are suitable to extract the relevant information for this particular task. We

show that these results can be applied to experimental gate certification and optimal control theory to significantly reduce the required experimental, respectively numerical, effort. We furthermore illustrate how optimal control theory can be used to find control schemes that successfully implement pivotal tasks of quantum information in open quantum systems. By using a realistic model for two physical systems of current interest, we illustrate the potential beneficial impacts of environmental degrees of freedom on the one hand while outlining strategies to mitigate their detrimental effects on the other hand.

This thesis is organised as follows: Section 2 is devoted to a brief overview on the general description of states of open and isolated quantum systems as well as the notion of observables and their measurement. Furthermore, we will review the mappings on the set of states that an open quantum system can physically implement. In particular, we will discuss the case of vanishing initial environmental correlations which leads to the notion of dynamical maps. An especially important case is given by unitary dynamical maps, in the context of quantum information usually called (unitary) gates, representing an evolution that is effectively identical to that of an isolated system. In Sec. 3 we will identify an algebraic criterion for the assessment of whether a given set of input states is sufficient for the identification of the unitary transformation that gives rise to a unitary dynamical map. We show how this criterion can be expanded to answer the question regarding minimal sets of input states which allow for unique characterisation of a unitary dynamical map and reconstruction of the corresponding unitary gate. Section 4 discusses the consequences of these results for practical certification of unitary dynamical maps and illustrates how fidelity measures deduced from reduced set of states behave with respect to a physically meaningful gate error. Furthermore, we will show how combining these sets of input states with state-of-the-art statistical schemes can lead to a reduction in computational resources as well as various experimental resources for the task of unitary gate certification.

After concluding the analysis of experimental certification we turn in Sec. 5 to the question of how to control open quantum systems such that they implement a certain task. To this end we will employ optimal control theory (OCT), in particular Krotov's algorithm [7–9]. We show how the reduced set of states derived in the previous sections can be applied in the context of OCT to formulate optimisation functionals that allow for a significant reduction in the numerical effort required for the optimisation algorithm. Finally, Sections 6 and 7 are devoted to the analysis of control strategies for two problems of great current interest: preparation of pure states, in particular the cooling of internal degrees of freedom of a quantum system, and the realisation of quantum gates. We will extensively discuss the vibrational cooling of molecules as an example for the former and show how environmentally induced Markovian evolutions can be efficiently exploited for cooling tasks. Moreover, we will generalise the employed scheme to a larger class of cooling processes. In a second example, we will show how environmentally induced non-Markovian evolutions of a superconducting phase qudit can be utilised to extend the reachable set of quantum gates under the limited experimental control resource of having amplitude control only. Section 8 concludes and gives a brief outlook on the impact of the results obtained in this work.

## 2 Quantum States, Observables and Dynamical Maps

Before we can attempt to answer the question of how to most efficiently characterise a quantum system, we have to establish the mathematical framework which allows an adequate description of the state of a physical system. Effectively, this means one should be able to associate to any such state an element of some set  $\mathcal{S}$ , apply operations to it (corresponding to for example its evolution in time) and obtain another element of  $\mathcal{S}$  which we can then uniquely identify with another state. We will take in this thesis a quantum information perspective in that we are firstly interested in the description of states on a physical system and point-to-point transformations on these states, representing a computational operation. Only when we introduce the concept of quantum control will we need to describe the continuous evolution of a state in time, i.e. full quantum system dynamics, which will be treated in Sec. 5.

The most general choice of the set  $\mathcal{S}$  for an isolated quantum system turns out to be a complex  $L^2$ -Hilbert space. We will illustrate how the physical requirements on the mathematical frameworks are being reflected in the characteristics of the Hilbert space formalism. It turns out that the necessity of normalisation of quantum states requires any physical state to be associated with an equivalence class of Hilbert space vectors rather than a single vector. Additionally, we will discuss how observable quantities and measurements on a physical system translate into this mathematical framework.

The Hilbert space formalism enables only the description of general states of isolated quantum systems, i.e. pure states. The generalisation of the theory to admit a proper description of open quantum systems necessitates the introduction of mixed state. They illustrate the remarkable difference between incoherent and coherent superpositions in quantum systems which represents one of the most striking differences between classical and quantum mechanics. While pure states are described by state vectors in Hilbert space, mixed states are associated with density matrices in Liouville space, an extension of Hilbert space in which the set of pure states forms a lower-dimensional subset. Just like in Hilbert space, density matrices need to obey a normalisation condition that does, however, not coincide with the norm induced by the canonical scalar product.

After having established the framework for the description of physical systems by states in Hilbert space (for isolated quantum systems) or Liouville space (for open quantum systems) we can turn to the question of how to properly describe a change of the state via a physical process, i.e. operations on the physical system. One expects that the mathematical properties of the state are preserved, i.e. normalisation and, in Liouville space, positive definiteness. It turns out that correlations with the environment can lead to unexpected behaviour, for example the loss of positivity of the transformation [10, 11]. We will briefly discuss what are the transformations that appropriately describe operations on open quantum systems. If no initial correlations exists, transformations that preserve all properties of an arbitrary input density matrix can be identified as so-called dynamical maps. We will discuss a general mathematical description of these dynamical maps via Choi's theorem [12] and review their equivalent description by a density matrix in a higher-dimensional Liouville space via the Choi-Jamiołkowski isomorphism [12–14].

In the special case of isolated quantum systems a dynamical map reduces to a unitary transformation on Hilbert space. We will conclude this section by demonstrating the equivalence between unitary dynamical maps and elements of the projective unitary group. This will set the stage for the derivation of the main theorems about characterisation of unitary transformations in open quantum systems in Sec. 3.

## 2.1 Breakdown of Local Realism and the Copenhagen Interpretation

From classical mechanics we expect any physical system to be characterisable by a certain set of real-valued quantities. Furthermore, any measurement of some property of one or multiple particles will be predetermined and those measurements will not (at least instantaneously) influence the state in phase space, i.e. other particles. This is usually summarised by stating that classical physics is a realistic and local theory [15]. A physical theory is said to be realistic if the result of a measurement of a property of the physical system is determined a priori, even if no prior knowledge about the state of the system exists. It is said to be local if the process of measurement of the state of a subsystem of the total physical system does not influence the state of other parts of the subsystem. Usually, the combined assumption of realism and locality is termed “local realism” [6, 16]. Local realism implies certain relations about correlation of experimental observables in spatially separated physical systems. These can be mathematically formalised into so-called Bell inequalities [3].

Evidently, as shown by many experiments [4, 5, 17], physical systems do not obey local realism. The fact that classical mechanics predicts local realism shows the need for a theory that foregoes this notion - the theory of quantum mechanics. This immediately leads to the question whether the assumption of locality or realism has to be discarded, or even both. One of the earliest, and also most widely accepted, answers to this question is given by the so-called Copenhagen interpretation of quantum mechanics which took their origin in the 1920s and was pioneered by Heisenberg and Bohr [18].

Despite its long history and broad acceptance, John Cramer states in his 1986 review article about the Copenhagen interpretation the following: “*Despite an extensive literature which refers to, discusses, and criticizes the Copenhagen interpretation of quantum mechanics, nowhere does there seem to be any concise statement which defines the full Copenhagen interpretation.*” [19]. He identified five key axioms that can be summarised as follows.

**Axiom** (Copenhagen Interpretation of Quantum Mechanics).

1. *The uncertainty principle: It is impossible to know all properties of a physical system at the same time.*
2. *State vectors: The state of a physical system at a certain time  $t$  is completely described by a wave function  $\psi(t)$ . The wave function is a continuous function of time except when a measurement is performed.*
3. *Statistical interpretation: The square modulus of the wave function  $|\psi|^2$  can be interpreted as a probability distribution. Observable quantities can be described as linear operators on the wave function. Their measurement results in a discontinuous change, or “collapse”, of the wave function to one of the eigenspaces of the observable.*
4. *Complementary principle: The uncertainty principle is a fundamental limit to the accuracy of a simultaneous measurement of certain variables. It is intrinsic to nature and cannot be circumvented, no matter the fidelity of the experimental apparatus. An interpretation of experimental results must take into account this complementary character of certain observables as it is specifically pronounced in the wave-particle duality of matter.*
5. *Positivism: The question of whether there is a hidden universe concealed behind what we can observe, that still obeys the law of determinism and local realism, is meaningless. A physical*

*theory must only be concerned with the prediction of outcomes of actually observable features of nature.*

The Copenhagen Interpretation clearly contradicts realism, since by the uncertainty principle it is impossible to attain perfect knowledge of all observables of a physical system at a certain time. It should be emphasised that while complete knowledge of the state of the system is represented in the form of a wave function, the statistical nature of quantum mechanics prevents this knowledge to extend to the level of arbitrary sets of observable quantities. Moreover, the Copenhagen interpretation also opposes locality due to the way measurements impact the wave function. It is this locality-violating axiom of the Copenhagen interpretation that lead Einstein to his famous remark of “*spooky action at a distance*” [1] and to the famous paper by Einstein, Podolsky and Rosen from 1935 [2]. We will review the mathematical framework of quantum mechanics in light of the central axioms of the Copenhagen interpretation.

We want to briefly note that there exist proposals of a quantum mechanical theory that deviate from the Copenhagen interpretation and name two examples. A comparatively well-known alternative formulation of quantum mechanics that preserves realism but still opposes locality is the so-called pilot wave theory, first pioneered by de Broglie in 1927 [20] and rediscovered and reformulated by Bohm in 1952 [21, 22]. More recently, in 1989, Weinberg analysed the effect of nonlinear corrections to a linear quantum mechanical theory and their implications [23]. However, it has been pointed out that such a nonlinear formulation potentially encounter the problem of allowing arbitrarily fast communication, often called supraluminal communication, which would be in contradiction to special relativity beyond the violation of non-locality via the Bell inequalities [24, 25].

## 2.2 Hilbert Space

The first question regarding the mathematical framework following from the Copenhagen interpretation concerns the state space of the wave function. By the complementary principle of the Copenhagen interpretation we understand that every physical particle can be interpreted as a wave, as such we expect physical particles to follow the superposition principle. The fact that we have to allow for superposition motivates the assumption that the space of state vectors needs to allow for a vector space structure such that addition of wave functions is well-defined<sup>1</sup>.

The statistical interpretation of quantum mechanics is manifested in the notion, that the modulus square of the state vector can be regarded as a probability distribution  $w = |\psi|^2$ . From a mathematical perspective this means that  $w$  needs to be nonnegative and normalised to 1. Since the statistical interpretation explicitly states that the probability is given by the modulus square, the norm can be identified with the so-called  $L^2$  norm. For the continuous variable of position corresponding to the representation of the state of a single particle via the wavefunction  $\psi(\vec{x})$  with  $\vec{x} \in \mathbb{R}^3$ , one can conclude that a suitable space for this specific spatial representation of a single-particle wave functions is the space  $L^2(\mathbb{R}^3)$ .

The next question concerns the underlying field of the vector space of quantum states. From a mathematical standpoint complex numbers are favourable to real numbers since they form an algebraically closed field, i.e. any non-constant polynomial with coefficients in the field has a root

---

<sup>1</sup>For an even stronger argument, we refer to the work by Abrams and Lloyd [26], who showed that nonlinearity of quantum mechanics would imply polynomial-time solvability of NP-complete and #P problems and interpret this result as evidence for the exact linearity of quantum mechanics.

in the field. This is equivalent to the statement that,  $\forall n \in \mathbb{N}$ , any matrix representing a map from  $\mathbb{C}^n$  admits a set of  $n$  generalised eigenvectors, a notion of great importance for the Copenhagen interpretation that demands a collapse of the wavefunction to eigenspaces of operator on the state space. An even stronger, and more physical, perspective was pointed out in Ref. [27] where it has been shown that the so-called quantum de-Finetti theorem is only consistent with a complex (and neither real nor quaternionic) formulation of quantum mechanics.

Since the  $L^2$  norm is at the core of the statistical interpretation of quantum mechanics we briefly present a more general perspective. For any index set  $I$ , one defines the space  $l_{\mathbb{C}}^2(I)$  as the set of all sequences  $(z_k)_{k \in I}$  with  $z_k \in \mathbb{C}$  such that

$$\sum_{k \in I} |z_k|^2 < \infty.$$

Following the Copenhagen interpretation, the proper mathematical tool to describe the state of a quantum mechanical system is to interpret it as an element of some  $l_{\mathbb{C}}^2(I)$  space. In fact, these spaces are even Hilbert spaces, i.e. Banach spaces with an inner product  $\langle \cdot, \cdot \rangle$  such that the norm is given by  $\|\cdot\| = \sqrt{\langle \cdot, \cdot \rangle}$ . There is an intimate relation between  $l^2$  spaces and general Hilbert spaces, which states that for any complex Hilbert space  $\mathcal{H}$  there exists an index set  $I$  such that  $\mathcal{H}$  is isomorphic to the space  $l_{\mathbb{C}}^2(I)$  [28]. Moreover, in physics one almost always deals with separable Hilbert spaces, i.e. those with a countable orthonormal basis. This allows for an even more precise statement: For any separable Hilbert space  $\mathcal{H}$  there are only two possibilities. If  $\dim(\mathcal{H}) = d < \infty$ , then  $\mathcal{H}$  is isomorphic to  $\mathbb{C}^d$  with the Euclidean norm. If  $\dim(\mathcal{H}) = \infty$ , then  $\mathcal{H}$  is isomorphic to  $L^2(\mathbb{R}^n)$  for arbitrary  $n \in \mathbb{N}$  with the canonical  $L^2$  norm.

In this thesis we will only discuss separable, in fact mostly finite-dimensional, Hilbert spaces. The fact that all Hilbert spaces of equal dimensionality are isomorphic to each other is the mathematical motivation why one sometimes speaks of “the” Hilbert space. The only mathematically relevant difference between Hilbert spaces lies in their dimensionality. In particular, the description of the state of any physical system in a Hilbert space of dimension  $d$  is equivalent to a description in the space  $\mathbb{C}^d$  with the Euclidean norm.

There is one subtle detail regarding the Hilbert space picture. Strictly speaking, the normalisation condition on wave functions is not compatible with a vector space structure. This can be immediately seen by observing that if  $|\psi\rangle$  is a properly normalised state vector<sup>2</sup> then the only  $\lambda \in \mathbb{C}$  that allows  $\lambda|\psi\rangle$  to still be properly normalised are those with  $|\lambda| = 1$ . Additionally, it turns out that no measurement can measure the absolute phase of a state vector  $|\psi\rangle$ . Only the relative phase between two state vectors leads to a physically observable difference in behaviour. The positivism axiom of the Copenhagen interpretation encourages to not include this phase in the mathematical description of the physical state space. This “physically unimportant global phase” is sometimes formalised by the statement that for each Hilbert space  $\mathcal{H}$  the group  $U(1)$  is a gauge group of first kind. Hence for a given Hilbert space  $\mathcal{H}$ , any state  $\lambda|\psi\rangle \in \mathcal{H}$  for arbitrary  $\lambda \in \mathbb{C} \setminus \{0\}$  is equivalent. More precisely, states of quantum systems are bijectively identified not with elements of Hilbert spaces but rather with elements of so-called projective Hilbert spaces [29]. The projective Hilbert space  $P(\mathcal{H})$  corresponding to  $\mathcal{H}$ , if  $\dim \mathcal{H} = d$  often called  $\mathbb{C}P^{d-1}$ , is given by the equivalence class of vectors

---

<sup>2</sup>In physics it has been historically established that vectors in Hilbert space are denoted by so-called kets  $|\psi\rangle$ , the corresponding dual space element by the Fréchet-Riesz representation theorem is denoted by a so-called bra  $\langle\psi|$ .

$|\psi\rangle \in \mathcal{H}$  with the equivalence relation  $\sim$  given by

$$|\psi_1\rangle \sim |\psi_2\rangle \text{ if } \exists \lambda \in \mathbb{C}, \lambda \neq 0 : \lambda |\psi_1\rangle = |\psi_2\rangle . \quad (2.1)$$

The elements of a projective Hilbert space are called rays. The Copenhagen interpretation hence motivates the notion, that quantum mechanical states are represented by rays in separable complex Hilbert spaces.

This description is strictly true only for so-called pure states. We will amend this in Sec. 2.4 and focus on pure states in this and the following subsection. Furthermore we will henceforth simply talk about “states in Hilbert space” where the identification with the corresponding equivalence class in the projective Hilbert space is implied.

To describe how quantum systems interact with each other it is necessary to find an adequate description of the composite state of two physical systems whose individual states are elements of a Hilbert space each. From a mathematical standpoint two solutions seem plausible - the tensor sum  $\oplus$  or the tensor product  $\otimes$ . The dimension of Hilbert space can be identified with the number of different configurations in which the physical system can be theoretically prepared, cf. Sec. 2.4. If one considers two physical systems, with  $d_1$  and  $d_2$  possible configurations respectively, the tensor sum implies that the composite system has a number of different configurations equal to the sum of different configurations of the individual system. Conversely, the tensor product implies that it is the product of different configurations. If one measures the properties on the two subsystems individually, and the two subsystems are completely independent, one expects no collapse in the other subsystem. As a consequence, it is evident that after a measurement on the first subsystem has been performed, the second subsystem needs to retain the possibility to be in any of its  $d_2$  configurations. Summing now over all  $d_1$  possible measurement results on the first system one can see that  $d_1 \cdot d_2$  is the proper number of configurations for the total system.

As a conclusion, the composite state space of two physical systems described by Hilbert spaces  $\mathcal{H}_1$  and  $\mathcal{H}_2$  is given by the tensor product Hilbert space  $\mathcal{H}_1 \otimes \mathcal{H}_2$ . It is important to keep in mind that the projective Hilbert space of the composite system  $P(\mathcal{H}_1 \otimes \mathcal{H}_2)$  is not equal to  $P(\mathcal{H}_1) \otimes P(\mathcal{H}_2)$ . This is just another way of illustrating that the global phase of a quantum system is irrelevant but the relative phase between any two subsystems is not.

## 2.3 Observables and Measurements

We will now turn to address the nature of observables in the framework of Hilbert space. By the Copenhagen interpretation, observables are represented by linear operators on the state space. To allow for a simple spectral decomposition of these operators, they should ideally be continuous. In fact, if the Hilbert space is finite-dimensional, every linear operator is continuous [28]. However, in an infinite-dimensional Hilbert spaces not even the position operator  $\vec{x}$  is continuous and it is mathematically not straightforward to define eigenvectors which are required to describe the action of a position measurement. This problem can be treated by looking for eigenvectors not in the Hilbert space but in an “extended Hilbert space” including for example the space of tempered distributions [28]. These generalised eigenvectors can then be properly mathematically characterised. In the following we will restrict ourselves to finite-dimensional Hilbert spaces which is sufficient in the context of this thesis. Since several results can be generalised, potentially under additional constraints,

for the infinite-dimensional case we will nonetheless try to keep the notation general, if possible.

A measurement of an observable leads to a discontinuous collapse of the wave function onto one of its eigenspaces. If we associate each eigenspace with a measurement result, then the statistical interpretation of quantum mechanics leads to the following assumption: The likelihood of a measurement associated with the observable  $O$  to collapse the state  $|\psi\rangle$  onto an eigenspace of  $O$  with corresponding projector  $P$  is equal to  $\|P|\psi\rangle\|^2$ .  $|\psi\rangle$  collapses according to the so-called Lüders projection,  $|\psi\rangle \mapsto \frac{P|\psi\rangle}{\|P|\psi\rangle\|}$  [30]. Such a measurement is usually termed “measurement of first kind” [31, 32].

There is some confusion in the literature about what precisely constitutes a Pauli measurement of first kind. In his original formulation [31], Pauli gave two definitions, namely that the result of a measurement of first kind will be identical upon repetition, whereas his second definition states that the probability distribution of obtaining a particular result is the same immediately before and after the measurement. We know nowadays that these definitions are not equivalent and in modern quantum mechanics the second definition is usually adopted. Measurements following the first definition are usually called repeatable and it is clear that repeatable measurements are of first kind but not all first-kind measurements are repeatable.

A special kind of repeatable measurements are so-called quantum nondemolition measurements (QNDs) [33, 34]. QND measurements usually do not only demand that the measurement result is identical after an immediate re-measurement but also after an additional free evolution of the system. It should be emphasised that a QND does not imply that the wave function does not collapse but only that the back-action on the system via the measurement is minimised in a way that makes repeated measurements possible.

A measurement of second kind alters the state of the system in such a way, that it changes the measurement statistics of the state through the measurement. For example, photon counting with destruction of photons by absorption represents a measurement of second kind. No matter whether a photon is detected or not, there will be no photons left after the measurement has been performed. One could now argue that a repeatable measurement also alters the measurement statistics since it always collapses the wave function such that the state after the measurement only admits a single result in a repetition. However, it is not the measurement that changed the statistics but rather the selection according to the recorded measurement result. This is in contrast to the photon counting by absorption in which the very measurement will destroy the photon no matter which measurement result actually has been recorded.

To emphasise this two-step approach to a measurement in terms of a preparation and a selection component, one often employs the weak von Neumann projection,  $|\psi\rangle \mapsto \sum_i \frac{P_i|\psi\rangle\langle\psi|P_i}{\|P_i|\psi\rangle\|^2}$  to describe the preparation of the state by the measurement, with  $\{P_i\}$  being the set of projectors on the eigenspaces of the corresponding observable [32]. The resulting state is a statistical mixture that yields the same probability distribution as the original state but has no definite value of the observable yet. It is rather in an incoherent superposition, i.e. a mixed state, of the possible values. We will discuss the corresponding extension of state space in the next section. Such a measurement without an actual recording of the measurement result, or, equivalently, an immediate discarding of the information about the result, is sometimes called non-selective measurement. This is in contrast to selective measurements which select from the ensemble obtained via von Neumann projection a subensemble corresponding to a unique value of the measured property. For the case of a one-dimensional projector corresponding to this measurement result this leads to a pure state and coincides with a Lüders

projection. Although it appears that the Lüders projection and the von-Neumann projection with selection of the measurement result yield different post-measurement states if the projector has dimension reater than one, it can be shown that both descriptions are equivalent [35]. For an extensive mathematical analysis on different kinds of measurement see e.g. Ref. [36]. An overview and comparison of the various projection postulates corresponding to different measurements was recently given in Ref. [35]. In the following we will usually refer to selective measurements when we speak of measurements being performed on a quantum system.

A measurement result is usually attributed to the eigenvalue of the measured observable corresponding to the eigenspace onto which the wave function collapsed. By that interpretation, the operator  $O$  should at least be normal since normal operators obey the relation that different eigenvalues correspond to orthogonal eigenspaces<sup>3</sup>. It is this property that allows us to talk about a proper projection onto an eigenspace corresponding to the measurement result. However, in practice, measurement results need to be classical in order to be observable by the classical sensors of an experimenter, e.g. their ears or eyes. For this reason, the measurement results and corresponding properties of the quantum systems are usually thought of as real. Consequently, observables need to be represented by diagonalisable, linear operators with real spectrum<sup>4</sup>. The corresponding operators are called self-adjoint or Hermitian<sup>5</sup>.

In summary, physical observables are represented by Hermitian operators on Hilbert space. Measurements correspond to a projection of the state vector of the physical system onto an eigenspace of the operator with likelihood equal to the squared modulus overlap of the state vector with the eigenspace. The eigenvalue of the operator on this eigenspace corresponds to the measurement result.

In terms of operators it makes no difference whether we consider them on the projective Hilbert space or the ordinary Hilbert space, since any linear operator  $A$  fulfils  $\forall \lambda \in \mathbb{C} : A(\lambda |\psi\rangle) = \lambda (A|\psi\rangle)$ . The action of a linear operator on a single vector in Hilbert space already defines its action on the whole ray completely. The term observable will refer, depending on context, either to the operator describing this system property in the mathematical framework of Hilbert spaces or to the set of classical measurement results of a certain system property. In mathematical terms the first case refers to a Hermitian operator on Hilbert space while the second case refers to the operator's spectrum.

Under certain restrictions, the space of operators on Hilbert space forms a Hilbert space itself. A compact operator  $A$  on a separable Hilbert space  $\mathcal{H}$  is called a Hilbert-Schmidt operator if  $\sum_i s_i^2 < \infty$  where  $\{s_i\}$  is the set of singular values of  $A$ . The set of Hilbert Schmidt operators is called  $\text{HS}(\mathcal{H})$ . The sesquilinearform

$$\forall A, B \in \text{HS}(\mathcal{H}) : \langle A | B \rangle = \text{Tr} [A^\dagger B] \quad (2.2)$$

defines a scalar product on  $\text{HS}(\mathcal{H})$  which induces the so-called Hilbert-Schmidt norm,

$$\|A\|_{\text{HS}} = \sqrt{\sum_i s_i^2}, \quad (2.3)$$

<sup>3</sup>This is strictly true only as long as the corresponding eigenvalues lie in the field of the vector space. In quantum mechanics one employs Hilbert spaces over the algebraically closed field of complex numbers which is why this is not an issue in this context.

<sup>4</sup>As pointed out, the fact that the spectrum of observables is assumed to be real is rather a matter of convention than a mathematical necessity since any normal operator allows for a complete and orthonormal eigenbasis. We will return to this point in Sec. 4.9.

<sup>5</sup>There is a subtle mathematical difference between these two concepts for infinite-dimensional Hilbert spaces [28]. However, since this thesis will mainly concern the finite-dimensional case we can use these two terms interchangeably.

where  $\{s_i\}$  is the set of singular values of the Hilbert-Schmidt operator  $A$ . Hence,  $\text{HS}(\mathcal{H})$  is a Hilbert space [28].

For finite-dimensional Hilbert spaces all operators are Hilbert-Schmidt operators. This allows us to obtain a natural Hilbert space structure for the space of operators including the notion of orthogonality and orthonormal bases. In the following, the space of operators will always be interpreted as the Hilbert space of Hilbert-Schmidt operators on  $\mathcal{H}$ .

## 2.4 Liouville Space

Maximal information about the state of a quantum system is represented by a set of measurement results obtained via measurement a maximal set of commuting observables [37]. Such a set of observables  $\mathcal{A} = \{A_i\}$  on  $\mathcal{H}$  is called a CSCO (complete set of commuting observables). More formally, the set  $\mathcal{A}$  is a CSCO if there exists exactly one orthonormal basis of  $\mathcal{H}$ , up to phase factors on the individual elements, which contains common eigenstates of all elements of  $\mathcal{A}$  [37].

Conversely, any element of a Hilbert space  $\mathcal{H}$  is completely determined by the measurement results of a sequence of measurements involving all elements of a CSCO. States obtained this way are called pure states, the process of obtaining a pure state this way is called preparation. Any state  $|\psi\rangle \in \mathcal{H}$  can be prepared by measuring a CSCO where  $|\psi\rangle$  is a common eigenstate to all observables in this set.

There is a statistical nature to quantum mechanics by virtue of the statistical outcomes of some measurements performed on quantum states. This is true even for pure states if the pure state is not an eigenstate to the observable corresponding to the measurement. Nevertheless, to any pure state in a Hilbert space  $\mathcal{H}$  there exists a CSCO for which the measurement results are not statistical, i.e. no matter how often an experiment on these observables is performed the result will always be the same. However, it is conceivable that we want to describe states for which we do not know the result of any measurement with certainty yet, for example by having measured a non-complete set of commuting observables on a completely unknown states. Such states are called weakly prepared. Specifically, consider a CSCO  $\mathcal{A}$  from which a proper subset  $\mathcal{A}_0 \subset \mathcal{A}$  has been measured. This means that the state of the system is in a common eigenstate of the subset  $\mathcal{A}_0$ . Let  $\{|\psi_i^{(0)}\rangle\}$  be an arbitrary orthonormal basis of  $\mathcal{A}_0$  in  $\mathcal{H}$ , then, the physical system can be interpreted to be with some probability  $p_i$  in the state  $|\psi_i^{(0)}\rangle$ . Nevertheless, this is not equivalent to saying that the physical system is in a pure state representing an equal superposition of the  $|\psi_i^{(0)}\rangle$  (since that would mean we could predict the measurement results of observables in  $\mathcal{A}/\mathcal{A}_0$  with certainty). To differentiate these two kinds of superposition, the quantum superposition of states in Hilbert space to form a pure state is called coherent superposition while the statistical superposition due to incomplete information is called incoherent superposition. Clearly, the expectation value of the measurement result of some observable in  $A \in \mathcal{A}/\mathcal{A}_0$ , for which one can attribute an eigenvalue  $a_i$  to the eigenvector  $|\psi_i^{(0)}\rangle$ , should be given by

$$\langle A \rangle = \sum_i p_i a_i = \sum_i p_i \langle \psi_i^{(0)} | A | \psi_i^{(0)} \rangle. \quad (2.4)$$

With  $\{|\psi_i\rangle\}$  being an orthonormal basis of  $\mathcal{H}$  one can write

$$\begin{aligned} \langle A \rangle &= \sum_{ij} p_i \langle \psi_i^{(0)} | \psi_j \rangle \langle \psi_j | A | \psi_i^{(0)} \rangle = \sum_j \left\langle \psi_j \left| A \sum_i p_i \right| \psi_i^{(0)} \right\rangle \left\langle \psi_i^{(0)} \left| \psi_j \right\rangle \right. \\ &= \sum_j \left\langle \psi_j \left| A \left[ \sum_i p_i P_i^{(0)} \right] \right| \psi_j \right\rangle = \text{Tr} \left[ A \sum_i p_i P_i^{(0)} \right] = \left\langle A, \sum_i p_i P_i^{(0)} \right\rangle_{\text{HS}}, \end{aligned} \quad (2.5)$$

where  $P_i^{(0)}$  corresponds to the projector onto  $|\psi_i^{(0)}\rangle$ . This motivates the definition of incoherent ensembles not as states on the Hilbert space  $\mathcal{H}$  but as operators on them. If one defines  $\rho = \sum_i p_i P_i^{(0)}$  then one can write the expectation value of an observable  $A$  simply as the overlap of  $A$  with  $\rho$ .  $\rho$  is called the density operator or, if  $\mathcal{H}$  is finite-dimensional, the density matrix. Note that if the  $p_i$  are to be interpreted as probabilities, they need to be nonnegative and they need to sum up to 1. More formally, any density matrix on this Hilbert space can be written as

$$\rho = \sum_i p_i |\psi_i\rangle \langle \psi_i|, \quad \forall i: p_i \geq 0, \quad \sum_i p_i = 1, \quad (2.6)$$

where  $\{|\psi_i\rangle\}$  is an orthonormal basis of  $\mathcal{H}$ .  $|\psi_i\rangle \langle \psi_i|$  denotes the dyadic product of the vector  $|\psi_i\rangle$  with itself. The dyadic product  $|\psi_i\rangle \langle \psi_i|$  is identical to the rank 1 projector  $P_i$  on  $|\psi_i\rangle$ . If at least two  $p_i$  are nonzero,  $\rho$  is called a mixed state. Otherwise, it is called a pure state. It is easy to see that the Hilbert-Schmidt norm of a density matrix is equal to 1 if and only if it is pure, otherwise it is strictly smaller than one. For this reason the quantity  $\|\rho\|_{\text{HS}}$  is often called the purity of  $\rho$ . Note, that this definition of pure states is consistent with the one from Sec. 2.2 since any pure density matrix can be uniquely identified with a state in projective Hilbert space.

The space of linear operators on a finite-dimensional Hilbert space,  $L(\mathcal{H})$ , is isomorphic to  $\mathcal{H} \otimes \mathcal{H} \cong \mathbb{C}^d \otimes \mathbb{C}^d \cong \mathbb{C}^{d^2}$  with  $d = \dim \mathcal{H}$ . The space  $\mathcal{H} \otimes \mathcal{H}$  is called Liouville space and we will denote it consistently with  $\mathcal{L}_{\mathcal{H}}$  to indicate its intimate connection with the Hilbert space it originates from. The consideration of projective Hilbert spaces is not necessary in this context, cf. Sec. 2.2, since in Liouville space the invariance under a global phase is incorporated by construction<sup>6</sup>. The set of density matrices is a proper subset of Liouville space. However, the set of density matrices does not obey a vector space structure and, in contrast to pure states and projective Hilbert spaces, no isomorphism to a Hilbert space can be found. It should be emphasised that while the property of having trace 1 is usually called normalised, it neither means that the operator norm nor that the Hilbert-Schmidt norm of a corresponding density matrix needs to be equal to 1.

## 2.5 Open Quantum Systems

A common approach concerning the description of open quantum systems is to start from a natural partitioning of state space into the primary system, described by a Hilbert space  $\mathcal{H}_S$ , and its environment, described by a Hilbert space  $\mathcal{H}_E$  [38]. The state of the total system is then described as an element of the bipartite tensor product Hilbert space  $\mathcal{H} = \mathcal{H}_S \otimes \mathcal{H}_E$ . Consequently, a general mixed state on the total Hilbert space is described by an element of the Liouville space

<sup>6</sup>This can be immediately seen by the following argument: Let  $\mathcal{H}$  be a Hilbert space and  $\lambda \in \mathbb{C}, |\lambda| = 1$ . Consider an arbitrary pure state, then  $\forall \lambda \in \mathbb{C}, |\lambda| = 1, |\psi\rangle \in \mathcal{H}: \rho_{\lambda|\psi} = |\lambda\psi\rangle \langle \lambda\psi| = \lambda^* |\psi\rangle \langle \psi| \lambda = |\lambda|^2 |\psi\rangle \langle \psi| = |\psi\rangle \langle \psi| = \rho_{|\psi}$ .

$\mathcal{L}_{\mathcal{H}} = L(\mathcal{H}) = L(\mathcal{H}_S \otimes \mathcal{H}_E) \cong L(\mathcal{H}_S) \otimes L(\mathcal{H}_E) = \mathcal{L}_{\mathcal{H}_S} \otimes \mathcal{L}_{\mathcal{H}_E}$ . A state  $\rho \in \mathcal{L}_{\mathcal{H}}$  is called a product state if there exist density matrices  $\rho_S \in \mathcal{L}_{\mathcal{H}_S}$  and  $\rho_E \in \mathcal{L}_{\mathcal{H}_E}$  such that

$$\rho = \rho_S \otimes \rho_E. \quad (2.7)$$

It is called separable if it is a convex superposition of product states, i.e.

$$\exists c_i \in \mathbb{R}, |c_i| \leq 1, \sum_i c_i = 1 : \rho = \sum_i c_i \rho_i \quad (2.8)$$

with all  $\rho_i$  being product states. A state that is not separable is called entangled. As a matter of fact the violation of local realism in the theory quantum mechanics is closely connected to the concept of entanglement. Entanglement itself can be seen as the property that makes a quantum state actually “quantum”<sup>7</sup> [6].

Given a density matrix on  $\mathcal{L}_{\mathcal{H}}$ , describing the total state of a physical system and its environment, what is the corresponding density matrix on  $\mathcal{L}_{\mathcal{H}_S}$  that describes only the information on the system? In other words, how does one obtain a reduced description of the total system only including the relevant degrees of freedom for the primary system.

We characterise the system state  $\rho_S \in \mathcal{L}_{\mathcal{H}_S} \equiv \mathcal{L}_S$  by measuring some set of observables  $\mathcal{M}_S \in \mathcal{L}_S$ . Let us consider a particular observable  $M_S \in \mathcal{M}_S$ . First, we need to figure out what is the measurement operator on the total system  $M$  corresponding to  $M_S$ . Consider first of all the special case that  $\rho_S$  is a pure state, corresponding to a  $|\psi_S\rangle \in \mathcal{H}_S$ , that is an eigenstate to  $M_S$  corresponding to the measurement result  $m_S$ . Then, if the state on the total Hilbert space were the pure state  $|\psi_S\rangle \otimes |\psi_E\rangle$  with  $|\psi_E\rangle \in \mathcal{H}_E$  arbitrary, we expect that a measurement of  $M$  yields the measurement result  $m_S$  with probability 1 and leaves the state on  $\mathcal{H}_S$  unchanged (since it is already in an eigenstate). Because this must be independent on  $|\psi_E\rangle$ , an obvious choice seems to be  $M = M_S \otimes \mathbb{1}_E$  leading to  $|\psi_S\rangle \otimes |\psi_E\rangle$  being an eigenstate to  $M$  with eigenvalue  $m_s$ , independently on  $|\psi_E\rangle$ . It is also the only choice since the fact that the eigenspaces of  $M$  need to be of the form  $E_i^{(S)} \otimes \mathcal{H}_E$ , with  $E_i^{(S)}$  being the eigenspaces of  $M_S$ , automatically implies  $M = A \otimes \mathbb{1}_E$ . Thus, the equivalence of  $M$  to  $M_S$  on the system then leads to  $M$  as defined above.

Now consider some  $\rho \in \mathcal{L}_{\mathcal{H}}$ . What is the proper reduced description  $\rho_S \in \mathcal{L}_S$ ? Clearly, the expectation value of a measurement of  $M_S$  on  $\rho_S$  needs to be the same as the measurement of the corresponding operator  $M_S \otimes \mathbb{1}_E$  on  $\rho$ ,

$$\text{Tr}[M_S \rho_S] = \text{Tr}[(M_S \otimes \mathbb{1}_E) \rho]. \quad (2.9)$$

$\rho_S$  will be the image of  $\rho$  under some linear operator  $\Theta : \mathcal{L} \mapsto \mathcal{L}_S$ , i.e.  $\rho_S = \Theta(\rho)$ . Let  $\{M_S^{(i)}\}$  be an orthonormal basis of  $\mathcal{L}_S$ , then by Eq. (2.9),

$$\Theta(\rho) = \sum_i M_S^{(i)} \text{Tr} \left[ M_S^{(i)} \Theta(\rho) \right] = \sum_i M_S^{(i)} \text{Tr} \left[ \left( M_S^{(i)} \otimes \mathbb{1}_E \right) \rho \right]. \quad (2.10)$$

---

<sup>7</sup>It should be noted at this point that recently a notion of “classical entanglement” started to emerge which describes Bell inequality violating correlation particularly in the context of classical light. It should be emphasised that this classical entanglement does not violate locality since it happens between degrees of freedom of a single system. This is in contrast to quantum entanglement which violates locality by nonclassical correlations between spatially separated systems. For a more detailed discussion on this subject see e.g. the work by Töppel et al. [39] and references therein.

Since  $\rho$  was arbitrary this is a unique prescription of the operator  $\Theta$ , called the partial trace  $\text{Tr}_E$  [6]. The partial trace maps the state of system and environment into a state of only the system by retaining all observable quantities that one would obtain by measuring system properties on the total system. Since the operators  $\{|\psi_i\rangle\langle\psi_j|\}$ , with  $\{|\psi_i\rangle\}$  being an orthonormal basis of  $\mathcal{H}_S$ , form an orthonormal basis of  $\mathcal{L}_S$  we can define the partial trace  $\text{Tr}_E$  of  $\rho$  with respect to  $\mathcal{H}_E$  as

$$\text{Tr}_E(\rho) = \sum_{ij} |\psi_i\rangle\langle\psi_j| \text{Tr}[(|\psi_i\rangle\langle\psi_j| \otimes \mathbf{1}_E) \rho]. \quad (2.11)$$

For any pure state  $\rho \in \mathcal{H}$ ,  $\text{Tr}_S(\rho)$  is a pure state if and only if  $\rho$  is separable with respect to the separation  $\mathcal{H}_S \otimes \mathcal{H}_E$  [40].

The partial trace allows us to clearly elucidate why density matrices are necessary for the description of open quantum systems. Let  $\mathcal{H}$  be the Hilbert space of a physical system with its environment and let us assume that in this total Hilbert space the system state can be described as a pure state. Any experiment on the physical system will concern observables on the Hilbert space corresponding to the system,  $\mathcal{H}_S \subset \mathcal{H}$ . For this reason, cf. the positivism axiom of the Copenhagen interpretation, it only makes sense to consider the state on the Hilbert space  $\mathcal{H}_S$  for all intents and purposes. However, the reduced state of the physical system on  $\mathcal{H}_S$  given by the partial trace will only be pure if there was no entanglement between the system (described by the Hilbert space  $\mathcal{H}_S$ ) and its environment (described by  $\mathcal{H}_E \equiv \mathcal{H}/\mathcal{H}_S$ ). In other words, as soon as the state of a physical system becomes entangled with its environment it must be described as a mixed state in Liouville space instead of a pure state in Hilbert space.

Finally, we want to illustrate the connection between quantum states and the information contained in them. It is common to rather define the entropy, i.e. the disorder, which describes the absence of information. In analogy to the classical Shannon entropy, one defines for quantum systems the so-called von Neumann entropy  $S$  [6],

$$S = -\rho \log_2 \rho. \quad (2.12)$$

If  $\mathcal{H}$  is finite-dimensional and  $\{\lambda_i\}$  is the set of eigenvalues of  $\rho$  (including repetitions due to degeneracy), then  $S$  can be written as

$$S = -\sum_i \lambda_i \log_2 \lambda_i, \quad (2.13)$$

with  $\lambda_i \log_2 \lambda_i = 0$  for  $\lambda_i = 0$  (in accordance with  $\lim_{\epsilon \rightarrow 0} (\epsilon \log_2 \epsilon) = 0$ ).  $S$  is nonnegative and it is minimal if  $\rho$  is a pure state, corresponding to maximal information contained in these kind of states. This is the reason why the preparation of pure states is a central paradigm of quantum information processing, a fact we will return to in Sec. 6.

## 2.6 Dynamical Maps

How does the state of an open quantum system evolve from one point in time to another? As already pointed out in Sec. 2.1 the theory of quantum mechanics is linear. It furthermore seems straightforward to demand that any such mapping map needs to map density matrices onto density matrices, i.e. they need to preserve Hermiticity, trace and positive semidefiniteness. In the following we will abbreviate positive semidefiniteness of a matrix by stating that the matrix is positive. For

any Hilbert space  $\mathcal{H}$  and  $A \in L(\mathcal{H})$ ,  $A$  is called positive if  $\forall x \in \mathcal{H} \langle x, Ax \rangle \geq 0$ .  $A$  is called trace-preserving if  $\forall x \in \mathcal{H}, \text{Tr}(x) = 1 : \text{Tr}(Ax) = 1$ . From this condition it then follows automatically that  $\forall x \in \mathcal{H} : \text{Tr}(x) = \text{Tr}(Ax)$ .

In short, a map that preserve the properties of a density matrix needs to be positive and trace-preserving. However, there is one caveat. If the mapping is supposed to be physically sensible, one requires a stronger form of positivity - complete positivity.  $A$  is called completely positive if it is  $m$ -positive  $\forall m \in \mathbb{N}$ .  $A$  is called  $m$ -positive if for all Hilbert spaces  $\mathcal{H}_m$  with  $\dim(\mathcal{H}_m) = m$  the map  $A \otimes \mathbf{1}_m \in L(\mathcal{H} \otimes \mathcal{H}_m)$  is positive. Physically, this means that if we consider a map on a quantum system where the system is coupled to another quantum system whose state is left invariant, the resulting map on the total system should still be positive. If this condition were not fulfilled, then there would not exist a natural extension of the map to a higher-dimensional Liouville spaces which would be unphysical. Complete positivity makes sure that this problem is avoided.

Similarly to the discussion from the previous subsection, we now employ a partitioning of Liouville space into a Liouville space of the system  $\mathcal{L}_S$  and a Liouville space of the environment  $\mathcal{L}_E$ . Consider an initial state  $\rho_S \in \mathcal{L}_S$ , that originates from some state  $\rho \in \mathcal{L}_S \otimes \mathcal{L}_E$  of the total system via the partial trace. Then, the image of  $\rho_S$  can be obtained by considering the image of  $\rho$  under some unitary<sup>8</sup> map on  $\mathcal{L}_S \otimes \mathcal{L}_E$  and computing the partial trace over the environmental degrees of freedom. A remarkable observation is the fact that if no restrictions are imposed on the relation between the initial density matrix in  $\mathcal{L}_S$  and the initial density matrix in  $\mathcal{L}_S \otimes \mathcal{L}_E$ , the resulting image of arbitrary initial density matrices in  $\mathcal{L}_S$  is not guaranteed to be a proper density matrix [10, 41]. However, one can prove that a proper completely positive dynamical map on  $\mathcal{L}_S$  is guaranteed if and only if  $\rho_S \in \mathcal{L}_S$  originates from a separable state in  $\mathcal{L}_S \otimes \mathcal{L}_E$ ,

$$\rho = \rho_S \otimes \rho_E, \quad (2.14)$$

with fixed  $\rho_E \in \mathcal{L}_E$  when the evolution on the total system is unitary [11].

Effectively, this means that when initial correlation between system and environment exist, i.e. the initial state on the combined Hilbert space of system and environment cannot be written in the form of Eq. (2.14), then the mapping on the system Liouville space  $\mathcal{L}_S$  is not necessarily completely positive. This effect has been observed experimentally in the context of process tomography [42]. It is even conceivable for the resulting map to be nonlinear [11]. Note that these non-linear maps are not contradictory to central theorems of quantum information or even special relativity, cf. Sec. 2.1, as only under very specific circumstances such a violation of linearity can appear and the evolution of the total system is still linear [43].

In the remainder of this thesis we will mainly focus on completely positive, trace-preserving maps (CPTP maps) on Liouville space. We will call these maps “dynamical maps”<sup>9</sup>. The general form in which these dynamical maps can be represented is given by a theorem first formulated by Choi [12] which reads for mappings from  $\mathbb{C}^d$  onto itself as follows.

**Theorem 2.1** (Choi). *Let  $\Phi : \mathbb{C}^d \mapsto \mathbb{C}^d$  be a linear map.  $\Phi$  is completely positive if and only if it is  $d$ -positive. Furthermore,  $\Phi$  is completely positive if and only if  $\exists \{E_k\}_{k=1, \dots, d^2}$  with  $E_k : \mathbb{C}^d \mapsto \mathbb{C}^d$*

<sup>8</sup>We postpone the reasoning why unitary evolution on the total system is a reasonable assumption to Sec. 2.8.

<sup>9</sup>While in the literature the term “dynamical map” may sometimes refer to arbitrary linear transformations on Liouville space [44], we reserve it for CPTP maps.

linear such that  $\forall x \in \mathbb{C}^d$

$$\Phi(x) = \sum_k E_k x E_k^\dagger. \quad (2.15)$$

Choi's theorem is the finite-dimensional version of a more general result on completely positive operators on  $C^*$  algebras called the Stinespring factorisation theorem [45]. The operators  $E_k$  in Eq. (2.15) are usually called Kraus operators. It can easily be seen that  $\Phi$  is trace-preserving if and only if

$$\sum_k E_k^\dagger E_k = \mathbb{1}_d. \quad (2.16)$$

More generally, a quantum operation is defined as a completely positive map fulfilling only  $\sum_k E_k^\dagger E_k \leq \mathbb{1}_d$  which is shorthand notation for saying that  $\sum_k E_k^\dagger E_k$  is a Hermitian operator whose eigenvalues are all less or equal 1 [6]. With respect to the nomenclature employed in this thesis, a dynamical map is a quantum operation that fulfils a normalisation according to Eq. (2.16).

There exists no bijection between CPTP maps and a corresponding set of Kraus operators. However, it can be proven that two dynamical maps  $\mathcal{D}, \mathcal{D}'$  from  $\mathbb{C}^d$  onto itself, with Kraus operator sets  $\{E_k\}, \{E'_k\}$  such that<sup>10</sup>  $|\{E_k\}| = |\{E'_k\}| = m$ , are equal if and only if there exists a unitary matrix  $U \in \mathbb{C}^{m \times m}$  with matrix elements  $u_{kl}$  such that  $E_k = \sum_l u_{kl} E'_l$  [6].

This freedom in the choice of Kraus operators can be exploited in terms of obtaining an orthogonal set  $\{\bar{E}_k\}$  such that  $\forall \rho \in \mathbb{C}^d$  [46]

$$\mathcal{D}(\rho) = \sum_k \bar{E}_k \rho \bar{E}_k^\dagger, \quad \sum_k \bar{E}_k^\dagger \bar{E}_k = \mathbb{1}_d. \quad (2.17)$$

A special kind of dynamical maps are unital dynamical maps which means that  $\mathcal{D}(\mathbb{1}_d) = \mathbb{1}_d$ . It is easy to see that  $\mathcal{D}$  is unital if and only if

$$\sum_k E_k E_k^\dagger = \mathbb{1}_d. \quad (2.18)$$

## 2.7 The Choi-Jamiołkowski Isomorphism

An arbitrary linear operator  $L : \mathbb{C}^d \mapsto \mathbb{C}^d$  can be identified with a vector in the space  $\mathbb{C}^d \otimes \mathbb{C}^d$  due to the isomorphism  $L(\mathbb{C}^d, \mathbb{C}^d) \cong \mathbb{C}^d \otimes \mathbb{C}^d$ . This idea leads to an especially convenient isomorphism between linear operators on a Liouville space and density matrices in another Liouville space, the Choi-Jamiołkowski isomorphism, sometimes also called channel-state isomorphism [12, 14].

**Definition 2.2** (Choi-Jamiołkowski isomorphism). Let  $\mathcal{H}$  be a finite-dimensional Hilbert space with  $\dim \mathcal{H} = d$  and let  $L(\mathcal{L}_{\mathcal{H}})$  the Hilbert space of linear operators on the corresponding Liouville space. Let  $\{|\psi_i\rangle\}$  be an orthonormal basis<sup>11</sup> of  $\mathcal{H}$  and define the unnormalised state  $|\phi\rangle = \sum_i |\psi_i\rangle \otimes |\psi_i\rangle$  as an element of the bipartite Hilbert space  $\mathcal{H} \otimes \mathcal{H} \cong \mathcal{L}_{\mathcal{H}}$ . The map  $\Lambda : L(\mathcal{L}_{\mathcal{H}}) \mapsto \mathcal{L}_{\mathcal{H}} \otimes \mathcal{L}_{\mathcal{H}}$  with

$$\Lambda(X) = (\mathbb{1}_{\mathcal{L}_{\mathcal{H}}} \otimes X) (|\phi\rangle \langle \phi|) = \sum_{ij} |\psi_i\rangle \langle \psi_j| \otimes X(|\psi_i\rangle \langle \psi_j|) \quad (2.19)$$

<sup>10</sup>This equality is without loss of generality. If the sets are unequal, one can pad the set with lower cardinality with zero operators until they match in size.

<sup>11</sup>Usually, this basis is chosen to be the canonical basis which motivates speaking of *the* Choi-Jamiołkowski isomorphism and *the* Choi matrix.

is called Choi-Jamiołkowski isomorphism.

Since  $\mathcal{L}_{\mathcal{H}} \otimes \mathcal{L}_{\mathcal{H}} \cong \mathcal{L}_{\mathcal{H} \otimes \mathcal{H}}$ , the Choi-Jamiołkowski isomorphism maps an operator on  $\mathcal{L}_{\mathcal{H}}$  to a state in the Liouville space corresponding to the bipartite extended Hilbert space  $\mathcal{H} \otimes \mathcal{H}$ . If one calculates the matrix elements of  $\mathcal{C}(X)$  in the orthonormal basis  $\{|\psi_i\rangle\langle\psi_j|\}_{i,j=1,\dots,d}$  one obtains the so-called Choi matrix<sup>12</sup> [46, 47]. The Choi matrix is most conveniently represented by associating the single index  $\alpha$  of an operator  $\tau_\alpha = |\psi_k\rangle\langle\psi_i|$  to the ordered pair  $(k, i)$ . Analogously, one can define  $\tau_\beta = |\psi_l\rangle\langle\psi_j|$ . Then, one obtains the following expression for the Choi matrix  $\Lambda$  [48],

$$\begin{aligned}\Lambda_{\alpha\beta} &= \langle\psi_k|X(|\psi_i\rangle\langle\psi_j|)|\psi_l\rangle \\ X &= \sum_{\alpha\beta} \Lambda_{\alpha\beta} \tau_\alpha \rho \tau_\beta^\dagger.\end{aligned}\tag{2.20}$$

While the Choi-Jamiołkowski isomorphism is an isomorphism between linear operators and bipartite states in the extended Liouville space, it is not an isomorphism between dynamical maps and density matrices (as elements of  $\mathcal{L}_{\mathcal{H} \otimes \mathcal{H}}$ ). This is because surjectivity of this mapping is violated, specifically note that  $\forall X \in L(\mathcal{L}_{\mathcal{H}}) : \text{Tr}_B(\Lambda(X)) = \mathbb{1}_{\mathcal{H}}$  where  $\text{Tr}_B$  is the partial trace over the second Liouville space of the bipartite Liouville space [49]. Calling the Choi-Jamiołkowski isomorphism a channel-state isomorphism is consequently problematic. However,  $\mathcal{C}$  is a linear injection on the space of dynamical maps, i.e. the image is still unique. Furthermore, for any  $X \in L(\mathcal{L}_{\mathcal{H}})$  if  $X$  is Hermiticity preserving then  $\Lambda(X)$  is hermitian. In addition,  $X$  is completely positive if and only if  $\Lambda(X)$  is positive [49]. This allows to identify properties of the mapping with properties of a density matrix which is usually much more convenient.

## 2.8 Unitary Dynamical Maps (UDMs)

What characterises dynamical maps that correspond to the evolution of an isolated<sup>13</sup> system? A canonical assumption for the evolution of an isolated system is that it is reversible which implies that information cannot be lost during the evolution. Clearly, information also cannot be created by evolution in an isolated system. Since entropy is a measure for information, this motivates the notion that isolated quantum systems evolve by linear, entropy-preserving transformations. This might seem like a strong assumption, specifically in terms of the Second Law of Thermodynamics. However, note that the Second Law describes macroscopic systems in which entropy is conserved for reversible processes. Classical thermodynamics still predicts increases in entropy even for isolated systems, for example when looking at an ideal gas in a box which is initially confined to exactly half of the box's volume. Nevertheless, one has to be careful since different notions of entropy are considered in this context. Notably, the classical Shannon entropy is linear (extensive) while the quantum von Neumann entropy is strongly sublinear [6]. For a more in depth analysis of classical

<sup>12</sup>It is important to note, that the Choi matrix  $\Lambda$  is usually not normalised in terms of having trace 1, the relation  $\text{Tr}[\Lambda] = d$  rather holds [46]. In the following, when we want to interpret the image of the Choi-Jamiołkowski isomorphism as a density matrix, we will imply the normalised matrix  $\frac{\Lambda}{d}$ .

<sup>13</sup>We will use in this thesis the term “isolated quantum system” to refer to what in the literature is usually called “closed quantum system”. This is to differentiate between quantum systems which truly experience no perturbation and those quantum systems which are steered by e.g. an outside laser field while still allowing a description in Hilbert space, hence admitting energy to flow in and out of the system. This distinction is also quite common in the field of thermodynamics [50]. In particular, these notions will become important in Sec. 5 when we turn to the subject of quantum dynamics and control. In this context, isolated systems are described in Hilbert space with an evolution induced by time-independent generators, whereas closed systems allow for time-dependent generators.

vs. quantum entropy see for example Ref. [51].

In Ref. [52] it was shown that a linear transformation on  $\mathcal{L}_{\mathcal{H}}$  is entropy-preserving if and only if it is unitary<sup>14</sup>. As a consequence, the evolution of isolated quantum systems should be described by unitary transformations. The fact that unitary transformations preserve information elucidates their pivotal importance for purposes of quantum information processing.

This immediately poses the question whether the Kraus decomposition for unitary dynamical maps (UDMs) can be written in a specific form. Indeed, it can be shown that a dynamical map  $\mathcal{D}$  is unitary if and only if it can be written as

$$\mathcal{D}(\rho) = U\rho U^\dagger, \quad (2.21)$$

for unitary  $U$ . For an explicit proof of this fact, see Appendix A.1.

We will consider now a finite-dimensional Hilbert space  $\mathcal{H}$  with  $d \equiv \dim(\mathcal{H})$ . By Eq. (2.21), we can identify any finite-dimensional unitary dynamical map on  $\mathcal{L}_{\mathcal{H}}$  with a unitary operator  $U$  on  $\mathcal{H}$  and hence with a unitary matrix  $U \in \mathbb{C}^{d \times d}$ . To examine the structure of the set of UDMs, we consider two unitary dynamical maps  $\mathcal{D}_1$ , with corresponding unitary Kraus operator  $U_1$ , and  $\mathcal{D}_2$ , with unitary Kraus operator  $U_2$ . Their concatenation is then given by  $\mathcal{D}_1\mathcal{D}_2$  and can be described by a single unitary Kraus operator  $U_1U_2$  since

$$\forall \rho \in \mathcal{L}_{\mathcal{H}} : (\mathcal{D}_1\mathcal{D}_2)(\rho) = \mathcal{D}_1(\mathcal{D}_2(\rho)) = U_1U_2\rho U_2^\dagger U_1^\dagger = U_1U_2\rho(U_1U_2)^\dagger. \quad (2.22)$$

This motivates to speak of a group of unitary dynamical maps and characterise them via the mapping given by Eq. (2.21) with the group of unitary transformations. However a proper identification of a UDM with a unitary matrix is only possible if this mapping is an isomorphism. We will now briefly motivate which is the proper isomorphism that has to be employed in this context.

The identification of concatenation with the group operation has been illustrated in Eq. (2.22). As pointed out in Sec. 2.6, the mapping between UDMs and the corresponding unitary Kraus operator is up to a complex number with modulus one (an element of  $U(1)$ ) on this Kraus operator. This equivalence is consequently described by the projective unitary group,  $PU(d)$ . It is defined as the quotient of the unitary group  $U(d)$  by  $U(1)$ . Elements of  $PU(d)$  can be interpreted as equivalence classes of elements of  $U(d)$  with respect to the scalar multiplication of a complex number with absolute value one<sup>15</sup>. By Eq. (2.21) any unitary dynamical map can be written  $\forall \rho \in \mathcal{L}_{\mathcal{H}}$  as  $\mathcal{D}(\rho) = U\rho U^\dagger$ . As discussed in Sec. 2.6,  $U$  is uniquely defined only up to a complex factor  $|z| = 1$ . Consequently, using the equivalence relation  $U \sim \tilde{U}$  if  $\exists \lambda \in \mathbb{C}, |\lambda| = 1 : \lambda U = \tilde{U}$ , there is a bijective mapping between a UDM and an element of the corresponding equivalence class. By definition, this space of equivalence classes is equal to the projective unitary group  $PU(d)$ . Since  $PU(d)$  is a group under multiplication, it can be directly associated to concatenation of the corresponding dynamical maps by Eq. (2.22). We can therefore conclude, that the mapping of a UDM to an element of  $PU(d)$ , representing its single Kraus operator, is an isomorphism. As a consequence, unitary dynamical maps in Liouville

<sup>14</sup>More precisely, it is even enough to demand continuity of the transformation and probabilistic linearity from which linearity of the transformation will follow. Alternatively, one can also show that any linear map that preserves entanglement of arbitrary decompositions of  $\mathcal{H}$  must be unitary [52].

<sup>15</sup>The group  $PU(d)$  is isomorphic to the group  $SU(d)$ . These are just two equivalent ways to account for the indefiniteness of the global phase in the transformation by either an equivalence class (in the  $PU(d)$  case) or by identifying the transformation with a special representative corresponding to determinant equal to 1 (in the  $SU(d)$  case). With this in mind it is evident that the projective special unitary group  $PSU(d)$ , which is defined analogously to  $SU(d)$  with respect to  $U(d)$ , is identical to  $PU(d)$ .

space can be equivalently described by elements of the projective unitary group.

### 3 Minimal Characterisation and Identification of UDMs

The core paradigm of quantum computation is the encoding of information in the state of a quantum system [6]. Manipulation or communication of this information, represented by unitary dynamical maps, then allows to perform a variety of tasks more efficiently than any classical computer ever would be able to [6]. However, the full characterisation of the information stored in a quantum system is a task that scales exponentially with the number of basic information carriers, in the simplest case represented by two-level systems called qubits in this context. While this exponential scaling represents on the one hand a powerful resource for quantum computation, it poses on the other hand a great experimental challenge. The experimental task of certifying that a quantum device manipulates arbitrary states in a desired way proves itself to be even more complex since it requires to show that for arbitrary input states, the corresponding output states are of the desired form. This motivates the search for the conditions on a minimal set of input states that enables the characterisation of unitary dynamical maps.

We will begin this section with a short introduction to the problem of exponential scaling, in particular we will illustrate why it is a fundamental property of quantum information carriers. We will then proceed to derive a powerful algebraic framework that allows to assess whether a set of states can differentiate between any two arbitrary UDMs. Specifically, we will determine what is the minimal amount of states in Liouville space that can perform this task and what are the central requirements such a minimal set of states has to fulfil. We will expand on these results by showing that the same set of states can also be used to answer the question whether a dynamical map is unitary in the first place. Combining these results we will be able to obtain the minimal requirements on a set of states to identify and characterise unitary quantum operations.

Several of the results presented in this section have been published in Ref. [53].

### 3.1 Exponential Scaling

Any pure state can be uniquely characterised by a measurement of a CSCO, cf. Sec. 2.4. It can be represented as an element of a Hilbert space  $\mathcal{H}$  with  $d \equiv \dim \mathcal{H}$  representing the amount of different sets of values one can obtain via measurement of the CSCO. In quantum information such a system is called a qudit. If  $d = 2$  the term qubit is employed, while for  $d = 3$  one speaks of a qutrit. If  $d$  is a prime  $p$ , the word qupit is commonly used to emphasise this fact.

In classical computation the fundamental information carrier is a bit, usually a transistor that can be in two voltage states representing 0 (low voltage), respectively 1 (high voltage). Analogously, the most fundamental information carrier in quantum information is the qubit. An arbitrary (pure) quantum state of a qubit can be written as

$$|\psi\rangle = \cos(\theta) |0\rangle + \sin(\theta) e^{i\varphi} |1\rangle, \quad \theta \in [0, \pi], \varphi \in [0, 2\pi]. \quad (3.1)$$

Naively one might assume, that an infinite amount of information can be encoded into such a qubit since the possible values the two angles  $\theta$  and  $\varphi$  can take are uncountably infinite. However, a readout of this information must be performed by a classical measurement of an observable, cf. Sec. 2.3. Any observable in the two-dimensional Hilbert space corresponding to a qubit can at most have two non-degenerate eigenspaces, hence only two possible outputs.

Let us assume Alice sends a qubit  $|\psi\rangle$  to Bob with the goal to communicate some information. If Alice tells Bob to measure with an operator for which  $|\psi\rangle$  is an eigenstate, Bob can acquire the information that either  $|\psi\rangle$  is in the eigenstate corresponding to  $|0\rangle$  or  $|1\rangle$ . This is the only sensible way to communicate information such that no statistical considerations come into play -  $|\psi\rangle$  must be pure and it must be an eigenstate corresponding to some fixed CSCO, i.e. it must not be an incoherent superposition or coherent superposition of eigenstates to the CSCO. This becomes especially apparent if Bob measures with an operator to which  $|\psi\rangle$  is not an eigenstate. Each measurement by Bob now only leads with a certain, non-unity likelihood to a result corresponding to either of the two eigenvalues. Bob is now, with only a single measurement, unable to retrieve any concrete information about the qubit due to the statistical nature of measurements. If he were to repeat the measurement on identical copies of the qudit, he could start to make statistical statements on the state. Nevertheless, it should be emphasised that he cannot make a statement about the qudit with absolute confidence other than that it is not an eigenstate to the observable he measured once he obtained two different measurement results.

More formally, it can be shown that an isolated system of  $n$  qubits cannot transmit more than  $n$  bits of classical information, which follows immediately from the so-called Holevo bound [6]. The Holevo bound shows, that even though theoretically a single qudit can hold an uncountable amount of information, practically it can only transmit the same amount of information as a classical bit. This immediately raises a question about the benefit in using quantum systems if they are only as powerful as classical systems. However, the Holevo bound only concerns isolated systems. By using ancillary qubits one can increase the capacity of a quantum channel. In the above discussion, if Alice and Bob both possess a single qubit of a two-qubit entangled state it is actually possible for Alice to transmit two classical bits of information by manipulating her qubit and sending it to Bob. This is called superdense coding [54]. Generally speaking, it is the fact that composite quantum systems can exhibit entanglement that allows them to break the computational and informational boundaries of

classical systems. If one wants to exploit the resource of quantumness, usage of composite, entangled quantum systems is consequently imperative.

Manufacturing a quantum device to process or communicate one or two bits of classical information is comparatively simple. However, the regime where quantum information devices truly become superior to classical devices is entered only when many qubits are combined. Furthermore, performing fault-tolerant quantum computation requires usually ancillary qubits and it is necessary to assert that the noise does not scale unfavourably with the corresponding increase in system size [55]. The process of adding computationally “atomic” structures on top of an existing architecture is called scaling. One of the most important differences between classical and quantum systems lies in their scaling behaviour.

If we consider a single classical bit, it can be either in the state 0 or 1. This means we can describe the state by a single number  $\{a\}$  with either  $a = 0$  or  $a = 1$ . If we scale this to a  $n$ -bit system, description of an arbitrary state of this system simply amounts to assigning to each of the  $n$  bits either the number 0 or 1. As a result, the total state of the system is described by the set  $\{a_i\}_{i=1,\dots,n}$  where  $a_i$  is the state of the  $i$ -th bit. This represents a linear scaling, since each additional bit only requires adding a single number to the set.

This linear scaling breaks down when quantum systems are considered. According to Eq. (3.1) the (pure) state of a qubit can be described by a set of two angles  $\{\theta, \varphi\}$ . This corresponds to the real dimensionality  $d = 2$  of the qubit’s projective Hilbert space. If quantum systems were to scale linearly, then a two-qubit system could be described by a set of four angles  $\{\theta_1, \varphi_1, \theta_2, \varphi_2\}$  corresponding to a real dimension of 4. However, the projective Hilbert space of the two-qubit Hilbert space has a real dimension of 6 due to the tensor product structure of composite quantum systems, cf. Sec. 2.2. More generally, the number of real parameters to describe the pure state is  $2 \cdot 2^n - 2$  for an  $n$ -qubit Hilbert space<sup>16</sup>, which indicates that quantum systems scale exponentially in their degrees of freedom. In fact, the naive approach to just add up the descriptions of the individual qudits only allows to describe separable states. Once again, the additional quantum resource of entanglement leads to a remarkable differences in the behaviour of quantum systems compared to classical systems.

As a conclusion, the increased power of qubits comes at a price: an increased difficulty in the characterisation of quantum systems. Due to the Choi-Jamiołkowski isomorphism this exponential scaling in the description of states immediately translates to an exponential scaling in the description of dynamical maps. To keep the description feasible it is consequently of great importance to find minimal characterisations of unitary (i.e. information preserving) dynamical maps. We will discuss various approaches to this in Sec. 3.4. In the following we will focus on the specific question on what is the minimal input of density matrices to uniquely identify the unitary matrix corresponding to a unitary dynamical map in terms of their action on some set of density matrices.

## 3.2 Unitary Characterisation in Liouville Space

Since unitary dynamical maps on Liouville space can be identified with unitary operators on Hilbert space, cf. Sec. 2.8, it is immediately clear that a unitary dynamical map can be uniquely characterised via its action on an orthonormal basis on Hilbert space. However, while Eq. (2.21) yields an isomorphism from the space of CPTP maps to the space of (projective) unitary operators on the

---

<sup>16</sup>A  $n$ -qubit Hilbert space is isomorphic to  $\mathbb{C}^{2^n}$ . Going to the corresponding projective Hilbert space reduces the real dimensionality by 2 due to the irrelevance of the global phase and the normalisation condition.

underlying Hilbert space, from a physical perspective it is rather relevant how we can characterise such a map by its action on states. After all, we can only indirectly access information of a dynamical map by performing measurements on states that underwent the action of the corresponding quantum channel. As mentioned previously, if we know the image of an orthonormal basis of Hilbert space vectors, we can uniquely characterise the corresponding unitary dynamical map. However, the image of the corresponding rank 1 projector density matrices is not enough to uniquely characterise the unitary dynamical map.

We will illustrate this somewhat surprising observation by an example. Let  $\{|\psi_i\rangle\}_{i=1,\dots,d}$  be an orthonormal basis of Hilbert space and  $\mathcal{P} = \{P_i\}_{i=1,\dots,d}$  the corresponding set of rank 1 projectors on the basis states. We consider a unitary dynamical map given by the unitary

$$U = \sum_i e^{i\varphi_i} |\psi_i\rangle \langle\psi_i|. \quad (3.2)$$

As long as the dimension  $d$  of the Hilbert space is greater than 1 the set of unitaries that can be written as in Eq. (3.2) cannot be identified with a single element of  $\text{PU}(d)$ . The corresponding UDMs,  $\mathcal{D}_U$ , map the set  $\mathcal{P}$  onto itself independently on the parameters  $\{\varphi_i\}_{i=1,\dots,d}$  since

$$\mathcal{D}_U(P_i) = UP_iU^\dagger = e^{i\varphi_i} P_i e^{-i\varphi_i} = P_i,$$

which implies that all UDMs derived from unitaries of the form of Eq. (3.2) are not differentiable by just considering the action on the set  $\mathcal{P}$ .

We want to point out that this issue somewhat illuminates why the density matrix picture can be regarded as more appropriate from a practical perspective, even in the absence of environmental effects. This is because the naive unitary characterisation in Hilbert space requires to probe a quantum system with a sequence of pure states whose individual global phases are locked and well-known in each individual experiment. This is unrealistic, since there is no way to prepare a pure state with a well-defined phase due to no measurement being able to access this phase. This was the motivation behind the introduction of projective Hilbert spaces, cf. Sec 2.2. Note that the density matrix formalism automatically takes the inaccessibility of the global phase of a quantum state into account, cf. Sec. 2.4. For this reason, it is necessary to probe in at least one experiment the behaviour of relative phases between the states of an orthonormal basis in addition to considering the mapping on the orthonormal basis itself<sup>17</sup>. This notion will be incorporated in the concept of “total rotation” that we will introduce later.

To find the specific requirements for the characterisation of unitary dynamical maps in terms of their action on elements of Liouville space, we need to introduce some definitions first. In the following we will identify elements of Liouville space with matrices in  $\mathbb{C}^{d \times d}$  with  $d$  being the dimension of the underlying Hilbert space.

**Definition 3.1** (Unitary Differentiating Sets). Let  $\{M_i\}$  be a set of matrices in  $\mathbb{C}^{d \times d}$ . We call this set unitary differentiating if it is possible to uniquely identify the matrix  $U \in \text{PU}(d)$  corresponding

---

<sup>17</sup>Alternatively one might employ an ancilla system to compare the phases of states in the primary system to. However, this would increase the dimensionality of the problem, in particular by requiring to prepare pure states of the composite system and performing measurements taking into account both the state of the primary system and the ancilla. Since we will show that solving the problem of identifying the proper phases consists in probing the primary system with a single additional state (independent on the system’s dimension), using an ancilla does not appear to be the best approach.

to a unitary dynamical map by the image of these matrices under the dynamical map, i.e. a set  $\{M_i\}$  is unitary differentiating if the unitary dynamical evolution map  $\Delta_{\{M_i\}}$  that maps  $U$  to the set  $\{M_i^{(U)}\}$  by  $M_i^{(U)} = UM_iU^\dagger$  is injective.

What characterises such a set of matrices to be unitary differentiating? To answer this question it is useful to introduce the concept of commutant spaces.

**Definition 3.2** (Commutant Space). Let  $M \in \mathbb{C}^{d \times d}$  and  $S$  be a set of elements of  $\mathbb{C}^{d \times d}$ . We call the set of operators

$$K_S(M) = \{S_i \in S \mid [S_i, M] = 0\} \quad (3.3)$$

the commutant space of  $M$  in  $S$ . The commutant space for a set  $\mathcal{M} = \{M_i\}$  in  $S$  is defined as

$$K_S(\mathcal{M}) = \bigcap_i K_S(M_i) . \quad (3.4)$$

With these definitions we can formulate our first main result about characterisation of UDMs in Liouville space.

**Theorem 3.3.** *A set of matrices  $\mathcal{M} = \{M_i\}$  with  $M_i \in \mathbb{C}^{d \times d}$  is unitary differentiating if and only if its commutant space in  $\text{PU}(d)$ ,  $K_{\text{PU}(d)}(\mathcal{M})$ , contains only the unit matrix  $\mathbb{1}_d$ .*

*Proof.* By Definition 3.1 we have to prove the injectivity of the map  $\Delta_{\{M_i\}}$  which maps any  $U \in \text{PU}(d)$  to the set of matrices  $\{M_i^{(U)}\}$ , i.e.  $\forall i : M_i^{(U)} = M_i^{(V)} \iff U = V$ . We first of all prove that this condition is equivalent to  $\forall i : M_i^{(U)} = M_i \iff U = \mathbb{1}_d$ .

Assuming  $\forall U, V \in \text{PU}(d)$  the validity of  $\forall i : M_i^{(U)} = M_i^{(V)} \iff U = V$  choose  $V = \mathbb{1}_d$ . Then  $M_i^{(V)} = M_i$  and the equivalence follows immediately.

Conversely, assume  $\forall i : M_i^{(U)} = M_i \iff U = \mathbb{1}_d$ . For arbitrary  $V, W \in \text{PU}(d)$  we set  $U = V^{-1}W = V^\dagger W$  which is possible due to  $\text{PU}(d)$  being a group and  $V^{-1} = V^\dagger$  since  $V$  is unitary. Then we know that

$$\begin{aligned} \forall i : M_i^{(V^\dagger W)} &= M_i \\ \iff \forall i : V^\dagger W M_i W^\dagger V &= M_i \\ \iff \forall i : W M_i W^\dagger &= V M_i V^\dagger \\ \iff \forall i : M_i^{(W)} &= M_i^{(V)} \end{aligned}$$

using the fact that  $VV^\dagger = V^\dagger V = \mathbb{1}_d$ . By assumption  $\forall i : M_i^{(V^\dagger W)} = M_i \iff V^\dagger W = \mathbb{1}_d$ , but since the condition  $\forall i : M_i^{(V^\dagger W)} = M_i$ , as shown in the calculation above, is equivalent to  $\forall i : M_i^{(W)} = M_i^{(V)}$  and the relation  $V^\dagger W = \mathbb{1}_d \iff W = V$  always holds if  $V, W \in \text{PU}(d)$  (since  $\text{PU}(d)$  is a group the inverse is unique) this immediately leads to the desired result:  $\forall i : M_i^{(U)} = M_i^{(V)} \iff U = V$ .

Thus, proving the theorem can be reduced to showing that  $K_{\text{PU}(d)}(\{M_i\}) = \mathbb{1}_d$  if and only if

$\forall i : M_i^{(U)} = M_i \iff U = \mathbf{1}_d$ . This can be seen as follows,

$$\begin{aligned}
& \forall i : M_i^{(U)} = M_i \\
& \iff \forall i : UM_iU^\dagger = M_i \\
& \iff \forall i : UM_i = M_iU \\
& \iff \forall i : UM_i - M_iU = 0 \\
& \iff \forall i : [U, M_i] = 0 \\
& \stackrel{(*)}{\iff} U = \mathbf{1}_d.
\end{aligned}$$

Since the equivalence relation  $(*)$  is only true if and only if the commutant space of  $\{M_i\}$  in  $\text{PU}(d)$  only contains the unit matrix, this proves the theorem.  $\square$

Theorem 3.3 answers the question which sets of density matrices can differentiate arbitrary unitary dynamical maps. If we return to the example from the beginning of this subsection we see that all unitaries given by Eq. (3.2) actually lie in the commutant space of  $\mathcal{P}$  and this means that the commutant space is strictly larger than  $\{\mathbf{1}_d\}$ .

### 3.3 Minimal Characterisation of UDMs

We can employ the results of Sec. 3.2 in our search for minimal unitary differentiating sets of density matrices. The commutant space for a set of density matrices in  $\text{PU}(d)$  contains all density matrices that are not yet differentiable, which is why we will start by formulating statements about its dimensionality. Moreover, if the commutant space in  $\text{PU}(d)$  will contain only identity, it needs to have a dimensionality of zero. Conversely, if a commutant space in  $\text{PU}(d)$  has dimensionality zero it will necessarily consist of only the identity matrix. That is because the identity matrix commutes with arbitrary matrices. Note that all dimensionalities in the following are the real dimensionalities, indicated by a subscript  $\mathbb{R}$ , i.e. they correspond to the required number of real parameters to represent an arbitrary element of the corresponding set in an arbitrary representation (canonically, we will usually use a matrix representation of  $\text{PU}(d)$  with respect to some fixed basis).

**Proposition 3.4.** *The commutant space in  $\text{PU}(d)$  of an arbitrary, diagonalisable matrix  $M \in \mathbb{C}^{d \times d}$  can be represented as*

$$\mathcal{K}_{\text{PU}(d)}(M) \cong \left[ \bigotimes_i U(g_i) \right] / U(1), \quad (3.5)$$

where  $g_i$  is the multiplicity of the  $i$ -th eigenvalue of the matrix  $M$ . Its dimension is given by

$$\dim_{\mathbb{R}} [\mathcal{K}_{\text{PU}(d)}(M)] = \left( \sum_i g_i^2 \right) - 1. \quad (3.6)$$

Any  $U \in \mathcal{K}_{\text{PU}(d)}(M)$  admits the decomposition

$$U = \bigotimes_i \tilde{U}_{\mathcal{E}_i(M)}, \quad (3.7)$$

where  $\tilde{U}_{\mathcal{E}_i(M)}$  is an element of  $U(g_i)$  acting on the eigenspace  $\mathcal{E}_i(M)$ .

*Proof.* See Appendix A.2. □

From this proposition it immediately follows that one needs at least two density matrices to be unitary differentiating. Because density matrices are Hermitian, hence diagonalisable, this allows the application of the above proposition. The expression  $(\sum_i g_i^2) - 1$  is minimal if  $\forall i : g_i = 1$  and only for the trivial case  $d = 1$  this minimal value will be equal to zero. Furthermore, one can conclude that an optimal density matrix to keep the commutant space as low dimensional as possible needs to contain no degeneracies which leads to a remaining dimensionality of the space of unitaries that cannot be differentiated equal to  $d - 1$ . It is then clear that these remaining unitaries share a common eigenbasis with the density matrix since two diagonalisable matrices commute if and only if they are simultaneously diagonalisable.

Proposition 3.4 allows us to conclude that two density matrices are sufficient to be unitary differentiating. We give an explicit example of this remarkable observation, by presenting a recipe to reconstruct the unitary matrix corresponding to a unitary dynamical map from the image of two such matrices under a UDM  $\mathcal{D}_U$ . The procedure consists of two steps: First, one chooses a diagonal density matrices without degeneracies, i.e.  $\rho_B$  with entries  $(\rho_B)_{ij} = \lambda_i \delta_{ij}$  with  $\lambda_i \geq 0$  and  $\sum_i \lambda_i = 1$  where  $\forall i \neq j : \lambda_i \neq \lambda_j$ . Next, one considers a second density matrix  $\rho_P$  with matrix elements given by  $(\rho_P)_{ij} = \alpha_i \delta_{ij} + \frac{1}{d^2} \delta_{1,j} + \frac{1}{d^2} \delta_{i,1} - \frac{2}{d^2} \delta_{11}$  where  $\sum_i \alpha_i = 1, \forall i \neq j : \alpha_i \neq \alpha_j$  and  $\forall i : \frac{1}{d} - \frac{1}{d^2} < \alpha(i) < \frac{1}{d} + \frac{1}{d^2}$ . The proof that  $\rho_P$  is a proper density matrix can be found in Appendix A.3. Furthermore, the set  $\{\rho_B, \rho_P\}$  is unitary differentiating, as we will see shortly. We denote by  $\{|\psi_k\rangle\}$  the canonical basis, i.e. the basis in which  $\rho_B$  and  $\rho_P$  are given by the equations above, and by  $\{|\tilde{\psi}_k\rangle\}$  an eigenbasis of  $\mathcal{D}_U(\rho_B)$  such that  $\mathcal{D}_U(\rho_B)|\tilde{\psi}_k\rangle = \lambda_k |\tilde{\psi}_k\rangle$ . In particular, this means that the ordering of the basis  $\{|\tilde{\psi}_k\rangle\}$  is such that it coincides with the ordering of  $\{|\psi_k\rangle\}$  in terms of the ordered set  $\{\lambda_k\}$ <sup>18</sup>. The unitary matrix corresponding to the UDM  $\mathcal{D}_U$  can then be written as

$$U = \sum_k e^{i\varphi_k} |\tilde{\psi}_k\rangle \langle \psi_k|, \quad (3.8a)$$

$$\varphi_k = \arg \langle \tilde{\psi}_k | \mathcal{D}_U(\rho_P) | \tilde{\psi}_1 \rangle, \quad (3.8b)$$

when setting  $\varphi_1 \equiv 0$  in accordance with  $U$  corresponding to an element of  $\text{PU}(d)$  instead of  $\text{U}(d)$ . A proof of this fact and an extensive discussion of the reconstruction recipe can be found in Appendix A.3.

After having presented a specific example of a minimal unitary differentiating set, we now turn to fully characterise the required properties of a set of density matrices to be unitary differentiating. This is accomplished by looking at the projectors of the density matrices in a candidate set onto their eigenspaces. We introduce the following definitions to facilitate nomenclature.

**Definition 3.5** (Basis Complete and Totally Rotating Projectors). Let  $\mathcal{H}$  be a finite-dimensional Hilbert space. A set  $\mathcal{P} \equiv \{P_i\}$  of projectors from  $\mathcal{H}$  onto itself is called basis complete if there exists a subset  $\mathcal{A} \subset \mathcal{P}$  which contains exactly  $d = \dim \mathcal{H}$  one-dimensional orthogonal projectors. A one-dimensional projector  $P_{TR}$  is called totally rotated with respect to the set  $\mathcal{A}$  if  $\forall P \in \mathcal{A} : P_{TR}P \neq 0$ .

<sup>18</sup>This is possible since  $\mathcal{D}_U$  is unitary and leaves the spectrum of  $\rho_B$  invariant. Furthermore the ordering is unique due to the nondegeneracy of the spectrum.

A set  $\mathcal{P} \equiv \{P_i\}$  of projectors is called complete and totally rotating if it is basis complete and there exists a one-dimensional projector  $P_{TR} \in \mathcal{P}$  such that  $P_{TR}$  is totally rotated with respect to  $\mathcal{A}$ .

**Definition 3.6** (Basis Complete and Totally Rotating Density Matrices). Let  $\mathcal{H}$  be a finite-dimensional Hilbert space. A set of density matrices  $\{\rho_i\}$  with  $\rho_i \in \mathcal{L}_{\mathcal{H}}$  is called basis complete if the set of projectors onto the eigenspaces of the set  $\{\rho_i\}$  is basis complete. It is called complete and totally rotating if the set of projectors on the eigenspaces of the  $\{\rho_i\}$  is basis complete and totally rotating.

*Remark.* The concept of total rotation formalises the requirement to check the relative phases between an orthonormal basis of pure states such that unitaries like those in Eq. (3.2) can be differentiated.

These definitions allow us to formulate a useful criterion to determine whether a given set of density matrices is unitary differentiating, leading to our second main result about characterisation of UDMs in Liouville space.

**Theorem 3.7.** Let  $\mathcal{H}$  be a finite-dimensional Hilbert space. A set of density matrices  $\{\rho_i\}$  with  $\rho_i \in \mathcal{L}_{\mathcal{H}}$  is unitary differentiating if it is complete and totally rotating.

*Proof.* This theorem follows from combining Proposition A.8 (see Appendix A.5) with Theorem 3.3.  $\square$

It is easy to see now that the set  $\{\rho_B, \rho_P\}$  from above is unitary differentiating since  $\rho_B$  is basis complete by definition and we prove in Appendix A.3 that  $\rho_P$  is totally rotated with respect to  $\rho_B$ .

While the restriction to density matrices in the above analysis is imperative from a practical point of view, the properties of commutant spaces in  $\text{PU}(d)$  of arbitrary matrices can be of interest for numerical analysis. Proposition 3.4 can be generalised for this case as follows.

**Proposition 3.8.** *The dimension of the commutant space in  $\text{PU}(d)$  of an arbitrary matrix  $M \in \mathbb{C}^{d \times d}$  can be estimated as*

$$\dim_{\mathbb{R}} [\mathcal{K}_{\text{PU}(d)}(M)] \leq \left( \sum_i g_i^2 \right) - 1, \quad (3.9)$$

where  $g_i$  is the algebraic multiplicity of the  $i$ -th generalised eigenvalue of the matrix  $M$ .

*Proof.* See Appendix A.2.  $\square$

Although Eq. (3.9) only gives an upper bound to the dimensionality of the commutant space it is clear that non-diagonalisable matrices are strictly better suited for the task of differentiating unitaries. In fact, one can show that the commutant space in  $\text{PU}(d)$  of the matrix  $M$  with matrix entries  $(M)_{ij} = \delta_{i+1,j}$ , i.e.

$$M = \begin{pmatrix} 0 & 1 & 0 & 0 & 0 & 0 \\ 0 & 0 & 1 & 0 & 0 & 0 \\ 0 & 0 & 0 & 1 & 0 & 0 \\ 0 & 0 & 0 & \ddots & \vdots & \vdots \\ 0 & 0 & 0 & \cdots & 0 & 1 \\ 0 & 0 & 0 & \cdots & 0 & 0 \end{pmatrix}, \quad (3.10)$$

contains only the unit matrix. Consequently, the matrix  $M$  given in Eq. (3.10) is unitary differentiating by itself. This fact is explicitly proven in Appendix A.4. However, it is currently not known

how to reconstruct the unitary matrix corresponding to the unitary dynamical map from the image of  $M$ .

### 3.4 Efficient Identification of Unitarity for Dynamical Maps

The analysis in Sec. 3.3 considered the case of prior knowledge with respect to the unitarity of the dynamical map under consideration. In other words, it represents the specific problem that one knows that a quantum channel is unitary and one only wants to determine the specific unitary as efficiently as possible. This assumption is rather restrictive, which gives rise to the question how to most efficiently determine whether an arbitrary dynamical map is unitary from its action on a small set of density matrices.

The following theorem presents a set of equivalent criteria to decide whether a dynamical map is unitary and represents our third main result about characterisation of UDMs in Liouville space.

**Theorem 3.9.** *Let  $\mathcal{H}$  be a finite-dimensional Hilbert space with  $d = \dim(\mathcal{H})$  and  $\mathcal{D}$  be a dynamical map on  $\mathcal{L}_{\mathcal{H}}$ . The following statements are equivalent.*

1.  $\mathcal{D}$  is unitary.
2.  $\mathcal{D}$  maps a set  $\mathcal{P}$  of  $d$  one-dimensional orthogonal projectors onto a set of  $d$  one-dimensional orthogonal projectors as well as a totally rotated projector  $P_{TR}$  (with respect to  $\mathcal{P}$ ) onto a one-dimensional projector.
3.  $\mathcal{D}$  is unital and there exists a complete and totally rotating set of density matrices whose spectrum is invariant under  $\mathcal{D}$ .
4.  $\mathcal{D}$  is unital and there exists a complete and totally rotating set of density matrices  $\mathcal{R}$  such that  $\forall \rho \in \mathcal{R}; k = 1, 2, \dots, d: \text{Tr}(\rho^k) = \text{Tr}(\mathcal{D}(\rho)^k)$ .

*Proof.* See Appendix A.5. □

Combining this theorem with Theorem 3.7 we see that a complete and totally rotating set (combined with the totally mixed density matrix  $\mathbb{1}_d$  to check unitality of the dynamical map) can identify whether a dynamical map is unitary and also uniquely identify the specific unitary transformation. Note that the density matrices  $\rho_B$  and  $\rho_P$  defined in Sec. 3.3 are complete and totally rotating, cf. Appendix A.3. As a consequence, the set of input states  $\{\rho_B, \rho_P, \mathbb{1}_d\}$  can be employed to decide whether a dynamical map is unitary and also uniquely identify it in terms of a corresponding element of  $\text{PU}(d)$ . This represents an efficient, scalable way to determine a unitary dynamical map uniquely in terms of their action on density matrices. It is an open question whether the number of density matrices can be reduced to two as it was the case for characterisation of a unitary dynamical map with prior information about its unitarity.

There is one caveat to the results presented in this section. By using a complete and totally rotating set (enriched with the completely mixed state) one can answer the question “Is a dynamical map unitary?” with yes or no. However, if the answer is negative, it is usually desirable to obtain some measure of distance with respect to a certain target unitary. Ideally, one would like to obtain a distance measure that leads to a physical interpretation on how close an experimental implementation is to the target unitary channel. This is usually called certification. In the next section we will illustrate the consequences of the results about efficient unitary characterisation and identification from

Theorems 3.3, 3.7, and 3.9 with respect to efficient and practical certification of unitary dynamical maps.

## 4 Tomography and Process Certification

Practical tomography of arbitrary quantum operations is a central requirement to assert the successful implementation of a physical task. The tomography of general quantum states was first suggested by Vogel and Risken [56] with the theory of quantum process tomography being developed by Chuang and Nielsen [57] and Poyatos et al. [58]. Recently, several attempts to reduce the scaling in resources for tasks of tomography and certification have been attempted, among which Monte Carlo sampling techniques and randomised benchmarking should be mentioned in particular [59–65]. Additionally, prior information in the form of sparsity of the Choi matrix in a given basis can be exploited to reduce the required experimental effort, which is usually termed “compressed sensing” [61, 62, 66–68]. Efficient approaches have been tested experimentally by Steffen et al. [69] and Schmiegelow et al. [62, 70], albeit so far only for two- and three-qubit operations, without taking advantage of the protocols’ savings by stochastic sampling. A common feat of most of these approaches is a scaling in the required resources for gate certification that is independent of system size if Clifford operations with Pauli measurements are considered. Clifford gates facilitate fault-tolerant computation [71] and yield a universal set when augmented by the proper local phase gate [72]. They can be used to prepare entangled states and perform quantum teleportation even though their computing power is not stronger than classical, a fact that is summarised in the famous Gottesmann-Knill theorem [73].

In this section we will apply our mathematical results on characterisation and identification of unitary dynamical maps. They allow to formulate fidelities that only require knowledge of the action of a dynamical map on a small set of input states instead of a complete orthonormal basis to assert the implementation of a unitary gate. We discuss how these fidelities compare to the average gate fidelity and analyse how, dependent on the particular reduced set of input states, numerical and analytical bounds can be formulated. We then combine these reduced fidelities with Monte Carlo process certification [59, 60] to improve the scaling of the certification’s complexity. In addition, we will show that this reduced scaling can be retained even for determining the average fidelity exactly, the only caveat being the requirement of entangled input states. We will also extend the result of efficient certification of Clifford operations for multi-qubit systems to the multi-qupit case, i.e. when the building blocks of the quantum information device can have arbitrary prime dimensions. In this context, we will derive the result that for qupits the generalised Pauli operators represent an optimal set of measurement operators in the sense that it yields a scaling of  $\mathcal{O}(1)$  in unitary process certification for as many unitaries as possible. The set of efficiently characterisable unitaries will turn out to be the generalised Clifford group, in analogy to the qubit case.

The combination of reduced fidelity approaches with Monte Carlo sampling has been published in Ref. [74]. The extension of the results on efficient tomography for Clifford gates to qupit systems has been published in Ref. [75]. The result that generalised Pauli operators as a measurement basis represent the most convenient choice to efficiently characterise as many unitaries as possible has been published in Ref. [76].

## 4.1 Process Tomography of General Dynamical Maps

Engineering a quantum device such that it implements an algorithm by the manipulation of input states in a well-defined way lies at the heart of quantum computing. As shown in Sec. 2.6, the action of most such devices can be described by a dynamical map on a suitable Liouville space. Effectively, this means that most quantum devices can be associated to such a map. The restriction to dynamical maps hinges on the fact that the device is initially uncorrelated with its environment, cf. Sec. 2.6. Carteret et al. analysed how initial correlations between a system and its environment can influence the proper interpretation tomographic results [11]. They point out, that “[...] *raw tomographic data often yields nonpositive dynamical matrices, which are usually considered unphysical. A maximum-likelihood estimation or other such technique is used to convert the experimental data into a (positive) dynamical matrix. We see that this can be justified for characterizing actual high-fidelity implementations of ‘known’ gates. However, when [the initial correlations] cannot be considered ‘small’ a different template such as a difference form should be used to fit the data when attempting linear inversion process tomography.*”. Keeping this in mind, we will focus the following analysis on the case of systems that can be prepared in arbitrary uncorrelated states with their environment. This allows us to use the formalism of dynamical maps.

The following presentation is inspired by Refs. [6] and [46]. Let  $\mathcal{H}$  be a Hilbert space with  $d = \dim \mathcal{H}$  and  $\mathcal{D}$  be a dynamical map on  $\mathcal{L}_{\mathcal{H}}$ . Then  $\mathcal{D}$  can be written according to Eq. (2.15) as

$$\mathcal{D}(\rho) = \sum_k E_k \rho E_k^\dagger.$$

Let  $\{A_i\}$  be an orthonormal basis of  $\mathcal{L}_{\mathcal{H}}$ . We can then expand  $E_k = \sum_i e_{ki} A_i$  which allows us to write the dynamical map as

$$\mathcal{D}(\rho) = \sum_{ijk} A_i \rho A_j^\dagger e_{ki} e_{kj}^*.$$

One can now define a so-called process matrix (sometimes also called chi matrix)  $\chi \in \mathbb{C}^{d^2 \times d^2}$  with respect to the basis  $\{A_i\}$  and entries  $\chi_{ij} \equiv \sum_k e_{ki} e_{kj}^*$ . The dynamical map can then be written as [6]

$$\mathcal{D}(\rho) = \sum_{ij} \chi_{ij} A_i \rho A_j^\dagger. \quad (4.1)$$

By comparison with Eq. (2.20) one can observe that the process matrix is identical to the Choi matrix up to unitary transformation, hence it inherits Hermiticity, trace and positivity of the Choi matrix<sup>19</sup> [48]. In particular, the Choi matrix is the process matrix corresponding to the orthonormal basis  $\{|\psi_i\rangle\langle\psi_j|\}_{i,j=1,\dots,d}$  where  $\{|\psi_i\rangle\}$  is the computational basis of  $\mathcal{H}$ , cf. Sec. 2.7. Knowledge of the Choi matrix or, equivalently, a process matrix with respect to an arbitrary orthonormal basis of  $\mathcal{L}_{\mathcal{H}}$  hence allows to find a set of Kraus operators for a dynamical map.

How does one measure the process matrix? Either of the following two approaches is usually followed.

1. Couple the system on which tomography should be performed to another physical system, a so-called ancilla, which can be described by a Hilbert space of equal dimensionality. Prepare the

<sup>19</sup>Just like the Choi matrix, the process matrix is usually not normalised in terms of having trace 1, cf. Footnote 12.

bipartite system of primary system and ancilla in the pure state  $|\phi\rangle = \frac{1}{\sqrt{d}} \sum_i |\psi_i\rangle$  where  $\{|\psi_i\rangle\}$  is an orthonormal basis of  $\mathcal{H} \otimes \mathcal{H}$ . Apply the dynamical map to the primary system. Then one can measure the state of the composite system. As a result, one obtains a density matrix on the extended Hilbert space by the Choi-Jamiolkowski isomorphism which is a faithful description of the dynamical map, cf. Sec. 2.7. This allows to determine the Choi matrix/process matrix. For an example of this approach see e.g. Ref. [77].

2. Choose an orthonormal basis  $\{|\psi_i\rangle\}$  of  $\mathcal{H}$ . Define, for example, the states  $|\psi_{ij}^+\rangle = \frac{1}{\sqrt{2}} (|\psi_i\rangle + |\psi_j\rangle)$  and  $|\psi_{ij}^-\rangle = \frac{1}{\sqrt{2}} (|\psi_i\rangle + i|\psi_j\rangle)$ . Note now that [6]

$$\forall i, j : |\psi_i\rangle \langle \psi_j| = |\psi_{ij}^+\rangle \langle \psi_{ij}^+| + i |\psi_{ij}^-\rangle \langle \psi_{ij}^-| - \frac{1+i}{2} |\psi_i\rangle \langle \psi_i| - \frac{1+i}{2} |\psi_j\rangle \langle \psi_j|. \quad (4.2)$$

This means that the orthonormal basis  $\{|\psi_i\rangle \langle \psi_j|\}_{i,j}$  of  $\mathcal{L}_{\mathcal{H}}$  can be obtained by a linear combination of the pure states from the set  $\mathcal{B} = \mathcal{B}^0 \cup \mathcal{B}^+ \cup \mathcal{B}^-$  with  $\mathcal{B}^0 = \{|\psi_i\rangle \langle \psi_i|\}_{i=1,\dots,d}$  and  $\mathcal{B}^{\pm} = \{|\psi_{ij}^{\pm}\rangle \langle \psi_{ij}^{\pm}|\}_{i,j=1,\dots,d;i>j}$ . Since dynamical maps are linear,  $\mathcal{D}(|\psi_i\rangle \langle \psi_j|)$  can be deduced from the results of applying  $\mathcal{D}$  to all elements of  $\mathcal{B}$ . As a consequence, by applying the dynamical map to the  $d^2 = |\mathcal{B}|$  density matrices in  $\mathcal{B}$  one obtains  $\mathcal{D}(|\psi_i\rangle \langle \psi_j|)$  from which the Choi matrix/process matrix of the dynamical map immediately follows if a full measurement of a CSCO is performed. For an example of this approach see e.g. Ref. [78].

In summary, tomography on an arbitrary dynamical map can be performed by either state tomography on a single pure density matrix on the extended Liouville space  $\mathcal{L}_{\mathcal{H} \otimes \mathcal{H}}$  or by state tomography on  $d^2$  pure density matrices in  $\mathcal{L}_{\mathcal{H}}$ . As a result one obtains the Choi matrix or, equivalently, a process matrix which then can be used to obtain the Kraus operators of the dynamical map.

## 4.2 State Tomography of General Density Matrices

We want to briefly review the general idea of state tomography of a general density matrix since, as pointed out in Sec. 4.1, tomography of a quantum operation can be mapped onto the tomography of density matrices. For a detailed discussion of state tomography for a two-qubit system see e.g. Ref. [79].

A density matrix is a positive operator on a Hilbert space  $\mathcal{H}$  with trace 1. If  $\dim \mathcal{H} = d$  it can generally be parametrised by  $d^2 - 1$  parameters. This is because a general linear operator on  $\mathcal{H}$  has  $2d^2$  real parameters. Hermiticity of the density matrix represents  $d^2$  constraints and  $\text{Tr}[\rho] = 1$  represents another constraint. Note that positivity, as long as Hermiticity is fulfilled, is a constraint given by an inequality which does not reduce the degrees of freedom of a density matrix any further. From these observations it is clear that any density matrix can be written as

$$\rho = \frac{1}{d} \mathbb{1}_d + \sum_k \omega_k W_k, \quad (4.3)$$

with  $\{W_k\}_{k=1,\dots,d^2-1}$  being a set of orthonormal, traceless, Hermitian operators in  $L(\mathcal{H})$  and  $\forall k : \omega_k \in \mathbb{R}$ . The density matrix according to Eq. (4.3) is written in such a way, that it is Hermitian and has unit trace by construction, hence automatically fulfilling the constraints discussed above. Note

that the coefficients

$$\omega_k = \langle W_k, \rho \rangle_{\text{HS}} = \text{Tr} [W_k \rho] \quad (4.4)$$

will correspond to the expectation value of a measurement of the observable  $W_k$  on the state  $\rho$ . An example for such a set of traceless orthonormal operators is given by the set [80]<sup>20</sup>

$$u_{jk} = \frac{1}{\sqrt{2}} (|j\rangle \langle k| + |k\rangle \langle j|), \quad (4.5a)$$

$$v_{jk} = \frac{-i}{\sqrt{2}} (|j\rangle \langle k| - |k\rangle \langle j|), \quad (4.5b)$$

$$w_l = \frac{1}{\sqrt{l(l+1)}} \sum_{i=1}^l (|i\rangle \langle i| - |l+1\rangle \langle l+1|), \quad (4.5c)$$

for  $1 \leq j < k \leq d$  and  $1 \leq l \leq d-1$  and  $\{|i\rangle\}_{i=1, \dots, d}$  being an orthonormal basis of  $\mathcal{H}$ .

Generally, one wants to determine all coefficients  $\omega_k$  in Eq. 4.3 such that they do not deviate more than  $\epsilon$  from their actual value with probability greater than  $\delta$ . To establish these statistical bounds the well-known Chebyshev inequality is usually employed. It states that for a random variable  $Z$  with expectation value  $\mu$  and variance  $\sigma^2$ , the following relation is fulfilled  $\forall k > 0$ ,

$$\Pr [|Z - \mu| \geq k\sigma] \leq \frac{1}{k^2}. \quad (4.6)$$

Such statistical considerations are necessary due to the inherent statistical nature of the measurement process in quantum mechanics, cf. Sec 2.3. Any single measurement of the observable  $W_k$  on  $\rho$  will return a measurement result in the interval  $[-1, 1]$  due to the fact that the  $W_k$  are normalised<sup>21</sup>. Let  $\omega_{k_i}$  be the measurement result of the  $i$ -th repetition of the measurement of  $W_k$  on a copy of  $\rho$ . If one performs  $N$  repetitions of the measurement then by the central limit theorem,

$$\lim_{N \rightarrow \infty} \sum_{i=1}^N \frac{\omega_{k_i}}{N} = \text{Tr} [W_k \rho] = \omega_k, \quad (4.7)$$

and in particular

$$\text{Var} \left( \omega_k^{(N)} \right) = \frac{\text{Var} \left( \omega_k^{(1)} \right)}{N}, \quad (4.8)$$

where  $\omega_k^{(1)}$  represents the random variable according to a single measurement and  $\omega_k^{(N)}$  represents the random variable corresponding to the average of  $N$  measurements. We will choose  $\omega_k^{(N)}$  as the random variable to apply the Chebyshev inequality to.

Clearly,  $\forall N \in \mathbb{N}$ , the expectation value of  $\omega_k^{(N)}$  is equal to  $\omega_k$ . Note that due to  $\omega_k^{(1)} \in [-1, 1]$  one can estimate  $\text{Var} \left( \omega_k^{(1)} \right) \leq 1$  and hence  $\text{Var} \left( \omega_k^{(N)} \right) \leq \frac{1}{N}$ . It is important to note that by the statistical nature of the above analysis, non-systematic experimental errors are included in the above derivation since they just add to the variance of the individual measurements. Choosing the number

<sup>20</sup>Note that in Ref. [80] there is a mistake for  $w_l$  (it is not properly normalised), which has been amended here.

<sup>21</sup>By the Cauchy-Schwarz inequality,  $|\omega_k| = |\text{Tr} [W_k \rho]| = |\langle W_k, \rho \rangle_{\text{HS}}| \leq \langle W_k, W_k \rangle_{\text{HS}} \langle \rho, \rho \rangle_{\text{HS}} \leq \langle W_k, W_k \rangle_{\text{HS}} = 1$ .

of repetitions to be  $N = \frac{1}{\epsilon^2 \delta}$  one obtains  $\sigma = \epsilon \sqrt{\delta}$  and choosing  $k = \frac{1}{\sqrt{\delta}}$  in Eq. (4.6) leads to

$$\Pr \left[ \left| \omega_k^{(N)} - \omega_k \right| \geq \delta \right] \leq \epsilon, \quad (4.9)$$

as desired. The number of experiments to determine a single  $\omega_k$  is independent on the dimension  $d$ . Performing full tomography on an arbitrary density matrix implies determining all  $\omega_k$ . The complexity is consequently upper bounded by  $\frac{d^2-1}{\epsilon^2 \delta}$  for deviation  $\epsilon$  and confidence  $\delta$  in all degrees of freedom of the density matrix according to Eq. (4.9), i.e. the scaling is  $\mathcal{O}(d^2)$ . It immediately follows that the experimental complexity of tomography of an arbitrary dynamical map is upper bounded by  $\mathcal{O}(d^4)$ .

There is one caveat to the above discussion. There is no guarantee that the resulting matrix is positive since we only could include those constraints that can be written as equalities for Eq. (4.3). This problem extends to tomography of general dynamical maps, cf. Sec 4.1, and is usually amended by postprocessing of the experimental data in terms of finding the density matrix that is most likely to be consistent with the experimental results [81]. Nevertheless, one should keep in mind that not all quantum system evolutions can be described by a dynamical map, cf. the discussion in Sec. 2.6. The postprocessing can thus be interpreted as finding the closest dynamical map that is consistent with the experimental observations.

As discussed in Sec. 3.1 the exponential scaling of quantum systems results in the dimensionality  $d$  going up exponentially when adding subsystems to an existing architecture. For this reason, general process tomography very quickly reaches its limit in terms of experimental feasibility. For example, implementation of the Shor code, that aims to implement a fault-tolerant gate on a single qubit [6], requires well over a billion measurements in standard tomographic schemes. This motivates the search for techniques to reduce the scaling, in particular by adapting the tomography protocol to the specific needs. In the following subsections we will show that certification, i.e. the question how close a given density matrix/dynamical map is to a desired one, is generally much easier to answer than full tomography. Furthermore, as indicated by our findings in Sec. 3, a restriction to the certification of unitary dynamical maps instead of general dynamical maps results in a dramatic reduction of the required set of input states to characterise the map. Another important point is to consider the choice of measurement basis. While Eqs. (4.5) represent an orthonormal basis of the space of traceless Hermitian matrices it is not immediately clear whether this is a good choice with respect to efficient tomography/certification. We will discuss in the following subsection a particularly convenient measurement basis for the most fundamental form of a scalable quantum device, the multi-qubit system.

### 4.3 Qubit Systems and Pauli Matrices - Stabilisers and the Clifford Group

An orthogonal, Hermitian basis of a qubit Hilbert space is given by the Pauli matrices,

$$\begin{aligned} \sigma_0 = \mathbb{1}_2 &= \begin{pmatrix} 1 & 0 \\ 0 & 1 \end{pmatrix}, & \sigma_1 = \sigma_x &= \begin{pmatrix} 0 & 1 \\ 1 & 0 \end{pmatrix}, \\ \sigma_2 = \sigma_y &= \begin{pmatrix} 0 & -i \\ i & 0 \end{pmatrix}, & \sigma_3 = \sigma_z &= \begin{pmatrix} 1 & 0 \\ 0 & -1 \end{pmatrix}. \end{aligned} \quad (4.10)$$

Consequently, an orthogonal Hermitian basis of an  $n$ -qubit Hilbert space (with dimension  $d = 2^n$ ) is given by all possible tensor products of Pauli matrices on the individual Hilbert spaces, i.e.

$$\bar{\mathcal{P}} = \left\{ \bigotimes_{j=1}^n \sigma_{k_j}^{(j)} \mid \forall j : k_j \in \{0, 1, 2, 3\} \right\}, \quad (4.11)$$

which we will call the set of Pauli observables. We will prove in Sec. 4.10, that in terms of efficient certification of unitary dynamical maps the set of Pauli operators is an optimal measurement basis. The derivation necessitates the concepts of stabilisers and Clifford gates which we will briefly introduce in the following.

The set of Pauli observables can be partitioned into  $d + 1$  subsets of  $d$  commuting operators, this property is often called ‘‘maximally partitioning’’ [82]. The resulting sets  $\mathcal{W}_A$  of  $d$  orthogonal commuting operators form a CSCO and the eigenvectors constituting their joint eigenbasis  $\{|\psi_i^A\rangle\}_{i=1,\dots,d}$  are called stabiliser states [6, 83]. The set of stabiliser states of  $\mathcal{W}_A$  has the property that the expectation value of a measurement of some Pauli observable  $P$  vanishes on any of those stabiliser states unless  $P \in \mathcal{W}_A$ . Furthermore all eigenbases to the sets  $\mathcal{W}_A$  are mutually unbiased, i.e. if  $A \neq A'$  then [82, 84]

$$\forall i, j : \left| \langle \psi_i^A \mid \psi_j^{A'} \rangle \right| = \frac{1}{d}, \quad (4.12)$$

a crucial concept we will often refer to in this section.

Not only does the set of Pauli matrices form an orthogonal basis of operator space but it also admits a group structure under multiplication if one includes Pauli matrices obtained via scalar multiplication of  $\pm 1$  and  $\pm i$  to the set. More formally, the set

$$\mathcal{P} = \left\{ i^a \omega^b \bigotimes_{j=1}^n \sigma_{k_j}^{(j)} \mid a \in \{0, 1\}; b \in \{0, 1\}; \forall j : k_j \in \{0, 1, 2, 3\} \right\} \quad (4.13)$$

forms the so-called Pauli group. The set of Pauli observables  $\bar{\mathcal{P}}$  is a proper subset of  $\mathcal{P}$ . The normaliser of  $\mathcal{P}$  in  $U(d)$  is called the Clifford group [85], i.e. it is given by those unitaries  $U_C \in U(d)$  which fulfil

$$\forall P \in \mathcal{P} : U_C P U_C^\dagger \in \mathcal{P}. \quad (4.14)$$

Specifically, any unitary conjugation induced via an element of the Clifford group maps a Pauli observable to another Pauli observable modulo a scalar prefactor of modulus 1. Clifford operations can also be defined in terms of their action on stabiliser states. Notably, Clifford operations map joint eigenstates of a set  $\mathcal{W}_A$  onto joint eigenstates of a set  $\mathcal{W}_{A'}$  (with possibly  $A = A'$ ) [86, 87].

The reason why Clifford gates and stabiliser gates are of great importance with respect to efficient certification is illustrated by the following theorem from Gottesmann and Knill [73]. The term ‘‘canonical basis’’ denotes the mutual eigenbasis of all Pauli observables that consist of only  $\sigma_0$  and  $\sigma_z$ .

**Theorem 4.1** (Gottesmann-Knill). *Consider a  $n$ -qubit system. The result of a measurement of a Pauli observable on a state obtained after the application of an arbitrary amount of Clifford operations to a state in the computational basis can be efficiently simulated on a classical computer.*

In this context, the notion of “efficient simulation” refers to a classical computational complexity that is at most polynomial in the number of qubits. As mentioned above, any stabiliser state can be obtained by applying a suitable Clifford operation to a state in the computational basis. The Gottesmann-Knill theorem shows a remarkable property of certain quantum operations and states in that they can be described in a way that does not scale exponentially in the number of qubits. For this reason these states/operations are of particular interest in quantum state/process certification and we will show in Sec. 4.7 that one can formulate certification protocols for these states/operations that do not scale with system size.

#### 4.4 Distance Measures and Fidelities

In order to certify an experimental realisation of a state or process with respect to some target, it is first of all necessary to define a distance measure, i.e. how far away is an implementation to the ideal case, or a fidelity, i.e. how well does an implementation correspond to the ideal case. There are three<sup>22</sup> central properties any such distance measure  $d(x, y)$  should fulfil with respect to two objects  $x$  and  $y$  from some set  $\mathcal{A}$ .

1.  $\forall x, y \in \mathcal{A} : d(x, y) \in \mathbb{R}, d(x, y) \geq 0$
2.  $\forall x, y \in \mathcal{A} : d(x, y) = d(y, x)$
3.  $d(x, y) = 0 \iff x = y$

Instead of a distance measure it is common to formulate fidelities  $F(x, y)$  instead. A fidelity does not denote how far away two object are, but it rather describes the closeness of two objects. Correspondingly, the properties above should be reformulated in following way<sup>23</sup>.

1.  $\forall x, y \in \mathcal{A} : F(x, y) \in \mathbb{R}, F(x, y) \geq 0$
2.  $\forall x, y \in \mathcal{A} : F(x, y) = F(y, x)$
3.  $F(x, y) = \sup_{x, y \in \mathcal{A}} F(x, y) \iff x = y$

In analogy to the situation in Hilbert space, one might naively employ the overlap by the Hilbert-Schmidt scalar product for a fidelity measure. Let  $\rho_C$  be the density matrix that is supposed to be certified as being equivalent to an ideal state  $\rho_0$ . Then this naive fidelity would read

$$F_X = \text{Tr}(\rho_C \rho_0) . \quad (4.15)$$

It turns out that this fidelity does not fulfil condition 3. As a simple counterexample, consider  $\rho_0 = \rho_C = \frac{1}{d} \mathbb{1}_d$ . In this case one obtains  $F = \frac{1}{d}$ , which is not equal to the supremum of the fidelity over all pairs of states corresponding to  $F = 1$ . Even worse, if  $\rho_0 = \frac{1}{d} \mathbb{1}_d$  one obtains the same value of the fidelity, i.e.  $F = \frac{1}{d}$ , even when  $\rho_0 \neq \rho_C$ . Most notably this happens when  $\rho_C$  is an arbitrary pure state.

<sup>22</sup>From a mathematical point of view a fourth property of distance measures, the triangular inequality, is usually also demanded. Such distance measures are then called metrics. For purposes of certification and optimal control it is however not strictly required, if one is only interested in the behaviour of the distance measure towards 0 (or equivalently the fidelity towards its maximal value).

<sup>23</sup>By convention, one usually limits the maximal value of the fidelity to one. However, this can always be achieved by renormalisation and does not represent a mathematical limitation.

A proper fidelity that fulfils all three properties for arbitrary mixed states is given by [88],

$$F_{\text{state}} = \text{Tr}^2 \left( \sqrt{\sqrt{\rho_C} \rho_0 \sqrt{\rho_C}} \right), \quad (4.16)$$

and only for pure states  $\rho_0$  Eq. (4.16) actually reduces to

$$F_{\text{state}} = \text{Tr}(\rho_C \rho_0). \quad (4.17)$$

The state fidelity in this case has a convenient physical interpretation. This can be seen by rewriting  $\rho_0 = |\psi_0\rangle\langle\psi_0|$  and  $\rho_C = \sum_k p_k |\psi_k\rangle\langle\psi_k|$  for an orthonormal basis  $\{|\psi_k\rangle\}$  of Hilbert space to obtain

$$F_{\text{state}} = \langle\psi_0 | \rho_C | \psi_0\rangle = \sum_k p_k |\langle\psi_k | \psi_0\rangle|^2. \quad (4.18)$$

Eq. (4.18) clearly elucidates that the state fidelity is the average likelihood that the state  $\rho_C$  coincides with the pure state  $|\psi_0\rangle$  in terms of a Hilbert space overlap. Consequently, it represents the natural extension of the state overlap in Hilbert space to Liouville space.

We will now turn to the question, which distance measures can be derived from Eq. (4.16). One example is to utilise the so-called Bures angle,

$$A(\rho_C, \rho_0) = \arccos(F_{\text{state}}(\rho_C, \rho_0)), \quad (4.19)$$

which turns out to coincide with the Fubini-Study metric<sup>24</sup> on projective Hilbert space if  $\rho_C$  and  $\rho_0$  are pure states and interpreted as elements of the projective Hilbert space [90]. The Bures angle represents the most straightforward way to convert the fidelity into a proper metric, i.e. it even fulfils the triangular inequality [6].

An alternative metric that is commonly employed is the trace metric, or Kolmogorov distance, which is defined by

$$D(\rho_C, \rho_0) = \frac{1}{2} \text{Tr} [|\rho_C - \rho_0|]. \quad (4.20)$$

The trace distance has a useful physical interpretation in that one can show that [6]

$$D(\rho_C, \rho_0) = \max_{P \in L(\mathcal{H}), P^2=P} \text{Tr}[P(\rho_C - \rho_0)]. \quad (4.21)$$

This allows to interpret the trace distance as the maximal probability difference between the two possible results of a measurement corresponding to a projector  $P$  when comparing two states. While the trace distance has no direct relation to the state fidelity, it is still possible to formulate a relationship between them according to the inequality [6]

$$1 - F_{\text{state}}(\rho_C, \rho_0) \leq D(\rho_C, \rho_0) \leq \sqrt{1 - F_{\text{state}}(\rho_C, \rho_0)^2}. \quad (4.22)$$

---

<sup>24</sup>The Fubini-Study metric is the natural metric on a projective Hilbert space. It is identical to the Bures metric corresponding to the distance measure  $B(\rho_1, \rho_2) = \sqrt{2(1 - \sqrt{F_{\text{state}}(\rho_1, \rho_2)})}$  [89].

Using the Choi-Jamiołkowski isomorphism, one can now formulate a generalisation of the state fidelity in Eq. (4.39) to quantum processes. We denote by  $\mathcal{D}_C$  the process matrix/Choi matrix of a quantum process and by  $\mathcal{D}_0$  the process matrix/Choi matrix of an ideal process. Then the process fidelity as a natural generalisation of the state fidelity, Eq. (4.16), is given by [64]

$$F_{\text{pro}} = \frac{1}{d^2} \text{Tr}^2 \left( \sqrt{\sqrt{\mathcal{D}_C} \mathcal{D}_0 \sqrt{\mathcal{D}_C}} \right), \quad (4.23)$$

where the trace is now over Liouville space instead of Hilbert space. Unitary dynamical maps correspond to pure process matrices. This is because the eigenvalues of the Choi matrix correspond to the weights in the representation of a dynamical map according to a set of orthogonal<sup>25</sup> Kraus operators [46]. Since a dynamical map is unitary if and only if it can be described by a single Kraus operator, cf. Appendix A.1, this means that the Choi matrix for unitary dynamical maps has only a single non-vanishing eigenvalue, analogously to the concept of pure states in Liouville space [46]. Consequently, one can once again simplify this expression to

$$F_{\text{pro}} = \frac{1}{d^2} \text{Tr} (\mathcal{D}_C \mathcal{D}_0), \quad (4.24)$$

if the ideal process  $\mathcal{D}_0$  is unitary. We will in the following denote ideal unitary processes by  $\mathcal{U}_0$  and the corresponding unitary by  $U_0$ .

The process fidelity is sometimes called entanglement fidelity when  $\mathcal{U}_0$  corresponds to identity [91]. By the interpretation according to the Choi-Jamiołkowski isomorphism, the process fidelity of a channel with respect to unity yields a measure how well the entanglement of the maximally entangled state  $|\phi\rangle$  of Definition 2.2 under the action of  $\mathbb{1}_d \otimes \mathcal{D}$  is preserved [91]. Due to this interpretation one sometimes uses the terms process fidelity and entanglement fidelity interchangeably even when  $\mathcal{U}_0$  is not the identity operation.

The physical interpretation of Eq. (4.24) is not as straightforward as it was the case for the state fidelity. This is due to the fact that the Choi matrix is more abstract than the density matrix, i.e. it does not allow for a simple probabilistic interpretation. However, it turns out that the process fidelity is almost identical to the so-called average fidelity  $F_{\text{ave}}$  [91],

$$F_{\text{pro}} = F_{\text{avg}} \left( 1 - \frac{1}{d} \right) + \frac{1}{d} \iff F_{\text{avg}} = \frac{dF_{\text{pro}} - 1}{d - 1}, \quad (4.25)$$

with the average fidelity given by

$$\begin{aligned} F_{\text{avg}} &= \int F_{\text{state}} (\mathcal{D}_C (|\psi\rangle\langle\psi|), \mathcal{U}_0 (|\psi\rangle\langle\psi|)) d\psi \\ &= \int \langle\psi| U_0^\dagger \mathcal{D}_C (|\psi\rangle\langle\psi|) U_0 |\psi\rangle d\psi. \end{aligned} \quad (4.26)$$

---

<sup>25</sup>Note, that in the Choi matrix/process matrix is usually not normalised. This necessitates to include a factor of  $\frac{1}{d^2}$  in Eq. (4.23), such that the maximal value of  $F_{\text{pro}}$  is equal to 1, cf. Footnotes 12 and 19.

where the integral is performed over the Fubini-Study measure<sup>26</sup>  $d\psi$  in projective Hilbert space [89]. The process fidelity is consequently directly related to the average state fidelity between an arbitrary pure state sent through the to be certified channel and the same pure state being sent through the ideal unitary channel.

There exist other notions of fidelity/distance between quantum processes, one of which we will briefly mention. The so-called diamond norm distance is defined as [64]

$$d_{\diamond}(\mathcal{D}_C - \mathcal{D}_0) = \sup_{\rho} \|(\mathcal{D}_C \otimes \mathbb{1}_d)\rho - (\mathcal{D}_0 \otimes \mathbb{1}_d)\rho\|_1, \quad (4.27)$$

where  $\|\cdot\|_1$  is the nuclear norm (or “trace norm”) given by  $\|A\|_1 = \text{Tr}(\sqrt{A^\dagger A})$ . It can be shown that the supremum in Eq. (4.27) is always taken at a pure state  $\rho$ , i.e. the supremum can be evaluated over the set of pure states [92]. The diamond norm has the interpretation to be the maximal likelihood to differentiate the channels  $\mathcal{D}_C$  and  $\mathcal{D}_0$  with a binary outcome measurement on an arbitrary initial state allowing for arbitrary ancillas [93]. The diamond norm distance represents an example for a “worst-case fidelity” which is more sensitive to errors than an average fidelity. Another example for such a worst-case fidelity would be to substitute the integral in Eq. (4.26) with an infimum. While the diamond norm has many useful qualities it is difficult to evaluate which is why in the following we will employ the average fidelity in terms of experimental certification. For an extensive overview of distance measures and fidelities for quantum processes, see Ref. [94].

From Eq. (4.26) one can observe that the average fidelity indeed averages information of the behaviour of a dynamical map in terms of its action on pure states in Liouville space. Equivalently, it is derived via Eqs. (4.23) and (4.25) from the Choi matrix/process matrix which includes information of the action of the dynamical map on an orthonormal basis in Liouville space, i.e. information from  $d^2$  pure state fidelities, cf. Sec. 4.1. Our findings in Sec. 3 allude to the possibility to formulate a fidelity which requires only a significantly reduced amount of information if the ideal transformation is unitary.

Let  $\{\rho_i\}_{i=1,2,3}$  be a complete and totally rotating set including  $\mathbb{1}_d$ , then we can define

$$F_{\min}(\mathcal{D}_C, \mathcal{U}_0) = \frac{1}{3} \sum_i F_{\text{state}}(\mathcal{D}_C(\rho_i), \mathcal{U}_0(\rho_i)). \quad (4.28)$$

Symmetry and positivity of  $F_{\min}$  directly follow from the corresponding properties of  $F_{\text{state}}$ . To see that  $F_{\min} = 1 \iff \mathcal{D}_C = \mathcal{U}_0$  we will argue that  $F_{\text{state}}(\mathcal{D}_C(\rho_i), \mathcal{U}_0(\rho_i)) = 1$  if and only if  $\mathcal{D}_C(\rho_i) = \mathcal{U}_0(\rho_i)$ . From Theorems 3.7 and 3.9 we observe, that for arbitrary dynamical maps the equality  $\mathcal{D}_C(\rho_i) = \mathcal{U}_0(\rho_i)$  implies that their spectra are identical which is the case if and only if  $\mathcal{D}_C$  is unitary. As a result,  $F_{\min} = 1$  can only be fulfilled if and only if  $\mathcal{D}_C$  is unitary and due to the set  $\{\rho_i\}_{i=1,2,3}$  being unitary differentiating, for unitary  $\mathcal{D}_C$  the equivalence  $\mathcal{D}_C(\rho_i) = \mathcal{U}_0(\rho_i) \iff \mathcal{D}_C = \mathcal{U}_0$  indeed holds. Consequently, Eq. (4.28) represents a proper fidelity for certification of unitary dynamical maps that requires only three state fidelity to be measured.

Nevertheless, there are two caveats to this fidelity. Firstly, since the set  $\{\rho_i\}_{i=1,2,3}$  needs to be basis complete with only three matrices, it must contain mixed states. Reliable preparation of

---

<sup>26</sup>Note that for fixed  $|\phi\rangle$  and arbitrary  $|\psi\rangle$  there exists a unitary such that  $U|\phi\rangle = |\psi\rangle$ . This allows the integral in Eq. (4.26) to be rewritten as an integral over all unitaries where the integral is then performed over the Haar measure  $dU$ . These two formulations are identical.

mixed states, albeit conceivable [95], is experimentally challenging since it usually requires a detailed control on decoherence. Furthermore, mixed states do not allow for a simplification of the state fidelity according to Eq. (4.17). Secondly, there is no clear physical interpretation of  $F_{\min}$ . To alleviate these concerns we will derive a reduced fidelity in the next chapter that employs a set of density matrices consisting of pure states only.

## 4.5 Minimal Fidelities involving Pure States for Certification of UDMs

According to Theorems 3.7 and 3.9, one requires a complete and totally rotating set of density matrices to unitarily identify a unital dynamical map. Since a set of density matrices is basis complete if there exists a complete and orthonormal set of projectors on one-dimensional eigenspaces, a restriction to pure states in a basis complete set immediately requires at least  $d$  one-dimensional projectors in this set. This is because any pure density matrix is equivalent to a one-dimensional projector. Since the formation of a complete and totally rotated set requires at least another density matrix, the minimal cardinality of a complete and totally rotating set of pure density matrices is  $d + 1$ .

Let  $\{|\psi_i\rangle\}_{i=1,\dots,d}$  be an orthonormal basis of  $\mathcal{H}$ ,  $|\phi\rangle = \frac{1}{\sqrt{d}} \sum_{k=1}^d |\psi_k\rangle$  and define for  $k = 1, \dots, d$

$$\rho_i = |\psi_i\rangle\langle\psi_i|, \quad \rho_{d+1} = |\phi\rangle\langle\phi|. \quad (4.29)$$

Then, the set of  $\{\rho_i\}_{i=1,\dots,d}$  is a set of  $d$  one-dimensional orthogonal projectors and  $\rho_{d+1}$  is a one-dimensional projector that is totally rotated with respect to the set  $\{\rho_i\}$ . With this in mind we can use the equivalence (1)  $\iff$  (2) of Theorem 3.9 and the observation that the set of pure states  $\{\rho_i\}_{i=1,\dots,d+1}$  can be used to identify whether a dynamical map is unitary and also to differentiate between any two UDMs. This motivates the definition of what we will call the arithmetic fidelity,

$$F_{\text{arith}}(\mathcal{D}_C, \mathcal{U}_0) = \frac{1}{d+1} \sum_i F_{\text{state}}(\mathcal{D}_C(\rho_i), \mathcal{U}_0(\rho_i)), \quad (4.30)$$

which is simply the arithmetic mean of the  $d + 1$  state fidelities of the minimal set of complete and totally rotating pure states.

After having eliminated the first caveat mentioned in Sec. 4.4 we can now turn to compare the arithmetic fidelity to the average fidelity. From the definition of the arithmetic fidelity it becomes immediately clear that it will be strongly dominated by the sum over the state fidelities of the basis complete set for increasing Hilbert space dimension. Consider a basis complete set of projectors  $\{P_i\}$  and the dynamical map

$$\mathcal{D}_{C_1}(\rho) = \sum_i P_i \rho P_i^\dagger.$$

If we were to compare this dynamical map to the identity operation we see that the state fidelities of all elements of the basis complete set are equal to one since

$$\forall k : \mathcal{D}_{C_1}(P_k) = \sum_i P_k P_i P_i^\dagger = P_k = \mathbb{1}_d P_k \mathbb{1}_d.$$

Only the state fidelity of the totally rotated state will indicate that  $\mathcal{D}_{C_1}$  is actually quite far from the dynamical map corresponding to identity. This issue can even arise when the to be certified

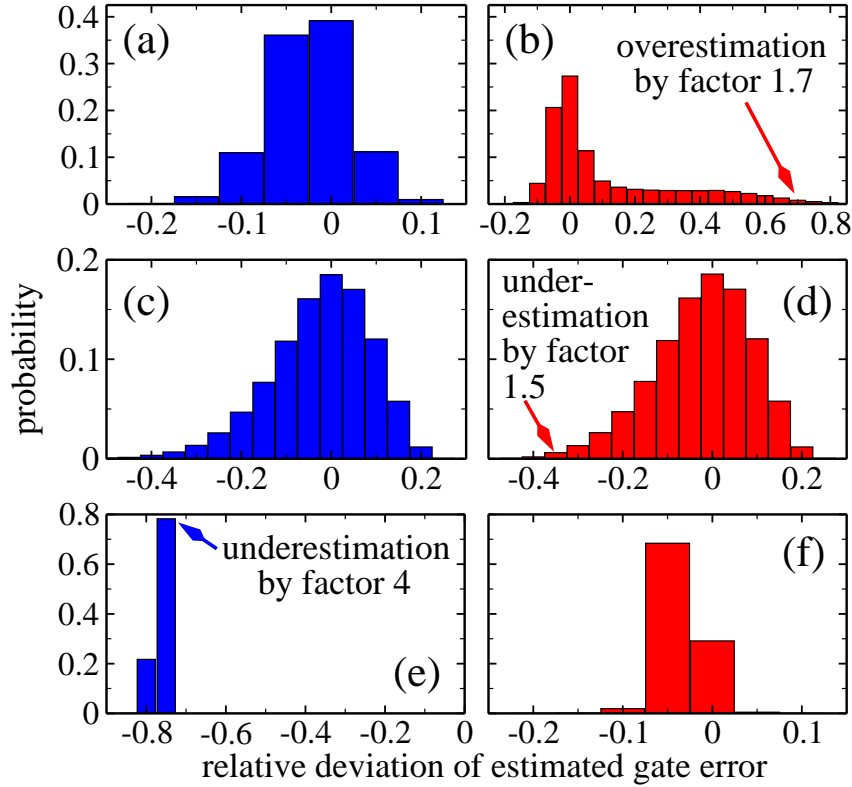


Figure 4.1: Probability of obtaining a relative deviation of the gate error via the arithmetic fidelity ( $1 - F_{\text{arith}}$ ) from the gate error via the average fidelity ( $1 - F_{\text{avg}}$ ), for 100.000 realisations when using  $F_{\text{arith}}$ , Eq. (4.30), (left column) and  $F_{\lambda}$ , Eq. (4.32), (right column). Shown are the results for randomised dynamical maps with  $O = \text{CNOT}$  (a, b), truly random unitaries with  $O = \text{CNOT}$  (c-d) and randomised unitaries with  $O = \mathbb{1}$  (e-f). Positive and negative values of the relative deviation, corresponding to under- and overestimation of the gate error, do not scale equivalently. The scale for overestimation ranges from zero to infinity while that for underestimation is confined to  $[-1, 0)$ .

dynamical map is unitary. Consider the ideal transformation  $O$  and a dynamical map implementing a unitary  $U$ , i.e.

$$\mathcal{U}_0(\rho) = O\rho O^\dagger, \quad \mathcal{D}_{C_2}(\rho) = U\rho U^\dagger.$$

Now, if  $U$  and  $O$  are both diagonal in terms of the basis complete set of projectors  $\{P_i\}$ , i.e.  $U = \sum_i e^{i\varphi_i} P_i$  and  $O = \sum_i e^{i\theta_i} P_i$ , then

$$\mathcal{U}_0(P_i) = P_i, \quad \mathcal{D}_{C_2}(P_i) = P_i$$

independent on the particular phases  $\{\varphi_i\}$  and  $\{\theta_i\}$ . This means that the state fidelities of all projectors in  $\{P_i\}$  is equal to one. Once again, the only indicator on the difference of  $\mathcal{U}_0$  and  $\mathcal{D}_{C_2}$  can be found in the state fidelity of the totally rotated projector whose contribution to  $F_{\text{arith}}$  becomes negligibly small for increasing dimension of the Hilbert space.

This effect can be directly observed in a numerical analysis. We sampled over a set of randomised unitaries with an eigenbasis very close to that of the projectors of the employed basis complete set. Figure 4.1(e) shows the relative deviation of the estimated gate error via the arithmetic fidelity with respect to the average fidelity, where we set  $O = \mathbb{1}_d$ . Figure 4.1(a) shows the probability of

obtaining a certain relative deviation of the estimated gate error for randomised dynamical maps and the CNOT gate as the target gate. The randomised dynamical maps were obtained by creating a random matrix [96] for twice as many qubits as there are system qubits. The random matrices were Hermitised, multiplied by a randomly chosen scaling factor and exponentiated. The resulting matrix was multiplied by the tensor product of the target unitary with  $\mathbb{1}_d$ , and the bath qubits were traced out. For most dynamical maps,  $F_{\text{arith}}$  yields a good estimate of the gate error. However, as already discussed above, if the state fidelities for the set of basis complete projectors are very high, but the fidelity for the totally rotated state is comparatively small, the arithmetic fidelity seriously underestimates the gate error. In other words, we have to account for the cases in which almost all the information is in the totally rotated basis leading to deceiving results for the arithmetic fidelity.

For brevity we define  $F^{(i)} = F_{\text{state}}(\mathcal{D}_C(\rho_i), \mathcal{U}_0(\rho_i))$  and  $F^{(TR)} = F_{\text{state}}(\mathcal{D}_C(\rho_{d+1}), \mathcal{U}_0(\rho_{d+1}))$ . With these abbreviations, we define the geometric fidelity,

$$F_{\text{geom}} = \frac{1}{d+1} + \left(1 - \frac{1}{d+1}\right) \left[ \left( \prod_i F^{(i)} \right) \cdot F^{(TR)} \right]. \quad (4.31)$$

The addition of the constant  $\frac{1}{d+1}$  is motivated by the observation that for unitary evolution the average fidelity lies in the interval  $\left[\frac{1}{d+1}, 1\right]$ . While the arithmetic fidelity accounts for that already implicitly, the geometric fidelity usually does not.

The geometric fidelity mostly takes small values since it is composed of a product of small numbers. It attains large numbers if all  $F^{(i)}$  are large and  $F^{(TR)}$  is large. More importantly, though, the geometric fidelity is very “strict” in a sense that it immediately takes small values if any of the projector images has a low fidelity. While in most cases this is in fact too strict, it proves itself numerically that especially in the cases where all projectors from the orthonormal set have good overlap one has to be careful since this indicates that information is shifted to  $F^{(TR)}$ , cf. the discussion above.

For this reason, we define the switching parameter  $\lambda \in [0, 1]$  and define the  $\lambda$ -fidelity,

$$F_\lambda = \lambda F_{\text{geom}} + (1 - \lambda) F_{\text{arith}}, \quad (4.32)$$

which has geometric character if  $\lambda$  is close to one and arithmetic character if  $\lambda$  is close to zero. It proves itself numerically that the following definition for  $\lambda$  is appropriate,

$$\lambda = \frac{\prod_i F^{(i)} - (\prod_i F^{(i)}) \cdot F^{(TR)}}{1 - (\prod_i F^{(i)}) \cdot F^{(TR)}} = \frac{1 - F^{(TR)}}{(\prod_i F^{(i)})^{-1} - F^{(TR)}} = 1 - \frac{1 - \prod_i F^{(i)}}{1 - (\prod_i F^{(i)}) \cdot F^{(TR)}}. \quad (4.33)$$

This choice of  $\lambda$  can be motivated as follows.

1.  $\lambda$  takes all values in the interval  $[0, 1]$ , hence covering the complete switching range.
2. If  $\forall i : F^{(i)} = 1$ , then  $\lambda = 1$  since this behaviour is an indicator that the gate error is mostly determined by the totally rotated state to which the geometric fidelity is more sensitive.
3. The smaller  $F^{(i)}$  is the smaller  $\lambda$  should be, too. An instructive special case is if  $F^{(TR)} = 0$ , then  $\lambda = \prod_i F^{(i)}$  and if most  $F^{(i)}$  are close to one, one should strongly weight the geometric fidelity (see point 2) whereas if not, then the arithmetic fidelity is adequate.

$N$	type of sample	$\alpha_{\text{arith}}$	$\beta_{\text{arith}}$	$\alpha_{\lambda}$	$\beta_{\lambda}$
2	randomised dynamical map	0.83	1.31	0.44	1.26
	random unitaries	0.76	2.35	0.75	1.92
	randomised unitaries	1.00	4.39	0.90	1.15
3	randomised dynamical map	0.96	1.04	0.51	1.03
	random unitaries	0.90	1.32	0.90	1.32
	randomised unitaries	1.00	8.67	0.91	1.20

Table 4.1: Numerically obtained bounds for over- and underestimation of the average fidelity in the form  $\alpha_i F_i \leq F_{\text{avg}} \leq \beta_i F_i$  for the arithmetic fidelity ( $i = \text{arith}$ ) and the  $\lambda$ -fidelity ( $i = \lambda$ ), using 100.000 realisations, for 2 and 3 qubits with  $O$  corresponding to CNOT ( $N = 2$ ), the Toffoli gate ( $N = 3$ ), respectively identity (randomised unitaries).

4. If  $F^{(TR)} = 1$ , then  $\lambda = 0$ , which corresponds to the  $\lambda$ -fidelity becoming identical to the arithmetic fidelity. This is because most information should be extractable from the propagation of the orthogonal projector set in this case.

It is still possible to manipulate the switching parameter  $\lambda$  by introducing another real, positive parameter  $k$  as follows,

$$\lambda_k = 1 - \frac{1 - \prod_i F^{(i)}}{1 - \left(\prod_i F^{(i)}\right)^k \cdot F^{(TR)}}. \quad (4.34)$$

All  $\lambda_k$  fulfil the properties 1 – 4 discussed above. For  $k = 1$  one retrieves the old choice of  $\lambda$ . For  $k > 1$  we decrease the value of  $\lambda$ , moving generally towards the arithmetic fidelity while for  $k < 1$  we increase the value of  $\lambda$  moving further towards the geometric fidelity. In the following we will for simplicity only consider  $k = 1$ .

The best estimates of the gate error in our numerical analysis are obtained using  $F_{\lambda}$  as shown in the right part of Fig. 4.1. Figure 4.1(a,b,e,f) presents results for randomised dynamical maps and randomised unitaries that were generated by exponentiating random Hermitian matrices. Since this is not truly random, we have also generated random unitaries based on Gram-Schmidt orthonormalisation of randomly generated complex matrices [97], cf. Fig. 4.1(c,d) with  $O$  being a CNOT gate. The  $\lambda$ -fidelity yields a faithful estimate of the gate error in all observed cases. On average, it underestimates the gate error by factors 1.03 (Fig. 4.1(b)), 1.11 (d) and 1.02 (f) and overestimates it by 1.16 (b), 1.08 (d), and 1.01 (f).

For three-qubit gates, we find the numerical bounds to be essentially contained by those for two-qubit gates, cf. Table 4.1. This suggests the numerical bounds to be independent of system size in the framework of this numerical analysis. A verification of this conjecture for larger system sizes is, however, hampered by the enormous increase in numerical effort for randomisation. For our examples of CNOT, the Toffoli gate and identity, we find the estimated gate error based on the  $\lambda$ -fidelity to deviate from the standard one in the worst case by a factor smaller than 2.5 and on average by a factor smaller than 1.2.

As a conclusion, the  $\lambda$ -fidelity seems to work in most cases very well. A recent analytical analysis showed that for an  $n$ -qubit system a nontrivial statement about a lower bound on the average fidelity can only be obtained if the arithmetic mean of the state fidelities of the basis complete set of pure states is above  $1 - 2^{n-1}$  [98]. In this work, a particular dynamical map was constructed that leads to a very low average fidelity while still having very high values for the arithmetic fidelity composed of a specific set of basis complete projectors and also leading to a  $F^{(TR)}$  which is close to one. In

this case the  $\lambda$  fidelity will also still be close to the arithmetic fidelity and could potentially strongly overestimate the average fidelity. The numerical analysis from Fig. 4.1 seems to indicate, however, that these instances are very unlikely to occur. Nonetheless, the results in Ref. [98] put further emphasis on the fact that while in most cases a naive processing of the information of the  $d + 1$  state fidelities from the minimal pure complete and totally rotating set can yield a good estimate on the average fidelity, in special cases a more careful approach might have to be taken. In particular, there are rare situations in which the minimal set cannot make a proper assessment on the average fidelity.

## 4.6 Classical Fidelities

A reduced set of pure state that allows for analytical and tight bounds to the process fidelity was found by Hofmann [99]. To achieve this he used two so-called classical fidelities to form these bounds.

Let  $\mathcal{H}$  be a Hilbert space and  $\dim \mathcal{H} = d$ . Let  $\{|k_i^{(1)}\rangle\}_{i=1,\dots,d}$  be an arbitrary orthonormal basis of  $\mathcal{H}$ . The classical fidelity of a channel is the fidelity that is equal to the average probability of obtaining the correct output for each of the  $N$  classically possible input states with respect to a certain, fixed basis. Hence, the classical fidelity with respect to the basis  $\{|k_i^{(1)}\rangle\}$  of a dynamical map  $\mathcal{D}_C$  with respect to a unitary dynamical map  $\mathcal{U}_0$  (corresponding to a unitary transformation  $U_0$ ) is given by

$$F_1 = \frac{1}{d} \sum_{i=1}^d \langle k_i^{(1)} | U_0^\dagger \mathcal{D}_C(|k_i^{(1)}\rangle \langle k_i^{(1)}|) U_0 | k_i^{(1)} \rangle. \quad (4.35)$$

Defining the rank 1 projectors,

$$P_i^{(1)} = |k_i^{(1)}\rangle \langle k_i^{(1)}|,$$

one can see that  $F_1$  corresponds to the arithmetic fidelity of the basis complete set of projectors  $\{P_i^{(1)}\}$ .

Next, Hofmann introduced a second classical fidelity with respect to a second orthonormal basis  $\{|k_n^{(2)}\rangle\}_{n=1,\dots,d}$  given by

$$|k_n^{(2)}\rangle = \frac{1}{\sqrt{d}} \sum_{m=1}^d e^{-i\frac{2\pi}{d}nm} |k_m^{(1)}\rangle. \quad (4.36)$$

The second classical fidelity then reads as follows,

$$F_2 = \frac{1}{d} \sum_{i=1}^d \langle k_i^{(2)} | U_0^\dagger \mathcal{D}_C(|k_i^{(2)}\rangle \langle k_i^{(2)}|) U_0 | k_i^{(2)} \rangle. \quad (4.37)$$

Once again, this expression can be interpreted as the arithmetic fidelity composed of another basis complete set of rank 1 projectors,

$$P_i^{(2)} = |k_i^{(2)}\rangle \langle k_i^{(2)}|.$$

Hofmann then showed that given the classical fidelities  $F_1$  and  $F_2$  the following bounds with respect

to the process fidelity holds,

$$F_1 + F_2 - 1 \leq F_{\text{pro}} \leq \min(F_1, F_2) . \quad (4.38)$$

These results can be understood in the framework of Sec. 3. It can be easily seen that any rank 1 projector from either set  $\{P_i^{(1)}\}$  or  $\{P_i^{(2)}\}$  is totally rotated with respect to the other. Moreover, the two bases  $\{|k_i^{(1)}\rangle\}$  and  $\{|k_j^{(2)}\rangle\}$  are mutually unbiased, i.e. they fulfil [100]

$$\forall i, j : \left| \langle k_i^{(1)} | k_j^{(2)} \rangle \right|^2 = \frac{1}{d} .$$

Mutual unbiasedness of two bases can be interpreted as the rank 1 projectors on the elements of either basis to be totally rotated with respect to each other. It can be shown that for an arbitrary dimension  $d$  there exist at least three mutually unbiased basis sets [101]. Furthermore, Hofmann's results can be generalised to not only hold for his particular construction according to Eq. (4.36) but for arbitrary mutually unbiased bases, cf. Appendix A.6. A set of two classical fidelities with respect to two mutually unbiased bases consequently enables strong analytical bounds on the process fidelity of a given dynamical map with respect to a certain unitary while requiring only the measurement of state fidelities for a set of  $2d$  pure input states.

## 4.7 Statistical Approaches to Tomography and Certification

In Sec. 4.2 we have shown how a straightforward approach to quantum state tomography leads to a complexity of  $\mathcal{O}(d^2)$  for general states and  $\mathcal{O}(d^4)$  for general dynamical maps. In recent years, several approaches to reduce this complexity have been attempted that are based on statistical considerations. The underlying idea to all those approaches is that instead of performing every measurement a fixed number of times, one rather performs a random measurement and can use tools of statistical mathematics to obtain an estimation for the actual density matrix/dynamical map with high confidence.

Three statistical approaches have been formulated recently: compressed sensing for tomography using the assumption of sparse states/maps [61, 68], randomised benchmarking for unitary certification, using the assumption of being able to implement a gate that transforms the to be certified unitary to identity [65], and Monte Carlo (MC) sampling for certification requiring no assumptions in the general case [59, 60]. The generality of the MC approach combined with its significant complexity reduction in special cases motivates the focus on this method in the context of this thesis. Nevertheless, we will briefly present the ideas underlying compressed sensing and randomised benchmarking.

The central paradigm of compressed sensing is the following: As pointed out in Sec. 4.2, a state, respectively dynamical map, is uniquely determined by a suitably chosen set of expectation values corresponding to certain measurements. If the set of measurement results fulfils the so-called restricted isometry property [61, 68] then it can be used, employing the solution of a convex optimisation problem, to determine an  $s$ -sparse<sup>27</sup> approximation to the actual density matrix/process matrix. Since any density matrix/process matrix is Hermitian, thus diagonalisable, there necessarily exists a basis in which it is sparse. If one were to know this basis a priori, then one could choose the measurement basis accordingly. Compressed sensing asserts that under certain conditions (most

<sup>27</sup>A matrix is  $s$ -sparse if it contains only  $s$  nonzero entries.

notably the above mentioned restricted isometry property) even without knowledge of the basis in which the matrix is sparse, one still can reduce the tomography complexity. For example, choosing for process tomography on an  $n$ -qubit system completely random input states and completely random measurements, the restricted isometry property is fulfilled with high (i.e. exponentially high) probability and the scaling reduces to  $\mathcal{O}(sn)$  where  $s$  is the actual sparsity of the process matrix, which in the worst case is  $d^2$ , and  $n$  is the number of qubits [61]. A caveat to this approach lies in the choice of completely random input states and measurement. This represents an experimentally very challenging task since it requires mixed states preparation. Nevertheless, at least for state tomography it was shown that using random Pauli measurements (cf. Sec. 4.3), the restricted isometry property is fulfilled with high probability and the scaling reduces to  $\mathcal{O}(sd)$  [68].

The idea of randomised benchmarking is that the process matrix element  $\chi_{mm}$  in the representation according to a complete orthogonal set of operators  $\{E_k\}$ , cf. Eqs. (2.15) and (2.20), can be efficiently determined by implementing the channel corresponding to the Kraus operator  $E_m^\dagger$  [65]. Note that if  $E_0$  is chosen to be the to be certified unitary  $U$ , then  $\chi_{00}$  determines the process fidelity of the implementation with respect to  $U$ , cf. Appendix A.6. The specific protocol for efficient characterisation employs randomly selecting elements of a so-called state 2-design and measuring the survival probability, i.e. the overlap of an initial state sent through the channel, of these states. The average over sufficiently many of these survival probabilities then yields the process fidelity, where the number of experiments to be performed is independent on system size. A related but slightly different approach is to apply these ideas to determine the average error of a given channel in terms of an average channel error over a set of random gates [63, 64]. This can be done efficiently if the set of Clifford gates is considered, a fact that is closely related to the fact that they form a unitary 2-design.

A particularly powerful tool for state/process certification is the MC sampling approach [59, 60]. It is based on the fact that the state fidelity can be spanned in an orthogonal<sup>28</sup> basis as follows,

$$F_{\text{state}} = \text{Tr}[\rho_C \rho_0] = \frac{1}{d} \sum_k \text{Tr}[\rho_C W_k^\dagger] \text{Tr}[W_k \rho_0]. \quad (4.39)$$

Here,  $\rho_C$  represents the state that is supposed to be certified and  $\rho_0$  represents the ideal state  $\rho_0$ . For the process fidelity, cf. Eq. (4.24), one obtains analogously

$$F_{\text{pro}} = \frac{1}{d^2} \text{Tr}[\mathcal{D}_C \mathcal{U}_0] = \frac{1}{d^4} \sum_{i,k} \text{Tr}[\mathcal{D}_C (W_i)^\dagger W_k] \text{Tr}[W_k^\dagger \mathcal{U}_0 (W_i)], \quad (4.40)$$

where  $\mathcal{D}_C$  represents the process that is supposed to be certified and  $\mathcal{U}_0(\rho) = U_0 \rho U_0^\dagger$  represents the ideal unitary dynamical map.  $\{W_k\}$  is a complete orthogonal set of operators in Liouville space fulfilling

$$\text{Tr}[W_i^\dagger W_k] = d \delta_{ik}. \quad (4.41)$$

For states one can define

$$\alpha_k = \text{Tr}[\rho_C W_k^\dagger], \quad \beta_k = \text{Tr}[W_k \rho_0]. \quad (4.42)$$

---

<sup>28</sup>In analogy to Refs. [59] and [60] we will not normalise the Pauli operators. This allows to use the unnormalised Pauli operators from Eq. (4.11) for the basis operators  $W_k$ .

For processes the definition is analogous,

$$\alpha_{ik} = \frac{1}{d} \text{Tr} \left[ \mathcal{D}_C(W_i)^\dagger W_k \right], \quad \beta_{ik} = \frac{1}{d} \text{Tr} \left[ W_k^\dagger \mathcal{U}_0(W_i) \right]. \quad (4.43)$$

Defining furthermore  $\text{Pr}(k) = \frac{1}{d} |\alpha_k|^2$ , respectively  $\text{Pr}(i, k) = \frac{1}{d^2} |\alpha_{ik}|^2$ , one obtains

$$F_{\text{state}} = \sum_k \text{Pr}(k) \frac{\alpha_k}{\beta_k} \quad (4.44)$$

for states and

$$F_{\text{pro}} = \sum_{ik} \text{Pr}(i, k) \frac{\alpha_{ik}}{\beta_{ik}} \quad (4.45)$$

for unitary gates [59,60]. The distribution  $\text{Pr}(k)$ , respectively  $\text{Pr}(i, k)$ , fulfils

$$\text{Pr}(k) \geq 0; \quad \sum_k \text{Pr}(k) = 1, \quad (4.46a)$$

$$\text{Pr}(i, k) \geq 0; \quad \sum_{i,k} \text{Pr}(i, k) = 1, \quad (4.46b)$$

and can be interpreted as a discrete probability distribution, in this context usually called relevance distribution.

An estimate on the state fidelity (resp. process fidelity) according to Eq. (4.44) (resp. Eq. (4.45)) can be obtained with the following approach [59,60].

1. Calculate the relevance distribution  $\text{Pr}(k)$  (resp.  $\text{Pr}(i, k)$ ) for the given target pure state  $\rho_0$  (resp. target unitary dynamical map  $\mathcal{U}_0$ ).
2. Draw an index  $k$  (resp. double index  $(i, k)$ ) according to the relevance distribution  $\text{Pr}(k)$  (resp.  $\text{Pr}(i, k)$ ).
3. Perform a measurement to obtain the quantity  $\alpha_k$  (resp.  $\alpha_{ik}$ ).
4. Given  $(\delta, \epsilon)$ , repeat steps 2 and 3 until  $L(\delta, \epsilon)$  draws of an index have been performed. Then, calculate  $Y = \frac{1}{L} \sum_{k=1}^L \frac{\alpha_k}{\beta_k}$  (resp.  $Y = \frac{1}{L} \sum_{(i,k)=1}^L \frac{\alpha_{ik}}{\beta_{ik}}$ ) to obtain an estimate for the fidelity  $F$  with  $\text{Pr}[|Y - F| \geq \delta] \leq \epsilon$ .

Complexity arises in this scheme at three points: Firstly, at step 1 one needs to classically compute the relevance distribution of the state  $\rho_0$  (resp. the transformation  $\mathcal{D}_0$ ). This task scales in general exponentially, however, if the set  $\{W_k\}$  is chosen to be the set of Pauli operators, cf. Sec. (4.3), it is a task that can be performed efficiently for stabiliser states (resp. Clifford gates). This is a direct consequence of Theorem 4.1 [59,60]. Secondly, while it is clear how to perform measurements in the case of state certification, it is not straightforward how operator inputs, i.e.  $\mathcal{D}_C(W_k)$ , have to be understood. One can circumvent this by drawing a random eigenstate of the ‘‘input operator’’  $W_i$  and apply the to be certified channel to this eigenstate [59]. Lastly, one needs to perform a sufficient number of experiments to get a sufficiently good estimate according to step 4. This depends generally on the state/process that should be certified. It can be shown that if the  $\{W_k\}$  are chosen to be the set of Pauli operators, for stabilisers (resp. Clifford gates) the number of experiments is independent

on system size [60]. The underlying reason for this fact is that stabiliser states (resp. Clifford gates) lead to a relevance distribution that has many vanishing entries with all remaining entries being equal to 1.

For a general state one obtains a scaling of  $L = \mathcal{O}(d)$  and for a general unitary transformation one obtains  $L = \mathcal{O}(d^2)$ . This is already a dramatic improvement on full tomography. The mathematical derivation of the bound on the number of draws as well as a more detailed explanation of the MC sampling procedure for the process fidelity of a unitary dynamical map can be found in Appendix A.7. Therein, it will also be explained why the complexity for Clifford gates becomes independent on the dimension of Hilbert space if Pauli operators are used as a measurement basis. The derivation in Appendix A.7 is already performed for the more general case of a non-Hermitian measurement basis which will become important when we extend our results to go beyond multi-qubit systems in Sec. 4.9.

## 4.8 Monte Carlo Process Certification with State Fidelities

We now turn to the question whether the complexity of Monte Carlo sampling can be lowered with the reduced pure state fidelities for unitary dynamical maps discussed in this Sec. 4.5. To this end, we will consider a  $n$ -qubit system, corresponding to Hilbert space dimension  $d = 2^n$ , using the Pauli operators  $\{W_k\}$  as an orthogonal measurement basis of Liouville space. We furthermore consider any fidelity given by an arithmetic mean over a set of  $I$  state fidelities of pure states represented by rank 1 projectors  $P_i$ , i.e.

$$F = \frac{1}{I} \sum_{i=1}^I F_{\text{state}}(\mathcal{U}_0(P_i), \mathcal{D}_C(P_i)) = \frac{1}{I} \sum_{i=1}^I \langle \mathcal{U}_0(P_i), \mathcal{D}_C(P_i) \rangle_{\text{HS}}. \quad (4.47)$$

In particular, as we will show later, this encompassed the arithmetic fidelity, Eq. (4.30), and arbitrary classical fidelities, Eq. (4.35).

The orthogonal basis of  $\mathcal{L}_{\mathcal{H}}$  given by the Pauli operators  $\{W_k\}$  fulfils

$$\langle W_k, W_l \rangle_{\text{HS}} = \text{Tr}[W_k W_l] = d \delta_{kl}, \quad (4.48)$$

where we can omit the dagger due to the Hermiticity of the Pauli operators.

Since the space  $\mathcal{L}_{\mathcal{H}}$  with the Hilbert-Schmidt scalar product is a Hilbert space, using Eq. (4.48) the following relation holds  $\forall \rho, \sigma \in \mathcal{L}_{\mathcal{H}}$ ,

$$\langle \rho, \sigma \rangle_{\text{HS}} = \frac{1}{d} \sum_{k=1}^{d^2} \langle \rho, W_k \rangle_{\text{HS}} \langle W_k, \sigma \rangle_{\text{HS}}. \quad (4.49)$$

Hence, we can rewrite any state fidelity  $F_{\text{state}}$  as

$$F_{\text{state}}(\mathcal{U}_0(P_i), \mathcal{D}_C(P_i)) = \frac{1}{d} \sum_{k=1}^{d^2} \text{Tr}[\mathcal{U}_0(P_i) W_k] \text{Tr}[W_k \mathcal{D}_C(P_i)]. \quad (4.50)$$

As a result, Eq. (4.47) can be rewritten as

$$F = \sum_{i=1}^I \sum_{k=1}^{d^2} \Pr(i, k) \frac{\beta_{ik}}{\alpha_{ik}}, \quad (4.51)$$

with

$$\alpha_{ik} = \text{Tr} [U_0 (P_i) W_k], \quad \beta_{ik} = \text{Tr} [W_k \mathcal{D}_C (P_i)], \quad (4.52)$$

$$\Pr(i, k) = \frac{1}{dI} |\alpha_{ik}|^2. \quad (4.53)$$

If  $\Pr(i, k)$  is supposed to represent a proper relevance distribution, it needs to be normalised, i.e.  $\sum_{kl} \Pr(i, k) = 1$ . This is proven in Appendix A.8. Evaluating Eq. (4.51) by Monte Carlo estimation involves randomly selecting  $L$  times a pair  $(i_l, k_l)$  of input states/measurement operators. The number of input states is given by  $I$ . The classical computational resources of the sampling step  $\mathcal{C}_{\text{class}}$  can be estimated by  $\mathcal{C}_{\text{class}} = N_{\text{input}} \times \mathcal{C}_{\text{single}}$  with  $\mathcal{C}_{\text{single}}$  being the classical computational cost for sampling a single state fidelity in Hilbert space ( $\mathcal{C}_{\text{single}} \sim n^2 2^{2n}$  [60]).

Analogously to standard Monte Carlo certification, we determine the sample size  $L$  by Chebyshev's inequality, Eq. (4.6). In our case,  $\mu = \langle Z \rangle = F$ ,  $Z = F_L = \sum_{l=1}^L X_l$ ,  $X_l = \beta_{i_l k_l} / \alpha_{i_l k_l}$  and  $k = \frac{1}{\sqrt{\delta}}$ . We show in Appendix A.9 that the variance of  $X_l$  is  $\leq 1$ , and thus  $\sigma^2 = \text{Var}(F_L) \leq \frac{1}{L}$ <sup>29</sup>. Then, the choice  $L = \frac{1}{\epsilon^2 \delta}$  guarantees that the probability for the estimate  $F_L$  to differ from  $F$  by more than  $\epsilon$  is smaller than  $\delta$ . Specifying the experimental inaccuracy and choosing the confidence level thus determines the sample size.

In order to estimate the number of required experiments, we first determine the number of experiments for an individual setting,  $N_l$ . For each  $l$ , the observable  $W_{k_l}$  has to be measured  $N_l$  times to account for the statistical nature of the measurement. The corresponding approximation to  $X_l$  is given by

$$\tilde{X}_l = \frac{1}{\alpha_{i_l k_l}} \frac{1}{N_l} \sum_{j=1}^{N_l} w_{lj}, \quad (4.54)$$

with  $w_{lj}$  the measurement result for the  $j$ -th repetition of experimental setting  $l$ , equal to  $\pm 1$  for Pauli operators. Since  $\tilde{X}_l$  is given as the sum of independent random variables,  $w_{lj}$ ,  $N_l$  can be determined using Hoeffding's inequality [102]. It provides an upper bound for the probability of a sum  $S = \sum_{i=1}^n Y_i$  of independent variables  $Y_i$  with  $a_i \leq Y_i \leq b_i$  to deviate from its expected value by more than  $\epsilon$ ,  $\forall \epsilon > 0$ ,

$$\Pr(|S - \langle S \rangle| \geq \epsilon) \leq 2 \exp\left(-\frac{2\epsilon^2}{\sum_{i=1}^n (b_i - a_i)^2}\right), \quad (4.55)$$

In our case,  $S = \tilde{F}_L = \frac{1}{L} \sum_{l=1}^L \tilde{X}_l$  and, using Eq. (4.54),  $\sum_{i=1}^n (b_i - a_i)^2 = \sum_{l=1}^L 4N_l [LN_l \alpha_{i_l k_l}]^{-2}$ . Inserting this into Eq. (4.55), it is evident that the choice

$$N_l = \frac{2}{L\epsilon^2 \alpha_{i_l k_l}^2} \log\left(\frac{2}{\delta}\right) = N_l(i_l, k_l) \quad (4.56)$$

<sup>29</sup>This follows from the fact that  $\text{Var}(\sum_i \alpha X_i) = \alpha^2 \text{Var}(X_i)$  for independent random variables  $X_i$ .

ensures the right-hand side of Eq. (4.55) to be  $\leq \delta$ . The setting  $l$  is chosen with probability  $\Pr(i_l, k_l)$ . The average number of times that this specific experiment (with input state index  $i_l$  and measurement operator  $W_{k_l}$ ) needs to be carried out is therefore given by

$$\begin{aligned} \langle N_l \rangle &= \sum_{i_l=1}^I \sum_{k_l=1}^{d^2} \Pr(i_l, k_l) N_l(i_l, k_l) \\ &= \frac{1}{dI} \sum_{i_l=1}^I \sum_{k_l=1}^{d^2} \alpha_{i_l k_l}^2 \frac{2}{\alpha_{i_l k_l}^2 L \epsilon^2} \log\left(\frac{2}{\delta}\right) \\ &\leq 1 + \frac{2d}{L\epsilon^2} \log\left(\frac{2}{\delta}\right). \end{aligned} \quad (4.57)$$

The total number of experiments that need to be carried can therefore be estimated by

$$\begin{aligned} \langle N_{\text{exp}} \rangle &= \sum_{l=1}^L \langle N_l \rangle \leq L \left[ 1 + \frac{2d}{L\epsilon^2} \log\left(\frac{2}{\delta}\right) \right] \\ &\leq 1 + \frac{1}{\epsilon^2 \delta} + \frac{2d}{\epsilon^2} \log\left(\frac{2}{\delta}\right). \end{aligned} \quad (4.58)$$

This number is sufficient to account for both the sampling error due to finite  $L$  and statistical experimental errors in the measurement results. Notably,  $\langle N_{\text{exp}} \rangle \sim d = 2^n$  only, i.e. the average number of experiments to estimate  $F$  scales like that required for characterising a general pure quantum state [60] and it is independent on the number of states that enter the arithmetic mean in the fidelity (4.51).

Clearly, the above result can be easily applied to the arithmetic fidelity, Eq. (4.47). However, due to the issues in finding a sensible bound of the arithmetic fidelity in terms of the actual process fidelity, cf. Sec. 4.5, it does not seem to be an optimal choice. A better approach is obtained by observing that the above result can also be applied to any classical fidelity. This can be seen as follows. Let  $\{|\psi_i\rangle\}$  be an orthonormal basis of  $\mathcal{H}$  and  $P_i = |\psi_i\rangle\langle\psi_i|$  be the corresponding rank 1 projectors/density matrices. The classical fidelity with respect to this orthonormal basis can be written as

$$\begin{aligned} F_{\text{class}} &= \frac{1}{d} \sum_{i=1}^d \langle \psi_i | U_0^\dagger \mathcal{D}(|\psi_i\rangle\langle\psi_i|) U_0 | \psi_i \rangle \\ &= \frac{1}{d} \sum_{i=1}^d \text{Tr} \left[ U_0 P_i U_0^\dagger \mathcal{D}(P_i) \right] \\ &= \frac{1}{d} \sum_{i=1}^d F_{\text{state}}(\mathcal{U}_0(P_i), \mathcal{D}_C(P_i)) \\ &= \frac{1}{d} \sum_{i=1}^d \langle \mathcal{U}_0(P_i), \mathcal{D}_C(P_i) \rangle_{\text{HS}}. \end{aligned} \quad (4.59)$$

By only evaluating two classical fidelities one can obtain already strong analytical bounds on the process fidelity, cf. Eq. (4.38). Both classical fidelities obey an average number of experiments scaling

as  $\mathcal{O}(d)$  and a factor of 2 is definitely worth this additional effort.

There is even a possibility to precisely estimate the average fidelity, and consequently the process fidelity, with a fidelity of the form of Eq. (4.47). This can be done by using the concept of quantum 2-designs [103]. A 2-design is a probability distribution, with probability coefficients  $p_i$  and elements  $\Psi_i$ , over pure quantum states which can duplicate properties of the probability distribution over the Fubini-Study measure for polynomials of degree 2 or less. Specifically, the average of any polynomial function of degree 2 over the 2-design is exactly the same as the average over the Fubini-Study measure, cf. Sec. 4.4. One can generalise this concept to quantum  $t$ -designs which then average polynomials of degree  $t$  [104]. Roughly speaking, let  $P$  be a polynomial of at most degree  $t$ . A  $t$ -design, i.e. a set  $(p_i, \Psi_i)$ , is given by the property that for all polynomials  $P$  the relation

$$\sum_i p_i P(\Psi_i) = \int P(\Psi) d\Psi \quad (4.60)$$

holds.

This can be applied to the average fidelity in the following way. Let  $X$  be a 2-design with uniform probability distribution, then

$$\begin{aligned} F_{\text{avg}} &= \int \langle \Psi | U_0^\dagger \mathcal{D}(|\Psi\rangle \langle \Psi|) U_0 | \Psi \rangle d\Psi \\ &= \frac{1}{|X|} \sum_{\Psi \in X} \langle \Psi | U_0^\dagger \mathcal{D}(|\Psi\rangle \langle \Psi|) U_0 | \Psi \rangle. \end{aligned} \quad (4.61)$$

This is valid since the average fidelity can be interpreted as a polynomial of degree 2 in terms of Eq. (4.60). Note that bras and kets are counted separately, which means that only at most two bras and two kets appear. It can be shown [105] that a possible set of two designs with uniform probability coefficients is given by the  $d(d+1)$  elements of the  $(d+1)$  mutually unbiased basis sets that exist in Hilbert spaces of dimensions with a prime number as base - specifically this implies the qubit case. Consequently,

$$F_{\text{avg}} = \frac{1}{d(d+1)} \sum_{i=1}^{d(d+1)} \langle \Psi_i | U_0^\dagger \mathcal{D}(|\Psi_i\rangle \langle \Psi_i|) U_0 | \Psi_i \rangle, \quad (4.62)$$

where  $\{|\Psi_i\rangle\}$  are the states from these  $(d+1)$  mutually unbiased basis sets. From Eq. (4.62) it is immediately clear that it is of the form of Eq. (4.47) and we can apply all previously obtained results in this subsection.

We conclude that the process fidelity/average fidelity of a general unitary transformation can be certified with complexity  $\mathcal{O}(d)$  which represents a saving of a factor of  $d$  compared to standard MC process certification. These savings come at the expense of (i) obtaining only bounds on the average fidelity when using two classical fidelities or (ii) the necessity to prepare entangled input states<sup>30</sup> when using two-designs. The latter scales quadratically in  $n$  [107]. Even factoring this additional cost in, Monte Carlo estimation of the average fidelity for a general unitary operation using two-designs is significantly more efficient than that based on the channel-state isomorphism. A comparison of all

<sup>30</sup>There is no full set of  $(d+1)$  mutually unbiased bases that consists of only separable states, see e.g. Ref. [106] and references therein.

approach	$\mathcal{C}_{\text{class}}$	$N_{\text{input}}$	$N_{\text{setting}}$	$\langle N_{\text{exp}} \rangle$
A	$\mathcal{O}(n^2 2^{4n})$	$6^n$	$\mathcal{O}(6^n 2^{2n})$	$\mathcal{O}(2^{2n})$
B	$\mathcal{O}(n^2 2^{4n})$	$2^n(2^n + 1)$	$\mathcal{O}(2^{4n})$	$\mathcal{O}(2^n)$
C	$\mathcal{O}(n^2 2^{3n})$	$2 \cdot 2^n$	$\mathcal{O}(2^{3n})$	$\mathcal{O}(2^n)$

Table 4.2: Resources required for determining the average gate error of a general unitary operation in terms of classical computational effort  $\mathcal{C}_{\text{class}}$  required for the random selection, number  $N_{\text{input}}$  of input states that need to be prepared, the number of experimental settings  $N_{\text{setting}}$  from which the actual experiments will be randomly chosen, and the average number  $\langle N_{\text{exp}} \rangle$  of experiments to be performed.  $N_{\text{setting}} = N_{\text{input}} \times N_{\text{meas}}$  with the number of measurement operators  $N_{\text{meas}} = 2^{2n}$  for all cases (A: standard Monte Carlo sampling [59, 60]; B: Monte Carlo sampling for two-designs; C: Monte Carlo sampling for classical fidelities).

approach	$\mathcal{C}_{\text{class}}$	$N_{\text{input}}$	$N_{\text{setting}}$	$\langle N_{\text{exp}} \rangle$
A	$\mathcal{O}(1)$	$6^n$	$\mathcal{O}(6^n 2^n)$	$\mathcal{O}(1)$
B	$\mathcal{O}(1)$	$2^n(2^n + 1)$	$\mathcal{O}(2^{3n})$	$\mathcal{O}(1)$
C	$\mathcal{O}(1)$	$2 \cdot 2^n$	$\mathcal{O}(2^{2n})$	$\mathcal{O}(1)$

Table 4.3: Resources required for determining the average gate error of a Clifford gate ( $N_{\text{setting}} = N_{\text{input}} \times 2^n$ ). Symbols as in Table 4.2.

discussed approaches can be found in Table 4.2 for general unitaries.

The scaling of  $\langle N_{\text{exp}} \rangle$  with the number of qubits changes also in the MC process certification approaches based on state fidelities, being strongly reduced for Clifford gates, as it was the case for the standard approaches. This is due to the property of Clifford gates to map eigenstates of a  $d$ -dimensional set of commuting Pauli operators into eigenstates of another such set, cf. Sec 4.3. The mutually unbiased bases entering the two classical fidelities or state 2-designs can be chosen to be such eigenstates [82]. Given a generic eigenstate  $|\Psi_j\rangle$  of a commuting set  $\mathcal{W}$  of Pauli operators, the coefficients for a Clifford gate,  $U_C$ , becomes

$$\begin{aligned}
\alpha_{i_l k_l} &= \text{Tr} \left[ W_k U_C |\Psi_i\rangle \langle \Psi_i| U_C^\dagger \right] \\
&= \text{Tr} [W_k |\Psi_j\rangle \langle \Psi_j|] = \begin{cases} \pm 1, & \text{if } W_k \in \mathcal{W} \\ 0, & \text{otherwise} \end{cases}.
\end{aligned} \tag{4.63}$$

The relevance distribution for Clifford gates,  $\text{Pr}(i_l, k_l) \sim \alpha_{i_l k_l}^2$ , is thus zero for many settings and uniform otherwise. Since settings with  $\text{Pr}(i_l, k_l) = 0$  will never be selected, the sampling complexity becomes independent of system size, cf. Sec. 4.7. Calculating  $\langle N_l \rangle$  according to Eq. (4.57) for a uniform relevance distribution, and accounting for the correct normalisations of  $\text{Pr}(i_l, k_l)$ ,  $\langle N_l \rangle$  is found to be independent of  $d$ ,  $\langle N_l \rangle \leq 1 + 2 \log(2/\delta)/(L\epsilon^2)$ , for all three approaches. Consequently, also  $\langle N_{\text{exp}} \rangle$  does not scale with system size,  $\langle N_{\text{exp}} \rangle \leq 1 + 1/(\epsilon^2 \delta) + 2 \log(2/\delta)/\epsilon^2$ , cf. Table 4.3. For Clifford gates, the three approaches require therefore a similar, size-independent number of measurements. A difference is found, however, for the number of possible experimental settings. For each input state  $i$ , there are only  $d$  (instead of  $d^2$ ) measurement operators  $W_k$  with non-zero expectation value. This leads to  $N_{\text{setting}} = N_{\text{input}} \times 2^n$  for Clifford gates, cf. Table 4.3. The larger  $N_{\text{setting}}$  required for approaches A and B in Table 4.3 comes with a potentially higher accuracy of the

estimate which is, however, limited by the experimental error of state preparation and measurement.

## 4.9 Qupit Systems and Generalised Pauli Operators

Qupits with dimension greater than  $d = 2$  occur naturally as the basic information carriers in the context of superconducting circuits [108,109], in orbital angular momentum modes of photons [110,111], or in the polarisation of biphotons [112,113]. Compared to qubits, they offer advantages in terms of increased security and higher channel capacity in quantum communication and better efficiency in quantum information [110–112]. Due to the Gottesmann-Knill theorem it seems natural to seek for generalisation of the Pauli group to arbitrary multi-qudit spaces. In fact, for qudits corresponding to Hilbert spaces of prime dimension  $p$ , so-called qupits, a generalisation of the Pauli group and correspondingly a generalisation to the formalism of stabiliser states and Clifford gates can be obtained.

Consider a Hilbert space  $\mathcal{H}$  of prime dimension  $p$  and an orthonormal basis  $\{|k\rangle\}_{k=1,\dots,p}$  of  $\mathcal{H}$ . Let  $\omega = e^{\frac{2\pi i}{p}}$  and define the operators [87]

$$Z = \sum_{n=1}^p \omega^n |n\rangle \langle n|, \quad (4.64)$$

$$X = \sum_{n=1}^p |n \oplus 1\rangle \langle n|, \quad (4.65)$$

where  $\oplus$  denotes addition modulo  $p$ . Then the generalised Pauli group is given by

$$\mathcal{P} = \{\omega^i Z^a X^b | a, b, i \in \{0, 1, \dots, p-1\}\}, \quad (4.66)$$

with an orthogonal basis of  $L(\mathcal{H})$  given by the subset  $\bar{\mathcal{P}}$  with [71,114]

$$\bar{\mathcal{P}} = \{Z^a X^b | a, b \in \{0, 1, \dots, p-1\}\}. \quad (4.67)$$

Note that all elements of the generalised Pauli group are unitary, hence normal.

The notion of a generalised Pauli group can be naturally extended to a Hilbert space that can be written as a tensor product of qupit Hilbert spaces. In fact, there exists a natural isomorphism of any finite-dimensional Hilbert space to such a Hilbert space by performing a prime factor decomposition on its dimension. With this in mind, the Pauli group can be defined for the total Hilbert space and notions of stabiliser states and Clifford operators can be introduced completely analogously to the multi-qubit case.

Most importantly, there exists a generalisation of the Gottesmann-Knill theorem to these general multi-qupit Hilbert space [87] which motivates the choice of generalised Pauli operators as an operator basis in terms of tomography and certification. There is an important caveat though. It is not possible to generalise the Pauli group for qupit systems with  $p > 2$  in such a way that one can retain a subset that forms an orthogonal basis which consists of only Hermitian operators. However, actual measurements of such non-Hermitian (but still normal) operators can be carried out utilising the concept of universal quantum circuits [87]. By the Copenhagen interpretation, any measurement results in a collapse of the physical system to an eigenstate of the measurement operator. However,

as already briefly mentioned in Sec. 2.3, as long as the operator is normal the operator still admits an orthonormal basis of eigenvectors of the underlying Hilbert space. In a sense, it is just convenient to ensure that all eigenvalues are real as this facilitates the interpretation of an eigenvalue as a measurement results. Nevertheless, as long as the complex spectrum of an arbitrary normal operator is mapped to a real measurement result by a suitable protocol, there is no obstacle to “measuring” non-Hermitian operators. One such approach in the framework of polarisation path qubits with  $p = 4$  has been utilised in Ref. [115]. Since the generalised Pauli operators are unitary, hence normal, it is consequently possible to use them as a measurement basis in terms of certification, respectively tomography. It turns out that one can straightforwardly generalise the MC sampling protocol to utilise the generalised Pauli operators as a measurement basis. This leads to efficient scaling for gate certification of generalised Clifford gates [75]. A Hermitised version of the measurement basis derived from generalised Pauli operators can also be utilised. While it does preserve the dimensionally independent scaling when certifying generalised Clifford gates it comes at the cost of non-local measurements in the sense that the basis operators cannot be written any more as a tensor product on the individual qubit Hilbert spaces [75].

#### 4.10 Optimal Choice of Measurement Basis

We will finish this section by giving a general prescription of an “optimal” measurement basis, i.e. a measurement basis which allows for a maximal amount of unitary transformations to be efficiently characterisable. In Appendix B we constructively prove for a general qubit Hilbert space  $\mathcal{H}$ , with  $\dim \mathcal{H} = p$  prime, the following results.

1. Any optimal measurement basis contains only operators with identical spectrum given by  $\{\lambda_k = e^{i\frac{2\pi k}{p}} \mid k = 0, \dots, p-1\}$  (modulo a global phase on the operators).
2. Any optimal measurement basis partitions into  $p+1$  Abelian groups consisting of  $p$  operators each, with the only common element in all of these sets being  $\mathbb{1}_p$ .
3. The common eigenbases of these Abelian groups form a set of  $p+1$  mutually unbiased bases.
4. A unitary is efficiently characterisable with respect to such an optimal measurement basis if and only if it keeps the partitioning of the  $p+1$  mutually unbiased bases in  $\mathcal{H}$  intact.

Evidently, the generalised Pauli operators from Sec. 4.9 are an example for such an optimal measurement basis which motivates their prevalence for process certification even from a mathematical perspective. The generalised Clifford group forms the corresponding set of efficiently characterisable unitaries.

For an  $n$ -qubit system it seems natural to construct the measurement operator basis to consist of tensor products of single-qubit operators to assure that their eigenstates are still product states. This is guaranteed if a tensor product structure for the measurement basis is chosen. For a Hilbert space of arbitrary dimension, one can obtain a partitioning into tensor products of smaller Hilbert subspaces by prime factor decomposition. A natural approach to identify optimal measurement bases on the total Hilbert space starts from maximising the number of efficiently characterisable unitaries on each subspace. This is achieved by finding an optimal measurement basis on each subspace as outlined above, using the fact that the dimension of each subspace is prime by construction. A measurement basis of the total Hilbert space is then constructed in terms of tensor products of the

operators defined on the subspaces. This yields an orthonormal basis of measurement operators on the total Hilbert space.

If one considers a partitioning involving subspaces of non-prime dimension, it remains an open question whether the explicit use of non-prime dimension subspaces can be used to increase the number of efficiently characterisable unitaries beyond the one following from the prime factor decomposition approach. Nonetheless, our conjecture that a measurement basis constructed from the prime factor decomposition represents indeed an optimal choice is motivated by the fact that existence of  $p + 1$  mutually unbiased bases is not guaranteed for non-prime dimension Hilbert spaces but seems to be a central prerequisite for obtaining efficiently characterisable unitaries [75].

## 5 Dynamics and Control of Open Quantum System

From the point of view of quantum information, the dynamical evolution of a quantum systems can be regarded as a family of point-to-point transformations that describe the continuous evolution of the system's state in time. For an isolated quantum system this family turns out to be a one-parameter unitary group [38]. This group is generated by the Hamiltonian of the physical system and gives rise to the Liouville equation as a first order differential equation for the density matrix, respectively the Schrödinger equation as a first order differential equation for the Hilbert space state vector. The corresponding answer for open quantum systems is significantly more complicated. If the evolution is infinitesimally divisible, representing a lack of memory of the environment, i.e. if it is Markovian, then it is often possible to describe the family of point-to-point transformations on an open quantum system as a one-parameter semigroup. In this case, the semigroup is generated by a so-called completely dissipative map. This gives rise to the Lindblad master equation as a first order differential equation for the density matrix [116, 117]. Sections. 5.1 and 5.2 will be devoted to a brief review on the derivation of these fundamental equations of motion from the perspective of quantum information.

Being able to describe the dynamics of quantum system allows to systematically explore the possibilities of coherent control of these systems, i.e. the steering of a physical process via some external control parameters. Coherent control can be performed either by using physical intuition, e.g. in the context of bichromatic control [118] or the STIRAP method [119], or by using analytical and/or numerical tools, see e.g. the book by Rice and Zhao [120], to find the optimal solution for the control problem at hand. The latter approach is called optimal control. Coherent control of isolated quantum systems is an established field of research with a wide variety of applications. This includes for example the realisation of a quantum computer, see e.g. the work by Sørensen et al. [121], or the steering of chemical processes, realised e.g. by Wollenhaupt et al. [122]. In contrast, studies on control of open quantum systems emerged only very recently.

In practice, one often uses mathematical algorithms to calculate the optimal field required to implement a desired process. This area of research is called optimal control theory and has been introduced more than 50 years ago by the seminal works of Pontryagin et al. [123] and Bellman [124]. It is usually very hard, or even impossible, to determine analytical solutions with these methods which is why in practice the use of numerical, iterative algorithms is prevalent. Using this approach for quantum mechanical control has been originally proposed for problems in chemical physics or theoretical chemistry, e.g. by Zhu et al. [125]. Algorithms to solve these control problems have been invented in areas such as engineering, e.g. the Krotov algorithm developed by Konnov and Krotov [7], or nuclear magnetic resonance in the context of which the GRAPE algorithm has been formulated by Khaneja et al. [126]. In Sec. 5.3 we will briefly review the formalism of optimal control and the iterative update equations for the optimisation of open quantum systems via the Krotov algorithm which we will employ in this thesis.

In the second half of this section, we will present a novel approach regarding the formulation of optimisation functionals for unitary gates in open quantum system: By employing reduced state fidelities, cf. Sec. 4.4, it is possible to significantly reduce the numerical effort both in terms of CPU time and required memory. It should be emphasised that this reduction via the formulation of specific functionals for the optimisation of unitary transformations does not hinge on the particular choice of the control algorithm. To illustrate the fact that reduced state fidelities can indeed replace

optimisation functionals using the full basis of Liouville space, we will show numerical results for optimisations utilising reduced optimisation functionals. In particular, we will compare the required computational resources in this context to optimisations involving an optimisation functional that employs the full basis.

A review of the Krotov algorithm for general isolated and open quantum systems has been published in Ref. [9]. Its application to the control of unitary gates in open quantum systems in the context of reduced functionals together with an extensive numerical analysis on their convergence behaviour has been published in Ref. [127].

## 5.1 Isolated Quantum System Dynamics

The main idea of quantum control is to generate an external perturbation to a quantum system which influences its dynamics in a certain, desirable way. To understand how one can mathematically describe this perturbation we will begin by discussing how an isolated quantum system behaves in the absence of control.

One expects an isolated quantum system to behave probabilistically linear, continuous and entropy-preserving [52] which means that at each point in time the dynamical map describing the evolution from time  $t_0$  to time  $t$  can be described as

$$\rho(t) = \mathcal{D}_{t,t_0}(\rho(t_0)) = U(t, t_0) \rho(t_0) U^\dagger(t, t_0), \quad (5.1)$$

cf. Sec. 2.8. Furthermore, one usually makes the assumption that the evolution of an isolated quantum system in absence of any external influence is homogeneous in time, in particular this means that the mapping  $\mathcal{D}_{t,t_0}$  will only depend on the time difference  $t - t_0$ . As a result, one obtains that a unitary dynamical map describing the evolution of isolated quantum systems is dependent on only a single parameter which we will simply denote by  $t$ . In particular, this means that  $\forall t' \in [0, t]$  the relation

$$\mathcal{D}_t(\rho) \equiv \mathcal{D}_{t,0}(\rho) = \mathcal{D}_{t,t'}(\mathcal{D}_{t',0}(\rho))$$

holds. Using Eqs. (5.1) and (2.22) this leads to

$$\begin{aligned} \mathcal{D}_t(\rho) &= U(t) \rho U^\dagger(t) = U(t, t') U(t', 0) \rho U^\dagger(t', 0) U^\dagger(t, t') \\ &= (U(t, t') U(t', 0)) \rho (U(t', 0) U(t, t'))^\dagger. \end{aligned}$$

In particular, this means that the set of unitaries describing the evolution of a isolated quantum system is a one-parameter group fulfilling

$$\forall t, s: U(t+s) = U(t)U(s) = U(s)U(t). \quad (5.2)$$

Furthermore, we expect by the Copenhagen interpretation that the state of a quantum system is continuously dependent on time<sup>31</sup>, i.e.

$$\lim_{t \rightarrow t_0} \mathcal{D}_t(\rho) = \mathcal{D}_{t_0}(\rho). \quad (5.3)$$

In particular this means for the unitary  $U$  that

$$\forall t, t_0 \in \mathbb{R}, \rho \in \mathcal{L}\mathcal{H}: \lim_{t \rightarrow t_0} U(t) \rho U^\dagger(t) = U(t_0) \rho U^\dagger(t_0),$$

which is obviously equivalent to

$$\forall t, t_0 \in \mathbb{R}, |\psi\rangle \in \mathcal{H}: \lim_{t \rightarrow t_0} U(t) |\psi\rangle = U(t_0) |\psi\rangle. \quad (5.4)$$

---

<sup>31</sup>Discontinuities arise when measurements are performed. However, a measurement violates the assumption that the system is isolated.

This property is called strong continuity [28] and a one-parameter group with this property is called a strongly continuous one-parameter unitary group. By Stone's theorem [128], there exists a Hermitian operator  $H$  on the Hilbert space  $\mathcal{H}$  such that<sup>32</sup>

$$\forall t \in \mathbb{R} : U(t) = e^{-iHt}. \quad (5.5)$$

As a consequence we can identify arbitrary homogeneous evolutions of an isolated quantum system with a Hermitian operator  $H$ , the so-called Hamiltonian of the evolution. The reason for this nomenclature can be seen by taking the derivative of  $\rho(t)$  with respect to time (using the abbreviation  $\rho = \rho(0)$ ),

$$\begin{aligned} \frac{d}{dt}\rho(t) = \frac{d}{dt}\mathcal{D}_t(\rho) &= \left[ \frac{d}{dt}U(t) \right] \rho U^\dagger(t) + U(t) \rho \frac{d}{dt}[U^\dagger(t)] \\ &= -iHU(t) \rho U^\dagger(t) + iU(t) \rho U^\dagger(t) H \\ \implies \frac{d}{dt}\rho(t) &= -i[H, \rho(t)], \end{aligned} \quad (5.6)$$

where we used that  $[H, U(t)] = 0$ , by definition. Eq. (5.6) is called the Liouville-von Neumann equation [38] and it stands in direct analogy to the Liouville equation in classical mechanics under the identification of  $H$  with the Hamilton function and of the commutator with the Poisson bracket (modulo a factor  $\frac{1}{i}$ ).

If  $\rho$  is a pure state, i.e. it can be identified with a Hilbert space vector  $|\psi\rangle$ , then the Liouville equation reduces to the so-called Schrödinger equation [129],

$$\frac{d}{dt}|\psi(t)\rangle = -iH|\psi(t)\rangle. \quad (5.7)$$

## 5.2 Open Quantum System Dynamics

The following presentation is inspired by Ref. [38].

The ideal situation of being truly isolated, i.e. the total lack of information exchange with another system, represents a rather unrealistic assumption in many physical system. The state of a physical system can often be at best understood as the element of a Hilbert space  $\mathcal{H}_S$  which is a subspace of a high-dimensional Hilbert space  $\mathcal{H}_{\text{tot}} = \mathcal{H}_S \otimes \mathcal{H}_E$ . Elements of  $\mathcal{H}_{\text{tot}}$  represent state vectors corresponding to an encompassing isolated system which we will refer to as the “total system”. Here, the Hilbert space  $\mathcal{H}_S$  describes the degrees of freedom of the primary system at hand and  $\mathcal{H}_E$  describes all other environmental degrees of freedom. In this case the state of the system at time  $t$  is given by the partial trace of a state in  $\mathcal{H}_{\text{tot}}$  over the environmental degrees of freedom in  $\mathcal{H}_E$ , or

$$\rho_S(t) = \text{Tr}_E \left[ U_{\text{tot}}(t) \rho_{\text{tot}} U_{\text{tot}}^\dagger(t) \right], \quad (5.8)$$

which leads via the Liouville-von Neumann equation immediately to

$$\frac{d}{dt}\rho_S(t) = -i\text{Tr}_E [H_{\text{tot}}, \rho_{\text{tot}}(t)], \quad (5.9)$$

---

<sup>32</sup>The minus sign in the exponent is a convention. Furthermore, one usually pulls a factor of  $\hbar^{-1}$  out of the operator  $H$  but for brevity we will set throughout the whole thesis  $\hbar = 1$ .

where  $H_{\text{tot}}$  is the Hamiltonian of the total system and  $U_{\text{tot}}(t) = e^{-iH_{\text{tot}}t}$ . Unfortunately, this equation is in general not very useful since one still requires knowledge of the state of the total system at all times to describe  $\rho_S(t)$ . The goal of an efficient description of the evolution of  $\rho_S(t)$  is to find a mapping  $\mathcal{D}_t : \rho_S(0) \mapsto \rho_S(t)$ . This mapping will still depend on the specific form of the initial state of the total system. It can be shown that if environment and system are initially entangled the mapping can be very complex, involving lack of positivity and even lack of linearity in special cases [11]. This motivates the so-called product state assumption, cf. Sec. 2.6,

$$\rho(0) = \rho_S(0) \otimes \rho_E(0). \quad (5.10)$$

With this assumption one can define the set of mappings  $\{\mathcal{D}_t | t \in \mathbb{R}, t \geq 0\}$  which map  $\rho_S(0)$  onto  $\text{Tr}_E[U_{\text{tot}}(t)(\rho_S(0) \otimes \rho_E(0))U_{\text{tot}}^\dagger(t)]$  according to Eq. (5.8). It can be shown that each  $\mathcal{D}_t$  is a completely positive, trace-preserving map [130]. Generally it turns out, however, that no simple differential equation for  $\mathcal{D}_t$  can be found, the main reason being that the evolution described by the family  $\mathcal{D}_t$  can allow for backflow of information. This means that it is not always possible to write the dynamical map  $\mathcal{D}_t$  as a product of two dynamical maps, e.g. the first describing the evolution from 0 to  $\frac{t}{2}$  while the second describes the evolution from  $\frac{t}{2}$  to  $t$ , i.e.  $\mathcal{D}_t = \mathcal{D}_{\frac{t}{2},t}^{(2)}\mathcal{D}_{0,\frac{t}{2}}^{(1)}$ . Although the initial state is a product state, it is possible that during the evolution entanglement is built up between system and environment which does not decay sufficiently fast such that the intermediate states can be considered as product states. Then, employing such an intermediate state as an initial state of another dynamical map usually fails.

A simple, yet often employed assumption for the family  $\{\mathcal{D}_t\}$  is given by the following formula,

$$\forall t, s \geq 0 : \mathcal{D}_{t+s} = \mathcal{D}_t\mathcal{D}_s = \mathcal{D}_s\mathcal{D}_t. \quad (5.11)$$

In analogy to Eq. (5.2), the set  $\{\mathcal{D}_t\}$  describes a one-parameter dynamical semigroup<sup>33</sup> of dynamical maps. This assumption is equivalent to homogeneity of the evolution in time in the sense that the evolution governed by the semigroup of dynamical map is having the same effect no matter how long the system already underwent evolution from the fixed initial product state. This becomes particularly clear by observing that from Eq. (5.11) it follows that

$$\forall n \in \mathbb{N}, t \in \mathbb{R} : \mathcal{D}_t = \left(\mathcal{D}_{\frac{t}{n}}\right)^n. \quad (5.12)$$

In particular, this means that the state of the total system at any point in time can still be regarded as a product state, since the evolution of the system between any two points in time can be described as a dynamical map. In other words, all entanglement between system and environment vanishes infinitely fast (or at least fast with respect to the natural system dynamics). At no point in time there is a shared information between the two subsystems, most notably at no point one can deduce any information on the state of the system via the state of the environment. This is often called the “lack of memory” of the environment. In particular, no backflow of information from the environment to the system is possible. This is why the generators of semigroups of dynamical maps are also sometimes called completely dissipative [116] and the resulting evolutions are called Markovian [38].

<sup>33</sup>Analogously to the strongly continuous one-parameter groups for isolated quantum systems, there are additional continuity requirements on a dynamical semigroup, cf. Ref. [116]. For simplicity, we will not further discuss them here.

Similarly to Stone's theorem, Lindblad proved [116] that one can write for any such semigroup of dynamical maps,

$$\mathcal{D}_t = e^{\mathcal{L}t}, \quad t \geq 0, \quad (5.13)$$

with

$$\frac{d\rho(t)}{dt} = \mathcal{L}\rho(t). \quad (5.14)$$

$\mathcal{L} \in L(\mathcal{L}_{\mathcal{H}})$  is a completely dissipative map if and only if it fulfils the so-called Lindblad master equation,

$$\mathcal{L}\rho = -i[H, \rho] + \sum_{k,l=1}^{d^2-1} c_{kl} \left( F_k \rho F_l^\dagger - \frac{1}{2} F_l^\dagger F_k \rho - \frac{1}{2} \rho F_l^\dagger F_k \right), \quad (5.15)$$

where  $H$  is traceless and Hermitian,  $\{F_k\}_{k=1, \dots, d^2-1}$  is an orthonormal set of traceless operators and the matrix whose elements are given by the coefficients  $c_{kl}$  is positive [117]. The condition of tracelessness of  $H$  and all  $F_k$  determines the generator uniquely. Due to the positive coefficient matrix, one can diagonalise Eq. (5.15) via a unitary transformation to obtain [38]

$$\mathcal{L}\rho = -i[H, \rho] + \sum_{k=1}^{d^2-1} \gamma_k \left( A_k \rho A_k^\dagger - \frac{1}{2} A_k^\dagger A_k \rho - \frac{1}{2} \rho A_k^\dagger A_k \right). \quad (5.16)$$

Since the all elements of the operator set  $\{F_k\}$  are traceless, so are the  $A_k$  and because the coefficient matrix was positive, all eigenvalues  $\gamma_k$  are nonnegative. Furthermore, as the transformation was unitary, the set  $\{A_k\}$  remains an orthogonal, traceless set. The operators  $A_k$  are called Lindblad operators. Note that the generator according to Eq. (5.16) is invariant under unitary transformations  $\sqrt{\gamma_k} A_k \rightarrow \sqrt{\gamma_k} \tilde{A}_k = \sum_l u_{kl} \sqrt{\gamma_l} A_l$  with  $u_{kl}$  being the coefficients to a unitary matrix [38]. The generator is also invariant under the inhomogeneous transformation  $A_k \rightarrow \tilde{A}_k = A_k + a_k \mathbb{1}_d$ ,  $H \rightarrow \tilde{H} = H + \frac{1}{2i} \sum_l \gamma_l (a_l^* A_l - a_l A_l^\dagger) + b \mathbb{1}_d$ , however, by demanding tracelessness of the  $A_k$  and  $H$  the generator in diagonal form is determined up to a unitary transformation on the set of Lindblad operators [38].

One can alternatively derive the Lindblad master equation by starting with a unitary evolution of the bipartite system/environment Hilbert space undergoing a unitary evolution starting from an initial product states. The necessary conditions for the result to be castable into the form of Eq. (5.16) are as follows [38]: Firstly, the influence of the system on the environment shall be small, i.e. the state of the environment remains essentially unchanged due to its interaction with the system. This is called the Born approximation. Moreover, one needs to perform a rotating wave approximation, sometimes also called secular approximation, which either requires the interaction of system and environment to be very strong or very weak on the timescale of system dynamics. If  $\tau$  represents the timescale of system-environment interaction and  $E_S$  the eigenvalues of the system Hamiltonian, the strong coupling case can be written as  $\forall E_S \in \text{spec}(H_S) : \int_0^\tau e^{iE_S t} dt \simeq 1$  and the weak coupling case as  $\forall E_S \in \text{spec}(H_S) : \int_0^\tau e^{iE_S t} dt \simeq 0$ . Finally, the reduced state of the system at a given time  $t$  shall be completely independent on the state of the system at previous times. Effectively this means that the Poincaré recurrence time of the environment needs to be much larger than the timescale that will be considered for system evolution.

While the semi-group approach by definition only admits Markovian evolutions, some quantum

master equation approaches go beyond that. One of the most prevalent techniques is the usage of memory kernels, see e.g. Ref. [131]. Another treatment is given by the method of the Surrogate Hamiltonian [132–134], where only the bath dynamics relevant on the time scale of the system’s evolution are considered. Finally, we want to briefly mention the description of the evolution of an open quantum system by a classical stochastic process in Hilbert space, termed “unravelling” or the “method of quantum trajectories”, see e.g. Refs. [135] and [136].

### 5.3 Optimal Control

Quantum control deals with the behaviour of isolated or open quantum systems under the influence of a controllable time-dependent perturbation, represented by a set of so-called controls  $\{u_k(t)\}$ . The most common example for a control is the classical electric field  $\epsilon(t)$  of a laser. The controls introduce a time dependence in the generators of the dynamical group/semigroup. Effectively, this means that Eqs. (5.7) and (5.14) read

$$\frac{d}{dt} |\psi(t)\rangle = -iH(t) |\psi(t)\rangle, \quad (5.17)$$

$$\frac{d\rho(t)}{dt} = \mathcal{L}(t) \rho(t), \quad (5.18)$$

where  $\forall t : H(t) = H(t)^\dagger$  and  $\mathcal{L}(t)$  is a completely dissipative map for all  $t$ . It can be shown [137] that Eq. (5.18) still gives rise to a canonical form of the generator  $\mathcal{L}(t)$  according to

$$\begin{aligned} \mathcal{L}(t) \rho(t) &= -i[H(t), \rho(t)] \\ &+ \sum_{k=1}^{d^2-1} \gamma_k(t) \left( A_k(t) \rho(t) A_k^\dagger(t) - \frac{1}{2} A_k^\dagger(t) A_k(t) \rho(t) - \frac{1}{2} \rho(t) A_k(t) A_k^\dagger(t) \right). \end{aligned} \quad (5.19)$$

If  $\forall k, t : \gamma_k(t) \geq 0$ , then the whole evolution is still completely positive since it can be regarded as the composition of infinitesimal completely positive evolutions. The dynamical maps resulting from the evolution are no longer one-parameter dynamical semigroups. Nevertheless, they still fulfil the condition

$$\mathcal{D}_{t,t_0} = \mathcal{D}_{t,t_1} \mathcal{D}_{t_1,t_0} \quad (5.20)$$

for all  $t_1 \in [t_0, t]$ .

If some coefficients  $\gamma_k(t)$  in Eq. (5.19) become negative, the evolution may but does not need to lose complete positivity [138]. This can occur if one relaxes the condition of complete dissipativity for the generator in Eq. (5.18) to linearity, Hermiticity and trace preservation. In this case, the evolution will lose the property of being Markovian. It is even possible to define non-Markovianity of an evolution described by a Liouvillian of the form (5.19) in terms of at least one coefficient  $\gamma_k(t)$  becoming negative at some point during the evolution [137]. In particular, the evolution then does not admit a decomposition according to Eq. (5.20). Note that this description of non-Markovianity is tied to equations of motion of the form of Eq. (5.19). In general, the characterisation of a non-Markovian evolution proves to be quite difficult. Although very recently a rather large variety of measures on non-Markovianity have been published [80, 139–143], there is nevertheless no common agreement on how to precisely quantify the non-Markovianity of an evolution due to the non-equivalence of many

of the proposed measures [144].

Closed quantum systems are described by introduction of a time-dependent Hamiltonian in Eq. (5.17). The total evolution is still unitary as long as  $H(t)$  is Hermitian at all points in time since it is the composition of infinitesimal unitary evolutions. The set of unitary transformation is not a one-parameter group anymore due to its dependence on an initial point in time, only fulfilling the condition

$$U(t, t_0) = U(t, t_1)U(t_1, t_0) \quad (5.21)$$

for all  $t_1 \in [t_0, t]$ .

The time dependence of the Hamiltonian or Liouvillian due to external influences can have controllable, e.g. a laser directed on an atom, or non-controllable time-dependent influences, e.g. stray electromagnetic fields in a solid state device. Usually, the time-dependence of the Hamiltonian in quantum control is solely due to a set of external controls  $\{u_k(t)\}$ , i.e. the Hamiltonian can be written in the following form,

$$H[\{u_k(t)\}] = H_0 + \sum_k u_k(t) H_k, \quad (5.22)$$

describing a so-called bilinear system [40]. In Eq. (5.22) the drift Hamiltonian  $H_0$  and all control Hamiltonians  $H_k$  are Hermitian operators.

The central question of optimal control of closed systems is the following: Given a set of initial states  $\{|\psi_n(0)\rangle\}$ , what is the optimal set of controls  $\{u_k(t)\}$ , among some set of admissible controls, in terms of maximising, respectively minimising, a certain figure of merit called the optimisation functional<sup>34</sup>,

$$J(\{|\psi_n\rangle\}, \{u_k\}) = J_T(\{|\psi_n(T)\rangle\}) + \int_0^T g(\{|\psi_n(t)\rangle\}, \{u_k(t)\}) dt, \quad (5.23)$$

where  $[0, T]$  represents the (usually fixed) optimisation interval in time. The first term in Eq. (5.23) corresponds to the desired state of the evolution at some final time and the second term introduces costs with respect to the pathway that the states and/or controls take during the evolution. It is very rare that such an optimisation problem can be treated analytically. This is due to the fact that the figure of merit depends on the states but one is looking for the optimal value of the controls with both states and controls being coupled via the equations of motion. For this reason one usually utilises iterative approaches combined with numerical solutions of the equations of motion. They consist in starting from some initial guess,  $\{u_k^{(0)}(t)\}$ , and improving the value of the optimisation functional step by step via iterative changes in the controls. There is a vast number of algorithms to obtain new sets of controls in such an iterative procedure, e.g. Gradient type quasi-Newton updates [126, 145] or simplex searches on reduced parametrisations of the set of controls [146].

A particularly powerful approach is to employ an idea originally proposed by Konnov and Krotov [7]. It consists in constructing an auxiliary functional that allows to independently consider changes in the value of the optimisation functional  $J$  via explicit changes in the states, respectively changes in the controls. Then, one can derive a condition on an iterated set of controls, which is guaranteed to lead to an improved value of  $J$  until convergence is reached. The Krotov algorithm can be applied to any quantum system as long as one is able to formulate the derivatives of the

---

<sup>34</sup>While the expression for  $J$  represents the full optimisation functional, we will occasionally utilise this term to only refer to the final-time part  $F$  if it is clear from context.

final-time functional  $F$  with respect to the states at final time and some smoothness conditions on the functional and the equations of motion are fulfilled [9].

One of the most common control problems requires a cost functional that prevents the control fields from changing too much in between iterations. When no further costs on either the states or controls are imposed this results in

$$g(\{u_k(t)\}) = \sum_k \frac{\lambda_k}{S_k(t)} \left( u_k(t) - u_k^{(\text{ref})}(t) \right)^2, \quad (5.24)$$

where  $u_k^{(\text{ref})}(t)$  is usually taken as the control field of the previous iteration, respectively the initial guess for the first iteration.  $\lambda_k$  represents a nonnegative weight and  $S_k(t)$  represents a nonnegative shape function which can be utilised to impose a certain temporal shape on the iterative control updates obtained from the algorithm. For additional costs of the form of Eq. (5.24) the update equations for the Krotov algorithm are given by [8, 9]

$$u_k^{(i+1)}(t) = u_k^{(i)}(t) + \frac{S_k(t)}{\lambda_k} \text{Im} \sum_n \left[ \left\langle \chi_n^{(i)}(t) \left| \frac{\partial H}{\partial u_k} \right| \psi_n^{(i+1)}(t) \right\rangle + \sigma(t) \left\langle \psi_n^{(i+1)}(t) - \psi_n^{(i)}(t) \left| \frac{\partial H}{\partial u_k} \right| \psi_n^{(i+1)}(t) \right\rangle \right]. \quad (5.25)$$

$\sigma(t)$  is an auxiliary function to ensure monotonic convergence. The initial states at time  $t = 0$ ,  $\{|\psi_n(0)\rangle\}$ , represent the initial conditions for the set of states entering the final-time functional. Evidently, they are fixed for each iteration. The evolution of the states  $\{|\psi_n(t)\rangle\}$  is described by the Schrödinger equation<sup>35</sup>,

$$\frac{d}{dt} \left| \psi_n^{(i)}(t) \right\rangle = -iH \left[ \left\{ u_k^{(i)}(t) \right\} \right] \left| \psi_n^{(i)}(t) \right\rangle, \quad (5.26)$$

$$\frac{d}{dt} \left| \psi_n^{(i+1)}(t) \right\rangle = -iH \left[ \left\{ u_k^{(i+1)}(t) \right\} \right] \left| \psi_n^{(i+1)}(t) \right\rangle, \quad (5.27)$$

and the so-called costates  $\left\{ \left| \chi_n^{(i)}(t) \right\rangle \right\}$  are given by

$$\left| \chi_n^{(i)}(T) \right\rangle = - \frac{\partial F}{\partial \langle \psi_n(T) | \left\{ \psi_n^{(i)}(T) \right\}}, \quad (5.28)$$

$$\frac{d}{dt} \left| \chi_n^{(i)}(t) \right\rangle = -iH \left[ \left\{ u_k^{(i)}(t) \right\} \right] \left| \chi_n^{(i)}(t) \right\rangle. \quad (5.29)$$

The Krotov algorithm can be generalised to more complicated cost functionals, e.g. involving spectral constraints on the control [147], non-linear Hamiltonians, e.g. for the description of Bose-Einstein condensation via the Gross-Pitaevskii equation [148], or state-dependent constraints [9, 149, 150].

For open quantum systems, the state-dependence of the functionals is represented in terms of a

<sup>35</sup>We consider here only Hamiltonians that are independent on the states, for a more general form of the update equations, see Refs. [8] and [9].

set of density matrices  $\{\rho_n(t)\}$  and the equations above generalise straightforwardly to<sup>36</sup> [127, 151]

$$u_k^{(i+1)}(t) = u_k^{(i)}(t) + \frac{S_k(t)}{\lambda_k} \text{Re} \sum_n \left[ \left\langle \Xi_n^{(i)}(t), \frac{\partial \mathcal{L}}{\partial u_k} \rho_n^{(i+1)}(t) \right\rangle_{\text{HS}} + \sigma(t) \left\langle \rho_n^{(i+1)}(t) - \rho_n^{(i)}(t), \frac{\partial \mathcal{L}}{\partial u_k} \rho_n^{(i+1)}(t) \right\rangle_{\text{HS}} \right], \quad (5.30)$$

$$\frac{d}{dt} \rho_n^{(i)}(t) = \mathcal{L} \left[ \left\{ u_k^{(i)}(t) \right\} \right] \rho_n^{(i)}(t), \quad (5.31)$$

$$\frac{d}{dt} \rho_n^{(i+1)}(t) = \mathcal{L} \left[ \left\{ u_k^{(i+1)}(t) \right\} \right] \rho_n^{(i+1)}(t), \quad (5.32)$$

$$\Xi_n^{(i)}(T) = - \left. \frac{\partial F}{\partial \rho_n(T)} \right|_{\{\rho_n^{(i)}(T)\}}, \quad (5.33)$$

$$\frac{d}{dt} \Xi_n^{(i)}(t) = -\mathcal{L}^\dagger \left[ \left\{ u_k^{(i+1)}(t) \right\} \right] \Xi_n^{(i+1)}(t). \quad (5.34)$$

It should be finally noted that the above approach also works if  $\rho_n(t)$  is not a density matrix but rather an arbitrary element of  $\mathcal{L}_{\mathcal{H}}$  by considering  $\rho_n(t)$  and  $\rho_n^\dagger(t)$  as independent variables and taking the derivative with respect to  $\rho_n^\dagger(T)$  in Eq. (5.33), cf. the final-time conditions in Refs. [151] and [152]. This procedure can be understood analogously to the treatment of kets and bras in the Hilbert space case.

## 5.4 Optimisation Functionals for Open Quantum Systems

Finding suitable final-time functionals for particular optimisation tasks is a very similar problem to finding proper fidelities/metrics for certification: Firstly, optimisation functionals need to be real to admit an order relation, i.e. they need to be able to assess how well a desired process is actually implemented under a given set of controls. Furthermore, an optimisation functional needs to become extremal only if a desired evolution takes place such that maximisation/minimisation of the functional is guaranteed to lead to the desired process - this property we will call “reliable”. Ideally, any set of set of states that corresponds to the desired behaviour of the system will correspond to a maximal/minimal value of the functional - we will call these functionals “encompassing”. This strengthens the condition to become extremal “only if” a desired process is implemented to “if and only if”. Not all reliable functionals will be encompassing since, in contrast to certification, there is not necessarily a unique set of states at final time that corresponds to implementing a certain physical goal. We will present a simple example to these concepts in the following.

In quantum computation one of the most important tasks is the implementation of unitary quantum operations, representing loss-less processing of quantum information [6]. On a Hilbert space  $\mathcal{H}$  with  $\dim \mathcal{H} = d$  a unitary transformation is uniquely defined by its action on an orthonormal basis  $\{|n\rangle\}$  of  $\mathcal{H}$ . Two suitable optimisation functionals for this task are given by the so-called real part functional,  $J_{\text{re}}$ , and the square modulus functional,  $J_{\text{sm}}$  [153], here shown in the formulation for a

<sup>36</sup>Note the real part in Eq. (5.30) in contrast to the imaginary part in Eq. (5.25) due to the different convention in the generators, cf. Eqs. (5.17) and (5.18).

minimisation problem<sup>37</sup>,

$$J_{\text{re}} = 1 - \frac{1}{d} \sum_n \text{Re} \langle \psi_n(T) | O | \psi_n(0) \rangle, \quad (5.35)$$

$$J_{\text{sm}} = 1 - \frac{1}{d} \sum_n |\langle \psi_n(T) | O | \psi_n(0) \rangle|^2, \quad (5.36)$$

where  $O$  is the target transformation and  $|\psi_n(0)\rangle \equiv |n\rangle$ . This can be easily seen by noting that for a closed quantum system the evolution is unitary, hence  $\exists U : \forall n : |\psi_n(T)\rangle = U |\psi_n(0)\rangle$ . This allows to write

$$\sum_n \langle \psi_n(T) | O | \psi_n(0) \rangle = \sum_n \langle \psi_n(0) | U^\dagger O | \psi_n(0) \rangle = \text{Tr} [U^\dagger O] = \langle U, O \rangle_{\text{HS}}.$$

Note now that  $\|U\|_{\text{HS}} = \|O\|_{\text{HS}} = 1$  due to their unitarity and hence, via the Cauchy-Schwarz inequality  $|\langle U, O \rangle_{\text{HS}}| = 1$  if and only if  $U = e^{i\varphi} O$  for some  $\varphi \in [0, 2\pi]$ . Since the only physically relevant part of a unitary transformation is captured in the projective unitary group, cf. Sec. 2.8, both the square modulus and the real part functional become minimal only if  $U$  and  $O$  correspond to the same element in  $\text{PU}(d)$ , i.e. both are reliable. However, only  $J_{\text{sm}}$  is encompassing since  $J_{\text{re}}$  also requires  $U$  and  $O$  to be identical as an element of  $\text{U}(d)$  instead of only  $\text{PU}(d)$ . For this reason, in general,  $J_{\text{sm}}$  will be a more suitable functional since it does not unnecessarily restrict the optimisation algorithm by introducing additional constraints beyond asserting the minimal requirements for the implementation of the target. There are technical reasons why sometimes real part functionals can be preferable to square modulus functionals in a practical numerical application, an example will be briefly mentioned in Sec. 6 in the context of state-to-state transformations.

If one considers now the optimisation of a unitary transformation for an open quantum system, the most straightforward approach is to simply use an optimisation functional according to Eq. (4.24) which reads<sup>38</sup>

$$J_{\text{pro}} = 1 - \frac{1}{d^2} \text{Re} \left[ \sum_k \langle \mathcal{D}_T(W_k), \mathcal{D}_0(W_k) \rangle_{\text{HS}} \right], \quad (5.37)$$

where  $\mathcal{D}_T$  represents the evolution from initial time to final time  $T$  and  $\mathcal{D}_0$  represents the dynamical map corresponding to the ideal transformation.  $\{W_k\}$  is an arbitrary orthonormal basis of  $\mathcal{L}_{\mathcal{H}}$ . This choice of fidelity has already been applied in the literature [151, 152]. Note that  $J_{\text{pro}}$  is not reliable if the target transformation  $\mathcal{D}_0$  is not unitary since the transformation is then not guaranteed to conserve the Hilbert-Schmidt norm of arbitrary states in  $\mathcal{L}_{\mathcal{H}}$ . We will give a simple example to elucidate this issue in the following.

Consider a single qubit with the ideal transformation being a perfect phase damping channel, i.e.

$$\mathcal{D}_0 = P_0 \rho P_0 + P_1 \rho P_1, \quad (5.38)$$

with  $P_0 = |0\rangle\langle 0|$  and  $P_1 = |1\rangle\langle 1|$  where  $\{|0\rangle, |1\rangle\}$  are eigenstates to  $\sigma_z$ . Then, choosing the normalised

<sup>37</sup>For simplicity, we will keep throughout this thesis all optimal control tasks formulated in terms of minimisation.

<sup>38</sup>Analogously to the Hilbert space case,  $J_{\text{pro}}$  can also be formulated with a square modulus. Note however, that in Liouville space this does not change whether the functional is encompassing when unitary transformations are considered since the projective unitary formulation is implicit for dynamical maps. For this reason, using the real part formulation with its simpler mathematical structure (i.e. linear dependence on propagated matrices) is usually preferred.

Pauli basis for the set  $\{W_k\}$ , we observe that

$$\begin{aligned}\mathcal{D}_0\left(\frac{1}{\sqrt{2}}\mathbb{1}_2\right) &= \frac{1}{\sqrt{2}}\mathbb{1}_2, \\ \mathcal{D}_0\left(\frac{1}{\sqrt{2}}\sigma_z\right) &= \frac{1}{\sqrt{2}}\sigma_z, \\ \mathcal{D}_0\left(\frac{1}{\sqrt{2}}\sigma_x\right) &= \mathcal{D}_0\left(\frac{1}{\sqrt{2}}\sigma_y\right) = 0.\end{aligned}$$

This means that if  $\mathcal{D}_T = \mathcal{D}_0$  then  $J_{\text{pro}} = \frac{1}{2}$ . However, the same value of  $F_{\text{pro}}$  is obtained if  $\mathcal{D}_T$  is the identity operation. This means that the fidelity  $J_{\text{pro}}$  is generally not reliable. A possibility to fix this issue by formulating the functional in terms of the backwards propagated targets has been performed in Ref. [152].

This behaviour is not entirely unexpected since Eq. (4.40) was derived for the specific case of unitary certification. The expression it originates from can be interpreted as the state fidelity from the state via the Choi-Jamiołkowski isomorphism, which only allows for a formulation via a simple Hilbert-Schmidt overlap if one of the states is pure, i.e. if the target transformation is unitary. If  $\mathcal{D}_0$  is unitary,  $J_{\text{pro}}$  coincides in this case with the process fidelity which we know is a proper fidelity for certification of unitary dynamical maps. This automatically implies that the optimisation functional is encompassing, since  $J_{\text{pro}} = 0$  if and only if the to be certified dynamical map is the ideal unitary. To preserve reliability and the encompassing property for the non-unitary case the Hilbert-Schmidt overlap needs to be substituted with the proper expression for the fidelity, i.e. for an orthonormal basis of positive operators  $\{W_k\}$ ,

$$\bar{J}_{\text{pro}} = 1 - \sum_k \frac{1}{d^2 \eta_k} \text{Tr}^2 \left( \sqrt{\sqrt{\mathcal{D}_T(W_k)} \mathcal{D}_0(W_k) \sqrt{\mathcal{D}_T(W_k)}} \right), \quad (5.39)$$

where normalisation factors  $\{\eta_k\}$  need to be employed if the optimal value should still correspond to  $\bar{J}_{\text{pro}} = 0$ . They are required to account for the fact that the individual traces might not become equal to one for the target transformation.

While the choice of a functional for unitary optimisation according to Eq. (5.37), respectively Eq. (5.39), is reliable and encompassing, it requires numerical propagation of the full set of  $d^2$  orthonormal operators in  $\mathcal{L}_{\mathcal{H}}$ . In Sec. 3 we have shown that a unitary dynamical map can be uniquely identified with the help of a set of only three states in  $\mathcal{L}_{\mathcal{H}}$ , independent of Hilbert space dimension. In the minimal formulation this set requires the inclusion of mixed states which is why a reliable and encompassing functional is given by

$$\bar{J}_{\text{min}} = 1 - \text{Re} \left[ \sum_{k=1}^3 \frac{1}{3\eta_k} \text{Tr} \left( \sqrt{\sqrt{\mathcal{D}_T(\rho_k)} \mathcal{U}_O(\rho_k) \sqrt{\mathcal{D}_T(\rho_k)}} \right) \right]. \quad (5.40)$$

with normalisation factors  $\{\eta_k\}$  required for the same reasons we mentioned above. As pointed out in Sec. 4.4, one generally loses reliability by using a simplified form of the state fidelity according to

Eq. (4.17),

$$J_{\min} = 1 - \operatorname{Re} \left[ \sum_{k=1}^3 \frac{1}{3\eta_k} \langle \mathcal{D}_T(\rho_k), \mathcal{U}_O(\rho_k) \rangle_{\text{HS}} \right]. \quad (5.41)$$

As we will see below the simplified minimal functional in Eq. (5.41) seems to still be reliable in practice and it has the great advantage of simple derivatives and monotonic convergence without requiring additional terms in the Krotov update formula [9].

Similarly to the observations in Sec. 4.5, a potential problem lies in the fact that while these functionals are reliable, they do not emulate the process fidelity very well, which is ultimately the quantity that is relevant in a practical implementation. In other words, if no solution with  $J_{\min} = 0$  can be found by the control algorithm, it is almost impossible to assess how close one actually is to the ideal transformation with respect to a physically motivated figure of merit. This leads to the formulation of the “ $d+1$  functional”,  $J_{d+1}$ , which is deduced from the arithmetic fidelity of a minimal set of pure states, cf. Sec. 4.5, or the “ $2d$  functional”  $J_{2d}$  formulated in terms of two classical fidelities of mutually unbiased basis which allows for analytical bounds on the process fidelity, cf. Sec. 4.6, i.e.

$$J_{d+1} = 1 - \operatorname{Re} \left[ \sum_{k=1}^{d+1} \frac{1}{d+1} \langle \mathcal{D}_T(\rho_k^{(d+1)}), \mathcal{U}_O(\rho_k^{(d+1)}) \rangle_{\text{HS}} \right], \quad (5.42)$$

$$J_{2d} = 1 - \operatorname{Re} \left[ \sum_{k=1}^{2d} \frac{1}{2d} \langle \mathcal{D}_T(\rho_k^{(2d)}), \mathcal{U}_O(\rho_k^{(2d)}) \rangle_{\text{HS}} \right], \quad (5.43)$$

Here, the set  $\{\rho_k^{(d+1)}\}_{k=1,\dots,d+1}$  can consist of e.g. the density matrices from Eq. (4.29) and  $\{\rho_k^{(2d)}\}_{k=1,\dots,2d}$  is composed from rank 1 projectors corresponding to two mutually unbiased bases of  $\mathcal{H}$ . Note that no normalisation factors are required for Eqs. (5.42) and (5.43) since all density matrices entering the functional are pure.

## 5.5 Unitary Transformations on Subspaces

In many implementations of unitary gates for quantum computation, the logical subspace in which the transformation takes place will be embedded in a larger Hilbert space. Usually a qudit or a multi-qudit system will be embedded in a total Hilbert space  $\mathcal{H}_{\text{tot}} = \mathcal{H}_1 \otimes \mathcal{H}_2$  where  $\mathcal{H}_1$  is the Hilbert space of the qudit(s) and  $\mathcal{H}_2$  is the Hilbert space of ancillary degrees of freedom or environmental degrees of freedom that cannot be traced out easily. This happens in particular, when the coupling of these environmental degrees of freedom to the qudit induces a strongly non-Markovian evolution. The case of  $\mathcal{H}_2$  representing ancillary degrees of freedom can be encountered e.g. in superconducting transmon qubit implementation [154,155], where the qubits are embedded in a cavity. In this context,  $\mathcal{H}_1$  corresponds to the description of the qubits and  $\mathcal{H}_2$  corresponds to the description of the cavity that is used to indirectly steer the qubits. An example for  $\mathcal{H}_2$  representing environmental degrees of freedom is given by a superconducting phase qudit with strongly coupled dielectric defects in its environment, a qudit implementation we will discuss in great detail in Sec. 7.

Another common occurrence is an embedding that can be represented by a tensor sum structure, i.e.  $\mathcal{H}_{\text{tot}} = \mathcal{H}_1 \oplus \mathcal{H}_2$ . This occurs most frequently when the qudits are encoded only in a subset of eigenstates of a higher-dimensional Hamiltonian acting on  $\mathcal{H}_{\text{tot}}$ . In this case,  $\mathcal{H}_1$  is given by the span of the eigenstates forming the so-called “logical subspace” while  $\mathcal{H}_2$  corresponds to the union of the

remaining eigenspaces. For example, in almost all superconducting qubit implementation qubits are encoded in the first two eigenstates of an anharmonic oscillator. Note, that the presence of a tensor product structure and a tensor sum structure is not mutually exclusive.

The tensor sum case is significantly easier to treat from a mathematical point of view. We will in the following reformulate Theorem 3.9 for this situation which will allows us to adjust our optimisation functionals from Sec. 5.4 to this setting. The Liouville space corresponding to a tensor sum Hilbert space also obeys a tensor sum structure according to  $\mathcal{L}_{\mathcal{H}_{\text{tot}}} = \mathcal{L}_{\mathcal{H}_1} \oplus \mathcal{L}_{\mathcal{H}_2}$ . If we consider a dynamical map  $\mathcal{D}$  with Kraus operators  $\{E_k\}$  on  $\mathcal{L}_{\mathcal{H}_{\text{tot}}}$ , we can write the reduced map  $\mathcal{D}_1$  on  $\mathcal{L}_{\mathcal{H}_1}$  as

$$\mathcal{D}_1(\rho) = P_1 \mathcal{D}(\rho \oplus 0) P_1 = \sum_k P_1 E_k (\rho \oplus 0) E_k^\dagger P_1, \quad (5.44)$$

where  $P_1$  is the projector on  $\mathcal{H}_1$  and  $\rho \oplus 0$  is the natural extension of a density matrix on  $\mathcal{L}_{\mathcal{H}_1}$  to the total Liouville space  $\mathcal{L}_{\mathcal{H}_{\text{tot}}}$ . Since  $\rho \oplus 0 = P_1 (\rho \oplus 0) P_1$  we can write

$$\mathcal{D}_1(\rho) = \sum_k (P_1 E_k P_1) (\rho \oplus 0) (P_1 E_k P_1)^\dagger. \quad (5.45)$$

The operators  $P_1 E_k P_1$  can be written as  $E_k^{(1)} \oplus 0$  with  $E_k^{(1)}$  being an operator on  $\mathcal{L}_{\mathcal{H}_1}$ . This means that  $\mathcal{D}_1$  can be written as

$$\mathcal{D}_1(\rho) = \sum_k E_k^{(1)} \rho (E_k^{(1)})^\dagger \quad (5.46)$$

which implies by Choi's theorem that the reduced map  $\mathcal{D}_1$  is Hermitian and completely positive on  $\mathcal{L}_{\mathcal{H}_1}$ . If we denote the identity on  $\mathcal{L}_{\mathcal{H}_1}$  as  $\mathbb{1}^{(1)}$  it can easily be checked whether  $\mathcal{D}_1$  is trace-preserving by analysing whether  $\mathcal{D}_1(\mathbb{1}^{(1)}) = \mathbb{1}^{(1)}$ . This leads to the expression

$$\mathcal{D}_1(\mathbb{1}^{(1)}) = \sum_k E_k^{(1)} (E_k^{(1)})^\dagger, \quad (5.47)$$

which is equal to  $\mathbb{1}^{(1)}$  if and only if  $\mathcal{D}_1$  is trace-preserving, cf. Sec. 2.6. This means that with respect to our results from Sec. 3, unitary certification on a tensor sum subspace only involves the additional requirement to ensure that  $\mathcal{D}_1(\mathbb{1}^{(1)}) = \mathbb{1}^{(1)}$  such that  $\mathcal{D}_1$  is indeed a dynamical map on  $\mathcal{L}_{\mathcal{H}_1}$ . However, this is equivalent to the standard test for unitality of a dynamical map, which needs to be performed anyway when a minimal set of states is employed.

More formally, the following corollary to Theorem 3.9 holds.

**Corollary 5.1.** *Let  $\mathcal{H} = \mathcal{H}_1 \oplus \mathcal{H}_2$  be a finite-dimensional Hilbert space with  $d_1 = \dim(\mathcal{H}_1)$  and let  $\mathcal{D}$  be a dynamical map on  $\mathcal{L}_{\mathcal{H}}$ . The following statements are equivalent:*

1. *The reduced map  $\mathcal{D}_1 : \mathcal{L}_{\mathcal{H}_1} \mapsto \mathcal{L}_{\mathcal{H}_1}$  given by  $\mathcal{D}_1(\rho) = \bar{\rho}$  with  $P_1 \mathcal{D}(\rho \oplus 0^{(2)}) P_1 = \bar{\rho} \oplus 0^{(2)}$  is a unitary dynamical map on  $\mathcal{H}_1$  with  $P_1 \in \mathcal{L}_{\mathcal{H}}$  being the projector onto  $\mathcal{H}_1$ .*
2.  *$\mathcal{D}$  maps a set  $\mathcal{P}_1$  of  $d_1$  one-dimensional orthogonal projectors on  $\mathcal{H}_1$  onto a set of  $d_1$  one-dimensional orthogonal projectors on  $\mathcal{H}_1$  as well as a totally rotated projector  $P_{TR} \in \mathcal{H}_1$  (with respect to  $\mathcal{P}_1$ ) onto a one-dimensional projector on  $\mathcal{H}_1$ .*
3.  *$\mathcal{D}(\mathbb{1}^{(1)} \oplus 0^{(2)}) = \mathbb{1}^{(1)} \oplus 0^{(2)}$  and there exists a complete and totally rotating set of density*

matrices in  $\mathcal{L}_{\mathcal{H}_1}$  whose spectrum is invariant under  $\mathcal{D}$ .

4.  $\mathcal{D}(\mathbb{1}^{(1)} \oplus 0^{(2)}) = \mathbb{1}^{(1)} \oplus 0^{(2)}$  and there exists a complete and totally rotating set of density matrices  $\mathcal{R}$  in  $\mathcal{L}_{\mathcal{H}_1}$  such that  $\forall \rho \in \mathcal{R}; k = 1, 2, \dots, d : \text{Tr}[(\rho \oplus 0^{(2)})^k] = \text{Tr}[\mathcal{D}(\rho \oplus 0^{(2)})^k]$ .

*Proof.* Following the above argument we can apply Theorem 3.9 to the reduced dynamical map on  $\mathcal{H}_1$  once we made sure that  $\mathcal{D}(\mathbb{1}^{(1)} \oplus 0^{(2)}) = \mathbb{1}^{(1)} \oplus 0^{(2)}$  which also automatically implies unitality of the reduced map. Note that if the set  $\mathcal{P}_1$  is mapped onto another set of  $d_1$  one-dimensional orthogonal projectors on  $\mathcal{H}_1$  this automatically implies  $\mathcal{D}(\mathbb{1}^{(1)} \oplus 0^{(2)}) = \mathbb{1}^{(1)} \oplus 0^{(2)}$  since  $\mathcal{D}$  is linear and  $\mathbb{1}^{(1)} \oplus 0^{(2)}$  is equal to the sum over all elements of an arbitrary set of one-dimensional orthogonal projectors on  $\mathcal{H}_1$ . Finally, note that the reduced map  $\mathcal{D}_1$  is well-defined since  $P_1 \mathcal{D}(\rho \oplus 0^{(2)}) P_1$  is guaranteed to have the form  $\bar{\rho} \oplus 0^{(2)}$  due to the projector sandwich  $P_1(\cdot)P_1$ .  $\square$

Corollary 5.1 allows us to use input states on the logical subspace to assess whether a given dynamical map is unitary on the logical subspace. Then, the results of Sec. 3 can be immediately applied on this subspace with respect to unitary identification. All fidelities from Sec. 5.4 can be straightforwardly translated to tensor sum Hilbert spaces if one considers the reduced set of density matrices as elements of the logical subspace undergoing a tensor sum with the zero operator on the remaining Hilbert space. As a result, one obtains in all cases reliable and encompassing fidelities for optimisation of unitary transformation on the logical subspace.

The situation for a tensor product partitioning of the total Hilbert space is more complicated since arguments involving projectors only work for tensor sum decompositions. If  $O_1$  is the target unitary transformation on  $\mathcal{H}_1$  then any  $O = O_1 \otimes O_2$  will result in an evolution that corresponds to the unitary  $O_1$  on  $\mathcal{H}_1$  for an arbitrary unitary  $O_2 \in L(\mathcal{H}_2)$ . This makes it difficult to create an encompassing functional that accounts for all evolutions on the total space which will lead to the target unitary on the product subspace. If the transformation on the total Liouville space is known to be unitary, then it is possible to construct a reliable and encompassing functional with respect to optimisation of unitary transformation on a tensor product subspace, see Ref. [156]. However, the assumption of a unitary evolution on the composite Hilbert space is very strong which is why it is beneficial to search for a more general formulation by relaxing the encompassing property of the resulting functional.

If the initial state of  $\mathcal{L}_{\mathcal{H}_2}$  is known, e.g. if  $\mathcal{H}_2$  represents some degrees of freedom initially in their ground state, and the states on the subsystems are not entangled we can make the following assumption on the dynamical map for the target evolution  $\mathcal{D}_0$ ,

$$\forall \rho^{(1)} \in \mathcal{L}_{\mathcal{H}_1} : \mathcal{D}_0(\rho^{(1)} \otimes \rho_0^{(2)}) = O_1 \rho^{(1)} O_1^\dagger \otimes \rho_0^{(2)}. \quad (5.48)$$

Then, we can consider a tensor sum decomposition of  $\mathcal{L}_{\mathcal{H}}$  as  $\mathcal{L}_{\mathcal{H}} = \mathcal{L}_\alpha \oplus \mathcal{L}_\beta$  with  $\mathcal{L}_\alpha$  spanned by the set  $\{\rho_k^{(1)} \otimes \rho_0^{(2)}\}_k$  where  $\{\rho_k^{(1)}\}_k$  is a complete orthonormal set in  $\mathcal{L}_{\mathcal{H}_1}$  and  $\rho_0^{(2)}$  is the known initial state on  $\mathcal{L}_{\mathcal{H}_2}$ . It follows directly from Eq. (5.48) that an optimal transformation leaves the subspace  $\mathcal{L}_\alpha$  invariant. Hence, we can interpret  $\mathcal{L}_\alpha$  as a logical subspace and the results derived above for tensor sums can be applied straightforwardly as long as  $\rho_0^{(2)}$  is pure<sup>39</sup>. The resulting functional is reliable in terms of implementing  $O_1$  on  $\mathcal{H}_1$  but not encompassing since we restricted the set of ideal

<sup>39</sup>If  $\rho_0^{(2)}$  is not pure, the optimisation functionals need to be formulated with respect to mixed states which requires special care, cf. Sec. 5.4.

transformations according to Eq. (5.48). It is possible to relax the restriction via Eq. (5.48) slightly by not requiring the states  $\rho_0^{(2)}$  to be the same on both sides of the equation<sup>40</sup>. In this case one needs to consider a reduced map that not only projects but also rotates the subspace  $\mathcal{L}_{\mathcal{H}_2}$  appropriately. Nevertheless, in most cases the assumption of Eq. (5.48) is not too restrictive. A common example for Eq. (5.48) representing a sensible assumption is given if the Liouville space  $\mathcal{L}_{\mathcal{H}_2}$  has a natural steady state in the absence of control fields, e.g. by being coupled to a  $T \simeq 0\text{K}$  bath. We will discuss a corresponding example in Sec. 7.5.

Corollary 5.1 can be also applied to formulate a functional that optimises an evolution to be as unitary as possible on a certain (tensor sum) subspace  $\mathcal{H}_S \subset \mathcal{H}$  with  $d = \dim \mathcal{H}_S$ . If we consider a complete and totally rotating set of density matrices on  $\mathcal{H}_S$  together with the completely mixed state  $\frac{1}{d}\mathbb{1}_{\mathcal{H}_S}$ ,  $\{\rho_k\}$ , then, by the equivalence (1)  $\iff$  (4) of Corollary 5.1, the functional

$$J_U = \sum_k \sum_{l=1}^d \text{Tr}^2 \left[ \mathcal{D}_T (\rho_k)^l - \rho_k^l \right] \quad (5.49)$$

is a reliable and encompassing functional for optimising towards a unitary evolution on  $\mathcal{H}_S$ . We used abbreviate notation by skipping the explicit tensor sum with 0 on  $\mathcal{H}/\mathcal{H}_S$ . This functional can be employed for example in the search of decoherence-free subspaces [157] under a non-unitary open system evolution.

## 5.6 Numerical Analysis of Reduced Optimisation Functionals

Functionals that are based on reduced fidelities are reliable and encompassing but they usually do not exhibit a straightforward relationship to the process fidelity/average fidelity, cf. Sec. 3. This can have disadvantageous effects on the convergence behaviour of a numerical control algorithm with respect to the average fidelity. Conversely, the fact that only a significantly smaller set of input states needs to be propagated to construct a reliable and encompassing optimisation functional leads to a decrease in the computational effort. We will briefly illustrate the interplay between these effects with two numerical examples, for more details see Ref. [127].

For the first example, we consider a bilinear control Hamiltonian as in Eq. (5.22) with a single control  $u_1(t)$  where  $H_0$  and  $H_1$  are diagonal in the same basis. All unitaries this control Hamiltonian can generate are as a result also diagonal in that basis. The control will only influence the eigenvalues of the unitary, i.e. the phases. We furthermore consider the case when the projectors for basis completeness in the employed minimal complete and totally rotating set are diagonal in the eigenbases of  $H_0$  and  $H_1$ . In this event the state fidelities corresponding to these density matrices in the functional will be completely insensitive to the phases. As a consequence, the whole burden of optimisation is put onto the totally rotating part. Generally speaking, the choice of optimisation functional is of great importance for the shape of the optimisation landscape, allowing the optimisation algorithm to see hills and valleys through which it tries to find extremal points. If only a small part of the functional is actually sensitive to the most relevant property in the optimisation (the phases in the above example), then the hills and valleys will be less pronounced which inhibits the ability of the algorithm to see the correct path in the landscape towards an optimal solution. If one is aware

<sup>40</sup>However, the resulting state on  $\mathcal{L}_{\mathcal{H}_2}$  on the right-hand side of Eq. 5.48 needs to be independent on  $\rho^{(1)}$ , otherwise one cannot perform the required tensor sum decomposition.

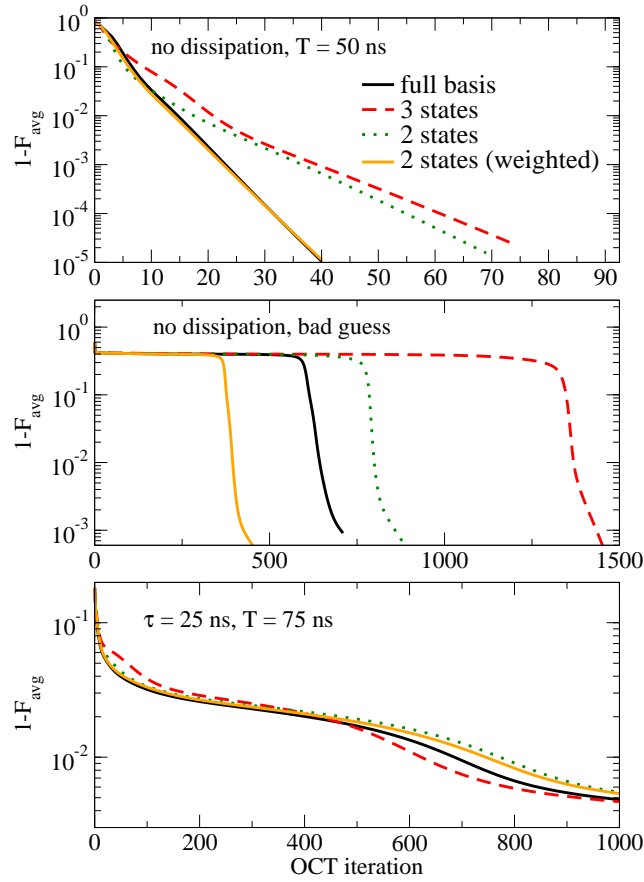


Figure 5.1: Convergence behaviour when optimising a controlled phase gate for two qubits, each represented by eigenstates of a trapped neutral atom. The control mechanism is given by excitation to a Rydberg state. The convergence is shown as the gate error,  $1 - F_{\text{avg}}$ , over OCT iterations, using the full basis of 16 states (solid black lines), as well as a reduced set of three states (red dashed lines) and a reduced set of two states (green dotted and orange solid line). The calculations employ equal weights for all states, except for those shown in orange where  $\lambda_2/\lambda_3 = 10$ , cf. Eq. (5.50). The top and middle panels show optimisations without any dissipation; the middle panel shows a calculation with the same parameters as the top panel except for the guess pulse, which is badly chosen. More details on this optimisation can be found in Ref. [127].

of this problem and the Hamiltonian admits such a special structure it can be advisable to rescale individual contributions to the functional to account for what is actually important in the specific problem at hand. Note that these observations are the analogue of the analysis in Sec. 4.5 from an OCT perspective.

Figure 5.1 shows the results of a numerical optimisation for such an optimisation problem in which only diagonal unitaries can be generated. The minimal set of states employed here is given by the three states

$$(\rho_1)_{ij} = \frac{2(d-i+1)}{d(d+1)}\delta_{ij}, \quad (\rho_2)_{ij} = \frac{1}{d}, \quad (\rho_3)_{ij} = \frac{1}{d}\delta_{ij}.$$

The employed functional for this minimal set is given by<sup>41</sup>

$$J_T^{(\min)} = - \sum_{k=1}^3 \frac{\lambda_k}{\langle \rho_k, \rho_k \rangle_{\text{HS}}} \langle \mathcal{D}_T(\rho_k), \mathcal{U}_O(\rho_k) \rangle_{\text{HS}}, \quad (5.50)$$

where we normalised the contributions to the fidelity according to the initial purity and allowed in addition for weighting factors  $\lambda_k$  for the individual states. This is motivated by the rescaling of individual contributions discussed above. In the absence of any dissipative effects the influence of proper weighting can be easily seen, compare the green and orange curve in Fig. 5.1. The green curve shows an optimisation using the minimal set of states while omitting the state  $\rho_1$  in the optimisation functional, since it contains no information about the optimisation progress. It performs, as expected, better than the red curve which contains all three states of the minimal set. If additional weighting is employed by increasing the emphasis on acquiring the proper phases, then the performance matches the one of the full basis. Note that despite the similar convergence speed in terms of OCT iterations, the numerical effort is much lower for the minimal set since it requires propagation of 2/3 matrices instead of the full basis of 16 matrices in Liouville space.

With the inclusion of dissipative effects the optimisation problem becomes harder since not only does the correct unitary need to be implemented but it is also now necessary to obtain a unitary dynamical map in the first place. This leads to a shift in the main task of the optimisation and all states in the minimal set are roughly equally sensitive to it. This is reflected in the numerical results which show similar behaviour for all employed sets of states, see Fig. 5.1. Note that due to the specific form of the dissipators in this optimisation problem an optimisation functional with only 2 states is reliable for this problem [127].

Figure 5.2 shows the result of numerical optimisations for a different physical example in which the reachable set of unitaries generated is not restricted to only diagonal ones. It can be clearly seen that the minimal sets do not make up their loss in comparability with the average fidelity with a sufficient increase in speed except in the asymptotic region of convergence. In contrast, the sets involving more states, using 5 states according to Eq. (5.42) respectively 8 states according to Eq. (5.43), perform better at each stage of the optimisation. Similar to the situation observed in Fig. 5.1, introducing a weighting for the minimal set improves the convergence behaviour in this problem. In the corresponding optimisations seen in Fig. 5.2 the mixed state  $\rho_1$  has been weighed 10 times more than either  $\rho_2$  and  $\rho_3$ . This is motivated by the fact that  $\rho_2$  only contains information about a single direction in Hilbert space (since it is pure) and  $\rho_3$  is insensitive with respect to specific unitaries (since all unitaries on the subspace map the totally mixed state onto itself). When accounted for this fact, the optimisation immediately converges faster. By employing a suitable weighting in the functional we conveyed the actual importance of the individual terms in the functional to the algorithm. While adjusting functionals to the specific needs of the optimisation is powerful, we can see from the results in Fig. 5.2 that the functionals which have at least some bound towards the average fidelity perform well even in the absence of such weighting.

We conclude from the above numerical analysis that reduced fidelities can be used to speed up convergence by reducing the amount of states that need to be propagated. Moreover, due to

<sup>41</sup>  $J_T^{(\min)}$  is not normalised such that it becomes 0 if the target is reached. In particular, it can become negative. If desired, this can be amended by an additive constant. However, from the point of view of the optimisation algorithm such an additive constant does not lead to different behaviour, i.e. it is merely a matter of aesthetics. Note that in all figures not the optimisation functional but the gate error, i.e. one minus the average fidelity, is displayed.

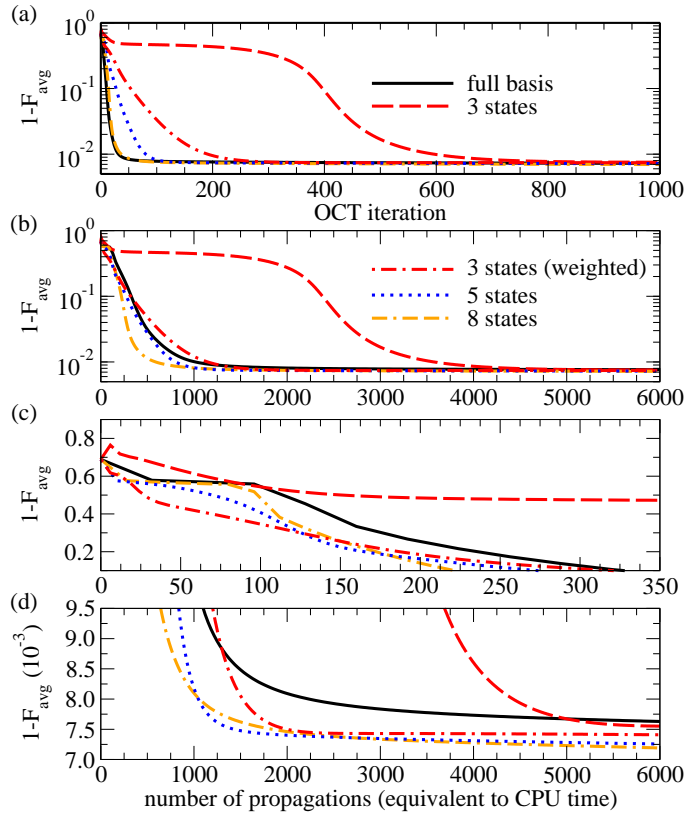


Figure 5.2: Convergence behaviour when optimising towards a  $\sqrt{i\text{SWAP}}$  gate in an implementation of two transmon qubits undergoing energy relaxation and pure dephasing. The panels from top to bottom show the gate error over the number of iterations; the gate error over the number of state propagations, indicative of the required CPU time; a zoom on the initial phase of the optimisation; and a zoom on the asymptotic convergence (panels (c) and (d) both using a linear scale). The number of propagations (x-axis in panels (b)-(d)) is a linear rescaling of the number of OCT iterations (x-axis in panel (a)), with 2 propagations per iteration and state, i.e. the lines of panel (a) are rescaled differently depending on the respective number of states. Since all panels only show different views on the same data, the line colours and styles are the same in all of them. More details on this optimisation can be found in Ref. [127].

fewer states entering the functional, the required memory to store these states during the numerical optimisation also goes down significantly. Among the reduced fidelities,  $J_{d+1}$  and  $J_{2d}$  perform best and do not require additional weighting of individual contributions to surpass optimisations utilising the full basis of Liouville space in their performance.



## 6 A Quantum Control Perspective on Cooling

Markovian open system evolutions represent environmental effects on a physical system that cannot increase the distinguishability of an arbitrary set of input states [139]. It is not difficult to see that a Markovian dynamics can only implement a unitary transformation if it is perfectly noiseless, i.e. if the system behaves like a closed quantum systems - we will briefly illustrate this in Sec. 6.1. From this perspective it is evident that Markovian open system evolutions do not yield any benefit in terms of realising unitary quantum gates. Nevertheless, it turns out that certain physical tasks are not only enhanced by an environment inducing such Markovian evolutions, but they are enabled by it in the first place. An important example for such a task is an evolution that aims to steer an arbitrary initial ensemble to a single pure state. Generally speaking, from the perspective of quantum information, the preparation of pure states as input states for quantum computation is of crucial importance as outlined by one of the so-called DiVincenzo criteria, representing one of the most widely accepted set of requirements towards the physical realisation of a quantum computer [158]. A common approach to achieve this goal is to cool the system to its (pure) ground state which allows to achieve arbitrary pure states via a suitable subsequent unitary transformation. We will present an example for the implementation of unitaries in open quantum systems via optimal control in Sec. 7 and focus on the cooling part in this section.

We will demonstrate how optimal control can be used to find control schemes that efficiently perform cooling tasks and discuss a specific example of great experimental interest: the vibrational cooling of molecules [159, 160]. Cooling via optical pumping makes use of the simplest quantum reservoir, the vacuum of electric field modes, and has led to the concept of quantum reservoir engineering [161]. We will show how control schemes derived from physical intuition can be translated into the mathematical formulation of a suitable optimisation functional. Due to the timescale separation of optical pumping and radiative decay in the context of vibrational cooling of molecules, the dissipative part of the evolution can be treated implicitly in the numerical simulation of the molecular dynamics. We find that control pulses obtained via optimal control show a significant performance boost with respect to simple experimental techniques like e.g. spectral cut-offs. We will discuss our numerical results extensively and we will show, that optimal control can successfully find cooling schemes that are applicable even if the molecular structure is inconvenient for vibrational cooling.

We finish this section by sketching a path towards generalised cooling via the cooling schemes derived for vibrational cooling. We will explicitly discuss these ideas in the framework of cavity QED, which proves to be a field of great current theoretical and experimental interest [162–164]. The analysis of the underlying Jaynes-Cummings Hamiltonian in terms of preparation of arbitrary control of the mode of a quantum electromagnetic field has been first performed by Law and Eberly [165] with improvements using numerically optimised schemes reported by Mischuk and Mølmer [166] in the context of superconducting qubits. Transformation of the state of a cavity from an unknown initial ensemble to a certain desired pure state with the help of atoms flying through the cavity has been experimentally realised by Deléglise et al. [167]. We will outline the ideas required to generalise the optimisation functionals we developed for vibrational cooling, leading to a powerful tool in the context of quantum reservoir engineering.

The optimal control approach for vibrational cooling of molecules has been published in Ref. [168].

## 6.1 Cooling, Markovian Evolutions and Quantum Control

How can we use optimal control to find an evolution that maps an arbitrary initial state of a physical system to a predefined pure state? If the pure state that shall be reached is the ground state of the system Hamiltonian, this is nothing more than the mathematical description of an ideal cooling process<sup>42</sup>. As a matter of fact, a unitary evolution can actually never implement such a transformation since unitary transformations are bijective, i.e. any target state of such a transformation must have a unique state it originates from. This implies that no two distinct states can ever be mapped to the same state. In particular, no proper mixed state can be mapped to a pure state; unitary transformations cannot lead to so-called purification since they preserve entropy. However, a Markovian, non-unitary evolution can lead to such an effect which we want to briefly illustrate with a simple example.

Consider a single qubit evolving according to the Lindblad master equation, Eq. (5.16), with a Hamiltonian  $H = 0$  and a single Lindblad operator  $L_1 = \begin{pmatrix} 0 & 1 \\ 0 & 0 \end{pmatrix}$  with  $\gamma_1 = \frac{\Gamma}{2}$  for some  $\Gamma > 0$ . Then, an arbitrary density matrix  $\rho(0) = \begin{pmatrix} \rho_{00} & \rho_{01} \\ \rho_{10} & \rho_{11} \end{pmatrix}$  at initial time  $t = 0$  will evolve to the following form at time  $t$ ,

$$\rho(t) = \begin{pmatrix} 1 - \rho_{11}e^{-\Gamma t} & \rho_{01}e^{-\frac{\Gamma}{2}t} \\ \rho_{10}e^{-\frac{\Gamma}{2}t} & \rho_{11}e^{-\Gamma t} \end{pmatrix}. \quad (6.1)$$

In particular, independent on  $\rho(0)$ , in the limit  $t \rightarrow \infty$  the state of the system will evolve to the pure state  $\begin{pmatrix} 1 & 0 \\ 0 & 0 \end{pmatrix}$ . Such a state is called a fixed point of the evolution, and in the above case it is unique. In other words, the problem of ideal cooling can be translated to engineering a dissipative evolution which has the ground state of the system as its unique fixed point.

We want to briefly illustrate that the enabling of the cooling task via a Markovian evolution is diametrically opposed to realising unitary operations in such a quantum system. As discussed in Sec. 5, a Markovian open system evolution admits an arbitrary decomposition into a series of dynamical maps. Clearly, a dynamical map is unitary if and only if it maps arbitrary pairs of orthogonal rank 1 projectors onto orthogonal rank 1 projectors<sup>43</sup>. It can be shown [6] that the state fidelity is monotonic under any dynamical map, i.e. for any two density matrices  $\rho, \sigma$  and any dynamical map  $\mathcal{D}$

$$F_{\text{state}}(\mathcal{D}(\rho), \mathcal{D}(\sigma)) \geq F_{\text{state}}(\rho, \sigma). \quad (6.2)$$

Since Markovian evolutions are concatenation of dynamical maps this means that for any two density matrices at some time  $t_0$ ,  $\{\rho(t_0), \sigma(t_0)\}$ , that undergo a Markovian evolution, the following relation

<sup>42</sup>Such a process is of course not possible in reality due to the third law of thermodynamics but optimal control is about finding the best solution towards a certain goal, not necessarily reaching that goal.

<sup>43</sup>For the “if” part, consider that the mapping of arbitrary pairs of orthogonal rank 1 projectors to orthogonal rank 1 projectors implies that we can in particular consider pairs of a set of complete projectors. This shows that a complete set of orthogonal rank 1 projectors will be mapped onto another complete set of orthogonal rank 1 projectors. Now, consider a totally rotated projector which, by assumption, will also be mapped onto a rank 1 projector. Then, by Theorem 3.9, the map must be unitary. For the “only if” part, note that the Hilbert-Schmidt product is invariant if both arguments are subject to a unitary transformation. In particular, this means that for any two orthogonal rank 1 projectors  $P_i, P_j$  the state fidelity  $F_{\text{state}}(\mathcal{D}(P_i), \mathcal{D}(P_j))$ , cf. Eq. (4.16), must be equal to zero for the dynamical map to be unitary, corresponding to orthogonality of the images.

holds for all times  $t_1 \geq t_0$ ,

$$F_{\text{state}}(\rho(t_1), \sigma(t_1)) \geq F_{\text{state}}(\rho(t_0), \sigma(t_0)) .$$

If at some final time  $T$  the Markovian evolution is supposed to represent a unitary transformation, this means consequently that

$$\forall t \in [0, T] : F_{\text{state}}(\mathcal{D}_t(P_i), \mathcal{D}_t(P_j)) = 0 , \quad (6.3)$$

for all pairs of orthogonal rank 1 projectors  $\{P_i, P_j\}$ , where  $\mathcal{D}_t$  represents the evolution from time 0 to time  $t$ . In particular, this means that the Markovian evolution needs to be unitary at all points in time. As a conclusion, a Markovian evolution can only generate a unitary dynamical map if its dissipator vanishes, i.e. if the Liouvillian can be substituted by a Hamiltonian. Markovian noise will consequently always be harmful when the optimisation goal is a unitary transformation. Note however, that non-Markovian noise does not necessarily follow this rule which we will exploit in Sec. 7.

In contrast to the destructive properties in terms of achieving a unitary gate, we see that from the perspective of cooling, or equivalently pure state preparation, the environment represents a fundamental resource. This can be seen as a special case of quantum reservoir engineering [161, 169–171] where methods of coherent control are employed to steer the interaction between system and environment for particular control tasks. In the section we will demonstrate how OCT can be used to find controls that use the environment to purify arbitrary initial states of the system towards a unique pure state. We start with the specific example of vibrational cooling of molecules, where the goal is to reach the vibrational ground state of the ground electronic surface from an initial arbitrary incoherent mixture of vibrational eigenstates on the ground electronic surface.

## 6.2 Laser Cooling

Laser cooling of atoms or molecules relies on the repeated excitation and spontaneous emission of light [172]. When the atom or molecule reaches a dark state, i.e. a state that does not interact with the laser light, it escapes from the cooling cycle. If this occurs before the particle is sufficiently cooled, repumping is required. The presence of too many levels that act as dark states has prevented laser cooling to work for most molecular species. However, dark states can also be used to an advantage in laser cooling when they are populated only by the cooled particles. This is utilised for example in subrecoil cooling based on velocity selective coherent population trapping [173]. Dark states also play a crucial role in the laser cooling of internal degrees of freedom [174–176]. The presence of many internal levels requires a broadband optical excitation which can be realised by femtosecond laser pulses. Cooling occurs if the target level is populated by spontaneous emission but remains dark to the laser pulse [175, 176]. The dark state can be realised by destructive interference or simply by removing the frequency components corresponding to excitation of the target level. The latter has recently been realised experimentally, resulting in successful demonstration of laser cooling of vibrations [159, 160, 177–181]. An extension to cooling rotations is feasible as well [182–184].

In the experiments of Refs. [159, 160, 177–180, 183, 184], cooling the internal degrees of freedom by broadband optical pumping was preceded by standard laser cooling of atoms to temperatures of

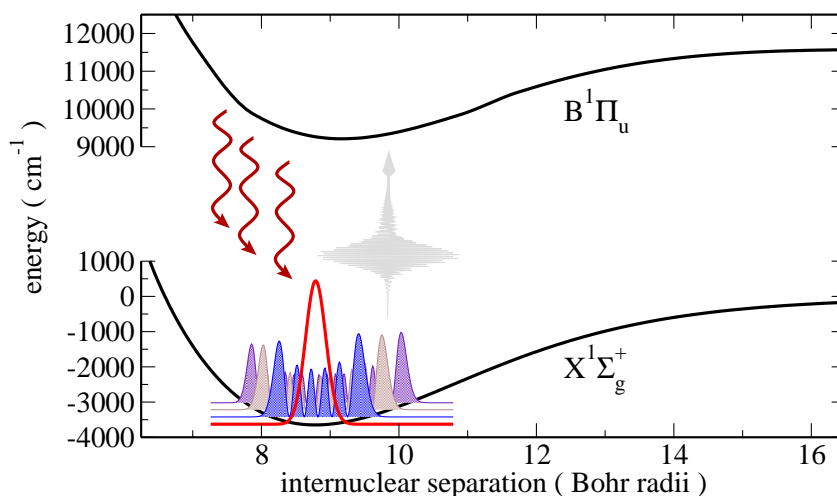


Figure 6.1: Potential energy curves of the  $\text{Cs}_2$  electronic states employed for the vibrational cooling by optimised optical excitation and spontaneous emission. The vibrational ground state (red solid curve) is the target state of the optimisation, vibrationally excited states (shown here  $v = 5, 10, 15$ ) make up the initial incoherent ensemble.

the order of  $100 \mu\text{K}$  and then photoassociating the atoms into weakly bound excited state molecules. Photoassociation [185, 186] is followed by spontaneous emission, yielding molecules in the ground electronic state. Depending on the choice of excited state potential, a significant part of the molecules might end up in ground state levels with comparatively small vibrational quantum numbers [159, 179]. The internal degrees of freedom of these molecules can be laser cooled by broadband optical pumping as illustrated in Fig. 6.1: An incoherent ensemble of molecules in different vibrational levels of the electronic ground state is excited by a broadband laser pulse to an electronically excited state. The electronically excited molecules will decay by spontaneous emission back to the ground state. The branching ratio for the different ground state vibrational levels is determined by the Franck-Condon factors or, more precisely, transition matrix elements, between ground and excited state levels. Some decay will always lead to the ground vibrational level. Repeated broadband optical pumping then accumulates the molecules in the ground vibrational level [159].

The overall cooling rate is determined by the timescale of the dissipative step, i.e. the spontaneous emission lifetime [174–176]. It cannot be modified by the coherent interaction of the molecules with the laser pulse. However, the pulses can be shaped such as to populate those excited state levels which preferentially decay into the target level. We will show that this minimises the number of required optical pumping cycles. Moreover, we will demonstrate that optimal pulse shapes allow for cooling even in cases where the Franck-Condon map is preferential to heating rather than cooling. This is the case when the excited state levels show similar Einstein coefficients for many ground state vibrational levels. Rather than accumulating the molecules in a single target level, spontaneous emission then distributes the population incoherently over many levels, effectively heating the molecules up.

The coherent interaction of the molecules with the laser pulse, on the order of 10 ps, takes place on a very different timescale the spontaneous decay with excited state lifetimes of the order of 10 ns. It is consequently not numerically feasible to treat the full dissipative dynamics of the excitation/spontaneous emission cycle. Seeking a pulse that populates only those excited state levels with the largest Einstein coefficients with the target ground state level allows us to treat the decay

implicitly. With this approach the actual propagation in terms of the control algorithm can take place in Hilbert space where we use our knowledge of the nature of the radiative Markovian decay to prepare “optimal” initial states for the dissipation in terms of the cooling goal. In the end, we aim for the total ground state to be the steady state of the evolution given by iterated excitation/decay cycles with the initial state being restricted to some finite-dimensional subspace of the electronic ground state manifold.

The two optimisation functionals realise different cooling mechanisms: One is based on optical pumping from all thermally populated ground state levels symmetrically, whereas the other one forces the thermally populated ground state levels into an “assembly line”. Only the first level in the line is transferred to the excited state while population from all other levels is reshuffled, one after the other, via Raman transitions into the first level. This suppresses heating actively and allows us to answer the question of what is the fundamental requirement of the molecular structure to allow for cooling. By imposing a certain cooling mechanism via the functional we forego its property to be encompassing but we stay reliable as we will show in Sec. 6.6. This presents also a way to “lead” the algorithm towards physically motivated solutions by not only prescribing the goal one has in mind but also a path that leads towards this goal. This reduction of complexity greatly increases numerical tractability and reduces the search space for the optimisation algorithm with the only downside being that one limits oneself to find only the solutions that are in accordance with the process one already has in mind.

### 6.3 Model for Optical Pumping Utilising Timescale Separation

We consider  $\text{Cs}_2$  and  $\text{LiCs}$  molecules in their electronic ground state after photoassociation and subsequent spontaneous emission. The excited state for optical pumping is chosen to be the  $B^1\Pi_u$  state as in the experiment for  $\text{Cs}_2$  molecules of Refs. [159, 160, 177, 178]. This state is comparatively isolated such that population leakage to other electronic states due to e.g. spin-orbit interaction is minimal. Neglecting polarisation effects, the Hamiltonian describing the interaction of the molecules with shaped femtosecond laser pulses in the rotating-wave approximation reads

$$H = \begin{pmatrix} T + V_{X^1\Sigma^+}(R) & \frac{1}{2}\epsilon^*(t)\mu \\ \frac{1}{2}\epsilon(t)\mu & T + V_{B^1\Pi}(R) - \omega_L \end{pmatrix}, \quad (6.4)$$

where  $T$  denotes the vibrational kinetic energy.  $V_g = V_{X^1\Sigma^+}(R)$  and  $V_e = V_{B^1\Pi}(R)$  are the potential energy curves as a function of interatomic separation,  $R$ , of the electronic ground and excited state (note that for  $\text{Cs}_2$  the  $X$  state is of gerade symmetry and the  $B$  state of ungerade symmetry).  $\mu$  is the transition dipole moment, approximated here to be independent of  $R$ . The laser pulse is characterised by its carrier frequency,  $\omega_L$ , and complex shape,  $\epsilon(t) = |\epsilon(t)|e^{i\phi(t)}$ , with the time-dependent phase  $\phi(t)$  referenced to the phase of the carrier frequency. The potential energy curves are found in Refs. [187] and [188] for the electronic ground state and in Refs. [189] and [190] for the electronically excited state of  $\text{Cs}_2$  and  $\text{LiCs}$ , respectively. For the numerical simulation of the wave packet dynamics under the Hamiltonian in Eq. (6.4) we used a representation on a Fourier grid [191] and we employed a Chebyshev propagator [192] for the solution of the Schrödinger equation.

The decay of the excited state molecules back to the electronic ground state is described by the

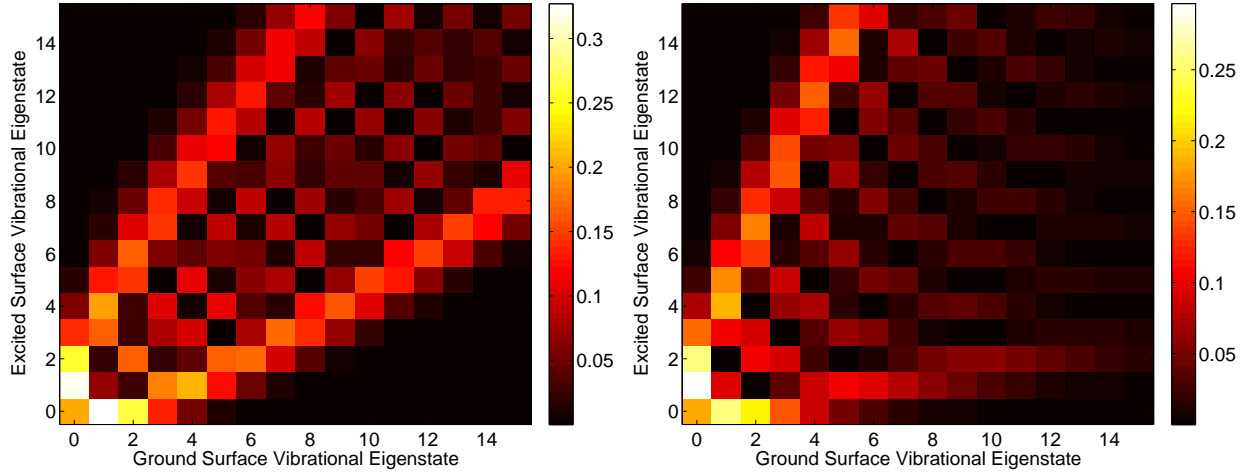


Figure 6.2: Franck-Condon map,  $\langle \varphi_{v'}^B | \mu | \varphi_{v''}^X \rangle$ , as a function of ground and excited state levels,  $v''$  and  $v'$ , respectively, for  $\text{Cs}_2$  (left) and  $\text{LiCs}$  (right). Optical pumping at the right edge of the compact parabola for  $\text{Cs}_2$  ensures cooling. This is in contrast to  $\text{LiCs}$  where absence of a compact boundary of the large transition matrix elements implies spontaneous emission towards levels with larger  $v''$ , i.e. heating.

spontaneous emission rates,

$$\gamma_{v'J'}^d = \sum_{v''J''} A_{v'J',v''J''}. \quad (6.5)$$

The Einstein coefficients  $A_{v'J',v''J''}$  are determined by the Franck-Condon factors,

$$A_{v'J',v''J''} = \frac{4\alpha^3}{3e^4\hbar^2} H_{J'} (E_{v'J'} - E_{v''J''})^3 \left| \langle \varphi_{v'J'}^B | \mu | \varphi_{v''J''}^X \rangle \right|^2, \quad (6.6)$$

where  $H_{J'}$  is the Hönl-London factor equal to  $(J'+1)/(2J'+1)$  for  $J' = J'' - 1$  and equal to  $J'/(2J'+1)$  for  $J' = J'' + 1$ ,  $\alpha$  denotes the fine structure constant and  $e$  the electron charge.  $|\varphi_{v''J''}^X\rangle$  and  $|\varphi_{v'J'}^B\rangle$  are the rovibrational eigenstates of the  $X^1\Sigma^+$  electronic ground state and the  $B^1\Pi$  excited state, respectively. We will neglect rotations in the following since the Einstein coefficients are essentially determined by the Franck-Condon factors,  $\langle \varphi_{v'J'}^B | \mu | \varphi_{v''J''}^X \rangle \approx \langle \varphi_{v'0}^B | \mu | \varphi_{v''0}^X \rangle$ .

Figure 6.2 displays the Franck-Condon map that governs the spontaneous emission for  $\text{Cs}_2$  and  $\text{LiCs}$ . A compact parabola of large transition matrix elements is observed for  $\text{Cs}_2$ , cf. left-hand side of Fig. 6.2. Excitation at the right edge of this parabola can be ensured by removing part of the broadband spectrum [159]. Spontaneous emission then will occur to levels with  $v'' \leq v''_{\text{initial}}$ , and repeated cycles of broadband excitation and spontaneous emission results in vibrational cooling [159]. The situation changes completely for  $\text{LiCs}$ , cf. right-hand side of Fig. 6.2. There is no strict separation between large and small transition matrix elements, and a given excited state level has many non-zero transition matrix elements of similar magnitude. Spontaneous emission will thus spread the population, and even worse, will do so preferentially toward levels with  $v'' \geq v''_{\text{initial}}$ , leading to heating rather than cooling. In the following two subsections we will derive optimisation functionals towards cooling schemes that circumvent these issues.

## 6.4 Symmetric Cooling

The main idea of this functional is to excite all vibrationally excited ground state levels symmetrically into those excited state levels which preferentially decay toward the target state  $|\varphi_0^g\rangle$  while minimising potential heating. Symmetric excitation ensures that all ground state levels in the thermal ensemble are treated homogeneously. The initial state for each laser pulse is given by an unknown incoherent distribution over ground state vibrational levels,  $|\psi_i(0)\rangle = |\varphi_i^g\rangle$ ,  $i = 1, \dots, n_{max}$ . Each of these levels is excited by the pulse and subject to the ensuing dynamics, giving rise to wavepackets  $|\psi_i(t)\rangle$  which decay by spontaneous emission to ground state vibrational levels. The spontaneous decay of the excited state component of the  $i$ -th wavepacket  $|\psi_i(t)\rangle$  to the target level  $|\varphi_0^g\rangle$  is determined by the temporally averaged overlap,

$$\sigma_i = \frac{1}{T_e} \int_T^{T+T_e} |\langle \psi_i(\tau) | P_e \mu | \varphi_0^g \rangle|^2 d\tau, \quad (6.7)$$

where  $T_e$  denotes the excited state lifetime and  $P_e$  is the projector onto the excited electronic state. Shifting the time axis by  $-T$ , inserting the completeness relation for vibrational levels on the excited state and denoting the Franck-Condon factors  $\langle \varphi_n^e | \mu | \varphi_m^g \rangle$  by  $\eta_{nm}$ , Eq. (6.7) becomes

$$\sigma_i = \frac{1}{T_e} \int_0^{T_e} \sum_{n,m} e^{i(E_n^e - E_m^e)t} \eta_{n0} \eta_{m0}^* \langle \psi_i(T) | \varphi_n^e \rangle \langle \varphi_m^e | \psi_i(T) \rangle dt,$$

where  $E_n^e$  is the eigenenergy corresponding to  $|\varphi_n^e\rangle$ . The integral is readily evaluated, yielding

$$\sigma_i = \sum_{n \neq m} \frac{1}{iT_e(E_n^e - E_m^e)} \left( e^{i(E_n^e - E_m^e)t} - 1 \right) \eta_{n0} \eta_{m0}^* \langle \psi_i(T) | \varphi_n^e \rangle \langle \varphi_m^e | \psi_i(T) \rangle + \sum_n |\eta_{n0}|^2 |\langle \psi_i(T) | \varphi_n^e \rangle|^2.$$

Due to the timescale separation,  $1/(T_e(E_n^e - E_m^e))$  is at most of the order  $10^{-4}$ , and the temporally averaged overlap is well approximated by the second term alone,

$$\sigma_i = \sum_n |\eta_{n0}|^2 |\langle \psi_i(T) | \varphi_n^e \rangle|^2. \quad (6.8)$$

The timescale separation also allows for neglecting the accidental creation of coherences in the ground state density matrix after each cooling cycle. While the initial ensemble most likely is a completely incoherent mixture, the state obtained on the ground electronic surface after one cooling cycle may contain coherences. Accidentally, this could lead to accumulation of molecules in an undesired dark state, i.e. a certain coherent superposition of vibrational eigenstates. However, the free evolution of the molecule introduces rapidly oscillating prefactors for each eigenstate. These oscillations are much more rapid than the time necessary for decay to the ground surface. Therefore, the system will be in a superposition of eigenstates with a fixed modulus but random phase before the next pulse arrives. If necessary, this can be strictly enforced by introducing a small, randomised waiting period between cycles. Since a dark state requires a fixed phase relation, accumulation in the dark state is effectively ruled out.

Ignoring coherences, the initial ensemble for each pulse is described only in terms of the vibrational

populations, and maximising the excitation of each vibrational level corresponds to minimising

$$J_{\text{yield}} = 1 - \sum_{n=1}^{n_{\text{max}}} \sigma_n . \quad (6.9)$$

Note that minimising  $J_{\text{yield}}$  also maximises the decay to the target level, since  $\sigma_n$  accounts for the matrix elements governing spontaneous emission, cf. Eq. (6.8). Symmetric excitation of all levels is ensured by balancing the yield with respect to an arbitrarily chosen level out of the initial ensemble,  $1 \leq n^* \leq n_{\text{max}}$ ,

$$J_{\text{sym}} = \sum_{n=1(n \neq n^*)}^{n_{\text{max}}} (\sigma_n - \sigma_{n^*})^2 . \quad (6.10)$$

$J_{\text{sym}}$  is required because otherwise the yield could be maximised by very efficiently exciting only some levels in the initial ensemble. This would result in incomplete cooling. In addition to efficiently exciting all vibrationally excited ground state levels, the target state must be kept dark. This is achieved by enforcing the steady-state condition,

$$J_{\text{ss}} = 1 - |\langle \varphi_0^g | U(T, 0; \epsilon) | \varphi_0^g \rangle|^2 . \quad (6.11)$$

A further complication arises from the fact that molecules could leave the considered subspace or, in the worst case, even dissociate during the cooling process. This is a source of loss and needs to be strictly prevented. The most efficient way of enforcing this requirement is to avoid leakage out of the initial ensemble of ground state vibrational levels,

$$J_{\text{leak}} = \sum_{m'=n_{\text{max}}+1} \sum_{m=0}^{n_{\text{max}}} |\langle \varphi_{m'}^g | U(T, 0; \epsilon) | \varphi_m^g \rangle|^2 + \sum_{m'=n_{\text{max}}+1} \sum_l \sum_{m=0}^{n_{\text{max}}} |\eta_{lm'}|^2 |\langle \varphi_l^e | U(T, 0; \epsilon) | \varphi_m^g \rangle|^2 . \quad (6.12)$$

The first term in Eq. (6.12) suppresses population transfer, via Raman transitions, from the initial ground state ensemble into higher excited ground state levels, whereas the second term suppresses population of excited state levels that have large Franck-Condon factors with ground state levels outside of the initial ensemble.  $J_{\text{leak}}$  does not only counter dissociation of the molecules but also undesired heating.

The complete final-time functional is given by the multi-objective target of keeping the target state dark, efficiently exciting all other vibrational levels in the initial ensemble and avoiding leakage out of the initial ensemble,

$$J_T^{\text{sym}} = \lambda_{\text{ss}} J_{\text{ss}} + \lambda_{\text{leak}} J_{\text{leak}} + \lambda_{\text{yield}} J_{\text{yield}} + \lambda_{\text{sym}} J_{\text{sym}} , \quad (6.13)$$

where the  $\lambda_j > 0$  allow to weight the separate contributions differently. The functional (6.13) will yield optimised pulses that cool when used in repeated excitation/deexcitation cycles, unless the molecule under consideration has a Franck-Condon map that strongly favours heating rather than cooling such that simultaneously fulfilling all targets imposed by the functional becomes very difficult. This raises the question concerning the minimum requirement on the transition matrix elements to obtain cooling and led us to define a second optimisation functional.

## 6.5 Assembly-Line Cooling

The main idea of this functional is to optimise population transfer to the electronically excited state only for a single ground state level  $n^*$ . The excited state levels that are reached from  $n^*$  need to have Franck-Condon factors that are favourable to cooling (in the extreme case, a single excited state level with favourable Franck-Condon factor is sufficient). The population of all other vibrationally excited ground state levels is simply reshuffled via Raman transitions, populating preferentially  $n^*$ . For example, if the cooling target is the ground state and we choose  $n^* = 1$ , all higher levels are reshuffled into the next lower level, forming an ‘‘assembly line’’ which ends in  $n = n^*$ .

The corresponding functional contains the steady state and leakage terms just as Eq. (6.13). The excitation term now targets only  $n^*$ , taken to be  $n^* = 1$ ,

$$\tilde{J}_{\text{yield}} = 1 - \sigma_1, \quad (6.14)$$

and population reshuffling towards lower vibrational levels is enforced by the assembly-line term,

$$J_{\text{ass}} = 1 - \frac{1}{n_{\text{max}} - 1} \sum_{n=2}^{n_{\text{max}}} |\langle \varphi_{n-1}^g | U(T, 0; \epsilon) | \varphi_n^g \rangle|^2. \quad (6.15)$$

Similarly to Eq. (6.13), the complete final-time functional for assembly line cooling is given by summing all contributions,

$$J_T^{\text{ass}} = \lambda_{\text{ss}} J_{\text{ss}} + \lambda_{\text{leak}} J_{\text{leak}} + \lambda_{\text{yield}} \tilde{J}_{\text{yield}} + \lambda_{\text{ass}} J_{\text{ass}} \quad (6.16)$$

with weights  $\lambda_j > 0$ . In Eq. (6.13), heating is countered only via the leakage term, whereas Eq. (6.16) avoids it actively.

Instead of the square modulus in the overlaps of Eqs. (6.8), (6.11), (6.12), and (6.15), it is also possible to use the real part of the overlap, cf. Sec. 5.4. This sets an unnecessary global phase but shows a better initial convergence for bad guess pulses. The latter is due to the specific form of the ‘‘initial’’ costates,  $|\chi_n^{(i)}(T)\rangle$ , which remain constant for real part functionals while depending linearly on the final-time forward propagated states,  $|\psi_n^{(i)}(T)\rangle$ , for the square modulus functional. As a result, costates for real part functionals cannot take values close to zero leading to very small gradients as is the case for square modulus functionals. This is important in particular for the assembly-line term, for which formulating a good guess pulse is difficult. Our results presented below were obtained with the real part instead of the square modulus in Eq. (6.15).

## 6.6 Optimisation Results for Vibrational Cooling

We choose our guess pulses such as to avoid small gradients at the beginning of the optimisation. In all examples, they are taken to be Gaussian transform-limited pulses of moderate intensity with central frequency and spectral width chosen to excite a number of transitions that are relevant for the cooling process. The latter are easily read off the Franck-Condon matrices in Fig. 6.2. The choice of the  $\lambda_j$  is determined by the relative importance of the individual terms in the optimisation functionals. Large values for the steady-state and leakage terms are crucial since a low value of these functionals will prevent a high repeatability of the excitation/deexcitation steps, effectively reducing

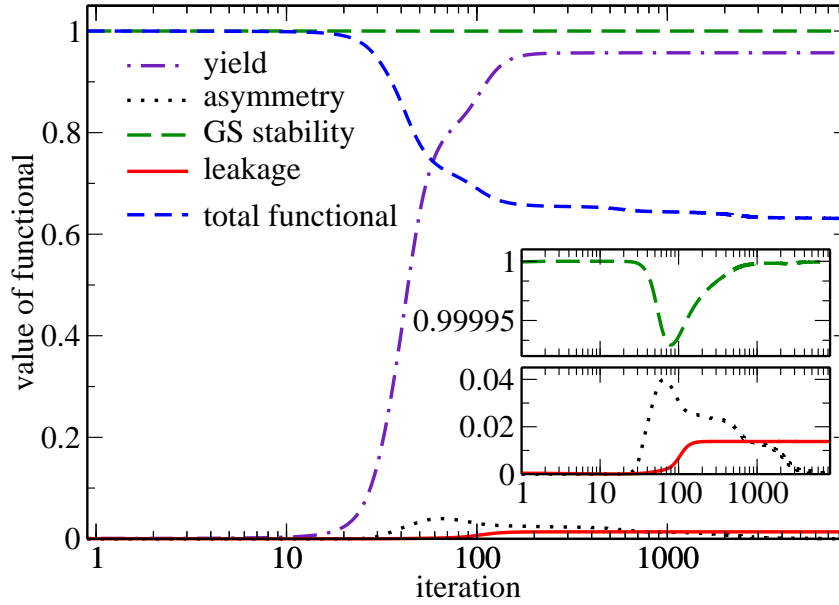


Figure 6.3: Optimising the vibrational cooling of  $\text{Cs}_2$  molecules using symmetrised excitation: Value of the total functional, Eq. (6.13), and its components vs iterations of the optimisation algorithm ( $n_{\text{max}} = 10$ ).

the attainable yield. In contrast, a slightly lower yield for an individual step can easily be amended by additional cycles. Consequently, as a rule of thumb,  $\lambda_{\text{ss}}$  and  $\lambda_{\text{leak}}$  should be chosen larger than  $\lambda_{\text{yield}}$  and  $\lambda_{\text{sym}}$  or  $\lambda_{\text{ass}}$ , respectively. This is more important for the symmetrised cooling since in the assembly line case the leakage is much easier to prevent by virtue of the mechanism. Hence it proved in our calculation sufficient to choose all  $\lambda$  equal to one for the assembly line functional while it proved useful to choose  $\lambda_{\text{leak}} = \lambda_{\text{sym}} = 1$ ,  $\lambda_{\text{ss}} = 2$  and  $\lambda_{\text{yield}} = 0.4$  for the symmetrised functional.

We first study vibrational cooling of  $\text{Cs}_2$  molecules, taking  $n_{\text{max}} = 10$ . Due to the favourable Franck-Condon map, optimisation is not required in this case but helps to reduce the number of cooling cycles. The behaviour of the individual contributions to the optimisation functional as well as its total value are plotted in Fig. 6.3 for  $J_T^{\text{sym}}$  and in Fig. 6.4 for  $J_T^{\text{ass}}$ . In both cases, monotonous convergence is observed for the total functional as expected, cf. blue dashed lines in Figs. 6.3 and 6.4. The dark-state condition for the target state is perfectly obeyed for symmetrised excitation throughout the optimisation (green long-dashed line in the inset of Fig. 6.3) but presents a slightly more difficult constraint to fulfil for assembly-line cooling (green long-dashed line in the inset of Fig. 6.4, note that the stability of the ground state is given by  $1 - J_{\text{ss}}$ ). For optimisation using  $J_T^{\text{sym}}$ , the excitation yield, given by  $1 - J_{\text{yield}}$ , measures excitation of all levels in the initial ensemble, and reaches a value above 0.9, cf. purple dot-dashed line in Fig. 6.3. This together with the fact that the final value of  $J_{\text{sym}}$  (black dotted line in Fig. 6.3) is  $10^{-6}$  implies that a pulse that excites all levels in the initial ensemble with similar efficiency can indeed be found. For optimisation using  $J_T^{\text{ass}}$ , the excitation yield,  $1 - \tilde{J}_{\text{yield}}$ , takes a smaller final value (purple dot-dashed line in Fig. 6.4). This reflects the fact that  $1 - \tilde{J}_{\text{yield}}$  measures only excitation out of  $v'' = 1$  and its maximum is given by 0.335, whereas the population reshuffling of the other levels is captured by  $1 - J_{\text{ass}}$  (black dotted line in Fig. 6.4). The latter takes a final value close to one, suggesting that the pulse reshuffles all higher excited ground state levels in the desired way. This indicates efficient excitation at the end of the assembly line as desired. Thus, both optimisation functionals, Eq. (6.13) and Eq. (6.16), yield pulses

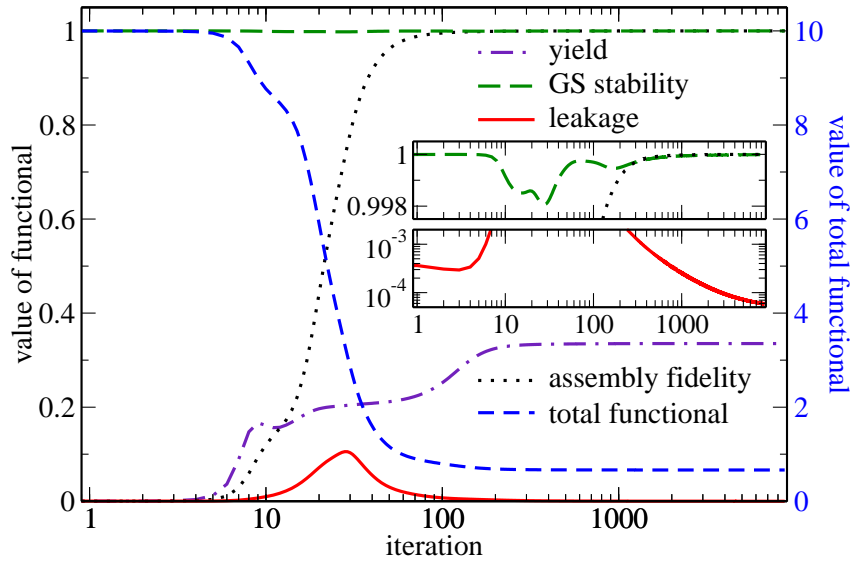


Figure 6.4: Optimising the vibrational cooling of  $\text{Cs}_2$  molecules using assembly-line cooling: Value of the total functional, Eq. (6.16), and its components vs iterations of the optimisation algorithm ( $n_{\max} = 10$ ).

which effectively excite all higher vibrational levels while keeping the target state dark. A striking difference between optimisation with  $J_T^{\text{sym}}$  and  $J_T^{\text{ass}}$  is found only in the ability of the optimised pulses to suppress leakage out of the initial ensemble (red solid lines in Fig. 6.3 and 6.4). While  $J_{\text{leak}}$  takes a final value of about 0.014 for symmetrised excitation, it can be made smaller than  $10^{-4}$  for assembly line cooling. In the latter case,  $J_{\text{leak}}$  could be further decreased by continued optimisation, cf. the slope of the red line in Fig. 6.4. This is in contrast to Fig. 6.3 where  $J_{\text{leak}}$  remains essentially unchanged after about 200 iterations, suggesting that a hard limit has been reached. Leakage from the cooling subspace thus starts to pose a problem for symmetrised excitation when a few hundred cooling cycles are required. The different performance of the two optimisation functionals is not surprising since  $J_T^{\text{ass}}$  is constructed to actively suppress leakage from the initial ensemble (and the ensuing vibrational heating) by allowing spontaneous emission only from the most favourable instead of all accessible levels.

The optimised pulses and their spectra for vibrational cooling of  $\text{Cs}_2$  are shown in Fig. 6.5, comparing symmetrised excitation (left-hand side) and assembly-line cooling (right-hand side). The spectral width of the optimised pulses covers about  $500 \text{ cm}^{-1}$ , corresponding to transform-limited pulses of 30 fs. This is well within the standard capabilities of current femtosecond technology. A similar conclusion can be made with respect to the integrated pulse energies: We find  $1 \mu\text{J}$  for the pulse obtained with  $J_T^{\text{sym}}$  in the left-hand side of Fig. 6.5 and  $4 \mu\text{J}$  for that obtained with  $J_T^{\text{ass}}$  in the right-hand side of Fig. 6.5.

We now turn to the example of LiCs molecules for which the Franck-Condon map is not favourable to cooling. Broadband optical pumping with unshaped pulses will thus lead to heating rather than cooling, cf. Fig. 6.2. We demonstrate in the following that shaping the pulses does, however, yield vibrational cooling. Note that by employing the  $B^1\Pi$ -state, we have chosen the most favourable out of all potential energy curves correlating to the lowest excited state asymptote (Li 2s + Cs 6p). For example, the  $A^1\Sigma^+$  state is expected to be even less suited for cooling. While the  $A^1\Sigma^+$ -state potential is more deeply bound and could thus be somewhat better in terms of the Franck-Condon map, it

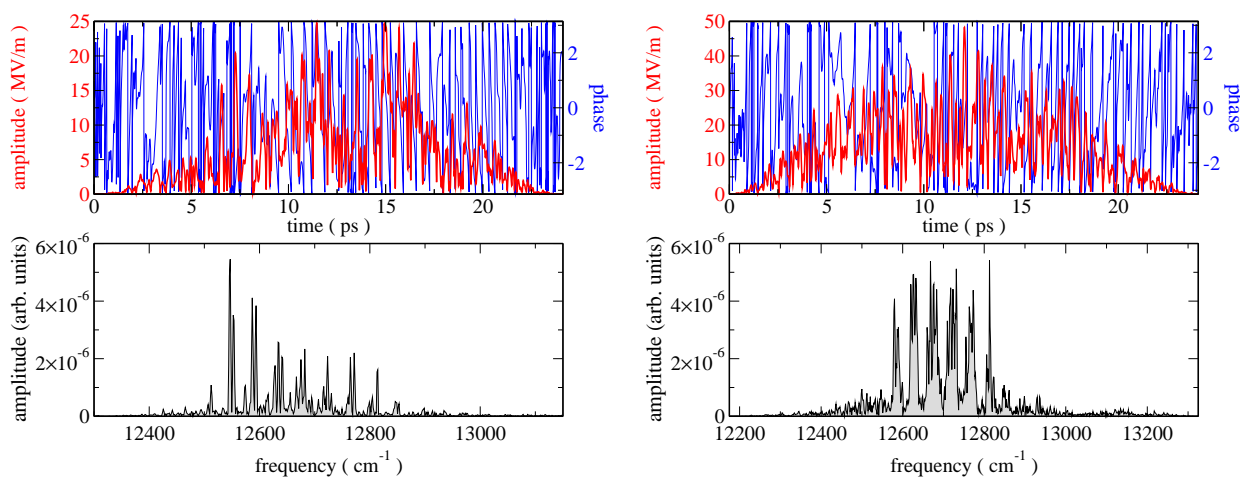


Figure 6.5: Optimised pulses (top) and their spectra (bottom) for the vibrational cooling of  $\text{Cs}_2$  molecules using symmetrised excitation (left) and assembly-line cooling (right).

is strongly perturbed by the spin-orbit interaction. The resulting coupling to triplet states implies a loss from the cooling cycle that, due to the timescale separation of excitation and spontaneous emission, cannot be prevented by shaping the pulse.

Since the  $B^1\Pi$ -state of LiCs is comparatively shallow [190], leakage out of the initial ensemble and dissociation of the molecules is a more severe problem than for  $\text{Cs}_2$ . We therefore first discuss  $n_{\text{max}} = 5$  and show later that assembly-line cooling allows also for larger  $n_{\text{max}}$ . The behaviour of the optimisation functionals and their individual contributions is displayed in Fig. 6.6 for  $J_T^{\text{sym}}$  and in Fig. 6.7 for  $J_T^{\text{ass}}$ . The overall behaviour of the functionals and their components is very similar to that observed for  $\text{Cs}_2$  in Figs. 6.3 and 6.4. In particular, both algorithms converge monotonically (dashed blue lines in Figs. 6.6 and 6.7), the dark-state condition can be very well fulfilled (green long dashed lines), and the excitation is efficient (purple dot-dashed and black dotted lines). The behaviour with respect to leakage changes, however, dramatically when going from  $\text{Cs}_2$  to LiCs (red lines in Figs. 6.6 and 6.7):  $J_{\text{leak}}$  takes final values of 0.16 for symmetrised excitation and 0.009 for assembly-line cooling. This reflects the Franck-Condon map being much more favourable to heating rather than cooling, cf. Fig. 6.2 (right), that even with shaped pulses it is difficult to ensure cooling. In particular, the result for symmetrised excitation is insufficient since  $J_{\text{leak}} = 0.16$  implies that losses from the cooling cycle will occur already after few excitation/deexcitation steps. For  $n_{\text{max}} = 5$ ,  $J_{\text{leak}}$  reaches a plateau for symmetrised excitation and assembly-line cooling alike. This is easily rationalised by inspection of the Franck-Condon map in Fig. 6.2 (right). In particular, the excited state levels which are reached from  $v'' = 5$ , such as  $v' = 2$ , show a large leakage toward higher ground state vibrational levels. We have therefore also investigated  $n_{\text{max}} = 10$  for assembly-line cooling. Most of the levels into which e.g.  $v' = 2$  decays, and which represent leakage for  $n_{\text{max}} = 5$ , are then part of the ensemble. Moreover,  $J_{\text{leak}}$  continues to decrease after 1000 iterations, albeit not as steeply as in Fig. 6.4 for  $\text{Cs}_2$ , allowing to push the value of  $J_{\text{leak}}$  below  $10^{-3}$ .

Figure 6.8 shows the optimised pulses (top) and their spectra (bottom) for LiCs with  $n_{\text{max}} = 5$  and symmetrised excitation (left) and assembly-line cooling (right). The bottom left panel of Fig. 6.8 displays furthermore the spectrum of the optimised assembly-line pulse obtained for  $n_{\text{max}} = 10$ . The spectral width obtained for  $n_{\text{max}} = 5$  covers less than  $3000 \text{ cm}^{-1}$ , corresponding to the bandwidth of a transform-limited pulse of a few femtoseconds. The integrated pulse energy amounts to  $3.4 \mu\text{J}$ .

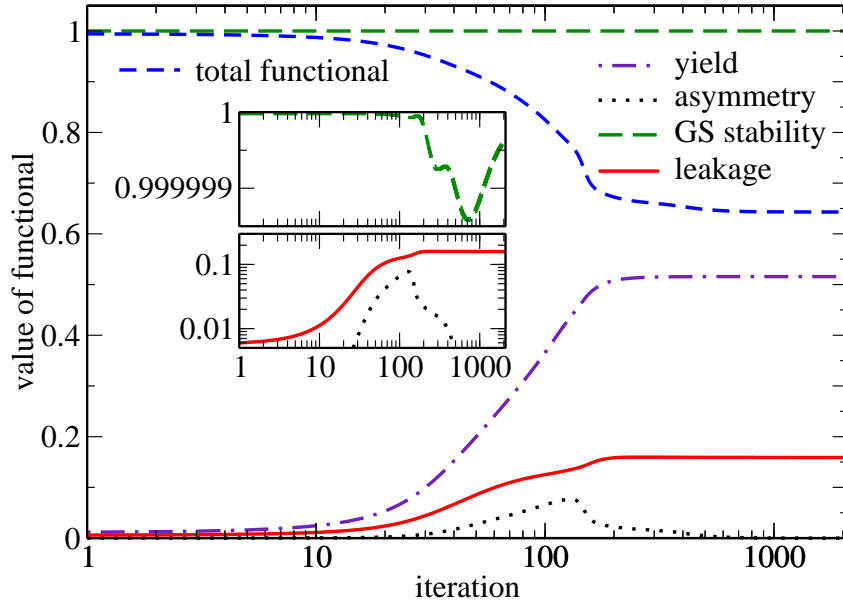


Figure 6.6: Optimising the vibrational cooling of LiCs molecules using symmetrised excitation: Value of the total functional, Eq. (6.13), and its components vs iterations of the optimisation algorithm ( $n_{\max} = 5$ ).

		# cycles for 90%	max. target state yield	# cycles for max. yield
Cs <sub>2</sub> ( $n_{\max} = 10$ )	$J_T^{\text{sym}}$	23	0.992	125
Cs <sub>2</sub> ( $n_{\max} = 10$ )	$J_T^{\text{ass}}$	26	0.9993	100
LiCs ( $n_{\max} = 5$ )	$J_T^{\text{sym}}$	not achieved	0.80	97
LiCs ( $n_{\max} = 5$ )	$J_T^{\text{ass}}$	26	0.96	137
LiCs ( $n_{\max} = 10$ )	$J_T^{\text{ass}}$	30	0.99	84

Table 6.1: Accumulation of molecules in the target  $v'' = 0$  level.

For  $n_{\max} = 10$ , significantly more transitions need to be driven, cf. Fig. 6.2. It is thus not surprising that both the spectral width of the optimised pulse and its integrated energy are larger than for  $n_{\max} = 5$ . The latter amounts to  $16 \mu\text{J}$ . Such a pulse is more difficult to realise experimentally than those found for Cs<sub>2</sub> although its spectral width could be reduced by employing spectral constraints in the optimisation algorithm [147, 150]. Nevertheless, we were able to demonstrate that optimised pulses lead to vibrational cooling even for molecules with unfavourable Franck-Condon map. This is evident from Fig. 6.7 and further substantiated by simulating the cooling process using the optimised pulses.

To this end, we assume the initial incoherent ensemble to be given by equal population in the levels  $v'' = 1, \dots, 10$  of the electronic ground state for both Cs<sub>2</sub> and LiCs. We calculate the wavepacket dynamics under the optimised pulse, and determine the ensemble that represents the initial state for the next pulse, identical to the previous one, by redistributing the population according to the Einstein coefficients, Eq. (6.6). The depletion of the excited vibrational levels and accumulation of population in  $v'' = 0$  is demonstrated in Fig. 6.9 and Table 6.1. A ground state population of 90% is obtained after just a few tens of excitation/spontaneous emission cycles for both Cs<sub>2</sub> and LiCs. This is in contrast to spectrally cut pulses without any further shaping which require several thousand

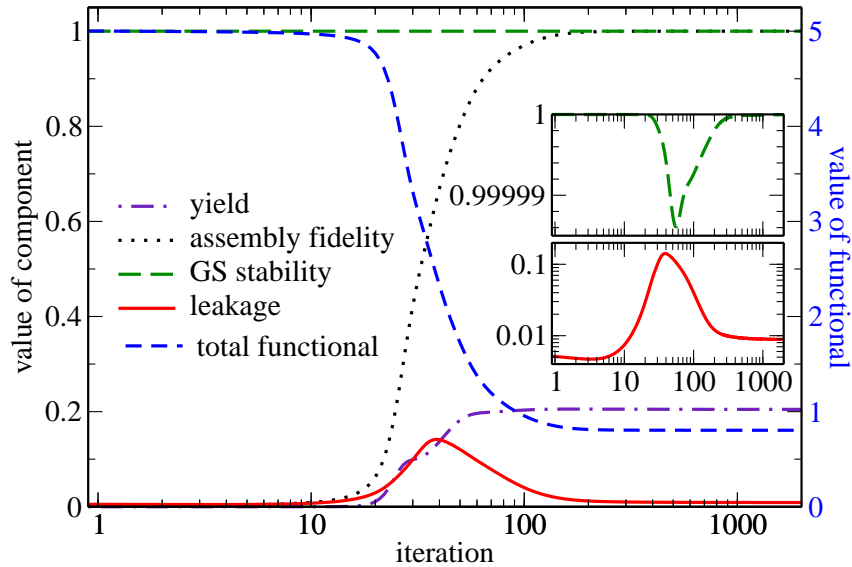


Figure 6.7: Optimising the vibrational cooling of LiCs molecules using assembly-line cooling: Value of the total functional, Eq. (6.16), and its components vs iterations of the optimisation algorithm ( $n_{\max} = 5$ ).

cycles for  $\text{Cs}_2$  and would fail altogether for LiCs. Moreover, a high degree of purity,  $\mathcal{P} > 0.98$ , is obtained for our optimised pulses with only of the order of 100 excitation/spontaneous emission cycles for both molecular species.

All results discussed above are obtained for  $v = 0$  as the target state. It is natural to ask whether other vibrational levels could also be chosen as target and whether such a choice would be more favourable for the cooling process. In fact, after reaching a pure state and full purification of the initial ensemble has been achieved, transforming this pure state to different pure states on the ground electronic surface is a comparatively easy task, e.g. by using a Raman transition. Experimentally, vibrational cooling has been demonstrated in  $\text{Cs}_2$  for target levels  $v = 1, 2, 7$  [160]. In order to determine which ground state level is most suitable as cooling target, we calculate, for each excited state level, the sum of transition matrix elements that lead to leakage from the cooling subspace. For both  $\text{Cs}_2$  and LiCs, we find that  $v' = 0$  has the smallest probability to induce leakage. For LiCs in particular, the leakage probability quickly increases with vibrational excitation. This implies that  $v' = 0$  is the only excited state level of practical use for assembly-line cooling. The most suitable target level is now simply determined as the ground state level with the largest decay probability. This is  $v = 1$  instead of  $v = 0$  in the example of LiCs, while  $v = 0$  turns out to be optimal for  $\text{Cs}_2$ .

## 6.7 Perspectives for Quantum Reservoir Engineering

We will turn now to a more general description of a cooling/purification problem on a physical system whose state can be described in a tensor product Hilbert space  $\mathcal{H} = \mathcal{H}_1 \otimes \mathcal{H}_2$ . In the case of vibrational cooling discussed above,  $\mathcal{H}_1$  represents the Hilbert space of the ground electronic surface while  $\mathcal{H}_2$  corresponds to the excited electronic surface. Due to its relevance in current experiments [162, 167] and inspired by previous work [193] we will discuss in the following the case of  $\mathcal{H}_1$  describing the state of a cavity field and  $\mathcal{H}_2$  describing the state of an atom that interacts with this cavity by passing through it. To be specific and in view of this concrete physical example, we will refer to  $\mathcal{H}_1$

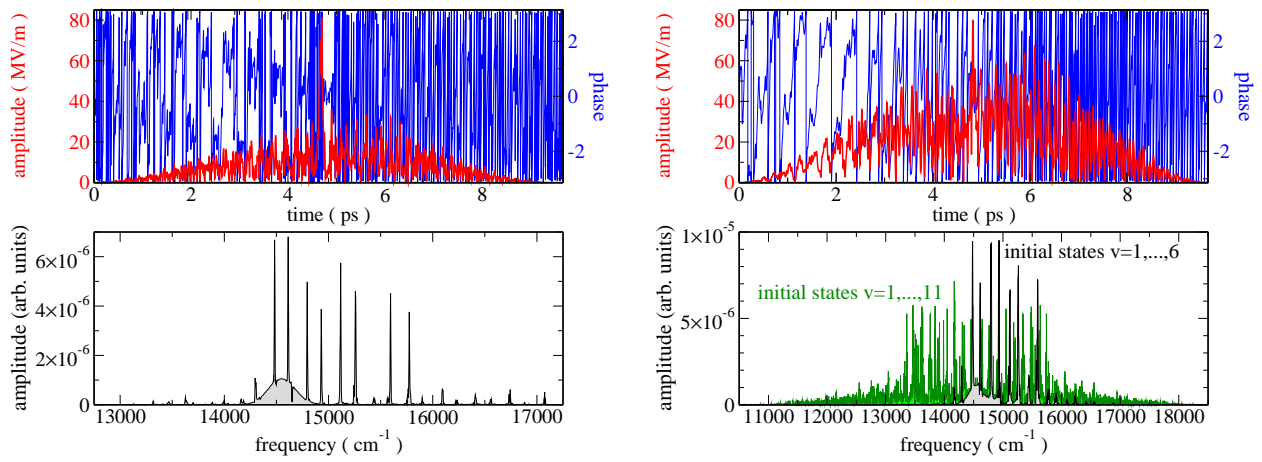


Figure 6.8: Optimised pulses (top) and their spectra (bottom) for the vibrational cooling of LiCs molecules using symmetrised excitation (left,  $n_{\max} = 5$ ) and assembly-line cooling (right,  $n_{\max} = 5$  in the top panel,  $n_{\max} = 10$  in the bottom panel).

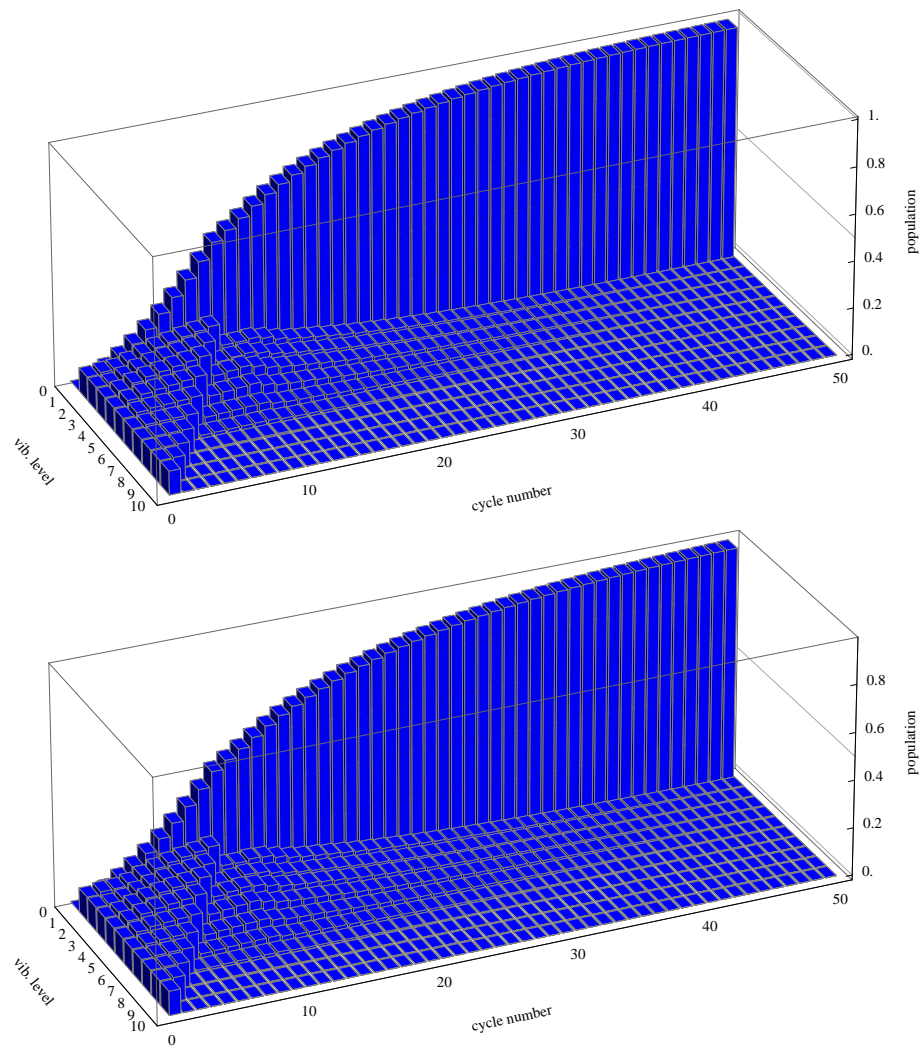


Figure 6.9: Demonstration of assembly-line cooling for  $\text{Cs}_2$  (top) and LiCs (bottom) molecules: Population of ground state vibrational levels vs number of excitation/spontaneous emission cycles. The initial distribution is assumed to be an equipartition in the ground state vibrational levels  $v'' = 1, \dots, v'' = 10$ .

as the cavity Hilbert space,  $\mathcal{H}_c$ , and to  $\mathcal{H}_2$  as the atom Hilbert space,  $\mathcal{H}_a$ . The total Hilbert space is then given by  $\mathcal{H} = \mathcal{H}_c \otimes \mathcal{H}_a$ . Nevertheless, it should be emphasised that the following ideas are not restricted to a specific physical system. Rather, they can be interpreted in the general framework of a cooling process of a physical system whose state can be represented as an element of a Hilbert space  $\mathcal{H}_1$  while the environmental degrees of freedom are represented by a Hilbert space  $\mathcal{H}_2$ .

We will begin by considering unitary evolution on the total Hilbert space  $\mathcal{H}$  and an initial product state involving a known pure state of the atom,  $|\psi_a\rangle$ . The initial state of the cavity is not known and could even be a mixed state. For simplicity, we will stay initially in the Hilbert space framework by considering pure states only. How can we formulate an optimisation functional that finds a unitary transformation such that the final state of the cavity in the Hilbert space  $\mathcal{H}_c$  will be given by  $|\psi_{ss}\rangle$ ? Similarly to the discussion in Sec. 6.1, a single unitary transformation cannot produce such a behaviour for an arbitrary initial state of the cavity as long as  $\dim(\mathcal{H}_a) < \dim(\mathcal{H}_c)$ . This can be seen as follows: Let  $\dim(\mathcal{H}_a) = d_a$ ,  $\dim(\mathcal{H}_c) = d_c$ , and let  $\{|c_i\rangle\}_{i=1,\dots,N_c}$  be an orthonormal basis of  $\mathcal{H}_c$ . A hypothetical unitary transformation that leads to the desired behaviour would yield the mapping  $U(|c_i\rangle \otimes |\psi_a\rangle) = |\psi_{ss}\rangle \otimes |\phi_i\rangle$  for all  $i = 1, \dots, N_c$  where the  $|\phi_i\rangle$  are arbitrary states in  $\mathcal{H}_a$ . Since any unitary transformation  $U$  maps an orthonormal set of vectors onto another orthonormal set of vectors, the set  $\{|\psi_{ss}\rangle \otimes |\phi_i\rangle\}_i$  must be orthonormal, i.e. the  $|\phi_i\rangle$  form an orthonormal set in  $\mathcal{H}_a$ . Due to  $\dim(\mathcal{H}_a) = d_a$ , the maximal number of orthonormal vectors in  $\mathcal{H}_a$  is equal to  $d_a$  which means that such a unitary transformation can only exist for  $d_a \geq d_c$ . If the initial state of the cavity is known and pure then it is straightforward to perform optimisation towards a certain target state of the cavity with  $d_a = 2$ , for an extensive discussion of this special case see Ref. [193]. For the general case we can only try to find a purification scheme that reaches the desired final state  $|\psi_{ss}\rangle$  after several cycles of atoms interacting with the cavity.

For simplicity, we will consider  $\dim(\mathcal{H}_a) = 2$ . Accordingly, we consider an arbitrary orthonormal basis of  $\mathcal{H}_a$ ,  $\{|a_1\rangle, |a_2\rangle\}$ . In analogy to the case of vibrational cooling, we restrict the initial state to be in certain, finite-dimensional subspace of  $\mathcal{H}_c$ <sup>44</sup>. The following functional is reliable and encompassing in terms of ensuring that the unitary transformation  $U$  due to a single atom interacting with cavity, leaves the target state  $|\psi_{ss}\rangle$  invariant<sup>45</sup>,

$$\begin{aligned} J_{ss}^{\#} &= \sum_{i=1,2} |\langle \psi_{ss} \otimes a_i | U | \psi_{ss} \otimes \psi_a \rangle|^2 \\ &= \langle \psi_{ss} | \text{Tr}_a [U (|\psi_{ss} \otimes \psi_a\rangle \langle \psi_{ss} \otimes \psi_a|) U^\dagger] | \psi_{ss} \rangle. \end{aligned} \quad (6.17)$$

We will call it the steady state functional  $J_{ss}^{\#}$ , in analogy to the one defined in Sec. 6.4.

We will now go beyond the Hilbert space picture and consider the more general case of a dynamical map  $\mathcal{D}$  on the total system. This dynamical map describes the evolution of the atom-cavity system with the atom initially in the pure state  $|\psi_a\rangle$ . Atom and cavity interact for a certain time before the atom leaves the interaction zone with the cavity. Since the initial state of atom and cavity are uncorrelated and the information obtained by the atom about the cavity via interaction is discarded, i.e. the atom stops to interact with the cavity completely before the next atom arrives, the

<sup>44</sup>Clearly this subspace needs to include  $|\psi_{ss}\rangle$  since  $|\psi_{ss}\rangle$  must be a steady state of the total evolution.

<sup>45</sup>We employ the superscript # for all functionals in this subsection to distinguish them from the similar functionals for vibrational cooling introduced above.

total evolution can be seen as a Markovian process and is hence suitable for a cooling/purification task. Moreover, the formulation of the evolution of the total system as a dynamical map allows for the inclusion of additional dissipative effects on the atom and/or the cavity. If the evolution of the combined atom-cavity system is described by a dynamical map, the steady state functional straightforwardly generalises to

$$J_{ss}^\# = \langle \psi_{ss} | \text{Tr}_a [\mathcal{D}(|\psi_{ss}\rangle \langle \psi_{ss}| \otimes |\psi_a\rangle \langle \psi_a|)] | \psi_{ss} \rangle . \quad (6.18)$$

We want to accomplish after a sufficient number<sup>46</sup> of atomic interactions that the state of the cavity becomes the steady state  $|\psi_{ss}\rangle$ , independent on the initial state of the cavity, as long as it is an element of a finite-dimensional subspace  $\mathcal{L}_{\bar{\mathcal{H}}_c} \subset \mathcal{L}_{\mathcal{H}_c}$ . This can be done by using the steady state functional, Eq. (6.18), while also having finite yield (in analogy to the discussion for vibrational cooling) in a single interaction cycle for an arbitrary initial cavity state,  $\rho_{c,0} \in \mathcal{L}_{\bar{\mathcal{H}}_c}$ . We can formulate this as follows: Find  $\mathcal{D}$  such that

$$\forall \rho_{c,0} \in \mathcal{L}_{\bar{\mathcal{H}}_c} : \sigma(\rho_{c,0}) \equiv \langle \psi_{ss} | \text{Tr}_a [\mathcal{D}(\rho_{c,0} \otimes |\psi_a\rangle \langle \psi_a|)] | \psi_{ss} \rangle > 0 . \quad (6.19)$$

We will now proceed to show how an optimisation functional can be formalised that ensures condition (6.19). Let  $\bar{d}_c = \dim(\bar{\mathcal{H}}_c)$  and let  $\rho_{c,0}$  be arbitrary. Choose an orthonormal basis of Hermitian matrices  $\{\rho_i\}$  on  $\mathcal{L}_{\bar{\mathcal{H}}_c}$  such that it consists of  $\bar{d}_c$  diagonal matrices  $\{\rho_i^D\}$  and  $\bar{d}_c(\bar{d}_c - 1)$  off-diagonal matrices<sup>47</sup>  $\{\rho_i^{OD}\}$  in a fixed representation. In other words, we can write

$$\{\rho_i\}_{i=1, \dots, \bar{d}_c^2} = \{\rho_i^D\}_{i=1, \dots, \bar{d}_c} \cup \{\rho_i^{OD}\}_{i=1, \dots, \bar{d}_c(\bar{d}_c-1)} . \quad (6.20)$$

Spanning  $\rho_{c,0}$  in this basis one obtains coefficients  $c_i^D \in \mathbb{C}$  and  $c_i^{OD} \in \mathbb{C}$  such that

$$\rho_{c,0} = \sum_{i=1}^{\bar{d}_c^2} c_i \rho_i = \sum_{i=1}^{\bar{d}_c} c_i^D \rho_i^D + \sum_{i=1}^{\bar{d}_c(\bar{d}_c-1)} c_i^{OD} \rho_i^{OD} . \quad (6.21)$$

We choose for simplicity  $\rho_i^D = P_i \equiv |\psi_i\rangle \langle \psi_i|$  where  $|\psi_i\rangle$  is an arbitrary ONB of  $\bar{\mathcal{H}}_c$ . Due to  $\rho_{c,0}$  being a density matrix, we can conclude the following relations for the coefficients and the basis elements,

$$\forall i : c_i \in \mathbb{R} \quad (\text{since } \rho_0 \text{ is hermitian}), \quad (6.22a)$$

$$\forall i : c_i^D \geq 0 \quad (\text{since } \rho_0 \text{ is pos. semidefinite}), \quad (6.22b)$$

$$\forall i : |c_i^{OD}| \leq 1 \quad (\text{since } \text{Tr}[\rho_0^2] \leq 1) . \quad (6.22c)$$

<sup>46</sup>Theoretically infinite, practically large but finite, cf. Footnote 42.

<sup>47</sup>By an off-diagonal matrix we denote a matrix whose diagonal entries vanish. Note that the resulting matrix is not a density matrix but for simplicity we will still denote it with a  $\rho$ . In the context of numerical optimisation it is generally not an issue when matrices are employed that do not obey all criteria for being a density matrix. Furthermore, ensuring condition (6.19) for all elements of Liouville space will in particular guarantee that it is fulfilled for all density matrices.

Using the decomposition of  $\rho_{c,0}$  according to Eq. (6.21) we can rewrite the yield  $\sigma(\rho_0)$  as follows,

$$\begin{aligned} \sigma(\rho_0) &= \sum_i c_i^D \langle \psi_{ss} | \text{Tr}_a [\mathcal{D}(\rho_i^D \otimes |\psi_a\rangle \langle \psi_a|)] | \psi_{ss} \rangle \\ &\quad + \sum_i c_i^{OD} \langle \psi_{ss} | \text{Tr}_a [\mathcal{D}(\rho_i^{OD} \otimes |\psi_a\rangle \langle \psi_a|)] | \psi_{ss} \rangle . \end{aligned} \quad (6.23)$$

To shorten notation it is convenient to define

$$\eta_i \equiv \langle \psi_{ss} | \text{Tr}_a [\mathcal{D}(\rho_i^D \otimes |\psi_a\rangle \langle \psi_a|)] | \psi_{ss} \rangle , \quad (6.24)$$

$$\beta_i \equiv \langle \psi_{ss} | \text{Tr}_a [\mathcal{D}(\rho_i^{OD} \otimes |\psi_a\rangle \langle \psi_a|)] | \psi_{ss} \rangle . \quad (6.25)$$

Since  $\mathcal{D}$  is a dynamical map and  $\rho_i^D$  is positive,  $\mathcal{D}(\rho_i^D \otimes |\psi_a\rangle \langle \psi_a|)$  is a positive matrix. As a result, the expectation value in Eq. (6.24) is nonnegative and it follows that  $\forall i : \eta_i \geq 0$ . Then, it is clear that condition (6.19) is equivalent to achieving  $\forall i : \beta_i = 0$  and  $\forall i : \eta_i > 0$ . Using Eq. (6.22c) we can even employ the significantly weaker condition

$$\sum_i |\beta_i| < \min_i \eta_i . \quad (6.26)$$

To obtain a symmetrised and maximally efficient steering process towards the steady state for this problem, we propose, analogously to Eq. (6.13), the following functional,

$$J_T^\# = J_{ss}^\# + J_{\text{eff}}^\# + J_{\text{symm}}^\# + J_{\text{leak}}^\# . \quad (6.27)$$

The steady state functional,  $J_{ss}^\#$ , is given by Eq. (6.18). The efficiency functional,  $J_{\text{eff}}^\#$ , is responsible for obtaining a high total yield  $\sigma$  averaged over all possible initial states. Since the only guaranteed beneficial contribution is the one corresponding to the  $\eta_i$ , we need to maximise the value of the  $\eta_i$  and minimise the values of the  $\beta_i$  accordingly. This motivates the following efficiency functional,

$$J_{\text{eff}}^\# = \sum_i \eta_i - \sum_i |\beta_i|^2 . \quad (6.28)$$

The symmetrisation functional,  $J_{\text{symm}}^\#$ , is responsible for equally distributing the total yield over all  $\eta_i$ . Since the initial state in  $\mathcal{L}_{\bar{\mathcal{H}}_c}$  is unknown, each  $\eta_i$  is equally important. The canonical approach is to make sure that all the  $\eta_i$  are of the same magnitude, cf. Sec 6.4. This can be achieved by a telescope-type functional,

$$J_{\text{symm}}^{\#, \text{tele}} = \sum_{i=2} |\eta_i - \eta_{i-1}|^2 , \quad (6.29)$$

or a lock-in functional in which one compares all  $\eta_i$  to a certain ‘‘locked-in’’  $\eta_k$ ,

$$J_{\text{symm}}^{\#, \text{lock}} = \sum_{i \neq k} |\eta_i - \eta_k|^2 . \quad (6.30)$$

Since errors can accumulate in the telescope type functional, the lock-in functional seems to be the better choice in general which is why it also has been chosen in Eq. (6.10) for vibrational cooling. It is

also conceivable that efficiency and symmetrisation functional can be substituted by an assembly-line type functional as introduced in Sec. 6.5. If the coherences represented by the  $\beta_i$  are suppressed, we can once again split the initial density matrix into the contributions from its eigenstates. This allows to find a drain state towards the steady state with the remaining eigenstates being coherently transferred step by step to this drain state.

The leakage functional,  $J_{\text{leak}}^\#$ , has the objective to prevent population transfer out of the subspace  $\mathcal{L}_{\bar{\mathcal{H}}_c} \subset \mathcal{L}_{\mathcal{H}_c}$ . Using the same ideas presented already in Sec. 6.4 we propose the functional

$$J_{\text{leak}}^\# = \text{Tr} [P_{\bar{\mathcal{H}}_c} \text{Tr}_a [\mathcal{D} (\bar{d}_c^{-1} \mathbf{1}_{\bar{d}_c} \otimes |\psi_a\rangle \langle \psi_a|)] P_{\bar{\mathcal{H}}_c}] . \quad (6.31)$$

where  $\bar{d}_c^{-1} \mathbf{1}_{\bar{d}_c}$  is the totally mixed state on the subspace  $\mathcal{L}_{\bar{\mathcal{H}}_c}$ .

We will finish this section by briefly putting the special case of vibrational cooling in the perspective of the generalised scheme presented in this subsection. The radiative decay for vibrational cooling is diagonal with respect to the vibrational energy basis [194]. As a result, it was not necessary to consider coherences, i.e. off-diagonal contributions corresponding to non-vanishing  $c_i^{OD}$ 's. For this reason we could assume that  $c_i^{OD} = 0$ , in other words we were able to restrict ourselves to a certain subset of initial density matrices  $\rho_0 \in \mathcal{L}_{\bar{\mathcal{H}}_c}$ . Thus, all  $\beta_i$  vanished automatically and the efficiency functional reduced to

$$\tilde{J}_{\text{eff}}^\# = \sum_i \eta_i . \quad (6.32)$$

Due to the additional time scale separation between coherent dynamics and the decay process, it was possible to treat the whole purification task for vibrational cooling in Hilbert space.



## 7 A Quantum Control Perspective on a Non-Markovian Evolution

Once the correlations between a system and its environment do not decay sufficiently fast, it is not possible to describe the system evolution via a Markovian master equation [38]. Finding an adequate equation of motion for these cases turns out to be highly non-trivial. Nevertheless, the study of these non-Markovian evolutions is of great interest from the perspective of quantum control. The preservation of system-environment correlations for a sufficient time implies that the information exchanged with the environment might be recoverable with suitably chosen controls. This is in stark contrast to Markovian evolutions for which any information transfer to the environment immediately leads to an unrecoverable loss of information on the system. Moreover, since non-Markovian evolutions do not necessarily only decrease the distinguishability of states it is possible to use this environmental resource even in the context of unitary quantum control. One of the first demonstrations that environmental effects in the context of non-Markovian evolutions can in fact be harnessed for purposes of optimal control was reported by Schmidt et al. [195]. A comparative analysis of optimal control results, showing that in the non-Markovian case gate fidelities can improve substantially when the details of the system-bath coupling are taken into account, was performed by Floether et al. [196].

In this section we will study the non-Markovianity in superconducting qudits and its impact on the implementation of unitary gates. Superconducting qudits represent a physical system of great current interest for which non-Markovian effects have been theoretically described and experimentally observed [197, 198]. These implementations represent one of the most promising architectures in terms of achieving a powerful implementation for tasks of quantum information processing, not least because of their vast engineerability of system parameters [199]. The beginning of this section is devoted to the description of a superconducting phase qudit, first of all in the absence of environmental effects. It turns out that the corresponding Hamiltonian is that of a weakly anharmonic oscillator. To take into account the environment we will employ a general model of a harmonic oscillator interacting with a bath of two-level systems (TLS). In the context of superconducting qudits, environmental TLS turn out to correspond to dielectric defects in the Josephson junction. This TLS model finds widespread use in many fields from the theory of glasses to defects in superconducting circuits [200]. The set of environmental TLS will predominantly lead to single-exponential decay and dephasing effects but a small subset of these two-level system will be coupled more strongly to the anharmonic oscillator than to the rest of the environment. This leads to non-Markovian dynamics in a phase qudit architecture. Environmental models explaining this non-Markovianity observed in superconducting qudit architectures have been thoroughly discussed in the review by Paladino et al. [200]. Spectroscopic results supporting the TLS model were reported by Lisenfeld et al. [201] and Shalibo et al. [202]. We will explicitly discuss how the non-Markovianity can be exploited to increase the controllability of a phase qudit. In particular, we will thoroughly analyse this controllability gain via the strongly coupled environmental degrees of freedom and illustrate the principle, limits and scope of this novel control scheme for superconducting qudit implementations.

## 7.1 Superconducting Qudits

In this section we will present a brief review on the physics of superconducting qudits, in particular that of the Josephson junction, following Ref. [203].

An electrical circuit composed of various elements can be classically described by a pair of conjugate variables analogous to position and momentum, namely the charge  $Q$  and the flux  $\Phi$ , derived from the voltage and current in the circuit. If the circuit is in the quantum regime, e.g. it is superconducting, then charge and flux need to be quantised and it can be shown that they obey the canonical commutation relation,

$$[\Phi, Q] = i, \quad (7.1)$$

With this in mind, one can associate to a simple superconducting LC circuit the Hamiltonian

$$H_{LC} = \frac{Q^2}{2C} + \frac{\Phi^2}{2L}, \quad (7.2)$$

where  $L$  is the inductance of the coil and  $C$  is the capacitance of the capacitor.

A crucial circuit element for superconducting circuits is the so-called Josephson junction. It consists of a superconductor that is interrupted by an insulator or a non-superconducting metal. The charge that passes through the junction is quantised<sup>48</sup>,

$$\hat{Q} = -2e\hat{N}, \quad (7.3)$$

where  $2e$  is the charge of a Cooper pair. Essentially, this means that the charge operator  $\hat{Q}$  can be replaced by a number operator  $\hat{N}$  with a corresponding eigenbasis  $|N\rangle$ . It can be shown that the Hamiltonian describing the charge transfer along the junction is given by,

$$\hat{H}_J = \frac{E_J}{2} \sum_{N=-\infty}^{\infty} (|N\rangle\langle N+1| + |N+1\rangle\langle N|). \quad (7.4)$$

Note that the integer  $N$  in the number states can be positive and negative. This corresponds to the two directions in which charge can pass through the junction. One can now define the states,

$$|\delta\rangle = \sum_{N=-\infty}^{\infty} e^{iN\delta} |N\rangle, \quad (7.5)$$

for  $\delta \in [0, 2\pi]$ . Conversely

$$|N\rangle = \frac{1}{2\pi} \int_0^{2\pi} d\delta e^{-iN\delta} |\delta\rangle \quad (7.6)$$

and one can define a corresponding operator  $\hat{\delta}$  such that

$$\hat{\delta} = \frac{1}{2\pi} \int_0^{2\pi} d\delta e^{i\delta} |\delta\rangle\langle\delta|. \quad (7.7)$$

---

<sup>48</sup>Throughout this section we will indicate from this point onwards operators on Hilbert space with a hat to improve their distinguishability from scalar quantities.

Akin to the number and phase operator in quantum electrodynamics,  $\hat{N}$  and  $\hat{\delta}$  can be interpreted as a conjugate pair of number and phase and it is easy to see that  $[\hat{\delta}, \hat{N}] = i$ . Correspondingly, it follows immediately from their definitions that

$$\hat{N} = \frac{1}{i} \frac{\partial}{\partial \delta}. \quad (7.8)$$

This operator allows to rewrite the Hamiltonian in Eq. (7.4) as

$$\hat{H}_J = -E_J \cos \hat{\delta}, \quad (7.9)$$

where the Josephson energy  $E_J$  depends on the specific material properties of the junction. From these definitions it is straightforward to show that the flux  $\hat{\Phi}$  is proportional to the phase via  $\hat{\Phi} = \frac{\Phi_0}{2\pi} \hat{\delta}$  where  $\Phi_0 = \frac{h}{2e}$  is the magnetic flux quantum. Furthermore, one can derive the so-called Josephson relations for voltage and current,

$$\hat{U} = \frac{\Phi_0}{2\pi} \frac{\partial \hat{\delta}}{\partial t}, \quad (7.10a)$$

$$\hat{I} = I_c \sin \hat{\delta}, \quad (7.10b)$$

where  $I_c = \frac{2\pi}{\Phi_0} E_J$  is the so-called critical current.

A Josephson junction has a natural capacitance associated to it since one can interpret the two ends of the superconducting wire as a capacitor. If one adds an inductor with an inductance  $L$  to the circuit one can interpret the resulting circuit as an LC circuit with a tunnelling element. The Hamiltonian of such a circuit is consequently given by

$$\begin{aligned} \hat{H} = \hat{H}_{LC} + \hat{H}_J &= \frac{\hat{Q}^2}{2C} + \frac{\hat{\Phi}^2}{2L} - E_J \cos \hat{\delta} \\ &= \frac{2}{C} e^2 \hat{N}^2 + \left( \frac{\Phi_0}{2\pi} \right)^2 \frac{\hat{\delta}^2}{2L} - E_J \cos \hat{\delta} \\ \hat{H} &= -\frac{2e^2}{C} \frac{\partial}{\partial \delta^2} + \frac{1}{2L} \left( \frac{\Phi_0}{2\pi} \right)^2 \hat{\delta}^2 - \frac{I_c \Phi_0}{2\pi} \cos \hat{\delta}. \end{aligned} \quad (7.11)$$

At this point one can see that this Hamiltonian describes a harmonic oscillator with an anharmonic contribution to the potential that is induced by the Josephson junction. The power of such a superconducting circuit lies in the fact that one can control the parameters in the Hamiltonian (7.11) rather easily. For example, one can increase the flux in the circuit by coupling the inductor to another inductor - this is called flux bias. The phase  $\hat{\delta}$  on the Josephson junction is then defined with respect to the total flux, i.e.  $\frac{\Phi_0}{2\pi} \hat{\delta} = \hat{\Phi} + \Phi_b$  where  $\hat{\Phi}$  is the flux due to the current in the circuit and  $\Phi_b$  is the external flux bias. Consequently the flux due to the current in the circuit is now given by  $\hat{\Phi} = \frac{\Phi_0}{2\pi} \hat{\delta} - \Phi_b$  and the new Hamiltonian of the circuit reads

$$\hat{H}_{fb} = -\frac{2e^2}{C} \frac{\partial}{\partial \delta^2} + \frac{1}{2L} \left( \frac{\Phi_0}{2\pi} \hat{\delta} - \Phi_b \right)^2 - \frac{I_c \Phi_0}{2\pi} \cos \hat{\delta}, \quad (7.12)$$

which introduces a displacement to the harmonic part of the potential.

Alternatively, one can also introduce a current bias in the junction by connecting it to some external source of current  $I_b$ . This source of current can be interpreted as a very large inductor with inductance  $L$  and some very large flux  $\Phi_b$  such that  $\Phi_b, L \rightarrow \infty$  and  $\frac{\Phi_b}{L} \rightarrow I_b$ . Plugging this into Eq. (7.12) leads to

$$\hat{H}_{cb} = -\frac{2e^2}{C} \frac{\partial}{\partial \delta^2} - I_b \frac{\Phi_0}{2\pi} \hat{\delta} - \frac{I_c \Phi_0}{2\pi} \cos \hat{\delta}. \quad (7.13)$$

Such an additional linear term can also be interpreted as a displacement to the harmonic part of the potential since

$$\omega_0^2 \hat{\delta}^2 + \epsilon \hat{\delta} = \omega_0^2 \left( \hat{\delta} + \frac{\epsilon}{2\omega_0^2} \right)^2 - \frac{\epsilon^2}{4\omega_0^4}.$$

Combining these two types of bias leads to the following Hamiltonian for a Josephson circuit,

$$\hat{H} = -\frac{2e^2}{C} \frac{\partial}{\partial \delta^2} + \frac{1}{2L} \left( \frac{\Phi_0}{2\pi} \hat{\delta} - \Phi_b \right)^2 - \frac{\Phi_0}{2\pi} \left( I_b \hat{\delta} + I_c \cos \hat{\delta} \right). \quad (7.14)$$

This Hamiltonian does not yet cover the most general scenario since it does not account for the so-called gate charge which leads to the introduction of a charge bias. For simplicity we will only discuss flux and current bias in the following. From the Hamiltonian in Eq. (7.14) one can identify three energy scales [204] (i)  $E_C = \frac{2e^2}{C}$  associated with the excess number of Cooper pairs across the junction, representing the inverse mass of the quasiparticle in the oscillator, (ii)  $E_J = \frac{I_c \Phi_0}{2\pi}$  associated to the tunnel coupling across the junction, (iii)  $E_L = \frac{\Phi_0^2}{2L}$  associated to a flux quantum going through the circuit. In the following we will consider the regime  $E_J \gg E_C$  representing the phase qudit regime. In this regime the circuit will behave like a weakly anharmonic oscillator and a qudit can be encoded in its low-lying energy eigenstates [204].

It is evident from Eq. (7.14), that flux bias and current bias have very similar effects on the Josephson circuit. For simplicity, we will treat a constant flux bias  $\Phi_b$  and a controllable current bias  $I_c(t)$ . Then, one can diagonalise the drift Hamiltonian to obtain eigenenergies  $E_0, E_1, \dots$  such that in good approximation  $E_n = n\omega_0 + \beta \frac{n(n-1)}{2}$  where  $\beta$  is an anharmonicity energy constant which can be steered by the flux bias<sup>49</sup>. For small anharmonicities and as long as one considers only the energetically lowest few eigenstates, the Hamiltonian (7.14) can be written as [204],

$$\hat{H} = \omega_0 \hat{n} + \frac{\beta}{2} \hat{n} (\hat{n} - 1) + \kappa_1 I_c(t) \hat{n} + \kappa_2 I_c(t) (\hat{a} + \hat{a}^\dagger), \quad (7.15)$$

where  $\kappa_1$  and  $\kappa_2$  are constants. The operators  $\hat{n} = n|n\rangle\langle n|$ ,  $\hat{a} = \sqrt{n}|n-1\rangle\langle n|$ ,  $\hat{a}^\dagger = \sqrt{n+1}|n\rangle\langle n+1|$  are defined in analogy to a harmonic oscillator with  $|n\rangle$  being the  $n$ -th eigenstate of the Hamiltonian for  $I_c = 0$ .

---

<sup>49</sup>Note that while one obtains without the term  $I_c \cos \delta$  a simple displacement in the Hamiltonian (7.14) due to the flux bias, the presence of the Josephson energy changes this simple behaviour.

## 7.2 Control Strategies for Phase Qudits

We will first of all go into a rotating frame with respect to the oscillator frequency  $\omega_0$ , i.e. we perform the following transformation of the Hamiltonian in Eq. (7.15),

$$\hat{H} = \hat{V}^\dagger \hat{H} \hat{V} - i\hat{V}^\dagger \frac{\partial \hat{V}}{\partial t}, \quad (7.16)$$

with  $\hat{V} = e^{-i\omega_0 \hat{n} t}$ . Then,

$$\hat{H} = \frac{\beta}{2} \hat{n} (\hat{n} - 1) + \kappa_1 I_c(t) \hat{n} + \kappa_2 I_c(t) \left( \hat{V} \hat{a} \hat{V}^\dagger + \hat{V} \hat{a}^\dagger \hat{V}^\dagger \right), \quad (7.17)$$

since  $[\hat{n}, \hat{V}] = 0$ . Now it is easy to see that  $\hat{a} \hat{V}^\dagger = e^{i\omega_0 t} \hat{V}^\dagger \hat{a}$  and  $\hat{a}^\dagger \hat{V}^\dagger = e^{-i\omega_0 t} \hat{V}^\dagger \hat{a}^\dagger$  and consequently

$$\hat{H} = \frac{\beta}{2} \hat{n} (\hat{n} - 1) + \kappa_1 I_c(t) \hat{n} + \kappa_2 I_c(t) \left( e^{i\omega_0 t} \hat{a} + e^{-i\omega_0 t} \hat{a}^\dagger \right). \quad (7.18)$$

We will now consider two cases.

1. If the carrier frequency of the control  $I_c(t)$  is much smaller than  $\omega_0$ , then  $I_c(t) e^{\pm i\omega_0 t}$  will be a quickly rotating term in the complex plane and in the time evolution the contribution involving this fast oscillation will average out. This is because  $I_c(t)$  varies slowly over time intervals in which  $e^{i\omega_0 t}$  covers the whole complex unit circle and then  $\frac{1}{T} \int_0^T I_c(t) e^{\pm i\omega_0 t} dt \simeq I_c \frac{1}{T} \int_0^T e^{\pm i\omega_0 t} dt \simeq 0$  if  $T \gg \frac{1}{\omega_0}$ . Hence, the Hamiltonian for low-frequency control can be written as

$$\hat{H}_{\text{low}} = \frac{\beta}{2} \hat{n} (\hat{n} - 1) + \kappa_1 I_c(t) \hat{n}. \quad (7.19)$$

2. If the carrier frequency of the control is centred around  $\omega_0$  one can write<sup>50</sup>  $I_c(t) = \frac{1}{2} u(t) e^{-i\omega_0 t} + \frac{1}{2} u^*(t) e^{i\omega_0 t}$  with a slowly varying  $u(t)$ . As a result, the Hamiltonian (7.18) can be written as

$$\begin{aligned} \hat{H} &= \frac{\beta}{2} \hat{n} (\hat{n} - 1) + \frac{1}{2} \kappa_1 \left( u(t) e^{-i\omega_0 t} + u^*(t) e^{i\omega_0 t} \right) \hat{n} \\ &\quad + \frac{1}{2} \kappa_2 \left( u(t) (1 + e^{2i\omega_0 t}) \hat{a} + u^*(t) (1 + e^{-2i\omega_0 t}) \hat{a}^\dagger \right). \end{aligned} \quad (7.20)$$

With the same argument as in point 1, all oscillating terms can be neglected and we obtain the Hamiltonian for high-frequency control,

$$\hat{H}_{\text{high}} = \frac{\beta}{2} \hat{n} (\hat{n} - 1) + \frac{\kappa_2}{2} \left( u(t) \hat{a} + u^*(t) \hat{a}^\dagger \right). \quad (7.21)$$

For the special case of amplitude control at the transition frequencies of  $\hat{H}_{\text{high}}$ , i.e.  $u(t) = \sum_n u_n(t) \sqrt{n} e^{i\frac{\beta}{2} n(n-1)t}$ , one can perform the transformation  $\hat{V}(t) = e^{-i\frac{\beta}{2} \hat{n}(\hat{n}-1)t}$  to obtain the

<sup>50</sup>Another parametrisation would be  $I_c(t) = u(t) \cos(\omega_0 t + \varphi(t))$  with  $u(t), \varphi(t)$  real. Note that the simpler ansatz  $I_c(t) = u(t) \cos(\omega_0 t)$  is not general since it fixes the roots of  $I_c(t)$ . The factor  $\frac{1}{2}$  has been employed such that the fluence of  $I_c$  and  $u(t)$  matches.

following Hamiltonian,

$$\hat{H}_{\text{high}}^{(\text{amp})} = \sum_n \left[ \frac{1}{2} u_n(t) |n\rangle \langle n-1| + \frac{1}{2} u_n^*(t) |n-1\rangle \langle n| \right], \quad (7.22)$$

if the anharmonicity is comparatively “large”. In this context, the “large” anharmonicity needs to be large compared to the frequency corresponding to temporal variations<sup>51</sup> of the  $u_n(t)$  but still small compared to  $\omega_0$ . This condition is required to neglect the counter-rotating terms analogously to those observed in Eq. (7.20).

We will now perform a controllability analysis on the Hamiltonians  $\hat{H}_{\text{low}}$  and  $\hat{H}_{\text{high}}^{(\text{amp})}$ , assuming completely unitary evolution. The reachable set of unitaries is determined by the Lie group associated to the dynamical Lie algebra  $\mathcal{L}$  which is given by  $\text{span}_{\{u\} \in \mathcal{U}} \{-iH(\{u\})\}$  [40].  $\mathcal{U}$  is the set of admissible controls and  $H$  is the Hamiltonian of the system. For bilinear systems, cf. Eq. (5.22), the analysis on the dynamical Lie algebra is typically performed by computing nested commutators of drift and control Hamiltonians until the dimensionality is exhausted [40]. It is easy to see that the dimensionality of the Lie algebra for  $\hat{H}_{\text{low}}$  is equal to 2, since drift and control Hamiltonian commute. The dimensionality of the Lie algebra for  $\hat{H}_{\text{high}}^{(\text{amp})}$  is given by  $\frac{d(d-1)}{2}$  if we consider a cut-off<sup>52</sup> on the qudit Hilbert space at dimension  $d$ . This can be seen most easily if we choose  $u_n \in \mathbb{I}$  purely imaginary. Note that this assumption does not contradict the assumption of amplitude control since it represents a static phase. In Appendix C we show that a basis of this Lie algebra is given by the matrices  $\{|n\rangle \langle n-j| - |n-j\rangle \langle n|\}_{n,j}$  for  $n = 0, \dots, d-1$  and  $0 < j < n$ . This identifies the Lie algebra as the special orthogonal Lie algebra (since it is spanned by all real, skew-symmetric matrices) and correspondingly the reachable set of unitaries are those lying in the special orthogonal group  $\text{SO}(d)$  [40]. For the special case of  $d = 4$  it is possible to determine analytical solutions for the required controls to obtain an arbitrary matrix in  $\text{SO}(d)$  [205, 206].

From this controllability analysis it follows immediately that the combination of the control schemes 1 and 2 cannot yield arbitrary matrices in  $\text{SU}(d)$  for  $d > 2$ , i.e. the system is not fully controllable. This can be directly seen by considering a Cartan decomposition of  $\text{SU}(d)$ , i.e. any  $U \in \text{SU}(d)$  can be written as

$$U = k_1 A k_2, \quad (7.23)$$

with  $k_1, k_2 \in \text{SO}(d)$  and  $A$  being a diagonal, complex matrix with determinant 1 [40]. While the high-frequency control scheme yields arbitrary  $k_1$  and  $k_2$  the low frequency control scheme can only reach arbitrary diagonal  $A$  when  $d = 2$  since the dimensionality of the dynamical Lie algebra of Eq. (7.19) is two, independent on  $d$ .

If one were somehow able to extend the controllability of the low-frequency scheme to all diagonal matrices instead of only those along two directions in the Lie algebra, then full controllability of the

<sup>51</sup>This approximation is best fulfilled if  $u_n(t) = u_n$  constant. However, from a physical point of view there will always be the need to turn the control on and off which will introduce side bands in the Fourier transform that need to be compared to the anharmonicity, respectively the oscillator frequency.

<sup>52</sup>While the Hilbert space of an anharmonic oscillator is infinite-dimensional, in practice the anharmonic modelling of the phase qudit will break down at some point. To stay in the valid regime of the model, one usually truncates the Hilbert space and needs to make sure that in numerical simulations no artificial reflections at the upper level boundary are encountered. Note that in the model for our numerical simulations in Sec. 7.5 there is no possibility for such reflections since no excitation of the qudit levels, by either the control or the environment, are possible. In this case we can simply truncate the oscillator Hilbert space at the boundary of the qudit’s logical subspace.

system is obtained<sup>53</sup>. If we do not want to change the schemes by for example including phase control in the high-frequency case, then the only place left to look for a controllability increase is given by the environment. For this reason the next subsection will be devoted to an analysis of a model for describing the environment for Josephson junctions that is able to explain the most important characteristics of the experimentally observed environmental effects - the TLS model.

### 7.3 The Two-Level System Model

No Josephson junction is perfectly manufactured, most notably there is a high likelihood for atomic impurities in the non-superconducting part of the junction [204]. The most successful model to describe these impurities is the TLS model<sup>54</sup> which describes each impurity as a two-level system with a lower-lying ground state  $|g\rangle$  and an energetically excited configuration  $|e\rangle$  [200–202, 209]. Let  $E_{\text{TLS}}$  be the energy difference, then the Hamiltonian of the TLS is given by

$$\hat{H}_{\text{TLS}} = E_{\text{TLS}} |e\rangle \langle e|. \quad (7.24)$$

The coupling mechanism between the qudit and a defect is assumed to be that of an electric dipole with an electric field. As a matter of fact the Josephson junction itself can be seen as a capacitor leading to an electric field between the two plates, i.e. the ends of the superconducting wire. The interaction of these defect fields with the circuit's wave function, i.e. the qudit, can have on the most basic level two effects.

1. An excitation in the circuit can be transferred to an excitation in the TLS and vice versa, the corresponding interaction Hamiltonian reads

$$\hat{H}_{\text{int}} = v_{\perp} (\hat{a} \otimes |e\rangle \langle g| + \hat{a}^{\dagger} \otimes |g\rangle \langle e|), \quad (7.25)$$

where  $v_{\perp}$  is the so-called transversal interaction strength, representing a resonant interaction between the state of the junction and the TLS. This is similar to how the electric field of a cavity (i.e. a harmonic oscillator) would interact with an dipolar level transition between two states of an atom (i.e. a TLS) forming the well-known Jaynes-Cummings Hamiltonian. We used the corresponding rotating wave approximation (RWA), neglecting the double-excitation and double-annihilation terms. This RWA is justified since the coupling strength will usually be much smaller than the energy scales of both TLS and oscillator.

2. If we assume the TLS to be in the ground state initially, then the energies of the qudit eigenstates will only be stable if the TLS stays in the ground state. Once the TLS enters the excited state this will lead to a change in the total energy. Consider for example a dipole in a capacitor that flips around. This leads to a change in the energy carried by the capacitor since the dielectric

---

<sup>53</sup>Note that while low-frequency and high-frequency control Hamiltonian are obtained with respect to a different frame, the unitary transformation between them is diagonal. The different phases acquired in the different frames can consequently be absorbed by the diagonal unitaries obtained by the low-frequency scheme.

<sup>54</sup>Due to the observed spectral density of the bath, one of the primary noise effects that leads to a non-Markovian evolution in superconducting qudits is often called  $1/f$ -noise. The TLS model is a particular way to reproduce its most important characteristics [200]. Frequently, the name two-level fluctuators (TLFs) is also employed in this context to emphasise their natural state fluctuations if the temperature is at the order of magnitude of their energy splitting [197, 198, 207, 208].

between the plates changed<sup>55</sup>. This off-resonant coupling can be described by an interaction Hamiltonian of the form

$$\hat{H}_{\text{int}} = v_{\parallel} (\hat{n} \otimes |e\rangle \langle e|) , \quad (7.26)$$

with  $v_{\parallel}$  being the so-called longitudinal interaction strength, corresponding to a change in the oscillator frequency (proportionality to  $\hat{n}$ ) once the TLS is in the excited state.

Another strong motivation for the two interaction mechanisms indicated by Eqs. (7.25) and (7.26) is that they exactly correspond to the damping (respectively dephasing) model of a harmonic oscillator which we will turn to in the next subsection. The above model consequently already presents an explanation for observed loss effects (transversal interaction with TLS) and dephasing (longitudinal interaction with TLS). However, the interaction Hamiltonians presented above can be even used beyond a Markovian approximation of the combined evolution of the qudit with TLS defects. In particular, the validity of the approximation will depend on the following question: What is the relationship between the coupling strength between qudit and TLS compared to the coupling strength of this TLS with the rest of the environment (in particular with other TLS)? If the interaction between TLS and qudit is strong compared to the coupling of the TLS to the rest of the environment, then the Markovian approximation cannot be valid. This is because the information exchanged between these two systems will not decay to the rest of the environment before it can potentially return to the qudit. This seems intuitive for transversal interaction but it also holds for longitudinal interaction. It has been shown that the thermal fluctuation of the TLS can lead to a deviation from single-exponential dephasing in the long-time limit [207]. These fluctuations can be modelled by a so-called random telegraph process and can induce a non-Markovian behaviour of the qudit's dynamics [207].

We can characterise a TLS by its coupling strength  $v$  and its splitting  $E_{\text{TLS}}$ . Let  $\omega_0$  be the frequency of the harmonic oscillator and let us assume that  $k_B T \ll \omega_0$  (otherwise one could not properly operate the junction anyway). One can generally split the TLS into 4 groups where we employ the nomenclature from Ref. [200].

1.  $E_{\text{TLS}} \ll \omega_0$  : Transversal interaction is suppressed since the TLS and the junction are not resonant. However, the TLS with  $k_B T \lesssim \omega_0$  experience fluctuations in their state due to interaction with the thermal bath which, in turn, can lead to fluctuations of the energy level of the qudit by longitudinal interaction. This is called adiabatic noise and the TLS in this context are sometimes called fluctuators, cf. Footnote 54. These fluctuators can induce a non-Markovian evolution of the superconducting qudit [207].
2.  $E_{\text{TLS}} \simeq \omega_0$  and  $v$  is small compared to the coupling strength to other modes of the environment: The TLS is in the ground state at operating temperature and can take an excitation from the qudit. However, it cannot coherently return the excitation since the excitation dissipates quickly. This leads to an unrecoverable loss of excitation on the qudit and is called quantum noise.
3.  $E_{\text{TLS}} \simeq \omega_0$  and  $v$  is large compared to the coupling strength to other modes of the environment: The TLS is in the ground state at operating temperature and can take an excitation from the qudit. It is able to coherently return this interaction which leads to a recoverable loss indicating a memory effect. This noise is called strongly coupled noise.

---

<sup>55</sup>Note that while for flux and phase qudits a longitudinal electric-dipole-coupling mechanism is excluded since the average voltage across the junction is zero, the defects can still change the shape of the potential for the phase in the junction leading to a shift in the energy [201].

4.  $E_{\text{TLS}} \gg \omega_0$  : The TLS is in the ground state at operating temperature and cannot transversally interact with the junction since it is out of resonance. It is also not in a regime where thermal excitation matters, consequently these TLS do not influence the evolution of the junction at all.

To summarise, if the TLS couple more strongly to their own environment than to the qudit they can be treated as a classical part of the environment whose influence on the qudit can be described as purely Markovian. It is rather common that decoherence on the qudit is determined by a few TLS that are more strongly coupled to the qudit than others [200]. On the contrary, if the TLS is sufficiently strongly coupled to the environment, it means that the information about its state is continuously transferred to the environment and this prevents any quantum interference from taking place. As such, the relevant quantity determining whether the TLS can be considered as a classical fluctuator or needs to be treated as a quantum object is the ratio of the qudit-TLS coupling and the dephasing rate of the TLS [209].

Taking all effects we discussed above into account, the dynamics of the qudit's reduced density matrix,  $\hat{\rho}_Q(t)$ , is described by the following equation [200],

$$\hat{\rho}_Q(t) = \text{Tr}_{SC} \left\{ \langle \text{Tr}_T [\hat{\rho}(t|E(t))] \rangle_{E(t)} \right\}, \quad (7.27)$$

$E(t)$  describes the stochastic process used to simulate the adiabatic noise by long-time memory, low-frequency noise.  $\hat{\rho}$  is the density matrix of all quantum degrees of freedom and  $\langle \cdot \rangle_{E(t)}$  is the average over the stochastic processes. In other words, one should describe the qudit together with its strongly coupled TLS in a thermal bath and use a Markovian master equation for the time evolution; this yields  $\text{Tr}_T [\rho(t|E(t))]$ . Repeating this for a sufficient number of realisations of the stochastic process  $E(t)$ , one can then build the stochastic average afterwards. From the remaining strongly coupled degrees of freedom we can determine the qudit density matrix by a final partial trace eliminating all non-qudit degrees of freedom. As a consequence, we need to formulate a Hamiltonian  $\hat{H}$  for the combined system of junction and primary environment (strongly coupled TLS), with the secondary environment (weakly coupled fluctuators) being included according to a random telegraph process. The tertiary environment (thermal bath and short-memory TLS) is described by dissipative operators in a Lindblad master equation yielding a Markovian evolution.

## 7.4 Noise Models for a Harmonic Oscillator

To describe the effects of the tertiary environment, we will employ the following model: Consider a harmonic oscillator (represented by creation and annihilation operators  $\hat{a}, \hat{a}^\dagger$ ) with frequency  $\omega_0$  interacting with a thermal bath at  $T \simeq 0\text{K}$ . Since in superconducting qudit implementations the device is usually operated at very low temperatures, this approximation is well-motivated. We will then use the results from this model for the phase qudit represented by an anharmonic oscillator with an anharmonicity that is much smaller than the oscillator frequency. In this case we expect that the harmonic approximation is well fulfilled.

We will first describe excitation transfer between the oscillator and bath modes, i.e. we consider a system-bath interaction Hamiltonian of the form  $\hat{H}_{\text{int}} = \sum_i (\hat{\Gamma}_i \hat{a}^\dagger + \hat{\Gamma}_i^\dagger \hat{a})$  for some set of operators

$\{\hat{\Gamma}_i\}$  on the bath [210]. One can show that, neglecting the Lamb shift<sup>56</sup>, it is possible to obtain the following Lindblad master equation for the state of the oscillator  $\rho$  [210],

$$\mathcal{L}\hat{\rho} = -i\omega_0 [\hat{a}^\dagger \hat{a}, \hat{\rho}] + \gamma_1 \left( \hat{a} \hat{\rho} \hat{a}^\dagger - \frac{1}{2} \hat{a}^\dagger \hat{a} \hat{\rho} - \frac{1}{2} \hat{\rho} \hat{a}^\dagger \hat{a} \right). \quad (7.28)$$

where  $\gamma_1$  is a parameter that depends on specific assumptions on the bath, in particular the operators  $\hat{\Gamma}_i$ . This interaction represents an exchange of excitation between system oscillator and bath leading to amplitude damping of the oscillator, i.e. decay. A Lindblad master equation is an appropriate description to the oscillator dynamics for weak system-bath coupling and when one considers the system dynamics on a timescale that is much faster than the oscillator timescale [212]. This is in accordance with the validity of a Markovian equation of motion, cf. Sec. 5.2. Both approximations are well fulfilled for our modelling in terms of a tertiary bath as illustrated in Sec. 7.3. Indeed, the oscillator frequency is very large compared to the timescale of the dynamics we are interested in, cf. the RWA we performed in the beginning of Sec. 7.2. Furthermore, we only include the weakly coupled TLS of the environment in the tertiary bath description, which indeed allows us to describe their effects in terms of a Markovian master equation.

Another very common coupling mechanism ansatz between oscillator and bath is given by an interaction Hamiltonian of the form  $\hat{H}_{\text{int}} = \sum_i (\hat{\Gamma}_i \hat{a}^\dagger \hat{a} + \hat{\Gamma}_i^\dagger \hat{a} \hat{a}^\dagger)$  [210]. This operator represents an environmental monitoring of the number of excitations in the oscillator [38]. Neglecting once again the Lamb shift, this leads to a master equation of the general form [210]

$$\mathcal{L}\hat{\rho} = -i\omega_0 [\hat{a}^\dagger \hat{a}, \hat{\rho}] + \gamma_2 \left( \hat{a}^\dagger \hat{a} \hat{\rho} \hat{a}^\dagger \hat{a} - \frac{1}{2} (\hat{a}^\dagger \hat{a})^2 \hat{\rho} - \frac{1}{2} \hat{\rho} (\hat{a}^\dagger \hat{a})^2 \right), \quad (7.29)$$

where  $\gamma_2$  will again be a parameter that depends on specific assumptions on the bath, in particular the specific operators  $\hat{\Gamma}_i$ . The same restrictions for the validity of a description via a Markovian master equation apply as in the damping case. The evolution governed by Eq. (7.29) will not change the excitations in the harmonic oscillator since all Lindblad operators are diagonal in the eigenbasis of the oscillator. The off-diagonal elements of the density matrix will, however, decay. Since the off-diagonal elements represent the phase information of a given state between its projections on e.g. the energy eigenbasis, this effect is usually called dephasing.

If one represents  $\hat{\rho}$  in the energy eigenbasis of the harmonic oscillator, the damped oscillator according to Eq. (7.28) and the dephasing oscillator according to Eq. (7.29) lead to so-called single-exponential decay<sup>57</sup> of the diagonal and off-diagonal elements of  $\hat{\rho}$ . The corresponding exponential decay time  $\sim e^{-\frac{t}{T}}$  for the diagonal elements, or “populations”, is called  $T_1$  whereas for the off-diagonal elements, or “coherences”, it is called  $T_2$ . While this nomenclature is usually applied to two-level systems in the theory of nuclear magnetic resonance, the fundamental concept of these processes holds in a large variety of physical systems and also in the multi-level case under truncation [213].

For the damped harmonic oscillator the equation of motion of the individual matrix elements in

<sup>56</sup>The term Lamb shift refers to the change in the system’s Hamiltonian by environmental effects [38]. For the models we consider in this section the Lamb shift is usually only a shift in the oscillator frequency which we can simply absorb into  $\omega_0$ , see e.g. Ref. [211].

<sup>57</sup>As we will see shortly, the decay of matrix elements will not be described by a simple single exponential for a harmonic oscillators. The term “single-exponential decay” is strictly speaking only adequate if we consider initial density matrices that are restricted to the Liouville space corresponding to the Hilbert space of the lowest two eigenstates of the oscillator, i.e. the oscillator reduces to a two-level-system.

the energy representation is given by

$$\frac{d}{dt}\rho_{nm} = -i\omega_0(n-m)\rho_{nm} + \gamma_1\sqrt{(n+1)(m+1)}\rho_{n+1,m+1} - \gamma_1\frac{n+m}{2}\rho_{nm}. \quad (7.30)$$

For the diagonal elements this reduces to

$$\frac{d}{dt}\rho_{nn} = \gamma_1(n+1)\rho_{n+1,n+1} - \gamma_1n\rho_{nn}. \quad (7.31)$$

This equation is easily understood by interpreting the first summand as a gain of excitation via transfer from the next-highest level whereas the second summand represents a loss of excitation due to transfer to the next-lowest level. From Eq. (7.30) one can also see that coherences are transferred. This is in accordance with the population transfer from the next-highest level represented by the second summand. However, in contrast to the populations, the coherences will for  $t \rightarrow \infty$  vanish completely since the time derivative of the “lowest” coherence  $\rho_{10}$  still has a decaying term. The  $T_1$  time is given by the exponential decay time of  $\rho_{11}$  and the  $T_2'$  time<sup>58</sup> is given by the exponential decay time of the matrix element  $\rho_{10}$ . As a result, we see that

$$T_1 = \frac{1}{\gamma_1}, \quad T_2' = \frac{2}{\gamma_1} \implies \frac{1}{2T_1} = \frac{1}{T_2'}. \quad (7.32)$$

For the harmonic oscillator under pure dephasing we obtain the matrix element equations,

$$\frac{d}{dt}\rho_{nm} = -i\omega_0(n-m)\rho_{nm} - \frac{\gamma_2}{2}(n-m)^2\rho_{nm}, \quad (7.33)$$

and we see that populations remain unchanged while coherences decay proportional to  $(n-m)^2$ . This results in<sup>59</sup>

$$T_1^* = \infty, \quad T_2^* = \frac{2}{\gamma_2}.$$

An observed single-exponential decay of populations and coherences can be explained via the combination of damping and dephasing. Due to  $T_1^* = \infty$ , the measured  $T_1$  time corresponds directly to the damping constant  $\gamma_1$  whereas the measured  $T_2$  time will have two sources, i.e.

$$\frac{1}{T_2} = \frac{1}{T_2'} + \frac{1}{T_2^*} = \frac{1}{2T_1} + \frac{1}{T_2^*}, \quad (7.34)$$

Since damping corresponds to both population loss, more precisely “excitation loss”<sup>60</sup>, and dephasing, it is actually possible to overestimate both effects by observing the following relation for the

<sup>58</sup>The prime on  $T_2$  is used to indicate that it originates from a decay process. A similar distinction for  $T_1$  is unnecessary as we will see shortly.

<sup>59</sup>To indicate that these times originate from pure dephasing, a star superscript is employed.

<sup>60</sup>The total population of the density matrix needs to remain normalised of course. Rather, only the population of the excited levels is decaying (and transferred to the ground state) which we will call “excitation loss”.

combined coherence decay given by damping and dephasing,

$$\begin{aligned}
\frac{(n+m)}{2T_1} + \frac{(n-m)^2}{T_2^*} &\leq \frac{(n+m)}{2T_1} + \frac{(n+m)|(n-m)|}{2T_2^*} \\
&\leq \frac{(n+m)}{2\min(T_1, T_2^*)} + \frac{(n+m)}{2\min(T_1, T_2^*)} \cdot 2|n-m| \\
&= \frac{(n+m)}{2\min(T_1, T_2^*)} [1 + 2|n-m|] \\
&= \frac{(n+m)}{2\min\left(\frac{T_1}{1+2|n-m|}, \frac{T_2^*}{1+2|n-m|}\right)} \equiv \frac{(n+m)}{2T_1^{(\text{eff})}}
\end{aligned}$$

Defining an effective  $T_1$  time,

$$T_1^{(\text{eff})} = \frac{\min(T_1, T_2^*)}{1 + 2\max|n-m|}, \quad (7.35)$$

we can conclude that a damped oscillator with decay according to  $T_1^{(\text{eff})}$  undergoes at least as much excitation loss as a harmonic oscillator with  $(T_1, T_2^*)$  (since  $T_1^{(\text{eff})} \leq T_1$ ) and, by the calculation above, it also undergoes at least as much dephasing. If we perform a cut-off of the oscillator Hilbert space at dimension  $d$ , i.e. we only describe the ground state and the next  $d-1$  excited levels, then clearly  $\max|n-m| = d-1$  and we can write

$$T_1^{(\text{eff})} = \frac{\min(T_1, T_2^*)}{2d-1}. \quad (7.36)$$

We will use this relation in the next subsection. It proves that it is essentially possible to describe effects of decay and dephasing with only a single effective  $T_1$  time if one accepts overestimation of some decoherence effects. This allows for an easier numerical analysis by reducing the number of environmental parameters.

## 7.5 Controllability Gain via Environmental Degrees of Freedom

As pointed out in Sec. 7.3, superconducting qudits exhibit non-Markovian behaviour and as such it is possible that the environment can assist in generating certain unitary transformations. Inspired by the works presented in Refs. [201] and [204], we exploit the fact that experiments are able to determine all important parameters for the strongly coupled TLS with frequencies near the qudit frequency, including their  $T_1$  and  $T_2$  times [204]. Furthermore, the phenomenological  $T_1$  and  $T_2$  times of the qudit itself can be recorded [204]. We will neglect in the following the non-Markovianity of the evolution originating from the adiabatic noise, however, the dephasing induced by these environmental degrees of freedom is implicitly included in the experimentally measured  $T_2$  times<sup>61</sup>. Analogously, quantum noise will be treated in the form of the experimentally measured  $T_1$  times. The strongly coupled noise will be considered by explicitly regarding one or a few TLS near the qudit frequency and in the spirit of Eq. (7.27) they will be explicitly included in the dynamics. Furthermore, the  $T_1$  and  $T_2$  times will be modelled by a Lindblad master equation on the strongly coupled degrees of freedom as

<sup>61</sup>We expect non-Markovian effects from the secondary bath to be strongly overshadowed by the non-Markovian effects from the primary bath, i.e. the strongly coupled TLS. This is further encouraged by the observation that the adiabatic noise can often be equivalently described by the interaction with a single, strongly-coupled TLS [209].

discussed in Sec. 7.3. In addition, we will almost universally absorb the  $T_2$  time in an effective  $T_1$  time as pointed out in Eq. (7.27).

In accordance with the results shown in Refs. [201] and [204] we will consider only transversal coupling for the strongly coupled TLS since this mechanism seems to adequately explain the observed behaviour of TLS in proximity of a phase qudit<sup>62</sup>. To account for the TLS, we will go into the rotating frame with the transformation  $\hat{V}(t) = e^{-i\omega_0(\hat{n} + \hat{P}_e)t}$  where  $\hat{P}_e$  is the projector on the excited state of the TLS. After neglecting all rapidly oscillating terms in a low-frequency control scheme, the resulting total Hamiltonian for a single TLS in the primary environment is given by

$$\hat{H}_{SC} = \frac{\beta}{2} \hat{n}(\hat{n} - 1) + I_c(t) \hat{n} + (E_{\text{TLS}} - \omega_0) \hat{P}_e + \frac{S}{2} (\hat{a} \otimes |e\rangle \langle g| + \hat{a}^\dagger \otimes |g\rangle \langle e|) . \quad (7.37)$$

The coupling strength  $v$  is given by half the splitting,  $S$ , one observes on the qudit when it is on resonance with the TLS. This transformation is analogous to the one performed in Sec. 7.2. It leaves the interaction term invariant since the exponent of  $V(t)$  takes equal values for equal total occupation number of qudit and TLS and the interaction only couples subspaces with identical total occupation number. For simplicity, we furthermore absorbed  $\kappa_1$  in  $I_c(t)$  such that  $I_c(t)$  can be interpreted directly as the frequency shift imposed on the qudit. Note that it is possible that the control also couples to the TLS, however due to the presumably small size of the TLS this has been neglected in accordance with the discussion in Ref. [201]. The generalisation of Eq. (7.37) to multiple TLS is straightforward.

We propose the following control mechanism that leads to arbitrary controllability of the diagonal phases of a unitary transformation on a phase qudit: First, move the qudit close to resonance with a TLS, then pick up the desired phase shift using the enhanced interaction, and finally move the qudit back off resonance. This sequence will properly align all the phases in the four-level subspace and yields the desired phases. Since the moving into resonance is crucial, it seems natural to impose the final control to move the qudit frequency towards a TLS in the very beginning and back to  $\omega_0$  at the end of the optimisation time interval  $[0, T]$ , corresponding to  $I_c(0) = I_c(T) = 0$ .

The Hamiltonian  $H_{SC}$ , describing the strongly coupled degrees of freedom, is employed together with Lindblad operators of the form  $\hat{A}_n = \sqrt{n/T_1} |n-1\rangle \langle n|$  and  $\hat{A}_{\text{TLS}} = \sqrt{1/T_1^{(\text{TLS})}} |g\rangle \langle e|$  to form a Lindblad master equation of the strongly coupled degrees of freedom, cf. Eq. (5.16). For superconducting qudits, the tertiary (i.e. thermal) bath can in very good approximation assumed to be at  $T \simeq 0\text{K}$ , cf. the analysis in Ref. [204]. A generalisation to multiple TLS is straightforward, with all operators having identical form modulo padding with tensor products of identity on the subspaces corresponding to the other TLS. For the numerical simulation of the density matrix dynamics we employed a Newton propagator [214] to solve the resulting Lindblad master equations.

Due to the thermal bath being at  $T \simeq 0\text{K}$  and the fact that the evolution cannot increase the combined excitation of qudit and TLS, we choose as an optimisation goal the unitary  $U \otimes \mathbb{1}$  on the strongly coupled degrees of freedom. Here,  $U$  represents the unitary gate that is supposed to be implemented on the qudit. Since the initial state of all strongly coupled TLS in the environment is the ground state it will always be desirable to recover any excitation that is transferred to any TLS. In other words, the target final state for the TLS should be their ground states. As a result, we employ a tensor-sum type optimisation on the Hilbert space  $\mathcal{H}_q \otimes |g\rangle \langle g|$  where  $|g\rangle$  represents the

<sup>62</sup>In the following, closeness of TLS and qudit always refers to proximity of transition frequencies between their eigenstates, not spatial proximity.

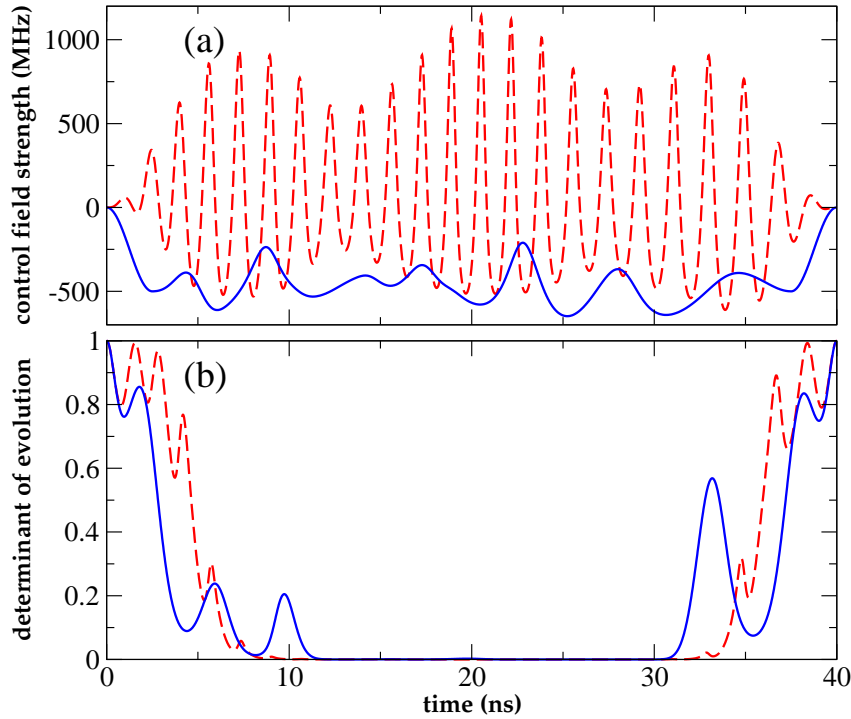


Figure 7.1: (a): Optimised amplitudes for an optimisation towards  $\text{diag}(1, -1, 1, 1)$  with the control shown in blue following a fixed ramp of  $\pm 500$  MHz over 2.5 ns at the beginning and end and the red dashed line obtained without imposing a ramp. The anharmonicity is given by  $\beta = 40$  MHz,  $\omega_0 - E_{\text{TLS}} = 550$  MHz,  $S = 60$  MHz,  $T_1^Q = 5 \mu\text{s}$ , and  $T_1^{\text{TLS}} = 1 \mu\text{s}$ . The optimised gate error (here and in the following this refers to  $1 - F_{\text{avg}}$ , cf. Eq. (4.26)) under the optimised pulse is given by  $1.529 \cdot 10^{-2}$  with ramp and  $1.648 \cdot 10^{-2}$  without ramp. (b): Liouville space determinant of the system evolution – increase of the determinant indicates non-Markovianity.

ground state of the TLS, cf. Sec. 7.3.

In the following, we will consider the lowest four levels of the qudit due to the existence of known analytical solutions for the  $\text{SO}(4)$  part of an arbitrary unitary transformation [205]. We choose  $U = \text{diag}(1, -1, 1, 1)$ <sup>63</sup> as a representative for the implementation of arbitrary diagonal unitaries. We have verified that optimisations towards diagonal unitaries with random phases yield very similar errors<sup>64</sup>. Note, however, that the phase corresponding to the ground state is fixed independently on the employed control. This is in accordance with the interpretation of unitaries as elements of  $\text{PU}(N)$ , cf. Sec 2.8. For the final-time optimisation functional we used Eq. (5.37), employing a full basis of Liouville space. This is motivated by the fact that we consider a comparatively low-dimensional problem and Eq. (5.37) can be directly related to the gate fidelity. The intermediate-time costs were chosen to be of standard form, cf. Eq. (5.24).

Figure 7.1 shows an example optimisation for some realistic system parameters. The red curve shows the optimised control if a squared sine shape function is employed. The result is a rather

<sup>63</sup>All target unitaries are written with an implicit rotation according to the transformation  $e^{-i\frac{\beta}{2}\hat{n}(\hat{n}-1)T}$  where  $T$  is the optimisation time. This was done to eliminate the drift part of the evolution which introduces a final-time dependent phase on the individual levels that leads to final-time dependent fidelities obtained via OCT. This is because without this rotation, in the absence of any TLS, the gate  $e^{-i\frac{\beta}{2}\hat{n}(\hat{n}-1)\tau}$  (simply by choosing  $I_c(t) = 0$ ) can be implemented perfectly if  $T = \tau$  but not if  $T = \tau \pm \epsilon$ . This dependence on final time is removed by the rotation since the effect of the drift is absorbed by it.

<sup>64</sup>For example, optimisation for 20 random diagonal unitaries, using the parameters of Fig. 7.1, yields errors between  $1.390 \cdot 10^{-2}$  and  $1.804 \cdot 10^{-2}$ , differing from that for  $U_1$  by less than a factor of 1.2, cf. Fig. (7.1).

rapidly oscillating control. This is undesirable since our approximations for the derivation of the Hamiltonian (7.37) require a slowly varying control. To direct the control algorithm towards a smooth implementation of this mechanism we employ a ramp-type shape function of the form

$$S(t) = \begin{cases} 0, & t \in [0, \tau] \\ \sin^2\left(\frac{\pi(t-\tau)}{T-2\tau}\right), & t \in [\tau, T-\tau] \\ 0, & t \in [T-\tau, T] \end{cases}, \quad (7.38)$$

for an optimisation time interval  $[0, T]$  and a ramp time  $\tau$ . This shape function is taken to be of the standard squared sine form in the middle of the optimisation time interval. At the very beginning and at the very end it is set such that the optimisation cannot change the guess pulse, cf. the update equation in Eq. (5.30).

The guess pulse has been accordingly chosen of the form

$$I_c^{(0)}(t) = \begin{cases} I_0 \sin^2\left(\frac{\pi t}{2\tau}\right), & t \in [0, \tau] \\ I_0 + \alpha e^{-\frac{1}{2}\frac{(t-t_0)^2}{2\sigma^2}}, & t \in [\tau, T-t] \\ I_0 \sin^2\left(\frac{\pi(T-t)}{2\tau}\right), & t \in [T-\tau, T] \end{cases}, \quad (7.39)$$

where  $I_0$  is the target offset the control should be centred around after the ramp and  $\alpha, t_0, \sigma$  are parameters of the Gaussian guess. The guess pulse will smoothly (note that  $I_c^{(0)}(t)$  and its first derivative are zero at  $t = 0$  and  $t = T$ ) ramp the pulse up and down. The success of this approach can be seen in the blue curve in Fig. 7.1 where an essentially identical gate fidelity could be obtained with a much smoother control that has a much smaller amplitude range in addition. Both properties are very desirable for experimental realisation of the numerically obtained control fields, in particular because the switching time of the controls in current experiments is technically limited [204].

Note that while anharmonicities for the anharmonic oscillators found in superconducting qubits are generally negative, from the perspective of this control scheme only the modulus of  $\beta$  has a relevant influence. This is because only the energy difference with respect to the TLS is relevant. Whether levels are below or above resonance only inverts the phase acquired during the interaction with the TLS. As a consequence, the sign of the anharmonicity merely swaps around the difficulty of particular diagonal gates. As long as we assert that we can reach any diagonal unitary our results can be applied both to the  $+\beta$  and  $-\beta$  case. From a physical perspective, the only change that needs to be implemented in the control scheme is with respect to the oscillator frequency  $\omega_0$  in absence of the control, in particular whether it should be set above or below the most strongly coupled TLS. This is because the higher level transitions always should increasingly move away from resonance with the TLS in the absence of a control field and not towards it. More precisely, one should choose  $\omega_0 < E_{\text{TLS}}$  if  $\beta < 0$  and  $\omega_0 > E_{\text{TLS}}$  if  $\beta > 0$ . As can be seen in Fig. 7.2, this adjusted control strategy indeed shows that the  $+\beta$  and  $-\beta$  case behave virtually identical if the initial position of the qudit frequency is chosen in accordance with the discussion above.

The dynamics under an optimised pulse utilising the ramping scheme is illustrated in Fig. 7.3. To visualise the optimised dynamics, we parametrise the joint state of system and strongly coupled TLS by  $r(t)(e^{i\varphi(t)} \cos(\theta(t)) |n, g\rangle + e^{i\chi(t)} \sin(\theta(t)) |n-1, e\rangle)$  with  $g, e$  representing the TLS ground state, respectively excited state. This makes use of the fact that, without loss due to finite  $T_1$  or

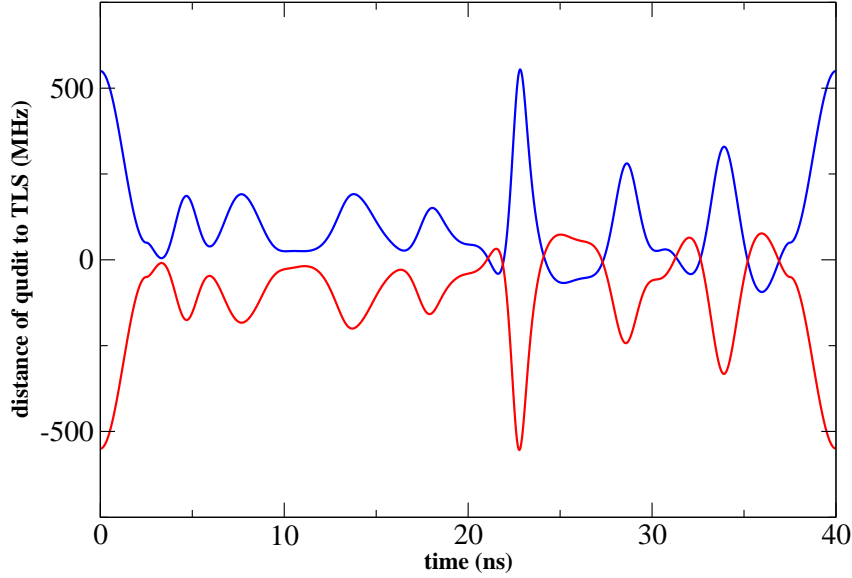


Figure 7.2: Optimised pulses for an optimisation towards  $\text{diag}(1, -1, 1, 1)$  for  $\beta = +40$  MHz in blue and  $\beta = -40$  MHz in red. The control fields in this figure have been shifted by  $+550$  MHz and  $-550$  MHz respectively to account for the different frequency of the qudit in absence of the control ( $\omega_0 - E_{\text{TLS}} = 550$  MHz for  $\beta = 40$  MHz and  $\omega_0 - E_{\text{TLS}} = -550$  MHz for  $\beta = -40$  MHz). The control field after the shift can be interpreted as the distance of the qudit frequency under the control with respect to the TLS, i.e. 0 MHz corresponds to resonance with the TLS. All remaining parameters are identical to those chosen in Fig. 7.1, however, a slightly different guess pulse has been chosen. The optimised gate error under the optimised pulse is given by  $1.504 \cdot 10^{-2}$  for  $\beta = +40$  MHz and by  $1.506 \cdot 10^{-2}$  for  $\beta = -40$  MHz.

dephasing due to finite  $T_2^*$ , any initial state  $|n, g\rangle$  evolves in a subspace of Hilbert spanned by  $|n, g\rangle$  and  $|n-1, e\rangle$ . In practice, the radius and angles are obtained in the following way<sup>65</sup>,

$$\alpha(t) = \langle n, g | \hat{\rho}(t) | 0, g \rangle, \quad (7.40a)$$

$$\beta(t) = \langle n-1, e | \hat{\rho}(t) | 0, g \rangle, \quad (7.40b)$$

$$r(t) = \sqrt{|\alpha(t)|^2 + |\beta(t)|^2}, \quad (7.40c)$$

$$\theta(t) = \arctan\left(\frac{|\beta(t)|}{|\alpha(t)|}\right), \quad (7.40d)$$

$$\varphi(t) = \arctan\left(\frac{\text{Im}(\alpha(t))}{\text{Re}(\alpha(t))}\right). \quad (7.40e)$$

$\hat{\rho}(t)$  is the propagated density matrix under the optimised pulse. It is evident that  $r(t)$  does not only capture excitation loss by the finite  $T_1$  on qudit and TLS (representing population leaving the parametrised subspace) but also dephasing due to  $\alpha(t)$  and  $\beta(t)$  being computed via coherences of  $\rho(t)$ . The phase  $\chi(t)$  is not relevant for our optimisation problem and a spherical coordinate representation is obtained with  $\theta = 0$  corresponding to the  $xy$ -plane. It is restricted to the northern hemisphere since  $\theta \in [0, \frac{\pi}{2}]$  is sufficient to parametrise any state in the subspace when  $\varphi, \chi \in [0, 2\pi]$ .

<sup>65</sup> $\alpha(t)$  and  $\beta(t)$  are also rotated to account for the rotation in footnote 63 but we will skip this transformation in the formulas for simplicity. As a matter of fact, this rotation does not even influence  $r(t)$  and  $\theta(t)$  since it only changes the phases of  $\alpha(t)$  and  $\beta(t)$ . For  $\varphi(t)$  only  $\alpha(t)$  is relevant, which is multiplied by  $e^{i\frac{\beta}{2}n(n-1)t}$ . The different sign in the exponent compared to the rotation of  $U$  is due to the correspondence to a state rotation, not an operator rotation.

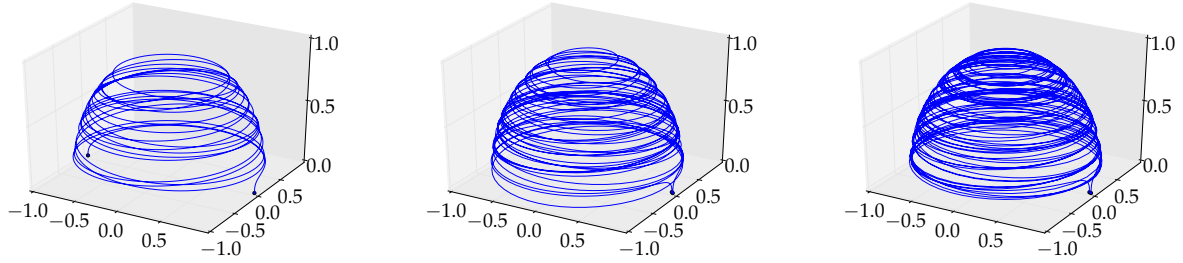


Figure 7.3: Time evolution of system levels  $n = 1, 2, 3$  (left to right) in the subspace spanned by  $|n, g\rangle$  and  $|n - 1, e\rangle$  for the ramped control. Parameters as in Fig. 7.1,  $T_1 = 5 \mu\text{s}$  (qudit),  $T_1^{(1)} = 1 \mu\text{s}$  (TLS).

Figure 7.3 displays the time evolution of each initial state  $|n, g\rangle$ ,  $n = 1, 2, 3$ , under the optimised control (level 0 is coupled to neither control nor the rest of Hilbert space): Level 1 acquires a final phase of  $\pi$ , whereas levels 2 and 3 return to their initial position as desired. During the evolution, the radii become slightly smaller than one, indicating Markovian decoherence effects. At intermediate times, the points leave the  $xy$ -plane which indicates excitation transfer to the TLS. The different numbers of revolutions correspond to the different frequency shifts the individual levels acquire via the control.

We will now directly illustrate how the optimised control utilises the strongly coupled environmental degrees of freedom to implement arbitrary diagonal unitaries. In panel (b) of Fig. 7.1 we see the determinant of the evolution at each point in time for the two control approaches, i.e. the determinant of the matrix  $e^{\mathcal{L}t}$  where  $\mathcal{L}$  is the Liouvillian corresponding to the Markovian evolution of the qudit degrees of freedom. A departure from monotonicity of this determinant represents a quantitative characterisation of the departure from Markovianity of the dynamical evolution [80]. As a matter of fact one can interpret the determinant as a description of the volume of accessible states when starting from an arbitrary density matrix in Liouville space at time  $t = 0$ . A reduction of the volume is in accordance with a purely Markovian evolution resulting in a potential loss of unitarity (representing rotation and consequently preservation of the Liouville space volume). More specifically, any Markovian evolution is contracting on Liouville space, i.e. it cannot increase the distance<sup>66</sup> between two density matrices [6]. It immediately follows that it cannot increase the volume of an arbitrary state set - dynamical maps are contractive. An increase of the Liouville space determinant represents a violation of contractivity and is consequently a reliable indicator of a non-Markovian evolution<sup>67</sup>. While, by construction, the evolution of the strongly coupled degrees of freedom is Markovian, hence contractive, the evolution of the qudit degrees of freedom is non-contractive for either optimised pulse as it can be clearly seen in Fig. 7.1. It is this non-Markovianity that yields an increase in controllability of the qudit system by interaction with the strongly coupled environmental degrees of freedom.

This point is further illustrated in Fig. 7.4 where the dependence of the best possible gate error on qudit anharmonicity and coupling strength between qudit and TLS is explored. For very small coupling to a TLS in the primary environment no solution can be found and the gate error remains

<sup>66</sup>Distance can refer to e.g. the trace distance or the negative state fidelity plus one.

<sup>67</sup>The evolution determinant is a rather weak measure for non-Markovianity, i.e. it is not very sensitive. Its relative ease of evaluation and reliability still motivates its usage for our purposes. An overview on different measures on non-Markovianity and how they compare with respect to each other can be found in Ref. [144].

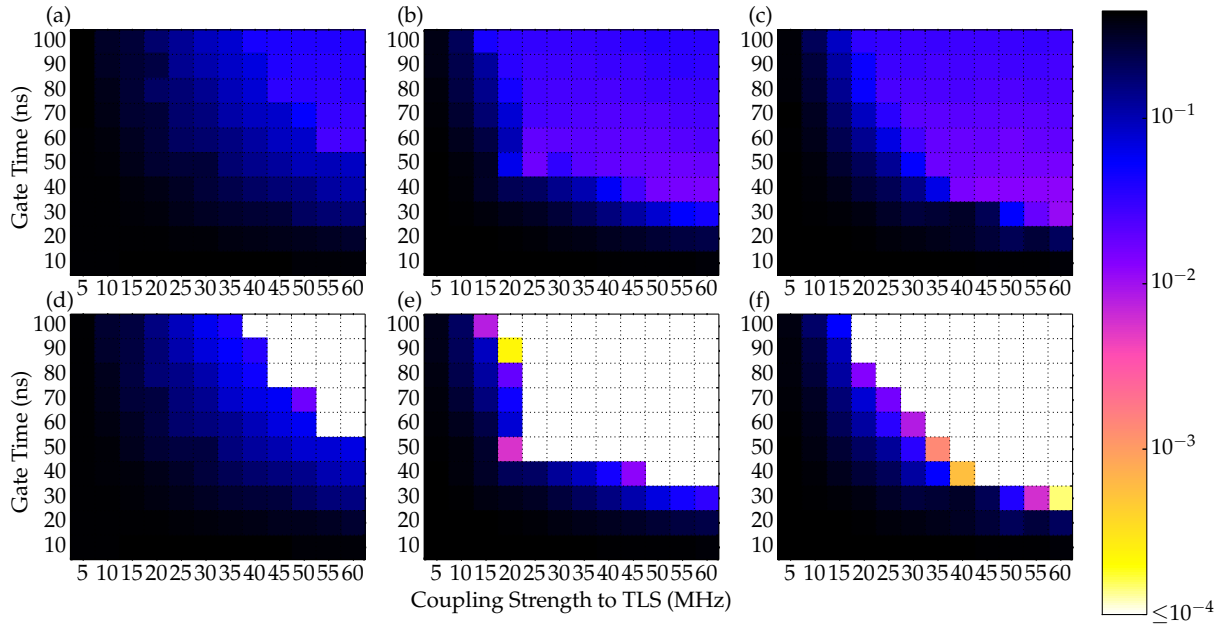


Figure 7.4: Error after optimisation for  $\text{diag}(1, -1, 1, 1)$  for  $T_1^Q = 5 \mu\text{s}$ ,  $T_1^{TLS} = 1 \mu\text{s}$  (a-c) and anharmonicities of  $\beta = 0 \text{ MHz}$  (a,d),  $40 \text{ MHz}$  (b,e),  $150 \text{ MHz}$  (c,f). For comparison, the error is also shown for infinite  $T_1$  of qudit and TLS (d-f). All remaining parameters are identical to those chosen in Fig. 7.1.

of the order one. In contrast, one moderately strongly coupled TLS in the primary environment is sufficient to yield good fidelities even for weak or zero anharmonicity. In the latter case (Fig. 7.4(a)), the desired diagonal unitaries can be realised if the operation time is sufficiently long. This can be successful only if the qudit has enough time to interact with the TLS in such a way that all levels “get back” their excitations and also acquire the correct phase. This is particularly hard for zero anharmonicity since all levels interact almost identically with the TLS due to the energy difference between all levels being the same. Only by utilising the level-dependent coupling strengths the levels are differentiated by the TLS-qudit interaction.

One can see in all panels of Fig. 7.4 a relatively sharp boundary, visible via an abrupt decrease in the optimal gate fidelity at a hyperbola  $y \sim \frac{1}{x}$  in the coupling strength ( $x$ ) - gate time ( $y$ ) plane. This boundary is determined by the control needing to implement the following steps: (i) ramp up the frequency of the qudit to be near-resonant with the TLS, (ii) transfer the wave function to the TLS, (iii) wait sufficiently long to acquire the proper phase, (iv) return the wave-function completely to the qudit and (v) return the qudit to its original frequency. The main bottleneck for the optimisation is most likely in steps (ii) and (iv), corresponding to the quantum speed limit (QSL) of this particular optimisation task [215]. The process can be roughly described in the language of atomic physics as acquiring a Rabi angle of  $\frac{\pi}{2}$  for the first excited level of the qudit if the goal is the unitary  $U = \text{diag}(1, -1, 1, 1)$ . The Rabi angle  $\varphi$  is proportional to the interaction time  $\tau$  and the coupling strength  $v$ , i.e.  $\varphi \sim \tau \cdot v$ . For fixed  $\varphi$  one immediately sees that  $\tau \cdot v = \text{const}$  which explains the observed hyperbola in Fig. 7.4. In the controllable region to the top-left of this hyperbola the gate error vanishes everywhere in the absence of decoherence, cf. the bottom panels of Fig. 7.4. In the presence of loss and dephasing, a large gate time leads to a decrease in the unitarity of the evolution which is why we get an additional bias towards short gate times  $\tau$ , cf. the bottom panels of Fig. 7.4.

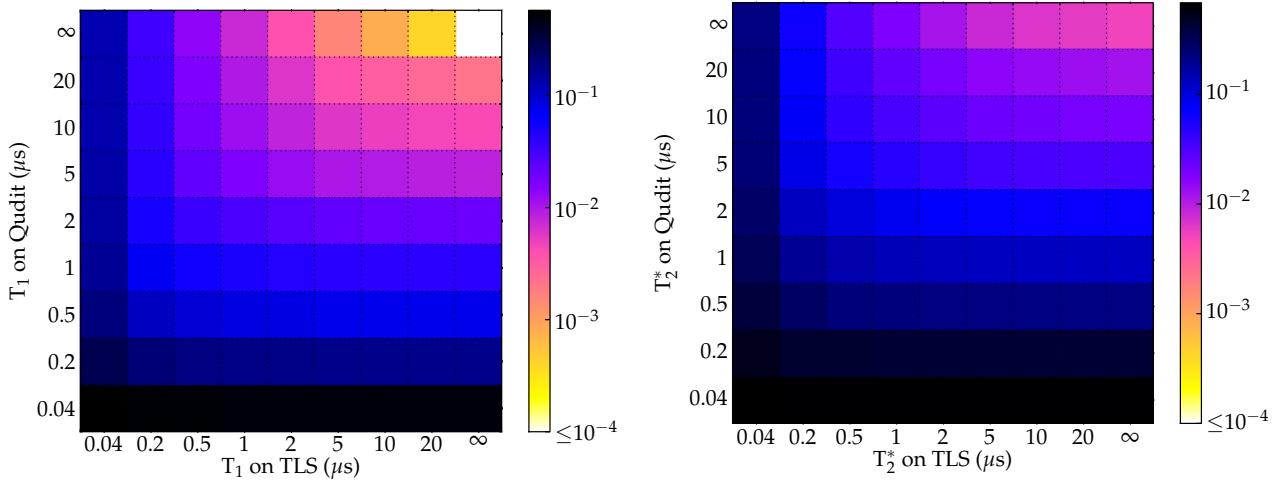


Figure 7.5: (left) Error after optimisation for  $\text{diag}(1, -1, 1, 1)$  as a function of  $T_1$  times of qudit and TLS for an optimisation time of  $T = 40$  ns (anharmonicity  $\beta = 40$  MHz,  $\omega_Q - \omega^{(1)} = 550$  MHz,  $S^{(1)} = 60$  MHz). (right) Error after optimisation for  $\text{diag}(1, -1, 1, 1)$  as a function of the  $T_2^*$  times with  $T_1$  fixed to  $10 \mu\text{s}$  for both qudit and TLS (parameters identical to left panel).

From this point of view, in the presence of multiple TLS in the environment, it is the best approach to couple the qudit to the most strongly coupled TLS which is as weakly coupled as possible to the remaining environment. There are some additional details to this general idea, which we will address later, but at least as long as all TLS are sufficiently far away from each other in terms of their energy splitting  $E_{\text{TLS}}$  this statement holds.

From the above discussion, one would expect that the reachable gate error is monotonically increasing for increasing coupling strength and increasing gate time. However, one can observe a few violations in Fig. 7.4, e.g. in panel (b) and (e) the point  $S = 20$  MHz and  $T = 60$  ns which represents a higher optimal gate error than the point at  $S = 20$  MHz and  $T = 50$  ns. These deviations are explained with numerical instabilities at the QSL boundary since the optimisation algorithm sometimes finds physically unreasonable solutions with very large spikes in the control field that numerically yield a better fidelity than any physically reasonable control. To limit this effect, a hard bound on the amplitude range of the control has been employed. Specifically, the optimisation is aborted once the algorithm tries to increase the control amplitude beyond a certain point. Nevertheless, there are still a few outliers remaining due to the slight arbitrariness of such an additional constraint in the algorithm. In particular, this makes the reachable fidelity dependent on the guess field and the details of the optimisation path in the landscape. Still, we can observe that in the vast majority of the cases the expected behaviour is reproduced in the numerical analysis.

The control problem becomes much easier for non-zero anharmonicity, with a subtle interplay between the requirements of resolving the qudit levels and sufficient interaction with all qudit levels. The latter corresponds to small anharmonicity (Fig. 7.4(b)) and subsequently allows good results even for weak coupling, whereas energy resolution is best for larger anharmonicity (Fig. 7.4(c)), which in turn allows for very short operation times. In other words, for small anharmonicity the level resolution is not as good and gate times need to generally be longer. On the other hand, many transitions can interact at the same time with the TLS allowing for a smaller coupling strength. This is illustrated best with regards to the light area in the middle of Figs. 7.4(b) and (e) compared to

$\Delta^{(2)}$	$S^{(2)}$	$T_1^{(2)}$	error	$\Delta^{(2)}$	$S^{(2)}$	$T_1^{(2)}$	error
50 MHz	40 MHz	2000 ns	$3.076 \cdot 10^{-2}$	450 MHz	40 MHz	2000 ns	$1.659 \cdot 10^{-2}$
50 MHz	40 MHz	200 ns	$4.052 \cdot 10^{-2}$	450 MHz	40 MHz	200 ns	$1.652 \cdot 10^{-2}$
50 MHz	40 MHz	40 ns	$7.867 \cdot 10^{-2}$	450 MHz	40 MHz	40 ns	$1.758 \cdot 10^{-2}$
50 MHz	10 MHz	2000 ns	$3.196 \cdot 10^{-2}$	450 MHz	10 MHz	2000 ns	$1.663 \cdot 10^{-2}$
50 MHz	10 MHz	200 ns	$3.564 \cdot 10^{-2}$	450 MHz	10 MHz	200 ns	$1.674 \cdot 10^{-2}$
50 MHz	10 MHz	40 ns	$4.241 \cdot 10^{-2}$	450 MHz	10 MHz	40 ns	$1.675 \cdot 10^{-2}$

Table 7.1: Error after optimisation for  $\text{diag}(1, -1, 1, 1)$  with two TLS in the primary environment (parameters for qudit and first TLS as in Fig. 7.1, second TLS positioned  $\Delta^{(2)}$  below  $\omega^{(1)}$ ). For comparison, the error obtained for a single TLS is  $1.652 \cdot 10^{-2}$ . All remaining parameters are identical to those chosen in Fig. 7.1.

Fig. 7.4(c) and (f). Conversely, for large anharmonicity the energy resolution is comparatively easy and the shortest gate times can be reached in this case. On the other hand, since only individual transitions can be tuned to resonance with the TLS at the same time due to their larger distance from each other, the coupling strength needs to be sufficiently high. This can be observed when looking at the QSL boundary for high coupling strengths which extends a little further towards shorter gate times for Figs. 7.4(c) and (f) compared to Figs. 7.4(b) and (e).

The effect of loss and dephasing on the strongly coupled degrees of freedom is illustrated in Fig. 7.5. We observe an exponential decay in the gate fidelity with decreasing  $T_1$  time in accordance with the exponential loss of excitations due to loss effects, cf. Sec. 7.4. Note that loss effects on the qudit have a slightly larger impact on the attainable gate fidelity since the prefactor in the exponent that governs decay is proportional to the level number, cf. Eq. (7.33). This situation remains unchanged, albeit slightly more pronounced, when an additional pure dephasing via a  $T_2^*$  time is introduced, see Fig. 7.5. In this case, higher levels are effected proportionally to the square of the level number, cf. Eq. (7.33), which leads to even higher gate errors for lower  $T_2^*$  times compared to lower  $T_1^*$  times.

When several TLS are in the strongly coupled degrees of freedom of the system, this will usually make the optimisation problem harder, at least if multiple noisy TLS are close to the “best” TLS (i.e. strong coupling, weak decoherence). This is because during the interaction with this TLS the qudit will also be weakly coupled to the other TLS and can potentially transfer excitations to them. This puts a further constraint on the optimisation in that it has to recover all excitations from multiple degrees of freedoms of the strongly coupled environment. The effect of a second TLS is illustrated in Table 7.1. As expected, if the TLS are not too close to each other, a suitable control can suppress the effect of the additional TLS even if it is strongly coupled and very noisy. On the other hand, the stronger a closely lying second TLS is coupled to the qudit, the more difficult it is to maintain good fidelities. In particular, if the two TLS are energetically very close, the gate time needs to be sufficiently long to resolve the energy difference between the two TLS. Adding more TLS to the primary environment does not change the general picture shown in Table 7.1: In optimisations with as many as four strongly coupled TLS, the error is increased by less than a factor of two compared to the error for a single TLS if none of the additional TLS is close to the favourable one ( $1.5 \cdot 10^{-2} \rightarrow 2.1 \cdot 10^{-2}$ ) and less than a factor of four if a moderately lossy TLS is in its vicinity ( $1.5 \cdot 10^{-2} \rightarrow 5.4 \cdot 10^{-2}$ ).

We want to finally emphasise, that our results are not restricted to superconducting phase qudit implementations. Our model is, in fact, quite general in that we considered an anharmonic oscillator

---

with an environment composed of two-level systems. Such a description can be applied to a variety of superconducting circuits, cf. the discussion in Secs. 7.1 and 7.3, or even NV centres in nanodiamonds [216]. As long as one or a few environmental modes are sufficiently isolated and sufficiently strongly coupled to the system, we expect that the environment can act as a resource for (almost) unitary quantum control.



## 8 Summary and Outlook

In this thesis, we derived highly efficient schemes for the certification and optimisation of unitary quantum operations in open quantum systems. In addition, we presented a quantum control perspective on two pivotal tasks of quantum information in the presence of environmental effects: preparation of pure states and implementation of quantum gates. To this end, optimal control has been applied for two examples of current experimental interest: the vibrational cooling of molecules and quantum information processing via superconducting qudits.

The mathematical concepts of commutant spaces in Liouville space and complete and totally rotating sets of density matrices have been introduced. They allowed to build a mathematical framework that enabled the derivation of fundamental theorems on the minimal amount of input states necessary to identify and reconstruct a unitary dynamical map on an open quantum system. These notions are independent upon the actual physical realisation of a quantum information device. In terms of experimental certification, state-fidelity based approaches to estimating the average fidelity of a given device with respect to a target unitary operation have been combined with Monte Carlo process certification. This allowed to significantly reduce the practical experimental effort of the certification task. Furthermore, we showed that control functionals derived from reduced set of states can reduce the numerical effort in OCT algorithms for the optimisation of unitary operations - both in terms of computational effort and required memory.

The preparation of pure states has been explored from the point of view of optimal control utilising two novel cooling schemes - symmetrised cooling and assembly-line cooling. These two schemes have been applied to the vibrational cooling of molecules for which they proved a significant improvement with respect to state-of-the-art experimental techniques. This improvement was not only restricted to an increase in efficiency but it also allowed for realisation of cooling almost independent on the electronic structure of the molecular species. Finally, it was shown that the implementation of unitary gates can be assisted by environmentally induced non-Markovian evolutions. We demonstrated that the controllability of a superconducting phase qudit can be increased when the strongly coupled environmental degrees of freedom are explicitly taken into account. This shows that beyond trying to merely reduce its detrimental effects, the environment of a physical system can also be exploited to assist in realising pivotal tasks of quantum information. All numerical programs written as a part of this thesis have been included in the library of programs for the simulation of time-dependent quantum molecular dynamics (QDYN) developed in the group of Prof. Christiane Koch at the University of Kassel.

The main theorems of this work, Theorems 3.3, 3.4, and 3.9, represent fundamental theoretical results regarding the limits of identification and certification of unitary dynamical maps. Significant steps towards a complete answer of the question how to best exploit a reduced set of input states in terms of a tight estimation of the average gate fidelity have been undertaken in this thesis. Our results already inspired further analysis on this subject in recent works [98, 217]. From a more general point of view, this poses the question whether similar reduced sets of states exist if the target operation is not unitary, but rather a different subset of dynamical maps. This could imply for example evolutions towards a steady state in the context of purification of quantum states. In addition, the work presented in this thesis regarding optimisation functionals allows for numerous applications, e.g. regarding the search of decoherence-free subspaces or in terms of quantum reservoir engineering. Finally, a detailed analysis of the environmental degrees of freedom in superconducting

qudits showed that non-Markovianity can extend the power of specific control approaches beyond their capabilities for a qudit that is isolated from its environment. While environmental effects often prove to be an experimental and theoretical challenge, this shows that a more rigorous understanding on when and how the environment can assist quantum control tasks is called for, in particular when non-Markovian evolutions are considered.

## A Proofs

### A.1 Kraus Operators for UDMs

**Lemma A.1.** *Let  $\mathcal{D} : \mathbb{C}^{d \times d} \mapsto \mathbb{C}^{d \times d}$  be a dynamical map represented by a set of Kraus operators  $\{E_k\}$ . The adjoint of  $\mathcal{D}$ ,  $\mathcal{D}^\dagger$ , is given by*

$$\mathcal{D}^\dagger(\rho) = \sum_k E_k^\dagger \rho E_k. \quad (\text{A.1})$$

$\mathcal{D}^\dagger$  is a dynamical map with Kraus operators  $\{E_k^\dagger\}$  if and only if  $\mathcal{D}$  is unital.

*Proof.* The adjoint of  $\mathcal{D}$  is defined as the mapping  $\mathcal{D}^\dagger : \mathbb{C}^d \mapsto \mathbb{C}^d$  which fulfils

$$\rho, \sigma \in \mathbb{C}^d : \langle \sigma, \mathcal{D}(\rho) \rangle = \langle \mathcal{D}^\dagger(\sigma), \rho \rangle.$$

Let  $\rho, \sigma \in \mathbb{C}^d$  be arbitrary, then using the invariance of the trace under cyclic permutation as well as its linearity,

$$\begin{aligned} \langle \sigma, \mathcal{D}(\rho) \rangle &= \text{Tr} \left[ \sigma^\dagger \sum_k E_k \rho E_k^\dagger \right] = \sum_k \text{Tr} \left[ E_k^\dagger \sigma^\dagger E_k \rho \right] \\ &= \sum_k \text{Tr} \left[ \left( E_k^\dagger \sigma E_k \right)^\dagger \rho \right] = \text{Tr} \left[ \left( \sum_k E_k^\dagger \sigma E_k \right)^\dagger \rho \right] = \left\langle \sum_k E_k^\dagger \sigma E_k, \rho \right\rangle. \end{aligned}$$

Defining

$$\mathcal{D}^\dagger(\rho) = \sum_k E_k^\dagger \rho E_k,$$

we see that  $\mathcal{D}^\dagger$  is a CP map and it is trace-preserving if

$$\sum_k E_k^\dagger E_k = \mathbf{1}_d,$$

which is equivalent to  $\mathcal{D}$  being unital. In this case  $\mathcal{D}^\dagger$  is a dynamical map with Kraus operators  $\{E_k^\dagger\}$ .  $\square$

**Lemma A.2.** *Let  $\mathcal{D} : \mathbb{C}^{d \times d} \mapsto \mathbb{C}^{d \times d}$  be a unitary dynamical map. Then  $\mathcal{D}$  is unital.*

*Proof.* Since  $\mathcal{D}$  is unitary it is an isometry. Let  $\tau \equiv \mathcal{D}(\frac{1}{d}\mathbf{1}_d)$ . Then

$$\langle \tau, \tau \rangle_{\text{HS}} = \left\langle \mathcal{D} \left( \frac{1}{d}\mathbf{1}_d \right), \mathcal{D} \left( \frac{1}{d}\mathbf{1}_d \right) \right\rangle_{\text{HS}} = \left\langle \frac{1}{d}\mathbf{1}_d, \frac{1}{d}\mathbf{1}_d \right\rangle_{\text{HS}} = \frac{1}{d}.$$

Since  $\mathcal{D}$  is a dynamical map  $\tau$  must be a density matrix. However, the only density matrix with norm  $\frac{1}{d}$  is  $\frac{1}{d}\mathbf{1}_d$ . Hence  $\tau = \mathcal{D}(\frac{1}{d}\mathbf{1}_d) = \frac{1}{d}\mathbf{1}_d$  and  $\mathcal{D}$  is unital.  $\square$

Now we can formulate the following proposition.

**Proposition A.3.** *Let  $\mathcal{D} : \mathbb{C}^{d \times d} \mapsto \mathbb{C}^{d \times d}$  be a dynamical map.  $\mathcal{D}$  is unitary if and only if it can be written as*

$$\mathcal{D}(\rho) = U\rho U^\dagger, \quad (\text{A.2})$$

with  $U : \mathbb{C}^d \mapsto \mathbb{C}^d$  being unitary.

*Proof.* Clearly any dynamical map given by  $\mathcal{D}(\rho) = U\rho U^\dagger$  is unitary since  $\mathcal{D}(\mathcal{D}^\dagger(\rho)) = UU^\dagger\rho U^\dagger U = \rho$ , i.e.  $\mathcal{D}\mathcal{D}^\dagger = \mathbb{1}_{d^2}$ .

Conversely, let  $\mathcal{D}$  be a unitary dynamical map. By Theorem 2.1 it can be written as

$$\mathcal{D}(\rho) = \sum_k E_k \rho E_k^\dagger,$$

with its adjoint given by

$$\mathcal{D}^\dagger(\rho) = \sum_k E_k^\dagger \rho E_k.$$

As pointed out in Sec. 2.6 we can assume w.l.o.g. that the set  $\{E_k\}$  is an orthogonal set. Any unitary transformation is unital by Lemma A.2, hence we know that

$$\sum_k E_k E_k^\dagger = \sum_k E_k^\dagger E_k = \mathbb{1}_d.$$

Since  $\mathcal{D}$  is unitary we know that  $\forall \rho \in \mathbb{C}^d$

$$\rho = \mathcal{D}(\mathcal{D}^\dagger(\rho)) = \sum_{kl} E_k E_l^\dagger \rho E_l E_k^\dagger.$$

Now combine  $(k, l)$  into a single index  $\alpha$  and define  $F_\alpha = E_k E_l^\dagger$  such that  $F_\alpha^\dagger = E_l E_k^\dagger$ , then

$$\mathcal{D}(\mathcal{D}^\dagger(\rho)) = \sum_\alpha F_\alpha \rho F_\alpha^\dagger = \mathbb{1}_d \rho \mathbb{1}_d. \quad (\text{A.3})$$

While the Kraus decomposition according to Eq. (A.3) is not necessarily unique, we know at least that there exists matrix elements  $u_{\alpha\beta}$  of a unitary matrix  $U$  such that

$$F_\alpha = \sum_\beta u_{\alpha\beta} \mathbb{1}_d,$$

as discussed in Sec. 2.6. Consequently,

$$\forall \alpha : F_\alpha \sim \mathbb{1}_d.$$

Since the  $\{E_k\}$  were chosen to be orthogonal this leads to

$$\text{Tr}[F_\alpha] = \text{Tr}[E_k E_l^\dagger] = \langle E_l, E_k \rangle \sim \delta_{lk},$$

which means that

$$\forall k, l : E_k E_l^\dagger \sim \delta_{lk} \mathbb{1}_d.$$

Specifically,

$$\forall k \exists c_k \in \mathbb{R}^+ : E_k E_k^\dagger = c_k \mathbb{1}_d,$$

with  $\sum c_k = 1$  due to  $\sum_k E_k E_k^\dagger = \mathbb{1}$  since by Lemma A.2,  $\mathcal{D}$  is unital due to being unitary. Note that  $c_k$  is positive since  $E_k E_k^\dagger$  is a positive operator. As a result, the Kraus operators can be written as  $E_k \equiv \sqrt{c_k} U_k$  with  $U_k$  unitary. This implies that  $\mathcal{D}$  can be written as

$$\mathcal{D}(\rho) = \sum_k c_k U_k \rho U_k^\dagger.$$

Now it only remains to show that all  $U_k$  are identical. Consider a pure state  $\rho = |\psi\rangle\langle\psi|$  and define  $\rho_k \equiv U_k |\psi\rangle\langle\psi| U_k^\dagger = |U_k \psi\rangle\langle U_k \psi| \equiv |\psi_k\rangle\langle\psi_k|$ . Clearly,  $\rho_k$  represents another pure state. Consequently, it is possible to write  $\mathcal{D}$  as follows,

$$\mathcal{D}(\rho) = \sum_k c_k |\psi_k\rangle\langle\psi_k|.$$

Because  $\mathcal{D}$  is an isometry,  $\mathcal{D}(\rho)$  also needs to be a pure state which is the case if and only if  $\forall k, l : |\psi_k\rangle = |\psi_l\rangle$ . This is because  $\mathcal{D}(\rho)$  is a convex combination of pure state which is only pure if and only if all pure states are the same. Since  $|\psi\rangle$  was arbitrary this means that  $\forall k, |\psi\rangle : U_k |\psi\rangle = |\phi\rangle$  for some fixed  $|\phi\rangle$  which immediately implies  $\forall k, l : U_k = U_l$  and we can finally conclude, using  $\sum_k c_k = 1$ , that indeed

$$\mathcal{D}(\rho) = U \rho U^\dagger.$$

□

## A.2 Commutant Spaces

**Proposition.** *The commutant space in  $\text{PU}(d)$  of an arbitrary, diagonalisable matrix  $M \in \mathbb{C}^{d \times d}$  can be represented as*

$$\mathcal{K}_{\text{PU}(d)}(M) \cong \left[ \bigotimes_i U(g_i) \right] / U(1), \quad (\text{A.4})$$

where  $g_i$  is the multiplicity of the  $i$ -th eigenvalue of the matrix  $M$ . Its dimension is given by

$$\dim_{\mathbb{R}} [\mathcal{K}_{\text{PU}(d)}(M)] = \left( \sum_i g_i^2 \right) - 1. \quad (\text{A.5})$$

Any  $U \in \mathcal{K}_{\text{PU}(N)}(M)$  admits the decomposition

$$U = \bigotimes_i \tilde{U}_{\mathcal{E}_i(M)}, \quad (\text{A.6})$$

where  $\tilde{U}_{\mathcal{E}_i(M)}$  is an element of  $U(g_i)$  acting on the eigenspace  $\mathcal{E}_i(M)$ .

*Proof.* Since  $M$  is diagonalisable we may write  $\mathbb{C}^d$  as the direct sum of the eigenspaces  $\mathcal{E}_i(M)$  of  $M$ , i.e.  $\mathbb{C}^d = \bigoplus_i \mathcal{E}_i(M)$ . The dimension of the subspace  $\mathcal{E}_i(M)$  is  $g_i$ . We show, that a matrix  $U \in \text{PU}(d)$  commutes with  $M$  as long as the operation does not allow vectors to leave these subspaces. Since  $U$

is an element of  $\text{PU}(d)$ , it is an isometry which generates rotations in this subspace. This is of course equivalent to  $U$  acting as a unitary operator on these subspaces.

One can see this by looking at the condition for a vanishing commutator,

$$[U, M] = 0 \iff [U, M] \vec{x} = \vec{0} \quad \forall \vec{x} \in \mathbb{C}^d.$$

Since  $\mathbb{C}^d = \bigoplus_i \mathcal{E}_i(M)$  we can write  $\vec{x} = \sum_i \nu_i \vec{e}_i$  with  $\vec{e}_i \in \mathcal{E}_i(M)$  for  $\nu_i \in \mathbb{C}$ . We will denote the corresponding eigenvalue of  $M$  to the eigenspace  $\mathcal{E}_i(M)$  by  $\lambda_i^{(M)}$ . Hence,

$$\begin{aligned} [U, M] \vec{x} &= \vec{0} \\ \iff \sum_i \nu_i U M \vec{e}_i &= \sum_i \nu_i M U \vec{e}_i \\ \iff \sum_i \nu_i \lambda_i^{(M)} U \vec{e}_i &= \sum_i \nu_i M U \vec{e}_i. \end{aligned}$$

Since this has to be fulfilled for any set  $\{\nu_i\}$  it follows that

$$\forall i : \lambda_i^{(M)} U \vec{e}_i = M U \vec{e}_i,$$

which means that  $U \vec{e}_i$  also has to lie in the eigenspace  $\mathcal{E}_i(M)$  (it has to be an eigenvector for  $M$  with eigenvalue  $\lambda_i^{(M)}$ ). Due to the argument being valid for all eigenspaces this means that any  $U$  in the commutant space allows for the following decomposition,

$$U = \bigotimes_i \tilde{U}_{\mathcal{E}_i(M)},$$

where  $\tilde{U}_{\mathcal{E}_i(M)}$  is an arbitrary element of  $U(g_i)$  acting on the eigenspace  $\mathcal{E}_i(M)$ .

Considering, that the final transformation should be in  $\text{PU}(d)$  we only consider the equivalence class with respect to division/multiplication with a complex number with absolute value 1. This leads to the desired result for the isomorphism,

$$\mathcal{K}_{\text{PU}(d)}(M) \cong \left[ \bigotimes_i U(g_i) \right] / U(1).$$

The dimensionality can be calculated directly, using the fact that  $\dim_{\mathbb{R}} [U(n)] = n$ ,

$$\dim_{\mathbb{R}} [\mathcal{K}_{\text{PU}(d)}(M)] = \left( \sum_i \dim_{\mathbb{R}} [U(g_i)] \right) - \dim_{\mathbb{R}} [U(1)] = \left( \sum_i g_i^2 \right) - 1.$$

This proves the proposition. □

**Proposition.** *The dimension of the commutant space in  $\text{PU}(d)$  of an arbitrary matrix  $M \in \mathbb{C}^{d \times d}$  can be estimated as*

$$\dim_{\mathbb{R}} [\mathcal{K}_{\text{PU}(d)}(M)] \leq \left( \sum_i g_i^2 \right) - 1, \tag{A.7}$$

where  $g_i$  is the algebraic multiplicity of the  $i$ -th generalised eigenvalue of the matrix  $M$ .

*Proof.* Since  $M$  is not necessarily diagonalisable, we may only find a decomposition of  $\mathbb{C}^{d \times d}$  in terms of the Jordan block invariant subspaces  $J_i(M)$ ,  $\mathbb{C}^{d \times d} = \bigoplus_i J_i(M)$ . The Jordan block invariant subspaces, i.e. the generalised eigenspaces, are given by  $\forall \vec{j}_i \in J_i(M) \exists k \in \mathbb{N} \setminus \{0\} : (M - \lambda_i \mathbb{1}_d)^k \vec{j}_i = \vec{0}$  where  $\lambda_i^{(M)}$  is the corresponding generalised eigenvalue of  $M$  to the Jordan block  $i$  [218]. Consider a  $U \in \mathcal{K}_{\text{PU}(d)}(M)$ , i.e.

$$\begin{aligned} [U, M] &= UM - MU = 0 \\ \iff M &= U^\dagger M U. \end{aligned}$$

Inserting this relation in the definition of the generalised eigenspaces, we obtain  $\forall \vec{j}_i \in J_i(M) \exists k \in \mathbb{N} :$

$$\begin{aligned} (U^\dagger M U - \lambda_i \mathbb{1}_d)^k \vec{j}_i &= \vec{0} \\ \iff U^\dagger (M - \lambda_i \mathbb{1}_d)^k U \vec{j}_i &= \vec{0} \\ \iff (M - \lambda_i \mathbb{1}_d)^k U \vec{j}_i &= \vec{0}, \end{aligned}$$

using the fact that  $UU^\dagger = U^\dagger U = \mathbb{1}_d$ . As a consequence, any unitary in the commutant space  $\mathcal{K}_{\text{PU}(d)}(M)$  needs to map the generalised eigenspaces to generalised eigenvalue  $\lambda_i$  to a generalised eigenspace to the same eigenvalue. In particular, this means that such unitaries cannot mix generalised eigenspaces to different generalised eigenvalues. This means that the dimension of eigenspaces of elements of  $\mathcal{K}_{\text{PU}(d)}(M)$  can at most correspond to the algebraic multiplicity of the generalised eigenvalues of  $M$ . Noting that for diagonalisable matrices algebraic and geometric multiplicity of eigenvalues coincide, we can now follow the arguments in the proof of Proposition A.2 for a diagonalisable matrix with the same (algebraic) eigenvalue structure as  $M$  to obtain an upper bound for the dimensionality of the commutant space. This proves the the proposition.  $\square$

### A.3 Reconstruction Matrices

**Lemma A.4.** *The matrix  $\rho_P \in \mathbb{C}^{d \times d}$  given by  $(\rho_P)_{ij} = \alpha_i \delta_{ij} + \frac{1}{d^2} \delta_{1,j} + \frac{1}{d^2} \delta_{i,1} - \frac{2}{d^2} \delta_{11}$  with  $\sum_i \alpha_i = 1, \forall i \neq j : \alpha_i \neq \alpha_j$  and  $\forall i : \frac{1}{d} - \frac{1}{d^2} < \alpha_i < \frac{1}{d} + \frac{1}{d^2}$  is a non-degenerate density matrix with full rank. Additionally, all eigenvectors of  $\rho_P$  have the form  $|\tilde{\psi}_i\rangle = \sum_j c_{ij} |\psi_j\rangle, \forall i, j : c_{ij} \neq 0$  where  $|\psi_j\rangle$  is the canonical basis, i.e. the basis  $\rho_P$  is represented in.*

*Proof.* We prove the three density matrix properties: Hermiticity, unit trace and positivity (we will even show positive definiteness). Furthermore, we will demonstrate that  $\rho_P$  is non-degenerate. The full rank condition follows from the positive definiteness, i.e. no eigenvalue is equal to zero.

1. Hermiticity is immediately seen from the construction.
2. Trace equal to one follows from  $\text{Tr}[\rho_P] = \sum_i \alpha_i + \frac{2}{d^2} - \frac{2}{d^2} = \sum_i \alpha_i = 1$  by assumption.
3. Positive definiteness is equivalent to  $\forall \vec{x} \in \mathbb{C}^N, \|\vec{x}\| = 1 : \langle \vec{x}, \rho_P \vec{x} \rangle > 0$ <sup>68</sup>. Note that we may write  $\rho_P$  as the sum of its diagonal part  $(\rho_P^D)_{ij} = \alpha_i \delta_{ij}$  and its off-diagonal part  $(\rho_P^{OD})_{ij} =$

<sup>68</sup>We will use vector notation here to emphasise the fact that we work in a matrix representation with respect to the canonical basis.

$\frac{1}{d^2}\delta_{1,j} + \frac{1}{d^2}\delta_{i,1} - \frac{2}{d^2}\delta_{11}$ . It is clear that  $\forall \vec{x} \in \mathbb{C}^N, \|\vec{x}\| = 1$  the following relation holds,

$$\langle \vec{x}, \rho_P \vec{x} \rangle = \langle \vec{x}, \rho_P^D \vec{x} \rangle + \langle \vec{x}, \rho_P^{OD} \vec{x} \rangle .$$

Obviously,  $\min_{\|\vec{x}\|=1} \langle \vec{x}, \rho_P^D \vec{x} \rangle = \min_i \alpha_i > \frac{1}{d} - \frac{1}{d^2}$  by assumption. Additionally we can estimate the second term  $\forall \vec{x} \in \mathbb{C}^N, \|\vec{x}\| = 1$  by  $|\langle \vec{x}, \rho_P^{OD} \vec{x} \rangle| \leq \|\rho_P^{OD}\|_1$  where  $\|\cdot\|_1$  represents the maximum absolute columns sum of a matrix<sup>69</sup>. It follows that

$$|\langle \vec{x}, \rho_P^{OD} \vec{x} \rangle| \leq \sum_{i=2}^N \frac{1}{d^2} = \frac{d-1}{d^2} = \frac{1}{d} - \frac{1}{d^2},$$

and obviously  $\forall \vec{x} \in \mathbb{C}^N, \|\vec{x}\| = 1$  one obtains

$$\begin{aligned} \langle \vec{x}, \rho_P \vec{x} \rangle &\geq \min_{\|\vec{x}\|=1} \langle \vec{x}, \rho_P^D \vec{x} \rangle - \max_{\|\vec{x}\|=1} |\langle \vec{x}, \rho_P^{OD} \vec{x} \rangle| \\ &\geq \min_i \alpha_i - \|\rho_P^{OD}\|_1 \\ &> \frac{1}{d} - \frac{1}{d^2} - \frac{1}{d} + \frac{1}{d^2} = 0, \end{aligned}$$

which shows positive definiteness.

We finally demonstrate the non-degeneracy of the eigenvalues. Since  $\rho_P$  is Hermitian it has  $d$  (possibly degenerate) eigenvalues. Let  $\lambda$  be an eigenvalue. Then the corresponding eigenvectors  $\vec{x}$  are given by the condition  $(\rho_P - \lambda \mathbb{1}_d) \vec{x} = \vec{0}$ . We show that  $\vec{x}$  can only lie in an one-dimensional subspace of  $\mathbb{C}^d$ , corresponding to multiplicity one of  $\lambda$ . Since  $\lambda$  was an arbitrary eigenvalue it follows that all eigenspaces are one-dimensional, hence  $\rho_P$  was non-degenerate. We will write the condition  $(\rho_P - \lambda \mathbb{1}_d) \vec{x} = \vec{0}$  componentwise,

$$\begin{aligned} (\alpha_1 - \lambda) x_1 + \frac{1}{d^2} \sum_{i=2}^d x_i &= 0, \\ \frac{1}{d^2} x_1 + (\alpha_2 - \lambda) x_2 &= 0, \\ \frac{1}{d^2} x_1 + (\alpha_3 - \lambda) x_3 &= 0, \\ &\dots \\ \frac{1}{d^2} x_1 + (\alpha_N - \lambda) x_N &= 0. \end{aligned}$$

Firstly, we may conclude that  $\forall i : \lambda \neq \alpha_i$ , which can be seen as follows. Assume the contrary, i.e.  $\lambda = \alpha_j$ . From the equation  $\frac{1}{d^2} x_1 + (\alpha_j - \lambda) x_j = 0$  it follows then that  $x_1 = 0$  and then one can see immediately that all the other  $x_i$  are zero but the zero vector is no proper eigenvector. Secondly, it is clear that  $\forall i : x_i \neq 0$ . This can be seen as follows. We already argued why  $x_1 = 0$  is impossible, hence assume an  $x_j$  with  $j \neq 1$  is equal to zero. From the corresponding equation  $\frac{1}{d^2} x_1 + (\alpha_j - \lambda) x_j = 0$  due to  $\lambda \neq \alpha_j$  (see the argument above) we may once again reduce this to the case  $x_1 = 0$  which is forbidden. Due to  $\forall i : x_i \neq 0$  the equations  $\forall i = 2, \dots, d : \frac{1}{d^2} x_1 + (\alpha_i - \lambda) x_i = 0$  can be written as

<sup>69</sup>It can easily be seen that for a Hermitian matrix  $\rho_P^{OD}$  with maximal eigenvalue  $\lambda_{max}$  one obtains  $\forall \vec{x} \in \mathbb{C}^N, \|\vec{x}\| = 1$  the inequality  $|\langle \vec{x}, \rho_P^{OD} \vec{x} \rangle| \leq \lambda_{max}$  and  $\lambda_{max} \leq \|\rho_P^{OD}\|_1$  since  $\|\cdot\|_1$  is a so-called induced norm [219].

$x_i = x_i(x_1)$ , i.e.  $x_i$  is a function of  $x_1$  and hence a single parameter (namely  $x_1$ ) determines the values of all components of the vector. But this means that the corresponding eigenspace is one-dimensional which completes the non-degeneracy proof. Moreover, showing the form of the eigenvectors stated in the second part of the proof is now trivial since  $\forall i : x_i \neq 0$  which means that an arbitrary eigenvector has no non-zero components with respect to the canonical basis.  $\square$

**Proposition A.5.** *The matrices  $\rho_B \in \mathbb{C}^{d \times d}$  with entries  $(\rho_B)_{ij} = \lambda_i \delta_{ij}$  with  $\lambda_i \geq 0$  and  $\sum_i \lambda_i = 1$  where  $\forall i \neq j : \lambda_i \neq \lambda_j$  and  $\rho_P \in \mathbb{C}^{d \times d}$  with entries  $(\rho_P)_{ij} = \alpha_i \delta_{ij} + \frac{1}{d^2} \delta_{1,j} + \frac{1}{d^2} \delta_{i,1} - \frac{2}{d^2} \delta_{11}$  with  $\sum_i \alpha_i = 1, \forall i \neq j : \alpha_i \neq \alpha_j$  and  $\forall i : \frac{1}{d} - \frac{1}{d^2} < \alpha(i) < \frac{1}{d} + \frac{1}{d^2}$  are unitary differentiating. Moreover, it is possible to reconstruct the unitary matrix corresponding to a unitary dynamical map  $\mathcal{D}_U$  from the images  $\mathcal{D}_U(\rho_B)$  and  $\mathcal{D}_U(\rho_P)$ .*

*Proof.* Since  $\rho_B$  is non-degenerate it is obviously basis complete. Furthermore, it is clear by the second part of Lemma A.4 that  $\rho_P$  is totally rotated with respect to  $\rho_B$ . We will now give an explicit recipe to reconstruct the unitary matrix corresponding to a unitary dynamical map by its action on the two matrices  $\rho_B$  and  $\rho_P$ .

Since  $\mathcal{D}_U(\rho_B)$  originates from a unitary transformation from  $\rho_B$  the spectrum of  $\rho_B$  and  $\mathcal{D}_U(\rho_B)$  is identical. Because the spectrum is non-degenerate we can decompose  $\mathcal{D}_U(\rho_B)$  and  $\rho_B$  in the following way,

$$\mathcal{D}_U(\rho_B) = \sum_i \lambda_i \tilde{P}_i, \quad (\text{A.9a})$$

$$\rho_B = \sum_i \lambda_i P_i, \quad (\text{A.9b})$$

where the  $P_i/\tilde{P}_i$  are unique, one-dimensional projectors<sup>70</sup>. Note that the ordering of the projector set  $\{P_i\}$  and  $\{\tilde{P}_i\}$  is fixed by the ordering of the non-degenerate spectrum  $\{\lambda_i\}$ . Using these projectors we can write

$$\mathcal{D}_U(\rho_B) = \sum_i \lambda_i \tilde{P}_i = \sum_i \lambda_i U P_i U^\dagger = U \rho_B U^\dagger.$$

A unitary transformation applied to one-dimensional projectors leads to a new set of one-dimensional projectors  $U P_i U^\dagger = P_i^{(U)}$ , consequently

$$\sum_i \lambda_i \tilde{P}_i = \sum_i \lambda_i P_i^{(U)}.$$

Multiplication with  $\tilde{P}_j$  from the right side leads to

$$\lambda_j \tilde{P}_j = \sum_i \lambda_i P_i^{(U)} \tilde{P}_j.$$

Multiplication with  $P_k^{(U)}$  from the left side leads to

$$\begin{aligned} \lambda_j P_k^{(U)} \tilde{P}_j &= \lambda_k P_k^{(U)} \tilde{P}_j \\ \iff (\lambda_j - \lambda_k) P_k^{(U)} \tilde{P}_j &= 0. \end{aligned}$$

<sup>70</sup>In practice these projectors are readily obtained via eigendecomposition of the corresponding matrices.

Due to  $\forall j \neq k : \lambda_j \neq \lambda_k$  (here the non-degeneracy comes into play) it follows immediately that

$$\forall j \neq k : P_k^{(U)} \tilde{P}_j = 0, \quad (\text{A.10})$$

whence follows (since the projectors were all one-dimensional)

$$P_j^{(U)} = c_j \tilde{P}_j,$$

with  $c_j \in \mathbb{C}$ . Any different relation between the two projectors sets would lead to a non-vanishing overlap according to Eq. (A.10). Note, that  $\forall j : |c_j| \stackrel{!}{=} 1$  or else  $P_j^{(U)}$  would not be idempotent which any projector needs to be. Note furthermore that  $\forall j : c_j \in \mathbb{R}^+$  or else  $P_j^{(U)}$  would not be positive which any projector needs to be. We may conclude that  $\forall j : c_j = 1$ , i.e.

$$\forall j : \tilde{P}_j = U P_j U^\dagger. \quad (\text{A.11})$$

We will now move to bra-ket notation. Let  $|\tilde{\psi}_j\rangle$  be a vector with  $\tilde{P}_j |\tilde{\psi}_j\rangle = |\tilde{\psi}_j\rangle$ . Then, by multiplication with  $\langle \tilde{\psi}_k|$  from the left and  $|\tilde{\psi}_k\rangle$  from the right, it follows from Eq. (A.11) that

$$\delta_{jk} = \langle \tilde{\psi}_k | U | \psi_j \rangle \langle \psi_j | U^\dagger | \tilde{\psi}_k \rangle = \left| \langle \tilde{\psi}_k | U | \psi_j \rangle \right|^2, \quad (\text{A.12})$$

with  $|\psi_j\rangle$  given by  $P_j |\psi_j\rangle = |\psi_j\rangle$ . As a result,  $U$  must map  $|\psi_j\rangle$  to a vector along  $|\tilde{\psi}_j\rangle$  or else not all components for  $j \neq k$  would vanish in Eq. (A.12). Since  $U$  is a isometry, i.e. it preserves norms, we may conclude for  $U$  that

$$\forall j : U | \psi_k \rangle = e^{i\varphi_k} | \tilde{\psi}_k \rangle,$$

for a set  $\{\varphi_k\}$  of yet to be determined phases. Since we know the action of  $U$  on an orthonormal basis we may consequently write

$$U = \sum_k e^{i\varphi_k} | \tilde{\psi}_k \rangle \langle \psi_k |. \quad (\text{A.13})$$

Note that while the vectors  $|\psi_k\rangle$  and  $\langle \tilde{\psi}_k|$  are only determined up to a global phase, since they are just defined as an eigenvector of a one-dimensional projector to eigenvalue 1, these phases can be absorbed in the  $e^{i\varphi_k}$ .

Finally, the phases  $e^{i\varphi_k}$  in Eq. (A.13) can be determined by applying the dynamical map  $\mathcal{D}_U$  to the matrix  $\rho_P$ . The corresponding image is given by

$$\begin{aligned} \mathcal{D}_U(\rho_P) &= \sum_{kl} \sum_{ij} e^{i(\varphi_k - \varphi_l)} \alpha_i \delta_{ij} | \tilde{\psi}_k \rangle \langle \psi_k | \psi_i \rangle \langle \psi_j | \psi_l \rangle \langle \tilde{\psi}_l | \\ &+ \sum_{kl} \sum_{ij} e^{i(\varphi_k - \varphi_l)} \frac{1}{d^2} \delta_{1j} | \tilde{\psi}_k \rangle \langle \psi_k | \psi_i \rangle \langle \psi_j | \psi_l \rangle \langle \tilde{\psi}_l | \\ &+ \sum_{kl} \sum_{ij} e^{i(\varphi_k - \varphi_l)} \frac{1}{d^2} \delta_{i1} | \tilde{\psi}_k \rangle \langle \psi_k | \psi_i \rangle \langle \psi_j | \psi_l \rangle \langle \tilde{\psi}_l | \\ &- \sum_{kl} \sum_{ij} e^{i(\varphi_k - \varphi_l)} \frac{2}{d^2} \delta_{11} | \tilde{\psi}_k \rangle \langle \psi_k | \psi_i \rangle \langle \psi_j | \psi_l \rangle \langle \tilde{\psi}_l | \end{aligned}$$

$$\begin{aligned}
\iff \mathcal{D}_U(\rho_P) &= \sum_{kl} \sum_{ij} e^{i(\varphi_k - \varphi_l)} \alpha_i \delta_{ij} \delta_{ki} \delta_{lj} |\tilde{\psi}_k\rangle \langle \tilde{\psi}_l| + \sum_{kl} \sum_{ij} e^{i(\varphi_k - \varphi_l)} \frac{1}{d^2} \delta_{1j} \delta_{ki} \delta_{lj} |\tilde{\psi}_k\rangle \langle \tilde{\psi}_l| \\
&+ \sum_{kl} \sum_{ij} e^{i(\varphi_k - \varphi_l)} \frac{1}{d^2} \delta_{i1} \delta_{ki} \delta_{lj} |\tilde{\psi}_k\rangle \langle \tilde{\psi}_l| - \sum_{kl} \sum_{ij} e^{i(\varphi_k - \varphi_l)} \frac{2}{d^2} \delta_{11} \delta_{ki} \delta_{lj} |\tilde{\psi}_k\rangle \langle \tilde{\psi}_l| \\
&= \sum_k \left( \alpha_k - \frac{2}{d^2} \delta_{k1} \right) |\tilde{\psi}_k\rangle \langle \tilde{\psi}_k| + \sum_k e^{i(\varphi_k - \varphi_1)} |\tilde{\psi}_k\rangle \langle \tilde{\psi}_1| \\
&+ \sum_k e^{i(\varphi_1 - \varphi_k)} |\tilde{\psi}_1\rangle \langle \tilde{\psi}_k|.
\end{aligned}$$

By freedom of the global phase, i.e.  $U$  is an element of  $\text{PU}(d)$ , we may set  $\varphi_1 = 0$  and it immediately follows  $\forall k \neq 1$  that

$$\begin{aligned}
\langle \tilde{\psi}_k | \mathcal{D}_U(\rho_P) | \tilde{\psi}_1 \rangle &= e^{i\varphi_k} \\
\implies \varphi_k &= \arg \langle \tilde{\psi}_k | \mathcal{D}_U(\rho_P) | \tilde{\psi}_1 \rangle.
\end{aligned} \tag{A.14}$$

□

## A.4 A Unitary Differentiating Matrix

**Proposition A.6.** *Consider the space  $\mathbb{C}^{d \times d}$ . The matrix  $M$  with  $(M)_{ij} = \delta_{i+1,j}$  is unitary differentiating.*

*Proof.* We show that  $\forall U \in \text{PU}(d) : [M, U] = 0 \implies U = \mathbf{1}_d$ . Assume that  $[M, U] = 0$ . We can directly calculate the matrix elements of this commutator, i.e. the following has to be fulfilled  $\forall a, b = 1, \dots, d$ ,

$$\begin{aligned}
([M, U])_{ab} &= (MU)_{ab} - (UM)_{ab} = \sum_i m_{ai} u_{ib} - \sum_i u_{ai} m_{ib} \\
&= \sum_i \delta_{a+1,i} u_{ib} - \sum_i u_{ai} \delta_{i+1,b} = \sum_i \delta_{a+1,i} u_{ib} - \sum_i u_{a,i-1} \delta_{ib} \\
&= u_{a+1,b} - u_{a,b-1},
\end{aligned} \tag{A.15}$$

where we defined  $u_{d+1,k} = 0 \forall k$  and  $u_{k,0} = 0 \forall k$  to facilitate notation.

Now it suffices to consider two cases: Firstly, for  $a = d$  the following relation follows directly from Eq. (A.15),

$$0 = u_{d+1,b} - u_{d,b-1} = -u_{d,b-1}.$$

In other words,  $\forall k \neq d$  the matrix elements  $u_{dk}$  have to vanish. But due to  $U \in \text{PU}(d)$  its column vectors have to be an orthonormal basis, hence  $u_{dd} \stackrel{!}{=} z \in \mathbb{C}, |z| = 1$ .

Secondly, consider the case  $a + 1 = b \equiv k \iff a = k - 1, b = k$  for arbitrary  $k = 2, \dots, d$ . Then we obtain from Eq. (A.15)

$$\begin{aligned}
u_{a+1,b} - u_{a,b-1} &= u_{kk} - u_{k-1,k-1} \stackrel{!}{=} 0 \\
\iff u_{kk} &= u_{k-1,k-1}.
\end{aligned}$$

Iteratively, it is easy to see that with the condition  $u_{dd} = z$  it follows that

$$u_{kk} = z \forall k = 1, \dots, d.$$

Now, since  $|z| = 1$  and the row (and column) vectors of  $U$  have to be normalised, it follows immediately that all non-diagonal elements of  $U$  have to vanish, i.e.

$$u_{ij} = z \delta_{ij}.$$

It follows, that a unitary  $U$  does not commute with  $M$ , it needs to be proportional to the unit matrix. Since  $U \in \text{PU}(d)$ , this implies immediately that  $z \stackrel{!}{=} 1$  and thus  $U \stackrel{!}{=} \mathbf{1}$ . As a result, the only element of  $\text{PU}(d)$  in the commutant space of  $M$  is the unit matrix. By Theorem 3.3 it follows that the set  $\{M\}$  with a single element is unitary differentiating. This completes the proof.  $\square$

## A.5 Proofs for Minimal Unitary Characterisation

In order to prove Theorem 3.9 we will first prove a series of auxiliary statements.

Our first goal is to prove that the only projective unitary matrix that commutes with each element of a complete and totally rotating set of states is the identity. In order to make use of the assumed commutation relations in the proof, we translate commutation of a unitary with a state into commutation of a unitary with one or more projectors. To this end, we introduce a lemma. Using commutation of a unitary with projectors, it is then straightforward to show that the unitary must be the identity.

**Lemma A.7.** *Let  $U \in \text{PU}(d)$  and  $\rho$  be a density matrix which has at least one non-degenerate eigenvalue  $\lambda_1$ . If  $[U, \rho] = 0$ , then the relation  $[U, P_1] = 0$  holds where  $P_1$  is the one-dimensional projector onto the eigenspace  $\mathcal{E}_1$  corresponding to the eigenvalue  $\lambda_1$ .*

*Proof.* Since  $\rho$  has a non-degenerate eigenvalue  $\lambda_1$ , we can expand it in a set of orthonormal projectors,  $\rho = \lambda_1 P_1 + \sum_{i=2}^d \lambda_i P_i$ , with  $P_1 = |\xi_1\rangle \langle \xi_1|$  the projector onto the one-dimensional eigenspace  $\mathcal{E}_1$ . By assumption,

$$\begin{aligned} [U, \rho] = 0 &= \lambda_1 U P_1 - \lambda_1 P_1 U + \sum_{i=2}^d (\lambda_i U P_i - \lambda_i P_i U) \\ &= \lambda_1 U P_1 U^\dagger - \lambda_1 P_1 + \sum_{i=2}^d (\lambda_i U P_i U^\dagger - \lambda_i P_i), \end{aligned}$$

where in the second line we have multiplied by  $U^\dagger$  from the right. Defining  $\bar{P}_i = U P_i U^\dagger$ , this is equivalent to

$$\lambda_1 \bar{P}_1 + \sum_{i=2}^d \lambda_i \bar{P}_i = \lambda_1 P_1 + \sum_{i=2}^d \lambda_i P_i.$$

The operator equality can be applied to  $|\xi_1\rangle$ , leading to

$$\lambda_1 \bar{P}_1 |\xi_1\rangle + \sum_{i=2}^d \lambda_i \bar{P}_i |\xi_1\rangle = \lambda_1 |\xi_1\rangle.$$

Inserting an identity,  $\sum_{i=1}^d \bar{P}_i = \mathbb{1}_d$ , in the right-hand side, we obtain

$$\lambda_1 \bar{P}_1 |\xi_1\rangle + \sum_{i=2}^d \lambda_i \bar{P}_i |\xi_1\rangle = \lambda_1 \bar{P}_1 |\xi_1\rangle + \sum_{i=2}^d \lambda_1 \bar{P}_i |\xi_1\rangle .$$

Multiplying from the left by  $\bar{P}_{i \neq 1}$  and using orthogonality of the  $\bar{P}_i$  and non-degeneracy of  $\lambda_1$ ,  $\lambda_{i \neq 1} \neq \lambda_1$ , we find that  $\bar{P}_i |\xi_1\rangle = 0$  for all  $i \neq 1$ . Therefore  $|\xi_1\rangle$  lies also in the one-dimensional eigenspace corresponding to  $\bar{P}_1$ , and the one-dimensional eigenspaces of  $P_1$  and  $\bar{P}_1$  must be identical. This implies

$$P_1 = \bar{P}_1 ,$$

and, by definition of  $\bar{P}_1$ , we find that  $U$  leaves the one-dimensional eigenspace corresponding to  $P_1$  invariant, hence commutes with  $P_1$ .  $\square$

*Remark.* Note that if a density matrix  $\rho$  that commutes with  $U$  has more than one non-degenerate eigenvalue, the lemma implies that  $U$  commutes with all the projectors onto the one-dimensional eigenspaces.

**Proposition A.8.** *The only projective unitary matrix  $U \in \text{PU}(d)$  that commutes with a complete and totally rotating set of states  $\{\rho_i\}$ , with  $\rho_i \in \mathbb{C}^{d \times d}$ , is the unit matrix.*

*Proof.* Repeated application of the lemma to states  $\rho_i$  yields a set of one-dimensional projectors that each commute with  $U$ . By definition of a complete and totally rotating set of states,  $d+1$  projectors within this set must be elements of  $\{\mathcal{P}_c, P_{TR}\}$ . We can thus choose the complete set of one-dimensional projectors  $\mathcal{P}_c$  to represent  $U$ ,  $U = \sum_{i=1}^d u_i P_i$ . An equally valid choice  $\{\tilde{P}_i\}$  employs the totally rotated projector,  $\tilde{P}_1 = P_{TR}$ , with  $\mathcal{E}_{TR}$  the corresponding eigenspace, and a suitable set of orthonormal one-dimensional projectors  $\{\tilde{P}_i\}_{i=2, \dots, d}$  for the space  $\mathcal{E}_{TR}^\perp$  such that  $U = \sum_{i=1}^d u_i \tilde{P}_i$ . The spectrum  $\{u_i\}$  is of course independent of the representation. Consider the action of  $U$  on a vector  $|\zeta\rangle \in \mathcal{E}_{TR}$ ,

$$\begin{aligned} U |\zeta\rangle &= \sum_{i=1}^d u_i P_i |\zeta\rangle = \sum_{i=1}^d u_i \tilde{P}_i |\zeta\rangle \\ &= u_1 |\zeta\rangle = \sum_{i=1}^d u_1 P_i |\zeta\rangle , \end{aligned} \tag{A.16}$$

where we have inserted  $\sum_{i=1}^d P_i = \mathbb{1}_d$  in the last step. By total rotation,  $P_{TR} P_i \neq 0 \forall P_i \in \mathcal{P}_c$ , or equivalently,  $P_i P_{TR} \neq 0$ . Applying this to  $|\zeta\rangle$ , we find

$$P_i P_{TR} |\zeta\rangle = P_i |\zeta\rangle \neq 0 \quad \forall i .$$

Since the  $P_i$  are one-dimensional orthonormal projectors, i.e.  $P_i = |\varphi_i\rangle \langle \varphi_i|$  with  $\{|\varphi_i\rangle\}$  a complete orthonormal basis of the Hilbert space, we can rewrite  $P_i |\zeta\rangle$ ,

$$P_i |\zeta\rangle = \mu_i |\varphi_i\rangle ,$$

with  $\mu_i \in \mathbb{C}$ ,  $\mu_i \neq 0$ . Inserting this into Eq. (A.16), we obtain

$$\sum_{i=1}^d u_1 \mu_i |\varphi_i\rangle = \sum_{i=1}^d u_i \mu_i |\varphi_i\rangle .$$

Comparing the coefficients yields  $u_1 \mu_i = u_i \mu_i \forall i$ . Due to total rotation,  $\forall i : \mu_i \neq 0$ , hence we can divide and obtain

$$u_1 = u_i \quad \forall i ,$$

i.e. a unitary with complete degeneracy in its eigenvalues. This necessarily has to be the matrix  $e^{i\varphi} \mathbf{1}_d$  for  $\varphi \in [0, 2\pi]$ , or, as an element of  $\text{PU}(d)$ , the unit matrix.  $\square$

We have thus shown that only the identity commutes with a set of states that is complete and totally rotating. This set of states is therefore unitary differentiating, leading to Theorem 3.7.

**Lemma A.9.** *Let  $\mathcal{D} : \mathbb{C}^{d \times d} \mapsto \mathbb{C}^{d \times d}$  be a unital dynamical map. If and only if there exists a set of  $d$  one-dimensional, orthogonal projectors that is mapped by  $\mathcal{D}$  onto another set of  $d$  one-dimensional orthogonal projectors, there exists a complete set of density matrices whose spectrum is invariant under  $\mathcal{D}$ .*

*Proof.* ( $\implies$  direction) We denote the set of  $d$  one-dimensional projectors  $P_i$  by  $\mathcal{P}$ . By assumption, we know that

$$\forall i : \mathcal{D}(P_i) = \tilde{P}_i ,$$

where the  $\tilde{P}_i$  also form a set of  $d$  one-dimensional, orthogonal projectors. Clearly,  $\text{spec}(P_i) = \text{spec}(\tilde{P}_i)$ , hence  $\forall P_i \in \mathcal{P}$

$$\text{spec}(\mathcal{D}(P_i)) = \text{spec}(P_i) = (1, 0, \dots, 0) .$$

Obviously,  $\mathcal{P}$  itself corresponds to a specific complete set of density matrices,  $\rho_i = P_i$ .

( $\impliedby$  direction) This part of the proof proceeds as follows: First we show that the assumption, a dynamical map leaving the spectrum of a given density matrix invariant, implies that  $\mathcal{D}$  maps projectors onto the eigenspaces of the initial density matrices into projectors onto the eigenspaces of the resulting density matrix with the same eigenvalue. As a consequence, a one-dimensional projector onto a corresponding one-dimensional eigenspace is mapped into a one-dimensional projector. We then repeat this argument for all density matrices in the complete set. In this set, by definition, there exist density matrices with  $d$  one-dimensional, orthogonal projectors onto one-dimensional eigenspaces which, according to the first step of the  $\impliedby$  proof, is mapped onto another set of one-dimensional projectors. We show in a second step that the set of the mapped one-dimensional projectors is also orthogonal.

We start by assuming that  $\mathcal{D}$  leaves the spectrum of a given density matrix,  $\rho$ , invariant,

$$\text{spec}(\mathcal{D}(\rho)) = \text{spec} \sum_k \left( E_k \rho E_k^\dagger \right) = \text{spec}(\rho) ,$$

where we have expressed  $\mathcal{D}$  in terms of Kraus operators  $E_k$ . We can write  $\rho = \sum_i \lambda_i P'_i$  where  $P' = \{P'_i\}$  is a set of  $M$  orthogonal projectors onto the eigenspaces of  $\rho$  with  $M$  the number of distinct eigenvalues of  $\rho$ . We assume the  $\lambda_i$  to be ordered by magnitude with  $\lambda_1$  corresponding to

the largest eigenvalue. Since we know that the spectrum of  $\mathcal{D}(\rho)$  to be identical to that of  $\rho$ , we can decompose  $\mathcal{D}(\rho)$ ,

$$\mathcal{D}(\rho) = \sum_i \lambda_i \tilde{P}'_i,$$

with  $\{\tilde{P}'_j\}$  another set of  $M$  orthogonal projectors. Note that neither the  $P'_i$  nor the  $\tilde{P}'_i$  have to be one-dimensional but for a given  $i$ ,  $\tilde{P}'_i$  has the same dimensionality as the corresponding  $P'_i$ . Specifically,

$$\mathcal{D}(\rho) = \mathcal{D}\left(\sum_i \lambda_i P'_i\right) = \sum_i \lambda_i \mathcal{D}(P'_i) = \sum_j \lambda_j \tilde{P}'_j.$$

Multiplying by another projector  $\tilde{P}'_p$  from the set, where  $p$  can take integer values between 1 and  $M$ , we obtain

$$\sum_i \lambda_i \mathcal{D}(P'_i) \tilde{P}'_p = \sum_j \lambda_j \tilde{P}'_j \tilde{P}'_p = \lambda_p \tilde{P}'_p, \quad (\text{A.17})$$

since  $\tilde{P}'_j, \tilde{P}'_p$  are orthogonal. Using proof by (transfinite) induction we now show that

$$\mathcal{D}(P'_k) = \tilde{P}'_k \quad \forall i = k, \dots, M.$$

The idea of the induction is the following: To show that indeed the projectors onto the eigenspaces of  $\rho$ ,  $P'_i$ , are mapped into projectors onto the eigenspaces of  $\mathcal{D}(\rho)$  with the same eigenvalue, we start with the projector onto the eigenspace with the largest eigenvalue and then inductively proceed to increasingly smaller eigenvalues. Furthermore, to prevent having to deal with a possible smallest eigenvalue of 0, we treat the lowest eigenvalue case separately. Calling the induction variable  $k$ , we have to show that  $\mathcal{D}(P'_k) = \tilde{P}'_k$  follows from the assumption  $\mathcal{D}(P'_i) = \tilde{P}'_i \forall i < k$ . Note that if  $k = M$ , i.e. for the smallest eigenvalue,

$$\sum_i \mathcal{D}(P'_i) = \mathcal{D}\left(\sum_i P'_i\right) = \mathcal{D}(\mathbf{1}_d) = \mathbf{1}_d, \quad (\text{A.18})$$

since, by definition, a unital dynamical map maps identity onto itself.

Hence, we assume  $k \neq M$ . Then  $\lambda_k > 0$  since it is not yet the smallest eigenvalue because each  $\lambda_k$  corresponds, by construction, to a different eigenspace. This implies that they are different. For brevity we will employ vector notation instead of bra-ket notation in the following. For  $k = p$ , we can rewrite Eq. (A.17), multiplying by an arbitrary normalised eigenvector  $\vec{x}_k \in \mathbb{C}^d$  of  $\tilde{P}'_k$  from the left and right,

$$\sum_i \lambda_i \vec{x}_k \cdot \mathcal{D}(P'_i) \cdot \vec{x}_k = \lambda_k. \quad (\text{A.19})$$

By assumption of the induction,  $\mathcal{D}(P'_i) = \tilde{P}'_i \forall i < k$ , therefore

$$\vec{x}_k \cdot \mathcal{D}(P'_i) \cdot \vec{x}_k = 0 \quad \forall i < k.$$

Introducing  $d_{kk}^{(i)} \equiv \vec{x}_k \cdot \mathcal{D}(P'_i) \cdot \vec{x}_k$ , Eq. (A.19) can be written as

$$\sum_{i \geq k} \lambda_i d_{kk}^{(i)} = \lambda_k. \quad (\text{A.20})$$

Due to Eq. (A.18) and the assumption of the induction,

$$\sum_i d_{kk}^{(i)} = \sum_{i \geq k} d_{kk}^{(i)} = \sum_i \vec{x}_k \cdot \mathcal{D}(P'_i) \cdot \vec{x}_k = 1,$$

and, since  $\mathcal{D}(P'_i)$  is the image of a positive matrix which has to be positive itself,

$$d_{kk}^{(i)} = \vec{x}_k \cdot \mathcal{D}(P'_i) \cdot \vec{x}_k \geq 0 \forall i.$$

Now remember that  $\lambda_k \neq 0$  is strictly larger than all the other  $\lambda_i$  with  $i > k$  since the eigenvalues are assumed to be ordered. In addition,  $d_{kk}^{(i)} \geq 0 \forall i$  and at least one  $d_{kk}^{(i)}$  with  $i \geq k$  must be non-zero, otherwise the  $d_{kk}^{(i)}$  would not sum up to 1. Then

$$\sum_{i \geq k} \lambda_i d_{kk}^{(i)} \leq \lambda_k \sum_{i \geq k} d_{kk}^{(i)} = \lambda_k,$$

with equality if and only if  $d_{kk}^{(i)} = 0$  for  $i \neq k$ . In fact, equality has to hold since otherwise we would contradict Eq. (A.20). We conclude that

$$d_{kk}^{(i)} = \vec{x}_k \cdot \mathcal{D}(P'_i) \cdot \vec{x}_k = \delta_{ik}.$$

Since  $\vec{x}_k$  is normalised and arbitrary as long as it lies in the eigenspace  $\tilde{\mathcal{E}}_k$  of  $\tilde{P}'_k$ ,  $\vec{x}_k$  must be an eigenvector of  $\mathcal{D}(P'_k)$  with eigenvalue 1. Consequently, the operator  $\mathcal{D}(P'_k)$  maps the eigenspace of  $\tilde{P}'_k$  onto itself. Now we are almost done with showing that  $\mathcal{D}(P'_k)$  and  $\tilde{P}'_k$  are indeed identical. Since  $\tilde{\mathcal{E}}_k$  is mapped by  $\mathcal{D}$  into itself,  $\mathcal{D}(P'_k)$  has at least  $\dim(\tilde{\mathcal{E}}_k)$  eigenvalues equal to 1. The fact that  $\mathcal{D}(P'_k)$  has exactly  $\dim(\tilde{\mathcal{E}}_k)$  eigenvalues equal to 1 follows from  $\mathcal{D}$  being trace-preserving:  $\text{Tr}[\mathcal{D}(P'_k)] = \text{Tr}[P'_k] = \dim(\mathcal{E}_k)$  and  $\dim(\mathcal{E}_k) = \dim(\tilde{\mathcal{E}}_k)$ , where  $\text{Tr}[\mathcal{D}(P'_k)]$  is the sum over the eigenvalues of  $\mathcal{D}(P'_k)$ . Since all eigenvalues of  $\mathcal{D}(P'_k)$  are non-negative, all other eigenvalues must vanish. Hence  $\mathcal{D}(P'_k) = \tilde{P}'_k$ . This completes the induction and concludes the first step of the  $\Leftarrow$  proof, i.e. we have shown that a unital dynamical map that leaves the spectrum of a given arbitrary density matrix invariant, maps projectors onto the eigenspaces of this density matrix onto projectors of the same rank. This is specifically true for one-dimensional projectors. Iterating the argument for all density matrices in the complete set and selecting a set  $\mathcal{P}$  of  $d$  orthogonal, one-dimensional projectors, it follows that these projectors will be mapped by  $\mathcal{D}$  onto another set of one-dimensional projectors.

In the second step of the  $\Leftarrow$  proof we still need to show that the mapped set is also orthogonal. We denote the complete set of projectors by  $\{P_i\}$ . From the first step of the  $\Leftarrow$  proof we know that the  $\tilde{P}_i$ ,

$$\mathcal{D}(P_i) = \tilde{P}_i,$$

need to be one-dimensional projectors. Using the unitality of  $\mathcal{D}$ , we see that

$$\mathbb{1}_d = \mathcal{D}(\mathbb{1}_d) = \mathcal{D}\left(\sum_i P_i\right) = \sum_i \mathcal{D}(P_i) = \sum_i \tilde{P}_i.$$

The unit matrix can only be summed by  $d$  one-dimensional projectors if these are orthogonal. Hence we have accomplished the second step, and the lemma follows.

Now we can turn to proving Theorem 3.9.  $\square$

**Theorem.** *Let  $\mathcal{H}$  be a finite-dimensional Hilbert space with  $d = \dim(\mathcal{H})$  and  $\mathcal{D}$  be a dynamical map on  $\mathcal{L}_{\mathcal{H}}$ . The following statements are equivalent.*

1.  $\mathcal{D}$  is unitary.
2.  $\mathcal{D}$  maps a set  $\mathcal{P}$  of  $d$  one-dimensional orthogonal projectors onto a set of  $d$  one-dimensional orthogonal projectors as well as a totally rotated projector  $P_{TR}$  (with respect to  $\mathcal{P}$ ) onto a one-dimensional projector.
3.  $\mathcal{D}$  is unital and there exists a complete and totally rotating set of density matrices whose spectrum is invariant under  $\mathcal{D}$ .
4.  $\mathcal{D}$  is unital and there exists a complete and totally rotating set of density matrices  $\mathcal{R}$  such that  $\forall \rho \in \mathcal{R}; k = 1, 2, \dots, d: \text{Tr}(\rho^k) = \text{Tr}(\mathcal{D}(\rho)^k)$ .

*Proof.* (1)  $\implies$  (2) : If  $\mathcal{D}$  is unitary, the action of  $\mathcal{D}$  on any state is described by  $\mathcal{D}(\rho) = U\rho U^\dagger$  according to Eq. (2.21). Specifically for orthonormal projectors  $P_i P_j = \delta_{ij}$ , we find

$$\mathcal{D}(P_i) \mathcal{D}(P_j) = U P_i U^\dagger U P_j U^\dagger = U P_i P_j U^\dagger = \delta_{ij} U P_i U^\dagger.$$

Since a one-dimensional projector can be written  $P_i = |\varphi_i\rangle \langle \varphi_i|$ , where  $\{|\varphi_i\rangle\}$  is a complete orthonormal basis of  $\mathcal{H}$ ,  $U P_i U^\dagger$  is also one-dimensional projector. By the same argument,  $P_{TR}$  is mapped onto a one-dimensional projector if  $\mathcal{D}(\rho) = U\rho U^\dagger$ . Therefore a dynamical map  $\mathcal{D}$  describing unitary time evolution maps a set of  $d$  orthonormal projectors,  $\{P_i\}$ , onto another such set,  $\{\tilde{P}_i = U P_i U^\dagger\}$ , and  $P_{TR}$  onto a one-dimensional projector.

(2)  $\implies$  (1) : We start with the representation of a dynamical map according to Theorem 2.1,

$$\mathcal{D} = \sum_{k=1}^K E_k \rho E_k^\dagger, \quad (\text{A.21})$$

by Kraus operators  $E_k$ , that fulfil

$$\sum_{k=1}^K E_k^\dagger E_k = \mathbb{1}_d. \quad (\text{A.22})$$

We employ the canonical representation in which the Kraus operators are orthogonal,  $\text{Tr}[E_k^\dagger E_l] \sim \delta_{kl}$ . By assumption, a set of  $d$  one-dimensional, orthonormal projectors  $\{P_i\}$  is mapped by  $\mathcal{D}$  onto another such set  $\{\tilde{P}_i\}$ ,

$$\mathcal{D}(P_i) = \sum_{k=1}^K E_k P_i E_k^\dagger = \tilde{P}_i. \quad (\text{A.23})$$

We need to show that this implies  $\mathcal{D}(\rho) = U\rho U^\dagger$ , or equivalently, as we demonstrate below, that  $\mathcal{D}$  is made up of a single Kraus operator  $E_1$  in the representation where  $\text{Tr}[E_k^\dagger E_l] \sim \delta_{kl}$ . In general, we can employ a polar decomposition for each Kraus operator, factorising it into a unitary and a positive-semidefinite operator,  $E_k = U_k \tilde{E}_k$ . For unitary evolution,  $U_k = \tilde{U}$  for all  $k$  and  $E_1 = U\mathbb{1}_d$  which is a special case of  $\tilde{E}_k$  being diagonal. We first show that the assumption for the  $d$  orthonormal projectors  $\{P_i\}$  implies  $U_k = \tilde{U}$  and diagonality of  $\tilde{E}_k$ . In a second step, we prove that the assumption for the totally rotated projector implies that there is only a single Kraus operator and  $\tilde{E}_1 = \mathbb{1}_d$ .

We first show that  $\tilde{E}_k = E_k U^\dagger$  is diagonal in the orthonormal basis  $\{|\varphi_i\rangle\}$  corresponding to the  $P_i$ . Eq. (A.23) suggests the definition of an operator  $\Pi_k^{(i)} \equiv E_k P_i E_k^\dagger$  which is obviously Hermitian and moreover positive semidefinite. The latter is seen by making use of  $P_i^2 = P_i$  and  $P_i = P_i^\dagger$ ,  $\langle \zeta | \Pi_k^{(i)} | \zeta \rangle = \langle \zeta | E_k P_i P_i E_k^\dagger | \zeta \rangle = \langle P_i E_k^\dagger \zeta | P_i E_k^\dagger \zeta \rangle = \langle \xi | \xi \rangle \geq 0$  for any  $|\zeta\rangle \in \mathcal{H}$ . Eq. (A.23) implies  $\sum_{k=1}^K \Pi_k^{(i)} = \tilde{P}_i$ . For the normalised vector spanning the eigenspace of  $\tilde{P}_i$ ,  $|\tilde{\varphi}_i\rangle \in \mathcal{E}_i$ , we find

$$\sum_{k=1}^K \left\langle \tilde{\varphi}_i \left| \Pi_k^{(i)} \tilde{\varphi}_i \right. \right\rangle = 1,$$

while for all  $|\xi\rangle \in \mathcal{E}_i^\perp$

$$\sum_{k=1}^K \left\langle \xi \left| \Pi_k^{(i)} \xi \right. \right\rangle = 0.$$

Due to positivity of  $\Pi_k^{(i)}$ , this implies  $\langle \xi | \Pi_k^{(i)} | \xi \rangle = 0$ . Reinserting the definition of  $\Pi_k^{(i)}$  leads to  $\langle \xi | E_k P_i E_k^\dagger | \xi \rangle = \langle P_i E_k^\dagger \xi | P_i E_k^\dagger \xi \rangle = 0$ , i.e. we find  $P_i E_k^\dagger | \xi \rangle = 0$  for all  $k, i$  and  $|\xi\rangle \in \mathcal{E}_i^\perp$ . For an arbitrary Hilbert space vector  $|\zeta\rangle$ ,  $(\mathbb{1}_d - \tilde{P}_i) |\zeta\rangle$  lies in  $\mathcal{E}_i^\perp$  such that  $P_i E_k^\dagger (\mathbb{1}_d - \tilde{P}_i) |\zeta\rangle = 0$  for all  $k$  and  $i$ . Therefore

$$P_i E_k^\dagger (\mathbb{1}_d - \tilde{P}_i) = 0 \iff P_i E_k^\dagger = P_i E_k^\dagger \tilde{P}_i \quad \forall i, k.$$

To make use of the orthogonality of the  $\tilde{P}_i$ , we multiply by  $\tilde{P}_j$ ,  $j \neq i$  from the right. Since  $\tilde{P}_j$  can be written as  $\tilde{P}_j = \tilde{U} P_j \tilde{U}^\dagger$  for a specific  $\tilde{U}$ , we obtain, for all  $i, k$  and  $j \neq i$ ,  $P_i E_k^\dagger \tilde{U} P_j \tilde{U}^\dagger = 0$ . Multiplication by  $\tilde{U}$  from the right yields

$$P_i E_k^\dagger \tilde{U} P_j = 0.$$

This implies that the operators  $E_k^\dagger \tilde{U}$  have to be diagonal in the basis corresponding to the  $P_i$ ,

$$E_k^\dagger \tilde{U} = \sum_{i=1}^d e_i^k P_i. \quad (\text{A.24})$$

Note that the unitary  $\tilde{U}$  is the same for all Kraus operators  $E_k$ .

In the second step, we now need to show that the right-hand side of Eq. (A.24) is equal to the identity, making use of the assumption that the totally rotated projector is mapped by  $\mathcal{D}$  onto a one-dimensional projector. The crucial information is captured in the coefficients  $e_i^k$ . Let us summarise what we know about the  $e_i^k$ . From orthogonality of the Kraus operators, we find  $\text{Tr}[E_k^\dagger E_l] = \text{Tr}[\sum_{i,j=1}^d e_i^k (e_j^l)^* P_i \tilde{U}^\dagger \tilde{U} P_j] = \sum_{i,j=1}^d e_i^k (e_j^l)^* \text{Tr}[P_i P_j] = \sum_{i,j=1}^d e_i^k (e_j^l)^* \delta_{ij} = \sum_{i=1}^d e_i^k (e_i^l)^* \stackrel{!}{\sim} \delta_{kl}$ . The last sum can be interpreted as a scalar product for two orthogonal vectors  $\vec{e}^k, \vec{e}^l \in \mathbb{C}^d$  with coefficients

$e_i^k, e_i^l$ . Defining the proportionality constants  $\mathcal{N}(k)$ ,

$$\mathcal{N}(k) \equiv \text{Tr} [E_k^+ E_k] = \sum_i e_i^k (e_i^k)^* = \langle \vec{e}^k, \vec{e}^k \rangle \geq 0, \quad (\text{A.25})$$

we find from Eq. (A.22) and  $\text{Tr}[\mathbb{1}_d] = d$  that  $\sum_{k=1}^K \mathcal{N}(k) = d$  (and, if we can show that  $\mathcal{N}(k) = d$  for one  $k$ , then the number of Kraus operators,  $K$ , must be one). Eq. (A.22) together with Eq. (A.24) yields yet another condition on the  $e_i^k$ :  $\mathbb{1}_d = \sum_{k=1}^K E_k^\dagger E_k = \sum_{i,j=1}^d \sum_{k=1}^K (e_i^k)^* e_j^k P_i P_j = \sum_{i,k} |e_i^k|^2 P_i$  such that  $\sum_k |e_i^k|^2 = 1$  for each  $i$ . This can be interpreted as normalisation condition for a vector  $\vec{e}_i \in \mathbb{C}^K$  with coefficients  $e_i^k$ ,

$$1 = \sum_{k=1}^K |e_i^k|^2 = \langle \vec{e}_i, \vec{e}_i \rangle. \quad (\text{A.26})$$

Since the vector sets  $\{\vec{e}_k\}$  and  $\{\vec{e}_i\}$  are not independent, it is clear that any information on the scalar product  $\langle \vec{e}_i, \vec{e}_j \rangle$  will be useful to determine  $\mathcal{N}(k)$  (such that we can check whether there is one  $k$  for which  $\mathcal{N}(k) = d$ ). To this end, we employ the assumption that  $P_{TR}$  is mapped by  $\mathcal{D}$  onto a one-dimensional projector,  $\tilde{P}_{TR} = \mathcal{D}(P_{TR})$ , i.e. the purity of  $P_{TR}$  is preserved,

$$\text{Tr} \left[ (\mathcal{D}(P_{TR}))^2 \right] = 1.$$

Inserting Eqs. (A.21) and (A.24), making use of the orthogonality of the  $P_i$  and of the trace being invariant under cyclic permutation, we find

$$\begin{aligned} \text{Tr} \left[ \mathcal{D}(P_{TR})^2 \right] &= \text{Tr} \left[ U \left( \sum_{ij} \sum_k \sum_{i'j'} \sum_{k'} (e_i^k)^* e_j^k (e_{i'}^{k'})^* e_{j'}^{k'} P_i P_{TR} P_j P_{i'} P_{TR} P_{j'} \right) U^\dagger \right] \\ &= \text{Tr} \left[ \sum_{ij} \sum_k \sum_{j'} \sum_{k'} (e_i^k)^* e_j^k (e_{j'}^{k'})^* e_{j'}^{k'} P_i P_{TR} P_j P_{TR} P_{j'} \right] \\ &= \sum_{ij} \sum_k \sum_{j'} \sum_{k'} (e_i^k)^* e_j^k (e_{j'}^{k'})^* e_{j'}^{k'} \text{Tr} \left[ P_i P_{TR} P_j P_{TR} P_{j'} \right] \\ &= \sum_{ij} \left| \sum_k (e_i^k)^* e_j^k \right|^2 \text{Tr} [P_i P_{TR} P_j P_{TR}] = \sum_{ij} |\langle \vec{e}_i, \vec{e}_j \rangle|^2 \text{Tr} [P_i P_{TR} P_j P_{TR}]. \end{aligned}$$

The trace over the projectors is easily evaluated in the basis  $\{|\varphi_i\rangle\}$ ,  $P_i = |\varphi_i\rangle \langle \varphi_i|$ , in which  $P_{TR} = |\Psi\rangle \langle \Psi|$ . It yields  $\text{Tr} [P_i P_{TR} P_j P_{TR}] = |\langle \varphi_i | \Psi \rangle|^2 |\langle \varphi_j | \Psi \rangle|^2 = |\mu_i|^2 |\mu_j|^2$  with  $\mu_i \equiv \langle \varphi_i | \Psi \rangle$  and  $\mu_i \neq 0$  due to total rotation,  $P_i P_{TR} \neq 0 \forall i$ . Estimating  $|\langle \vec{e}_i, \vec{e}_j \rangle|^2$  by the Cauchy-Schwarz inequality,  $|\langle \vec{e}_i, \vec{e}_j \rangle|^2 \leq \langle \vec{e}_i, \vec{e}_i \rangle \langle \vec{e}_j, \vec{e}_j \rangle$ , and making use of the normalisation of  $\vec{e}_i$ , cf. Eq. (A.26), we obtain

$$\begin{aligned} 1 = \text{Tr} \left[ \mathcal{D}(P_{TR})^2 \right] &= \sum_{ij} |\mu_i|^2 |\mu_j|^2 |\langle \vec{e}_i, \vec{e}_j \rangle|^2 \\ &\leq \sum_{ij} |\mu_i|^2 |\mu_j|^2 = 1. \end{aligned}$$

In the last step, we have used  $\sum_i |\mu_i|^2 = \sum_i |\langle \varphi_i | \Psi \rangle|^2 = \sum_i \langle \Psi | \varphi_i \rangle \langle \varphi_i | \Psi \rangle = \langle \Psi | \Psi \rangle = 1$ . Since we

find one on the left hand and right hand side, equality must hold for the inequality. Since  $\mu_i \neq 0$  for all  $i$ , this is possible only for

$$|\langle \vec{\epsilon}_i, \vec{\epsilon}_j \rangle|^2 = 1, \quad \text{or,} \quad |\langle \vec{\epsilon}_i, \vec{\epsilon}_j \rangle| = 1, \quad \forall i, j.$$

Therefore, the normalised vectors  $\vec{\epsilon}_i, \vec{\epsilon}_j$  are identical up to a complex scalar,  $|e_i^k| = |e_j^k|$  for all  $i, j$  and  $k$ . This implies for the proportionality constants  $\mathcal{N}(k)$ , Eq. (A.25), equality of all summands,

$$\mathcal{N}(k) = \sum_{i=1}^d e_i^k (e_i^k)^* = d (e_a^k)^* e_a^k.$$

Each component is thus given by  $e_i^k = \sqrt{\mathcal{N}(k)/d} \exp[i\phi_i]$  which, making use of the orthogonality of the vectors  $\vec{e}_k, \sum_i e_i^k (e_i^l)^* \sim \delta_{kl}$ , leads to

$$\begin{aligned} \sum_{i=1}^d e_i^k (e_i^l)^* &= \sum_{i=1}^d \frac{\sqrt{\mathcal{N}(k)\mathcal{N}(l)}}{d} \exp[i\phi_i] \exp[-i\phi_i] \\ &= \sqrt{\mathcal{N}(k)\mathcal{N}(l)} = 0 \quad \forall k \neq l. \end{aligned}$$

For this to be true, all  $\mathcal{N}(k)$  except one and consequently all  $E_k$  except one must be zero. By Eq. (A.24), its representation is

$$E = \tilde{U} \left[ \sum_i (e_i^1)^* P_i \right].$$

Making use of  $P_i P_j = \delta_{ij} P_i$  and  $P_i = P_i^\dagger$ , unitarity of the time evolution follows immediately since

$$\begin{aligned} E^\dagger E &= \sum_{i=1}^d e_i^1 (e_i^1)^* P_i = \sum_{i=1}^d \sqrt{\frac{\mathcal{N}(1)}{d}} P_i = \sum_{i=1}^d P_i = \mathbb{1}_d, \\ EE^\dagger &= \tilde{U} \left( \sum_{i=1}^d e_i^1 (e_i^1)^* P_i \right) \tilde{U}^\dagger = \tilde{U} \mathbb{1}_d \tilde{U}^\dagger = \mathbb{1}_d, \end{aligned}$$

such that

$$\mathcal{D}(\rho) = \tilde{U} \rho \tilde{U}^\dagger$$

for a unitary  $\tilde{U} \in \text{PU}(d)$ .

(2)  $\implies$  (3) : If  $\mathcal{D}$  maps a set of  $d$  one-dimensional orthogonal projectors onto another set of  $d$  one-dimensional orthogonal projectors, it leaves the spectrum of the projectors invariant. This can be seen as follows. Projectors are idempotent and positive semi-definite, hence their spectrum can only consist of zeros and ones. Since the projector is one-dimensional, its image under  $\mathcal{D}$  has to be one-dimensional, too, and there can only be one eigenvalue equal to one. Thus any one-dimensional projector has the spectrum  $\{1, 0, 0, \dots\}$  which must be invariant under a mapping between one-dimensional orthogonal projectors. We now use the linearity of dynamical maps to show that  $\mathcal{D}$  must be unital. Specifically, let  $\{P_i\}$  be the initial set of orthogonal projectors that is mapped to another set of orthogonal projectors,  $\{\bar{P}_i\}$ . We find for the image of the totally mixed state,

$$\rho_M = \frac{1}{d} \mathbb{1}_d,$$

$$\begin{aligned} \mathcal{D}(\rho_M) &= \mathcal{D}\left(\frac{1}{d} \sum_{i=1}^d P_i\right) = \frac{1}{d} \sum_{i=1}^d \mathcal{D}(P_i) \\ &= \frac{1}{d} \sum_{i=1}^d \bar{P}_i = \rho_M, \end{aligned}$$

i.e.  $\mathcal{D}$  maps identity onto itself, making it unital. We can thus use Lemma A.9 to obtain that the spectrum of a complete set of density matrices is invariant under  $\mathcal{D}$ . We now just have to add  $\rho_{TR} = P_{TR}$  to realise a complete and totally rotating set. The spectrum of  $\rho_{TR} = P_{TR}$  is also invariant under  $\mathcal{D}$  since it is a one-dimensional projector that is mapped onto another one-dimensional projector.

(3)  $\implies$  (2) : From Lemma A.9, we obtain that  $\mathcal{D}$  maps a set of  $d$  one-dimensional, orthogonal projectors onto another set of  $d$  one-dimensional orthogonal projectors. We are thus only left with showing that  $\mathcal{D}$  maps a totally rotated projector onto a one-dimensional projector: There always exists a density matrix with a one-dimensional eigenspace corresponding to a totally rotated projector  $P_{TR}$  whose spectrum is invariant under the action of  $\mathcal{D}$ . In the proof of Lemma A.9, we have shown that a dynamical map that leaves the spectrum of projectors invariant maps these projectors onto projectors of the same rank. Repeating the steps of the proof of Lemma A.9, we see that the image of  $P_{TR}$  has to be a one-dimensional projector.

(3)  $\implies$  (4) : Let  $\{\lambda_n\}_{n=1,\dots,d}$  be the set of eigenvalues of  $\rho$ . Then  $\forall k \in \mathbb{N} : \text{Tr}(\rho^k) = \sum_{n=1}^d \lambda_n^k$ . It follows immediately that if  $\rho$  and  $\mathcal{D}(\rho)$  have the same spectrum then  $\forall k \in \mathbb{N} : \text{Tr}(\rho^k) = \text{Tr}(\mathcal{D}(\rho)^k)$ , specifically this is true  $\forall k \leq d$ .

(4)  $\implies$  (3) : The characteristic equation of a matrix  $\rho$  is uniquely determined by the set  $\{\text{Tr}(\rho^k)\}_{k=1,\dots,d}$  [220]. Consequently, if  $\forall k \leq d : \text{Tr}(\rho^k) = \text{Tr}(\mathcal{D}(\rho)^k)$ , then the characteristic equations of  $\rho$  and  $\mathcal{D}(\rho)$  have identical roots. Since these roots correspond to the eigenvalues of  $\rho$ , respectively  $\mathcal{D}(\rho)$ , their spectrum is identical.  $\square$

## A.6 Analytical Bounds for Two Classical Fidelities Utilising MUBs

**Lemma A.10.** *Let  $d \in \mathbb{N}$ ,  $d \geq 2$  and  $a \in \mathbb{Z}$ ,  $|a| < d$ . Then*

$$\sum_{n=1}^d e^{i\frac{2\pi}{d}an} = d\delta_{a0}. \quad (\text{A.28})$$

*Proof.* For  $a = 0$  the statement is obvious. Let us assume that  $a \neq 0$ . We then use the summation formula of the geometric series,

$$\begin{aligned} \sum_{n=1}^d e^{i\frac{2\pi}{d}an} &= \sum_{n=0}^{d-1} e^{i\frac{2\pi}{d}a} e^{i\frac{2\pi}{d}an} \\ &= e^{i\frac{2\pi}{d}a} \sum_{n=0}^{d-1} \left(e^{i\frac{2\pi}{d}a}\right)^n = e^{i\frac{2\pi}{d}a} \frac{1 - e^{i\frac{2\pi}{d}ad}}{1 - e^{i\frac{2\pi}{d}a}} = e^{i\frac{2\pi}{d}a} \frac{1 - e^{i2\pi a}}{1 - e^{i\frac{2\pi}{d}a}} = 0, \end{aligned}$$

whence follows the lemma.  $\square$

**Theorem A.11.** *Let  $\mathcal{H}$  be a Hilbert space with  $\dim \mathcal{H} = d$ . Let  $\mathcal{B}_1 = \{|k_n^{(1)}\rangle\}_{n=1,\dots,d}$  be an orthonormal basis of  $\mathcal{H}$  and let  $\mathcal{B}_2 = \{|k_n^{(2)}\rangle\}_{n=1,\dots,d}$  be another orthonormal basis of  $\mathcal{H}$  that is mutually unbiased with respect to  $\mathcal{B}_1$ . Furthermore, let  $U_0 \in \mathcal{U}(d)$  and  $\mathcal{D}_C \in L(\mathcal{L}_{\mathcal{H}})$  be a dynamical map. Defining for  $\alpha = 1, 2$  the so-called classical fidelities,*

$$F_\alpha = \frac{1}{d} \sum_{i=1}^d \langle k_i^{(\alpha)} | U_0^\dagger \mathcal{D}_C(|k_i^{(\alpha)}\rangle\langle k_i^{(\alpha)}|) U_0 | k_i^{(\alpha)} \rangle, \quad (\text{A.29})$$

the following inequality holds,

$$F_1 + F_2 - 1 \leq F_{pro} \leq \min(F_1, F_2), \quad (\text{A.30})$$

where  $F_{pro}$  is the process fidelity between  $\mathcal{D}$  and the unitary dynamical map corresponding to  $U_0$ .

*Proof.* Let us consider the set of unitaries dynamical maps which yield a classical fidelity of  $F_1 = 1$  with respect to  $\mathcal{B}_1$ . An orthonormal set  $\mathcal{U}^{(1)}$  of unitaries spanning the this space is given by  $\mathcal{U}^{(1)} = \{\frac{1}{\sqrt{d}}U_m^{(1)}\}_{m=0,\dots,d-1}$  having the property

$$\forall m : U_m^{(1)} |k_n^{(1)}\rangle = e^{-i\frac{2\pi}{d}mn} U_0 |k_n^{(1)}\rangle, \quad (\text{A.31})$$

where we set  $U_0^{(1)} \equiv U_0$ . This immediately follows from the fact that the set of unitaries that cannot be differentiated from  $U_0$  by propagating the set  $\mathcal{B}_1$  is given by the commutant space<sup>71</sup>  $\mathcal{K}_{\mathcal{U}(d)}(\mathcal{B}_1)$  which by a straightforward generalisation of Proposition 3.4 is given by those unitaries that have a common eigenbasis with  $U_0$ . Furthermore the dimension of this space is  $d$ . To show that  $\mathcal{U}^{(1)}$  is indeed an orthonormal set spanning this commutant space it suffices to show that the  $d$  elements of  $\mathcal{U}^{(1)}$  are orthogonal which can be seen by direct calculation,

$$\begin{aligned} \text{Tr} \left[ \left( \frac{1}{\sqrt{d}} U_a^{(1)} \right)^\dagger \frac{1}{\sqrt{d}} U_b^{(2)} \right] &= \frac{1}{d} \sum_{n=1}^d \langle k_n^{(1)} | e^{i\frac{2\pi}{d}an} U_0^\dagger U_0 e^{-i\frac{2\pi}{d}bn} | k_n^{(1)} \rangle \\ &= \frac{1}{d} \sum_{n=1}^d e^{i\frac{2\pi}{d}(a-b)n} \langle k_n^{(1)} | U_0^\dagger U_0 | k_n^{(1)} \rangle \\ &= \frac{1}{d} \sum_{n=1}^d e^{i\frac{2\pi}{d}(a-b)n} = \delta_{ab}, \end{aligned}$$

with the last equality following from Lemma A.10.

Similarly we can define a second orthonormal set  $\mathcal{U}^{(2)}$  of unitaries spanning the commutant space  $\mathcal{K}_{\mathcal{U}(d)}(\mathcal{B}_2)$ . We use the same notation,  $\mathcal{U}^{(2)} = \{\frac{1}{\sqrt{d}}U_m^{(2)}\}_{m=0,\dots,d-1}$  with  $U_0^{(2)} = U_0$  having the property

$$U_m^{(2)} |k_n^{(2)}\rangle = e^{-i\frac{2\pi}{d}mn} U_0 |k_n^{(2)}\rangle. \quad (\text{A.32})$$

<sup>71</sup>We work here with the full unitary group instead of the projective unitary group for simplicity. Clearly unitary differentiation with respect to the unitary group automatically implies unitary differentiation with respect to the lower-dimensional projective unitary group.

The calculation for the orthonormality of the objects in the set  $\mathcal{U}^{(2)}$  is identical to the one for  $\mathcal{U}^{(1)}$ . Now we will furthermore show, that  $\forall a, b$  with  $a = 0, b = 0$  excluded the unitaries  $U_a^{(1)}$  and  $U_b^{(2)}$  are orthogonal. This is done by calculating the Hilbert-Schmidt scalar product,

$$\begin{aligned}
\text{Tr} \left[ \left( \frac{1}{\sqrt{d}} U_b^{(2)} \right)^\dagger \frac{1}{\sqrt{d}} U_a^{(1)} \right] &= \frac{1}{d} \sum_n \langle k_n^{(1)} | \left( U_b^{(2)} \right)^\dagger U_a^{(1)} | k_n^{(1)} \rangle \\
&= \frac{1}{d} \sum_{n,m} \langle k_n^{(1)} | k_m^{(2)} \rangle \langle k_m^{(2)} | \left( U_b^{(2)} \right)^\dagger U_a^{(1)} | k_n^{(1)} \rangle \\
&= \frac{1}{d} \sum_{n,m} \langle k_n^{(1)} | k_m^{(2)} \rangle \langle k_m^{(2)} | e^{i \frac{2\pi}{d} b m} e^{-i \frac{2\pi}{d} a n} | k_n^{(1)} \rangle \\
&= \frac{1}{d} \sum_{n,m} e^{i \frac{2\pi}{d} (b m - a n)} \langle k_n^{(1)} | k_m^{(2)} \rangle \langle k_m^{(2)} | k_n^{(1)} \rangle \\
&= \frac{1}{d} \sum_{n,m} e^{i \frac{2\pi}{d} (b m - a n)} \left| \langle k_n^{(1)} | k_m^{(2)} \rangle \right|^2.
\end{aligned}$$

Using the fact that the two bases are mutually unbiased we obtain that

$$\text{Tr} \left[ \left( \frac{1}{\sqrt{d}} U_b^{(2)} \right)^\dagger \frac{1}{\sqrt{d}} U_a^{(1)} \right] = \frac{1}{d^2} \sum_{n,m} e^{i \frac{2\pi}{d} (b m - a n)} = \frac{1}{d} d^2 \delta_{a0} \delta_{b0} = \delta_{a0} \delta_{b0},$$

where we used once again Lemma A.10. Hence the stated orthonormality follows.

It is possible to write a general dynamical map in the following way,

$$\mathcal{D}_C(\rho) = \sum_{ij=0}^{d^2-1} \xi_{ij} \bar{U}_i \rho \bar{U}_j^\dagger, \tag{A.33}$$

where the  $\bar{U}_i$  form an orthonormal basis of unitaries of the Liouville space  $\mathcal{L}_{\mathcal{H}}$  and  $\xi_{ij}$  is a process matrix, cf. Sec. 4.1. It is evident that we can choose the basis  $\{\bar{U}_i\}$  such that

$$\bar{U}_0 = \frac{1}{\sqrt{d}} U_0, \tag{A.34a}$$

$$\forall 1 \leq i \leq d-1 : \bar{U}_i = \frac{1}{\sqrt{d}} U_i^{(1)}, \tag{A.34b}$$

$$\forall d \leq i \leq 2(d-1) : \bar{U}_i = \frac{1}{\sqrt{d}} U_{i-d+1}^{(2)}. \tag{A.34c}$$

The remaining  $\bar{U}_i$  with  $2(d-1) \leq i \leq d^2$  are not relevant for the further discussion but can be constructed in such a way that they are orthonormal to the  $\bar{U}_i$  defined above. Note that  $\xi_{ij}$  is a positive Hermitian matrix. The process fidelity  $F_{\text{pro}}$  of  $\mathcal{D}_C$  with respect to the unitary dynamical map described by  $U_0$  is given by

$$F_{\text{pro}} = \frac{1}{d} \xi_{00}. \tag{A.35}$$

This can be seen by using Eq. (4.24),

$$F_{\text{pro}} = \frac{1}{d^2} \text{Tr} (\mathcal{D}_C \mathcal{U}_0) ,$$

with  $\mathcal{D}_C$  and  $\mathcal{U}_0$  representing the Choi matrices of the corresponding dynamical maps. Noting that the trace is invariant under unitary transformation, we can specifically use the Choi matrices in their representation with respect to the orthonormal basis  $\{\bar{U}_i\}$ . In this representation  $\mathcal{U}_0$  is matrix that is composed entirely of zeros except for the (0,0) entry which is equal to  $d$  and it immediately follows that indeed  $F_{\text{pro}} = \frac{1}{d} \xi_{00}$  which, as argued above, corresponds to the corresponding entry of  $\mathcal{D}_C$  in the representation with respect to  $\{\bar{U}_i\}$ .

Furthermore, it can be immediately seen by inserting the expansion of  $\mathcal{D}_C$  according to Eq. (A.33) in the definition equations for the classical fidelities, that

$$F_1 = \frac{1}{d} \sum_{n=0}^{d-1} \xi_{nn} , \quad (\text{A.36})$$

This can be seen by rewriting Eq. (A.33) in a different orthonormal basis of Liouville space leading to another process matrix  $\eta_{pq}^{rs} \equiv \xi_{(p,q)(r,s)}$  in terms of double indices,

$$\mathcal{D}_C(\rho) = \sum_{pqrs=0}^d \eta_{pq}^{rs} |U_0 k_p^{(1)}\rangle \langle k_q^{(1)}| \rho |k_r^{(1)}\rangle \langle U_0 k_s^{(1)}| .$$

Note that  $\{|U_0 k_i^{(1)}\rangle \langle k_j^{(1)}|\}_{i,j=1,\dots,d}$  is indeed an orthonormal basis of Liouville space due to

$$\begin{aligned} \text{Tr} \left[ \left( |U_0 k_i^{(1)}\rangle \langle k_j^{(1)}| \right)^\dagger |U_0 k_{i'}^{(1)}\rangle \langle k_{j'}^{(1)}| \right] &= \text{Tr} \left[ \langle k_j^{(1)}| \langle U_0 k_i^{(1)}| U_0 k_{i'}^{(1)}\rangle |k_{j'}^{(1)}\rangle \right] \\ &= \delta_{ii'} \delta_{jj'} . \end{aligned}$$

Thus, the classical fidelity  $F_1$  reads

$$\begin{aligned} F_1 &= \frac{1}{d} \sum_{j=1}^d \langle k_j^{(1)}| U_0^\dagger \mathcal{D}_C(|k_j^{(1)}\rangle \langle k_j^{(1)}|) U_0 |k_j^{(1)}\rangle \\ &= \frac{1}{d} \sum_{j=1}^d \sum_{pqrs=0}^d \eta_{ps}^{qr} \langle k_j^{(1)}| U_0^\dagger |U_0 k_p^{(1)}\rangle \langle k_q^{(1)}| k_j^{(1)}\rangle \langle k_j^{(1)}| k_r^{(1)}\rangle \langle U_0 k_s^{(1)}| U_0 |k_j^{(1)}\rangle \\ &= \frac{1}{d} \sum_{j=1}^d \eta_{jj}^{jj} . \end{aligned}$$

Now, note that from Eq. (A.31) it immediately follows that

$$\forall m = 0, \dots, d-1 : U_m^{(1)} = \sum_{n=1}^d e^{-i \frac{2\pi}{d} mn} |U_0 k_n^{(1)}\rangle \langle k_n^{(1)}| .$$

This means that the span of the orthonormal basis elements  $\{|U_0 k_j^{(1)}\rangle |k_j|\}_{j=1,\dots,d}$  in Liouville space is identical to the span of the orthonormal set  $\{\bar{U}_m^{(1)}\}_{m=0,\dots,d-1}$ . As a result, there exists a unitary transformation between them which means that the unitary transformation between the process matrices  $\xi$  and  $\eta$  has block structure. This block unitary transformation preserves the trace of the corresponding blocks of the process matrix, hence the partial coefficient sums of the process matrices  $\sum_{j=1}^d \eta_{jj}^{jj}$  and  $\sum_{j=0}^{d-1} \xi_{jj}$  need to be identical. This proves Eq. (A.36) and we can slightly rewrite it to obtain

$$F_1 = \frac{1}{d}\xi_{00} + \frac{1}{d}\sum_{i=1}^{d-1}\xi_{ii}, \quad (\text{A.37})$$

Analogously, one obtains the following equation for the second classical fidelity,

$$F_2 = \frac{1}{d}\xi_{00} + \frac{1}{d}\sum_{i=d}^{2(d-1)}\xi_{ii}. \quad (\text{A.38})$$

Due to the properties of the matrix  $\chi$  (namely positivity) it follows immediately that

$$F_1 \geq \frac{1}{d}\xi_{00} \text{ and } F_2 \geq \frac{1}{d}\xi_{00} \quad (\text{A.39})$$

as well as (using trace  $d$  of  $\chi$  combined with positivity),

$$\begin{aligned} F_1 + F_2 &= \frac{2}{d}\xi_{00} + \frac{1}{d}\sum_{i=1}^{2(d-1)}\xi_{ii} = \frac{1}{d}\xi_{00} + \frac{1}{d}\left(\xi_{00} + \sum_{i=1}^{2(d-1)}\xi_{ii}\right) \leq \frac{1}{d}\xi_{00} + 1, \\ \iff F_1 + F_2 - 1 &\leq \frac{1}{d}\xi_{00}, \end{aligned} \quad (\text{A.40})$$

such that with Eq. (A.35) the following bound can be formed,

$$F_1 + F_2 - 1 \leq F_{\text{pro}} \leq \min(F_1, F_2),$$

which is equivalent to the bound in Eq. (4.38) for the specific construction used by Hofmann.  $\square$

## A.7 Monte Carlo Certification for General Operator Bases

In this subsection we will discuss Monte Carlo certification of unitary dynamical maps for a general (not necessarily Hermitian) choice of the measurement basis, following the derivations in Refs. [59, 60] where a similar calculation for a Hermitian measurement basis has been performed.

Analogously to Eq. (4.45) we will introduce the quantities,

$$\alpha_{ik} = \frac{1}{d}\text{Tr}\left[\mathcal{D}(W_i)^\dagger W_k\right], \quad (\text{A.41a})$$

$$\beta_{ik} = \frac{1}{d}\text{Tr}\left[UW_i^\dagger U^\dagger W_k\right], \quad (\text{A.41b})$$

for an orthogonal set of Liouville space operators  $\{W_k\}_{k=1,\dots,d^2}$  fulfilling

$$\mathrm{Tr}\left(W_k^\dagger W_k\right) = d.$$

In general,  $\alpha_{ik}$  and  $\beta_{ik}$  are complex; they are real only if  $W_k$  is Hermitian. The process fidelity can be expressed in terms of  $\alpha_{ik}$  and  $\beta_{ik}$ ,

$$\begin{aligned} F_{\mathrm{pro}} &= \frac{1}{d^2} \sum_{i,k} \alpha_{ik} \beta_{ik}^* = \sum_{i,k} \frac{|\beta_{ik}|^2}{d^2} \frac{\alpha_{ik}}{\beta_{ik}} \\ &= \sum_{i,k} \mathrm{Pr}(i,k) \frac{\alpha_{ik}}{\beta_{ik}}, \end{aligned} \quad (\text{A.42})$$

with the real-valued relevance distribution,

$$\mathrm{Pr}(i,k) = \frac{|\beta_{ik}|^2}{d^2}. \quad (\text{A.43})$$

Note that if  $U_0$  is a (generalised) Clifford gate and the  $\{W_k\}$  are chosen to be (generalised) Pauli operators, then for any  $i$  there is only a single  $k$  such that  $\beta_{ik} \neq 0$ , taking the value  $\frac{1}{d^2}$ . This is because a (generalised) Clifford gate maps a (generalised) Pauli operator to another generalised Pauli operator. For Monte Carlo sampling we define now the complex random variable  $X$  on the event space given by the set of tuples  $(i,k)$ ,

$$X(i,k) = \frac{\alpha_{ik}}{\beta_{ik}}. \quad (\text{A.44})$$

It is easy to see that the expectation value of this random variable corresponds to  $F_{\mathrm{pro}}$ ,

$$\mathbb{E}(X(i,k)) = \sum_{i,k} \mathrm{Pr}(i,k) \frac{\alpha_{ik}}{\beta_{ik}} = F_{\mathrm{pro}}. \quad (\text{A.45})$$

The Monte Carlo approach seeks an estimate of  $F_{\mathrm{pro}}$  with additive error  $\epsilon$  and failure probability  $\delta$ . In other words, one wants to find an estimator  $Y$  such that the likelihood that this estimator  $Y$  is greater or equal  $\epsilon$  away from the fidelity  $F_{\mathrm{pro}}$  to be less or equal  $\delta$ ,

$$\mathrm{Pr}[|Y - F_{\mathrm{pro}}| \geq \epsilon] \leq \delta. \quad (\text{A.46})$$

The complex version of Chebyshev's inequality [221] states that,  $\forall t > 0$  and each complex random variable  $Z$  with expectation value  $\mu$ , the following relation is fulfilled

$$\mathrm{Pr}[|Z - \mu| \geq t|\mu|] \leq \frac{\mathbb{E}(ZZ^*) - \mathbb{E}(Z)\mathbb{E}(Z^*)}{t^2|\mu|^2}. \quad (\text{A.47})$$

Mapping  $t > 0$  onto  $t|\mu| \equiv \kappa > 0$  leads to

$$\mathrm{Pr}[|Z - \mu| \geq \kappa] \leq \frac{\mathbb{E}(ZZ^*) - \mathbb{E}(Z)\mathbb{E}(Z^*)}{\kappa^2}. \quad (\text{A.48})$$

Now one just needs to find a suitable estimator  $Y$  and calculate its expectation value and variance.

To this end, set the number of draws  $L$  from the event space given by the tuples  $(i, k)$  to  $L = \lceil \frac{1}{\epsilon^2 \delta} \rceil$  where  $\lceil \cdot \rceil$  is the ceiling, i.e. rounding up to the nearest integer. Choosing independently some events  $(i_1, k_1), \dots, (i_L, k_L)$  out of the total event space yields independent estimates  $X_1 = \frac{\alpha_{i_1 k_1}}{\beta_{i_1 k_1}}, \dots, X_L = \frac{\alpha_{i_L k_L}}{\beta_{i_L k_L}}$ . Now define  $Y = \frac{1}{L} \sum_{l=1}^L X_l$ . We explain how to estimate  $Y$  which in turn is an approximation to  $F_{\text{pro}}$ .

Consider the choice of  $(i_l, k_l)$  with  $l = 1, \dots, L$  chosen as explained above and  $i_l$  denoting the index of the input operator of the  $l$ -th measurement by  $k_l$  the index of the measured operator of the  $l$ -th measurement. For each  $l$  the operator  $W_{k_l}$  will be measured on the state that is obtained by sending a randomly drawn eigenstate  $|\phi_a^{i_l}\rangle$  of  $W_{i_l}$  with corresponding eigenvalue  $\lambda_a^{i_l}$  through the device ( $a$  is drawn out of the set  $\{1, \dots, d\}$ ). This is repeated a total number of  $m_l$  times where

$$m_l = \left\lceil \frac{4}{|\beta_{i_l k_l}|^2 L \epsilon^2} \log \left( \frac{4}{\delta} \right) \right\rceil. \quad (\text{A.49})$$

This choice of  $m_l$  guarantees that Eq. (A.46) is fulfilled as we show below. Note that each measurement gives an eigenvalue of the operator  $W_{k_l}$ . We denote these, in general complex, measurement results by  $w_{ln}$  with  $n$  referring to the  $n$ -th repetition of the  $l$ -th measurement. Each of these measurements results in an eigenvalue  $w_{ln} \in \text{spec}(W_{k_l})$ . We assume the expectation value of a measurement of an operator  $W_{k_l}$  for a state  $\rho$  to be given by

$$\langle W_{k_l} \rangle_\rho = \text{Tr} [\rho^\dagger W_{k_l}] = \text{Tr} [\rho W_{k_l}]$$

also for non-Hermitian operators. Let us define now  $A_{ln} = (\lambda_{a_n}^{i_l})^* w_{ln}$  where  $\lambda_{a_n}^{i_l}$  is the eigenvalue corresponding to the eigenstate  $|\phi_{a_n}^{i_l}\rangle$  of the operator  $W_{i_l}$ . Note that

$$\begin{aligned} \mathbb{E}(A_{ln}) &= \frac{1}{d} \sum_{a_n=1}^d (\lambda_{a_n}^{i_l})^* w_{ln} \\ &= \frac{1}{d} \sum_{a_n=1}^d (\lambda_{a_n}^{i_l})^* \text{Tr} \left[ \mathcal{D} (|\phi_{a_n}^{i_l}\rangle \langle \phi_{a_n}^{i_l}|)^\dagger W_{k_l} \right] \\ &= \frac{1}{d} \sum_{a_n=1}^d \text{Tr} \left[ (\lambda_{a_n}^{i_l})^* \mathcal{D} (|\phi_{a_n}^{i_l}\rangle \langle \phi_{a_n}^{i_l}|)^\dagger W_{k_l} \right] \\ &= \frac{1}{d} \text{Tr} \left[ \mathcal{D} \left( \sum_{a_n=1}^d \lambda_{a_n}^{i_l} |\phi_{a_n}^{i_l}\rangle \langle \phi_{a_n}^{i_l}| \right)^\dagger W_{k_l} \right] \\ &= \frac{1}{d} \text{Tr} \left[ \mathcal{D} (W_{i_l})^\dagger W_{k_l} \right] = \alpha_{i_l k_l}. \end{aligned} \quad (\text{A.50})$$

Estimators corresponding to  $X_l$ , denoted by  $\tilde{X}_l$ , can now be introduced,

$$\tilde{X}_l = \frac{1}{\beta_{i_l k_l}} \cdot \frac{1}{m_l} \sum_{n=1}^{m_l} A_{ln}. \quad (\text{A.51})$$

Since  $\mathbb{E}(B_{ln}) \equiv \langle A_{ln} \rangle = \alpha_{i_l k_l}$ , it is clear that  $\frac{1}{m_l} \sum_{n=1}^{m_l} A_{ln} \rightarrow \alpha_{i_l k_l}$ .

For the final step in the Monte Carlo estimation, let

$$\tilde{Y} = \frac{1}{L} \sum_{l=1}^L \tilde{X}_l. \quad (\text{A.52})$$

Just like  $\tilde{X}_l$  is an approximation to  $X_l$ ,  $\tilde{Y}$  is an approximation to  $Y$  or in other words an estimate for  $Y$ . The goal is to fulfil Hoeffding's inequality, which we prove below,

$$\Pr \left[ \left| \tilde{Y} - Y \right| \geq \epsilon \right] \leq \delta. \quad (\text{A.53})$$

The whole procedure uses the channel a total number of  $m = \sum_{l=1}^L m_l$  times. This value in estimation can be bounded by calculating  $\mathbb{E}(m_l)$  which is the expected number of experimental repetitions for the given setting  $(i_l, k_l)$ . In other words,  $\mathbb{E}(m_l)$  is the number of experiments one has to perform for a setting  $(i, k)$  multiplied by the probability that this setting is chosen. Denoting by  $m_l(i, k)$  the number of experiments for the tuple  $(i, k)$ , given by Eq. (A.49), the expectation value becomes

$$\begin{aligned} \mathbb{E}(m_l) &= \sum_{ik} \Pr(i, k) m_l(i, k) \\ &= \frac{1}{d^2} \sum_{ik} |\beta_{ik}|^2 \left\lceil \frac{4}{|\beta_{ik}|^2 L \epsilon^2} \log \left( \frac{4}{\delta} \right) \right\rceil \end{aligned} \quad (\text{A.54})$$

$$\leq 1 + \frac{4d^2}{L\epsilon^2} \log \left( \frac{4}{\delta} \right), \quad (\text{A.55})$$

where 1 accounts for the fact that the smallest integer greater than the expression in the ceiling  $\lceil \cdot \rceil$  is taken. The total number of experiments given by the sum of all  $m_l$  is found to be

$$\begin{aligned} \mathbb{E}(m) &= \sum_{l=1}^L \mathbb{E}(m_l) \leq L \cdot \left[ 1 + \frac{4d^2}{L\epsilon^2} \log \left( \frac{4}{\delta} \right) \right] \\ &\leq 1 + \frac{1}{\epsilon^2 \delta} + \frac{4d^2}{\epsilon^2} \log \left( \frac{4}{\delta} \right), \end{aligned} \quad (\text{A.56})$$

where the additive 1 appears for the same reason as above. Note that this scales as  $\mathcal{O}(d^2)$ .

For (generalised) Clifford gates and (generalised) Pauli measurements, there are only  $d^2$  nonvanishing entries the sum in Eq. (A.54) since for each  $k$  there exists only one  $l$  for which  $\beta_{kl} \neq 0$ . This leads to

$$\mathbb{E}(m_l) \leq 1 + \frac{4}{L\epsilon^2} \log \left( \frac{4}{\delta} \right) \quad (\text{A.57})$$

and consequently

$$\mathbb{E}(m) \leq 1 + \frac{1}{\epsilon^2 \delta} + \frac{4}{\epsilon^2} \log \left( \frac{4}{\delta} \right), \quad (\text{A.58})$$

resulting in a scaling of  $\mathcal{O}(1)$ .

Finally we prove validity of Eqs. (A.46) and (A.53). We first consider Eq. (A.46), where the

numerator of the right hand side of the Chebyshev inequality needs to be estimated for  $Z = X_l$ ,

$$\begin{aligned}
\mathbb{E}(X_l X_l^*) - \mathbb{E}(X_l) \mathbb{E}(X_l^*) &= \sum_{ik} \Pr(i, k) \frac{|\alpha_{ik}|^2}{|\beta_{ik}|^2} - \left| \sum_{ik} \Pr(i, k) \frac{\alpha_{ik}}{\beta_{ik}} \right|^2 = \frac{1}{d^2} \sum_{ik} |\alpha_{ik}|^2 - F_{\text{pro}}^2 \\
&= \frac{1}{d^4} \sum_{ik} \langle \langle \mathcal{D}(W_i) \| W_k \rangle \rangle \langle \langle W_k \| \mathcal{D}(W_i) \rangle \rangle - F_{\text{pro}}^2 \\
&= \frac{1}{d^4} \sum_{ik} \left| \text{Tr} \left[ W_k^\dagger \mathcal{D}(W_i) \right] \right|^2 - F_{\text{pro}}^2. \tag{A.59}
\end{aligned}$$

Obviously  $0 \leq F_{\text{pro}} \leq 1 \implies 0 \leq F_{\text{pro}}^2 \leq 1$ . The same is true for the first term. This can be seen most easily in terms of the process matrix, cf. Eq. (4.1). For any operator  $O$ , one can write

$$\mathcal{D}(O) = \sum_{nm} \chi_{nm} W_m O W_n^\dagger.$$

Clearly for  $O = W_i$ ,

$$\mathcal{D}(W_i) = \sum_{nm} \chi_{nm} W_m W_i W_n^\dagger.$$

It follows that

$$\begin{aligned}
\left| \text{Tr} \left[ W_k^\dagger \mathcal{D}(W_i) \right] \right|^2 &= \left| \sum_{nm} \chi_{nm} \text{Tr} \left[ W_k^\dagger W_m W_i W_n^\dagger \right] \right|^2 \\
&\leq \sum_{nm} |\chi_{nm}|^2 \left| \text{Tr} \left[ W_k^\dagger W_m W_i W_n^\dagger \right] \right|^2
\end{aligned}$$

For fixed  $i$  and  $k$ , the operator  $W_k^\dagger W_m W_i$  is proportional to a Pauli operator. Consider the expression

$$\sum_{ik} \left| \text{Tr} \left[ W_k^\dagger W_m W_i W_n^\dagger \right] \right|^2.$$

For fixed  $m, n$  and a certain  $i$  there exists exactly one  $k$  such that this is non-zero, namely if and only if

$$W_k^\dagger W_m W_i W_n^\dagger \sim \mathbb{1}_d. \tag{A.60}$$

That is,

$$W_k \sim W_m W_i W_n^\dagger.$$

Due to orthonormality of the operator basis, there is only one such  $k$  for which this relation can be fulfilled. For Pauli operators the proportionality constant has modulus 1, hence

$$\sum_{ik} \left| \text{Tr} \left[ W_k^\dagger W_m W_i W_n^\dagger \right] \right|^2 = d^2 \cdot d^2 = d^4.$$

This results in a trace of  $d$  for the  $d^2$  tuple  $(i, k)$  for which relation (A.60) holds. Consequently

$$\frac{1}{d^4} \sum_{ik} \left| \text{Tr} \left[ W_k^\dagger \mathcal{D}(W_i) \right] \right|^2 \leq \sum_{ik} |x_{ik}|^2.$$

Due to the Choi-Jamiołkowski isomorphism, the normalised Choi matrix<sup>72</sup> corresponds to a density matrix in the  $d^2$ -dimensional Hilbert space  $\mathcal{H} \otimes \mathcal{H}$ , cf. Sec. 2.7. It can easily be seen that  $\sum_{ik} |x_{ik}|^2$  corresponds to the purity of this density matrix which cannot be greater than 1. Therefore

$$\frac{1}{d^4} \sum_{ik} \left| \text{Tr} \left[ W_k^\dagger \mathcal{D}(W_i) \right] \right|^2 \leq 1.$$

Hence  $[\mathbb{E}(X_l X_l^*) - \mathbb{E}(X_l) \mathbb{E}(X_l^*)]$  is the difference between two numbers in the interval  $[0, 1]$  and consequently smaller than 1,

$$\mathbb{E}(X_l X_l^*) - \mathbb{E}(X_l) \mathbb{E}(X_l^*) \leq 1.$$

It follows for  $Y = \frac{1}{L} \sum_{l=1}^L X_l$  that

$$\begin{aligned} \mathbb{E}(Y Y^*) - \mathbb{E}(Y) \mathbb{E}(Y^*) &= \mathbb{E} \left( \left( \frac{1}{L} \sum_l X_l \right) \left( \frac{1}{L} \sum_{l'} X_{l'}^* \right) \right) - \mathbb{E} \left( \frac{1}{L} \sum_l X_l \right) \mathbb{E} \left( \frac{1}{L} \sum_{l'} X_{l'}^* \right) \\ &= \frac{1}{L^2} \sum_{l'} \mathbb{E}(X_l X_{l'}^*) - \frac{1}{L^2} \sum_{l'} \mathbb{E}(X_l) \mathbb{E}(X_{l'}^*) \\ &= \frac{1}{L^2} \sum_{l'} [\mathbb{E}(X_l X_{l'}) - \mathbb{E}(X_l) \mathbb{E}(X_{l'}^*)] = \frac{1}{L^2} \sum_l [\mathbb{E}(X_l X_l) - \mathbb{E}(X_l) \mathbb{E}(X_l^*)] \\ &\leq \frac{L}{L^2} = \frac{1}{L}, \end{aligned}$$

where use has been made of  $\mathbb{E}(X_l X_{l'}) = \mathbb{E}(X_l) \mathbb{E}(X_{l'})$  for the  $X_l \neq X_{l'}$  which are uncorrelated. Chebyshev's inequality, Eq. (A.47), consequently yields

$$\Pr[|Y - F| \geq \kappa] \leq \frac{1}{L \kappa^2}.$$

Now set  $\kappa = \sqrt{\frac{1}{L \delta}}$  and  $L = \frac{1}{\epsilon^2 \delta}$  to obtain

$$\Pr[|Y - F| \geq \epsilon] \leq \delta.$$

To show the validity of Eq. (A.53) we use the complex version of Hoeffding's inequality [222].

**Lemma A.12.** *Let  $\vec{a} \in \mathbb{R}^n$  and  $\{X_i\}_{i=1, \dots, N}$  be independent zero-mean complex-valued random variables with  $\forall i: |X_i| \leq a_i$ . Then  $\forall \delta > 0$*

$$\Pr \left( \left| \sum_{i=1}^N X_i \right| \geq \delta \right) \leq 4 \exp \left( - \frac{\delta^2}{4 \sum_{i=1}^n |a_i|^2} \right). \quad (\text{A.61})$$

<sup>72</sup>Note that due to the lack of normalisation of the  $\{W_k\}$ , the Choi matrix is actually normalised in this calculation.

**Corollary A.13.** *Let  $\vec{a} \in \mathbb{R}^n$  and  $\{X_i\}_{i=1, \dots, N}$  be independent complex-valued random variables with mean value  $\sum_{i=1}^N \langle X_i \rangle = \langle X \rangle$  where  $X = \sum_{i=1}^N X_i$  and  $\forall i: |X_i - \langle X_i \rangle| \leq a_i$ . Then  $\forall \delta > 0$*

$$\Pr(|X - \langle X \rangle| \geq \delta) \leq 4 \exp\left(-\frac{\delta^2}{4 \sum_{i=1}^n |a_i|^2}\right). \quad (\text{A.62})$$

*Proof.* Apply Hoeffding's inequality to the random variables  $X_i - \langle X_i \rangle$ .  $\square$

Specifically this means for  $\delta > 0$ ,  $n = L$  and  $\tilde{Y} = \frac{1}{L} \sum_{l=1}^L \tilde{X}_l$  with  $\langle \tilde{Y} \rangle = \frac{1}{L} \sum_{l=1}^L \langle \tilde{X}_l \rangle = \frac{1}{L} \sum_{l=1}^L X_l = Y$ . Note furthermore that the  $\tilde{X}_l$  themselves are composed of a sum of independent random variables  $A_{ln}$  corresponding to measurement results with modulus smaller than 1 and expectation value with modulus smaller than 1. As such we can write

$$\Pr\left[|\tilde{Y} - Y| \geq \epsilon\right] \leq 4 \exp\left(-\frac{4\epsilon^2}{C}\right), \quad (\text{A.63})$$

where

$$C = \sum_{l=1}^L \frac{1}{L} m_l |2c_l|^2, \quad c_l = \frac{1}{m_l \beta_{i k_l}} \quad (\text{A.64})$$

since the quantity  $[A_{ln} - \langle A_{ln} \rangle]$ , as discussed for Eq. (A.51), always takes values with modulus smaller than 2.

Calculating  $C$  leads to

$$\begin{aligned} C &= \sum_{l=1}^L \frac{4}{L^2 \beta_{i k_l}^2 m_l} = \sum_{l=1}^L \frac{4 \beta_{i k_l}^2 L \epsilon^2}{4 L^2 \beta_{i k_l}^2 \log\left(\frac{4}{\delta}\right)} \\ &= \sum_{l=1}^L \frac{\epsilon^2}{L \log\left(\frac{4}{\delta}\right)} = \frac{\epsilon^2}{\log\left(\frac{4}{\delta}\right)}. \end{aligned} \quad (\text{A.65})$$

Plugging this into Hoeffding's inequality yields

$$\begin{aligned} \Pr\left[|\tilde{Y} - Y| \geq \epsilon\right] &\leq 4 \exp\left(-\frac{4\epsilon^2}{C}\right) = 4 \exp\left(-4 \log\left(\frac{4}{\delta}\right)\right) \\ &= 4 \exp\left(\log\left(\frac{\delta^4}{256}\right)\right) = \frac{\delta^4}{256} \leq \delta. \end{aligned} \quad (\text{A.66})$$

Hence the failure probability is  $\leq \delta$ , as desired.

## A.8 Proper Normalisation of the Relevance Distribution for Reduced Fidelities

Consider an  $n$ -qubit Hilbert space  $\mathcal{H}$  with  $\dim \mathcal{H} = 2^n = d$ . In order to prove normalisation of the relevance distribution  $\Pr(i, k)$ , cf. Eq. (4.53), we first show that

$$\sum_{k=1}^{d^2} \langle \varphi_i | W_k | \varphi_j \rangle \langle \varphi_n | W_k | \varphi_m \rangle = d \delta_{im} \delta_{jn}, \quad (\text{A.67})$$

with  $\{|\varphi_j\rangle\}$  the canonical basis where  $W_k$  is an arbitrary Pauli operator on  $\mathcal{H}$ . Note that for each pair  $|\varphi_i\rangle, |\varphi_j\rangle$ , there are exactly  $d$  operators  $W_k$  with  $\langle\varphi_i|W_k|\varphi_j\rangle \neq 0$ . This is seen easily in the bit representation ( $W_k = \omega_k^1 \otimes \dots \otimes \omega_k^N$ ). For the  $m$ -th qubit, the scalar product vanishes if there is a bit flip between the two states at the  $m$ -th qubit and  $\omega_k^m = \sigma_0$  or  $\sigma_z$ . Analogously, the scalar product vanishes if the  $m$ -th qubit has the same value between the two states and  $\omega_k^m = \sigma_x$  or  $\sigma_y$ . There are thus only two choices of  $W_k$  for each qubit that lead to a non-zero scalar product. Repeating the argument over all  $n$  qubits gives exactly  $2^n = d$  possible operators  $W_k$  for which  $\langle\varphi_i|W_k|\varphi_j\rangle \neq 0$ .

Consider now  $\langle\varphi_i|W_k|\varphi_j\rangle \langle\varphi_n|W_k|\varphi_m\rangle$  for a certain  $W_k$  with  $|\varphi_i\rangle \neq |\varphi_m\rangle$  and  $|\varphi_j\rangle, |\varphi_n\rangle$  fixed. Since  $|\varphi_i\rangle \neq |\varphi_m\rangle$  there exists a qubit,  $l$ , where the two states differ. We differentiate two cases for this qubit.

1.  $|\varphi_j\rangle$  and  $|\varphi_i\rangle$  take the same value on the  $l$ -th qubit. Then  $\omega_k^l$  must be  $\sigma_0$  or  $\sigma_z$  for  $\langle\varphi_i|W_k|\varphi_j\rangle \langle\varphi_n|W_k|\varphi_m\rangle$  not to vanish. However, there exists an operator  $W_{k'}$  such that the contribution of the two operators to the sum, Eq. (A.67),

$$\langle\varphi_i|W_k|\varphi_j\rangle \langle\varphi_n|W_k|\varphi_m\rangle + \langle\varphi_i|W_{k'}|\varphi_j\rangle \langle\varphi_n|W_{k'}|\varphi_m\rangle ,$$

vanishes. This operator is identical to  $W_k$  except that  $\omega_{k'}^l = \sigma_0$  if  $\omega_k^l = \sigma_z$  and vice versa. Then

$$\langle\varphi_i|W_{k'} = -\langle\varphi_i|W_k \quad \text{and} \quad W_{k'}|\varphi_m\rangle = W_k|\varphi_m\rangle ,$$

with the minus sign due to  $\sigma_z$  on the  $l$ -th qubit for either  $W_k$  or  $W_{k'}$ .

2. Alternatively,  $|\varphi_j\rangle$  and  $|\varphi_i\rangle$  take different values on the  $l$ -th qubit. Then  $\omega_k^l$  must be  $\sigma_x$  or  $\sigma_y$  for  $\langle\varphi_i|W_k|\varphi_j\rangle \langle\varphi_n|W_k|\varphi_m\rangle$  not to vanish. Again, there exists an operator  $W_{k'}$  such that the contribution of the two operators to the sum, Eq. (A.67), vanishes. This operator is identical to  $W_k$  except that  $\omega_{k'}^l = \sigma_x$  if  $\omega_k^l = \sigma_y$  and vice versa. If  $|\varphi_i^l\rangle = |1\rangle$  (and thus  $|\varphi_m^l\rangle = |0\rangle$ ),

$$\langle\varphi_i|W_{k'} = -i\langle\varphi_i|W_k \quad \text{and} \quad W_{k'}|\varphi_m\rangle = -iW_k|\varphi_m\rangle .$$

Otherwise, if  $|\varphi_i^l\rangle = |0\rangle$  (and thus  $|\varphi_m^l\rangle = |1\rangle$ ),

$$\langle\varphi_i|W_{k'} = i\langle\varphi_i|W_k \quad \text{and} \quad W_{k'}|\varphi_m\rangle = iW_k|\varphi_m\rangle .$$

In both cases, the terms in the sum cancel.

Consequently, for each  $W_k$  and  $|\varphi_i\rangle, |\varphi_j\rangle, |\varphi_m\rangle, |\varphi_n\rangle$  with  $|\varphi_i\rangle \neq |\varphi_j\rangle$  there exists a ‘‘pair operator’’  $W_{k'}$  which cancels the contribution of  $W_k$  to Eq. (A.67) such that  $\sum_{k=1}^{d^2} \langle\varphi_i|W_k|\varphi_j\rangle \langle\varphi_n|W_k|\varphi_m\rangle = 0$  if  $|\varphi_i\rangle \neq |\varphi_m\rangle$ . Repeating the argument for  $|\varphi_j\rangle \neq |\varphi_n\rangle$  leads to

$$\begin{aligned} \sum_{k=1}^{d^2} \langle\varphi_i|W_k|\varphi_j\rangle \langle\varphi_n|W_k|\varphi_m\rangle &= \delta_{im}\delta_{jn} \sum_{k=1}^{d^2} \langle\varphi_i|W_k|\varphi_j\rangle \langle\varphi_n|W_k|\varphi_m\rangle \\ &= \delta_{im}\delta_{jn} \sum_{k=1}^{d^2} |\langle\varphi_i|W_k|\varphi_j\rangle|^2 , \end{aligned}$$

using Hermiticity of  $W_k$  in the last step. Now, validity of Eq. (A.67) follows simply from the fact that there exist, for each pair  $|\varphi_i\rangle, |\varphi_j\rangle$ , exactly  $d$  operators  $W_k$  with non-vanishing  $\langle\varphi_i|W_k|\varphi_j\rangle$ , and, in the canonical basis, these matrix elements are equal to one.

Expanding a general vector  $|\Phi\rangle$  in the canonical basis and using Eq. (A.67), we find our second intermediate result,

$$\begin{aligned} \sum_{k=1}^{d^2} |\langle\Phi|W_k|\Phi\rangle|^2 &= \sum_{k=1}^{d^2} \left| \sum_{i,j=1}^d c_i^* c_j \langle\varphi_i|W_k|\varphi_j\rangle \right|^2 \\ &= \sum_{k=1}^{d^2} \sum_{i,j,n,m=1}^d c_i^* c_j c_n^* c_m \langle\varphi_i|W_k|\varphi_j\rangle \langle\varphi_n|W_k|\varphi_m\rangle \\ &= \sum_{i,j,n,m=1}^d c_i^* c_j c_n^* c_m d \delta_{im} \delta_{jn} = d \left( \sum_{i=1}^d |c_i|^2 \right) = d. \end{aligned} \quad (\text{A.68})$$

It is now straightforward to prove normalisation of  $\text{Pr}(i, k)$ , starting from the definition

$$\text{Pr}(i, k) = \frac{1}{dI} |\alpha_{ik}|^2 = \frac{1}{dI} \left| \text{Tr} \left[ U_0 P_i U_0^\dagger W_k \right] \right|^2.$$

Writing  $P_i = |\psi_i\rangle\langle\psi_i|$  we obtain when evaluating the trace in some orthonormal basis  $\{|\psi_n\rangle\}$  containing  $|\psi_i\rangle$  as one element

$$\begin{aligned} \sum_{i=1}^I \sum_{k=1}^{d^2} \text{Pr}(i, k) &= \frac{1}{dI} \sum_{i=1}^I \sum_{k=1}^{d^2} \left| \text{Tr} \left[ U_0 P_i U_0^\dagger W_k \right] \right|^2 \\ &= \frac{1}{dI} \sum_{i=1}^I \sum_{k=1}^{d^2} \sum_{n,m=1}^d \langle\psi_n|UW_kU^\dagger|\psi_i\rangle \langle\psi_i|\psi_n\rangle \langle\psi_m|\psi_i\rangle \langle\psi_i|U^\dagger W_k U|\psi_m\rangle \\ &= \frac{1}{dI} \sum_{i=1}^I \sum_{k=1}^{d^2} \langle\psi_i|UW_kU^\dagger|\psi_i\rangle \langle\psi_i|U^\dagger W_k U|\psi_i\rangle = \frac{1}{dI} \sum_{i=1}^I d = 1, \end{aligned} \quad (\text{A.69})$$

where we have used Eq. (A.68) in the last line with  $|\Phi\rangle = U|\psi_i\rangle$ .

## A.9 Bounded Variance for the Random Variables Involved in Reduced Fidelities

Consider an  $n$ -qubit Hilbert space  $\mathcal{H}$  with  $\dim \mathcal{H} = 2^n = d$ .  $X_l$ , the random variable of the top level of sampling in the Monte Carlo estimation of arithmetic means of pure state fidelities, has been defined in Appendix A.7 as the ratio of the measurement outcomes for the actual dynamical map and the ideal unitary dynamical map,

$$X_l = \frac{\beta_{i_l k_l}}{\alpha_{i_l k_l}}. \quad (\text{A.70})$$

In analogy to the discussion in Sec. A.6 we will show that the variance of each  $X_l$  is not too large,

$$\begin{aligned}
\text{Var}(X_l) &= \mathbb{E}(X_l^2) - \mathbb{E}(X_l)^2 = \sum_{i=1}^I \sum_{k=1}^{d^2} \Pr(i, k) \left( \frac{\beta_{i_l k_l}}{\alpha_{i_l k_l}} \right)^2 - \left( \sum_{i=1}^I \sum_{k=1}^{d^2} \Pr(i, k) \frac{\beta_{i_l k_l}}{\alpha_{i_l k_l}} \right)^2 \\
&= \frac{1}{dI} \sum_{i=1}^I \sum_{k=1}^{d^2} \beta_{i_l k_l}^2 - \frac{1}{dI} \left[ \sum_{i=1}^I \text{Tr} [U P_i U^+ \mathcal{D}(P_i)] \right]^2 \\
&= \frac{1}{dI} \sum_{i=1}^I \sum_{k=1}^{d^2} \left| \text{Tr} [W_k \mathcal{D}(P_i)] \right|^2 - F^2, \tag{A.71}
\end{aligned}$$

with  $F$  being the fidelity from Eq. (4.51). Since  $0 \leq F \leq 1$  it follows that  $0 \leq F^2 \leq 1$ . The same is true for the first term. This can be seen as follows. Each term  $\mathcal{D}(P_i)$  can be written as a density matrix  $\rho_i$ ,

$$\mathcal{D}(P_i) = \rho_i = \sum_{n=1}^d \lambda_n^{(i)} |\phi_n^{(i)}\rangle \langle \phi_n^{(i)}|,$$

with eigenvectors  $|\phi_n^{(i)}\rangle$  and eigenvalues  $\lambda_n^{(i)}$ . Evaluating the trace for each  $i$  in the corresponding eigenbasis yields

$$\begin{aligned}
\frac{1}{dI} \sum_{i=1}^I \sum_{k=1}^{d^2} \left| \text{Tr} [W_k \mathcal{D}(P_i)] \right|^2 &= \frac{1}{dI} \sum_{i=1}^I \sum_{k=1}^{d^2} \left| \sum_{n,m=1}^d \langle \phi_m^{(i)} | W_k \lambda_n^{(i)} |\phi_n^{(i)}\rangle \langle \phi_n^{(i)} | \phi_m^{(i)} \rangle \right|^2 \\
&= \frac{1}{dI} \sum_{i=1}^I \sum_{k=1}^{d^2} \left| \sum_{n=1}^d \langle \phi_n^{(i)} | W_k \lambda_n^{(i)} |\phi_n^{(i)}\rangle \right|^2 \\
&\leq \frac{1}{dI} \sum_{i=1}^I \sum_{n=1}^d \left( \lambda_n^{(i)} \right)^2 \sum_{k=1}^{d^2} \left| \langle \phi_n^{(i)} | W_k |\phi_n^{(i)}\rangle \right|^2.
\end{aligned}$$

Using Eq. (A.68) from Appendix A.8 with  $|\Phi\rangle = |\phi_n^{(i)}\rangle$  and  $\text{Tr} [\rho_i^2] = \sum_{n=1}^d (\lambda_n^{(i)})^2 \leq 1$ , we obtain

$$\frac{1}{dI} \sum_{i=1}^I \sum_{k=1}^{d^2} \left| \text{Tr} [W_k \mathcal{D}(P_i)] \right|^2 \leq \frac{1}{I} \sum_{i=1}^I \sum_{n=1}^d \left( \lambda_n^{(i)} \right)^2 \leq \frac{1}{d} \sum_{i=1}^I 1 = 1. \tag{A.72}$$

Hence  $\text{Var}(X_l)$  is the difference between two numbers in the interval  $[0, 1]$  and therefore  $\leq 1$ .

## B Optimal Measurement Bases for MC Certification

Before we begin with the construction of optimal measurement basis sets for a qubit Hilbert space, we will first introduce two lemmas.

**Lemma B.1.** *Let  $p \in \mathbb{N}$  be prime. The only solution of*

$$\sum_{s=0}^{p-1} c_s e^{i \frac{2\pi s}{p}} = 0 \quad (\text{B.1})$$

for  $c_s \in \mathbb{N}_0$  under the additional constraint  $\sum_{s=0}^{p-1} c_s = p$  is  $c_s = 1$  for all  $s$ .

*Proof.* We use the fact that  $e^{i \frac{2\pi s}{p}}$  is a  $p$ -th root of unity for all  $s$  and then apply a theorem of Ref. [223] about sums over roots of unity. Abbreviating  $e^{i \frac{2\pi}{p}} = \omega$ , Eq. (B.1) becomes

$$\sum_{s=0}^{p-1} c_s \omega^s = 0. \quad (\text{B.2})$$

Since all  $c_s$  are non-negative integers, this can be rewritten as

$$\sum_{t=0}^{p-1} \Omega_t = 0, \quad (\text{B.3})$$

where  $\Omega_t$  is a  $p$ -th root of unity. We absorbed the integer values of  $c_s$  into the  $\Omega_t$  by allowing for repetitions in the sum. So for example if a  $c_s$  was greater than one, there would be multiple indices  $t$  in Eq. (B.3) with  $\Omega_t = \omega^s$ . Furthermore, some  $c_s$  could be zero which means that the corresponding root of unity  $\omega^s$  does not appear in the set of  $\Omega_t$ . Note furthermore that since we know that the  $c_s$  sum up to  $p$ , the sum in Eq. (B.3) indeed has  $p - 1$  elements.

Consider now the general situation of sums over  $p$ -th roots of unity with an arbitrary number of summands,  $n$ . As in Eq. (B.3), the same root of unity may appear multiple times. Lam and Leung showed [223] that if  $p$  is prime, such a sum can only be equal to zero if  $n$  is equal to a multiple of  $p$ . As a consequence there exists no proper subsum of the sum in Eq. (B.3) that goes to zero by itself. This property is called minimal. Moreover, Corollary 3.4. from Ref. [223] implies that for  $p$  prime the only minimal vanishing sum of  $p$  roots of unity, including repetitions, is given by

$$\sum_{t=0}^{p-1} \omega^t = e^{i \frac{2\pi t}{p}} = 0. \quad (\text{B.4})$$

This translates into the sum in Eq. (B.3) having no repetitions and every root of unity appears exactly once. Consequently,  $c_s = 1$  in for all  $s$  in Eq. (B.1) and the statement is proven.  $\square$

**Lemma B.2.** *The  $p \times p$  matrices given by the matrix elements*

$$(U^b)_{ik} = \delta_{k, (i-1) \cdot b \oplus 1}, \quad (\text{B.5})$$

for  $b = 2, \dots, p - 1$  with  $\oplus$  denoting modulo  $p$  addition, are unitary and contain on each (secondary)

*diagonal only one entry equal to one.*

*Proof.* For simplicity we use normal addition symbols but all algebraic manipulations are to be understood modulo  $p$ . We first note that each (secondary) diagonal contains only one entry equal to one with all others being zero. Consider a fixed  $b$  and a fixed diagonal  $t$ . An element on this (secondary) diagonal,  $(U^b)_{i,i+t}$  with  $i = 1, \dots, p$ , is non-zero according to Eq. (B.5) if and only if  $\delta_{i+t,(i-1) \cdot b+1} = 1$ . To prove that, given  $b$  and  $t$ , there is exactly one  $i$  for which this can happen, we consider the solutions of the equation

$$(i-1) \cdot (b-1) = t, \quad (\text{B.6})$$

which follows directly from  $(i-1) \cdot b + 1 = i + t$ . If we keep  $b$  fixed, showing that for each  $t$  there is one  $i$  for which Eq. (B.6) is fulfilled is equivalent to showing that for each  $i$  there is exactly one  $t$  for which Eq. (B.6) is fulfilled, i.e.  $t(i)$  is bijective. Then in each row a different diagonal acquires the value 1. Since the map  $t(i)$  maps the finite set  $\{1, \dots, p\}$  onto itself, injectivity implies surjectivity. Hence we only need to prove that  $t(i)$  is injective.

To do this, we need to find out how many solutions  $i$  are allowed for Eq. (B.6) with  $t \in \{0, \dots, p-1\}$ . At least one solution to Eq. (B.6) must exist since by construction of  $U_b$ , there is one entry equal to 1 on each row. According to the rules of modulo algebra, if one solution exists, then there are  $g$  solutions with  $g = \gcd(b-1, p)$  where  $\gcd$  denoting the greatest common divisor. Since  $b < p$  and  $p$  is a prime number,  $g = 1$  and there exists only one solution. This proves injectivity of  $t(i)$ . Therefore the map  $t(i)$  is bijective and so is  $i(t)$  which implies that the construction of  $U_b$ , Eq. (B.5), indeed fulfils the condition of exactly one entry equal to 1 on each (secondary) diagonal.

Next we show unitarity of  $U_b$ . By construction, there exists exactly one entry equal to 1 in each row. It remains to be shown that in each column there exists also only one entry equal to 1. Unitarity of  $U_b$  then follows immediately.

Let us consider for fixed  $b$  a column  $k$ . According to Eq. (B.5), an entry in the  $i$ -th row is non-zero if and only if  $\delta_{k,(i-1) \cdot b+1} = 1$ . To show that for fixed  $b$  and  $k$  there is exactly one  $i$  for which this can happen, we consider the solutions of the equation

$$(i-1) \cdot b + 1 = k. \quad (\text{B.7})$$

Eq. (B.7) defines a map  $k(i)$ . Showing that  $k(i)$  is bijective implies that for each  $k$  there exists only one  $i$  as a solution and vice versa, i.e. for each column there is only one row with an entry equal to 1. Employing the same argument as above, there exist  $g$  solutions to Eq. (B.7) with  $g = \gcd(b, p)$  and, since  $b < p$  and  $p$  is prime,  $g = 1$  and there exists only one solution. As a consequence the map  $k(i)$  is bijective and so is the map  $i(k)$ , i.e. the  $U_b$  constructed according to Eq. (B.5) are indeed unitary.  $\square$

We can now turn to constructing optimal measurement basis sets for qubit Hilbert spaces, i.e. Hilbert spaces of dimension  $p$  with  $p$  prime. Correspondingly, we define the set of efficiently characterisable unitaries  $\mathcal{U}_{\mathcal{M}}$  by the property that for all  $U \in \mathcal{U}_{\mathcal{M}}$  and  $M_i \in \mathcal{M}$  there exists a  $M_j \in \mathcal{M}$  such that  $UM_iU^\dagger = e^{i\phi_i}M_j$  with  $\phi_i \in \mathbb{R}$  some phase. This property guarantees a relevance distribution for the Monte Carlo sampling with  $p^2$  non-vanishing entries which is the minimal amount [75]. Furthermore, these entries all have equal magnitude.

We define an operator basis set  $\mathcal{M}$  to be optimal,  $\mathcal{M}^*$ , if  $|\mathcal{U}_{\mathcal{M}}| = u_{max}$  where  $u_{max} = \max_{\mathcal{M}'} |\mathcal{U}_{\mathcal{M}'}|$  and  $|\cdot|$  denotes the cardinality of a set. That is to say that an operator basis  $\mathcal{M}$  is optimal if the number of unitaries that map the basis onto itself is maximal amongst all possible operator bases. The map here is to be understood as the conjugation  $U : M \mapsto U M U^\dagger$ .

## B.1 Spectrum of the Basis Operators

Completeness of the operator basis implies that the set  $\mathcal{M}$  contains  $p^2$  elements. We include the identity in  $\mathcal{M}$  since  $\mathbb{1}_p$  is mapped onto itself by all unitaries. This provides a good starting point for the construction of  $\mathcal{M}^*$  which requires all  $M_i$  to be mapped to some  $M_j \in \mathcal{M}^*$  by as many unitaries as possible. We can thus restrict the following discussion to the  $d^2 - 1$  traceless operators in  $\mathcal{M}$ . Tracelessness of the remaining operators  $M_1, M_2, \dots, M_{p^2-1}$  in  $\mathcal{M}$  follows from their orthogonality to the identity. We denote this set by  $\tilde{\mathcal{M}}$ , i.e.  $\tilde{\mathcal{M}} = \mathcal{M} \setminus \mathbb{1}_p$ .

By assumption,  $M_1 \in \tilde{\mathcal{M}}$  is mapped to some  $M_j \in \tilde{\mathcal{M}}$  for any unitary  $U \in \mathcal{U}_{\mathcal{M}}$ , i.e.  $U M_1 U^\dagger = e^{i\phi_1} M_j$  with  $\phi_1$  a phase.  $M_j$  can either be  $M_1$  itself, and we speak of a cycle of degree 1, or some other element of  $\tilde{\mathcal{M}}$ . In the latter case, we take  $j = 2$  without loss of generality. Applying the map to  $M_2$ ,  $U M_2 U^\dagger = U U M_1 U^\dagger U^\dagger = U^2 M_1 (U^\dagger)^2$  yields either a result proportional to  $M_1$ , in which case we have a cycle of degree 2, or a result proportional to another  $M_j$  for which we can set  $j = 3$ . Note that the outcome of  $U M_2 U^\dagger$  cannot be  $M_2$  if  $M_2 = U M_1 U^\dagger$  due to the bijectivity of rotations. The cycle will necessarily be closed after a number of repeated applications of the map since this always leads to an element of  $\tilde{\mathcal{M}}$ , and there are only  $p^2 - 1$  elements in  $\tilde{\mathcal{M}}$ . We define the cycle to be of degree  $n$  on the set  $\tilde{\mathcal{M}}$  if  $U^n M_1 (U^\dagger)^n = e^{i\phi_n} M_1$  with  $n \leq p^2 - 1$  and  $\phi_n$  a phase.

An iterative argument shows that every operator  $M$  in the set  $\tilde{\mathcal{M}}$  is contained in at least one cycle. To see this, choose the lowest  $i$  such that  $M_i$  is not contained in a previously considered cycle and apply  $U$  repeatedly on  $M_i$  until  $U^n M_i (U^\dagger)^n = e^{i\phi_n} M_i$ . This procedure can be repeated until the complete set  $\tilde{\mathcal{M}}$  is exhausted. In fact, for a specific  $U \in \mathcal{U}_{\mathcal{M}}$ , every operator  $M \in \tilde{\mathcal{M}}$  appears exactly once in all the cycles generated by this  $U$ . As a consequence, the sum over the degrees of all cycles generated by  $U$  needs to be  $p^2 - 1$ . This can be seen follows: Since rotations are bijective,  $U : M_i \mapsto U M_i U^\dagger = e^{i\phi_i} M_j$  induces a mapping between the integers  $i$  and  $j$  which is also bijective. Therefore each  $i$  can also only occur in one cycle. The degree of a cycle measures how many indices  $i$  are present in this cycle. Since the total number of indices is  $p^2 - 1$ , summing over the degrees of all cycles must amount to  $p^2 - 1$ . The two extreme cases are that there are  $p^2 - 1$  cycles of degree 1 (e.g. when  $U$  is the identity) or that there is one cycle of degree  $p^2 - 1$ .

For the operator basis to be optimal, the unitary mappings on  $\tilde{\mathcal{M}}$  should allow for arbitrary cycle structures, i.e. cycles of degree 1, a single cycle of degree  $p^2 - 1$ , and anything in between. This guarantees that the number of unitaries in  $\mathcal{U}_{\mathcal{M}}$  is not limited by the cycle structure. While we do not prove this to be a strict requirement on the optimal set, it represents a very reasonable assumption in terms of avoiding unnecessary restrictions on the unitaries that map the operator basis onto itself. Specifically, for a cycle of degree  $p^2 - 1$  to exist, all operators in the set  $\tilde{\mathcal{M}}$  must have the same spectrum<sup>73</sup>. This is due to all elements in this cycle emerging from one another by unitary transformation which leaves the spectrum invariant. The requirement of an identical spectrum for

<sup>73</sup>There is always the freedom of a global phase on the spectrum of each measurement operator. It does not influence the relevance distribution and thus does not affect the property of efficient characterisability in any Monte Carlo protocol. For this reason we set the global phase to zero. Our term “the same spectrum” therefore corresponds to, strictly speaking, “the same spectrum up to a global phase”.

all  $M_i \in \tilde{\mathcal{M}}^*$  automatically also allows for the existence of cycles of all other degrees. We denote the spectrum of the operators in the set  $\tilde{\mathcal{M}}$  by  $\text{spec}(\tilde{\mathcal{M}})$ .

The condition of an identical spectrum together with the property that the operator basis is mapped onto itself by  $U \in \mathcal{U}_{\mathcal{M}}$  implies that the eigenvalues must form a closed cycle: From  $UM_iU^\dagger = e^{i\phi_i}M_j$  it follows that the spectrum needs to obey the condition  $e^{i\phi_i}\text{spec}(M_j) = \text{spec}(M_j)$ , i.e. if  $\lambda \in \text{spec}(\tilde{\mathcal{M}}^*)$  then  $e^{i\phi_i}\lambda \in \text{spec}(\tilde{\mathcal{M}}^*)$ . Multiplication by a complex number  $e^{i\phi_i}$  corresponds to rotating the eigenvalue by an angle  $\phi_i$  in the complex plane. Unless  $\phi_i$  is a multiple of  $2\pi$ , a new eigenvalue  $\mu = e^{i\phi_i}\lambda$  is obtained. Each application of  $U$  thus rotates an eigenvalue onto the next one until the cycle is closed. The degree of the cycle on the eigenvalues can be at most  $p$  since the operators in  $\tilde{\mathcal{M}}$  can at most have  $p$  distinct eigenvalues. Similarly to asking above for the existence of operator cycles of all degrees, asking for the longest eigenvalue cycle ensures that the number of unitaries in  $\mathcal{U}_{\mathcal{M}}$  is not unnecessarily restricted. This implies  $(e^{i\phi_i})^p = 1$ , i.e. the smallest possible rotation angle between two distinct eigenvalues is  $\phi_i = \frac{2\pi}{p}$ . As a consequence the spectrum in polar representation  $\lambda_i = r_i e^{i\phi_i}$  needs to fulfil  $r_i = r = \text{const.}$  and  $\phi_i = \frac{2\pi k}{p} + \phi_0$  with  $\phi_0$  arbitrary such that any rotation by  $\frac{2\pi}{p}$  leaves the spectrum invariant. The normalisation condition on the operator basis  $\mathcal{M}$  yields  $r = 1$ . Since a global phase on the spectrum is physically irrelevant we can choose  $\phi_0 = 0$ . To summarise, for an operator basis  $\mathcal{M}$  not to restrict the number of unitaries that map  $\mathcal{M}$  onto itself, the spectrum is identical for all  $M \in \mathcal{M} \setminus \mathbb{1}_p$  and  $p$ -nary, i.e. it consists of the  $p$ -th roots of unity,

$$\text{spec}(\mathcal{M}^*) = \left\{ \lambda_k = e^{i\frac{2\pi k}{p}} \mid k = 0, \dots, p-1 \right\}. \quad (\text{B.8})$$

In particular, this requires all measurement operators in  $\mathcal{M}$  to be unitary. As can be seen from Eq. (B.8), the operators in  $\mathcal{M}^*$  cannot be unitary and Hermitian at the same time for  $p > 2$ .

## B.2 Eigenbases of the Basis Operators

In the previous section, we have used the transformation of the operators  $M \in \mathcal{M}$  under a special class of rotations together with the requirement not to restrict the number of unitaries in this class to derive the spectral properties of the operator basis. We can now use orthogonality of the operator basis,

$$\text{Tr} \left[ M_a M_b^\dagger \right] = \delta_{ab} \quad \forall M_a, M_b \in \mathcal{M}, \quad (\text{B.9})$$

to obtain information about the eigenbases of the operators in  $\mathcal{M}^{74}$ . Since any orthogonal basis of the underlying Hilbert space is an eigenbasis of the identity, i.e. the eigenbasis of  $\mathbb{1}_p$  is undetermined, we only consider the  $p^2 - 1$  traceless operators in  $\tilde{\mathcal{M}} = \mathcal{M} \setminus \mathbb{1}_p$ .

We order the eigensystem according to the complex phase in the spectrum, Eq. (B.8), i.e.  $\lambda_k = e^{i\frac{2\pi k}{p}}$  for  $k = 0, \dots, p-1$  and consider two distinct arbitrary measurement operators  $M_a$  and  $M_b$ ,  $a \neq b$ , with corresponding eigenbases  $\{|\psi_k^a\rangle\}_{k=1, \dots, p}$  and  $\{|\psi_k^b\rangle\}_{k=1, \dots, p}$ . Employing a spectral decomposition,  $M_a = \sum_k \lambda_k |\psi_k^a\rangle \langle \psi_k^a|$ , and expanding the trace in Eq. (B.9) in the eigenbasis of  $M_a$ , we obtain

$$\text{Tr} \left[ M_a M_b^\dagger \right] = \sum_{klm} \lambda_k \lambda_l^* \langle \psi_m^a | \psi_k^a \rangle \langle \psi_k^a | \psi_l^b \rangle \langle \psi_l^b | \psi_m^a \rangle = \sum_{kl} \lambda_k \lambda_l^* |\langle \psi_k^a | \psi_l^b \rangle|^2 = 0.$$

<sup>74</sup> To be precise, the two properties that we have not yet exploited are orthogonality and completeness. However, completeness immediately follows from orthogonality and the fact that  $\mathcal{M}$  contains (by definition)  $p^2$  elements.

Inserting the ordered eigenvalues yields for the trace

$$\begin{aligned} \text{Tr} \left[ M_a M_b^\dagger \right] &= \sum_{kl} e^{i\frac{2\pi k}{p}} e^{-i\frac{2\pi l}{p}} |\langle \psi_k^a | \psi_l^b \rangle|^2 = \sum_{kl} e^{i\frac{2\pi(k-l)}{p}} |\langle \psi_k^a | \psi_l^b \rangle|^2 \\ &= \sum_s e^{i\frac{2\pi s}{p}} \sum_k |\langle \psi_{k\oplus s}^a | \psi_k^b \rangle|^2, \end{aligned} \quad (\text{B.10})$$

where in the last step we have shifted the index  $s$  to run from 0 to  $p-1$  and  $\oplus$  denotes addition modulo  $d$  corresponding to the group  $Z_p$  on the eigenbasis indices. Equation (B.10) can be interpreted as a change of basis between the eigenbases of  $M_a$  and  $M_b$ ,

$$U^{ab} = \sum_k |\psi_k^b\rangle \langle \psi_k^a|, \quad (\text{B.11})$$

together with a right-shift by  $s$  in the eigenbasis of  $M_a$ ,

$$S^a(s) = \sum_k |\psi_{k\oplus s}^a\rangle \langle \psi_k^a|. \quad (\text{B.12})$$

With the definitions of Eq. (B.12), we can rewrite the orthogonality condition as

$$\text{Tr} \left[ M_a M_b^\dagger \right] = \sum_s e^{i\frac{2\pi s}{p}} \sum_k |\langle \psi_k^a | S^a(s) U^{ab} | \psi_k^a \rangle|^2 = 0. \quad (\text{B.13})$$

To derive from Eq. (B.13) requirements that the operator eigenbases of operators in the optimal set  $\mathcal{M}^*$  must meet, we first assume  $M_a$  and  $M_b$  to commute and analyse the case of non-commuting operators afterwards.

We first show that a change of basis  $U^{ab}$  between the eigenbases of two measurement operators which commute,  $[M_a, M_b] = 0$ , is a permutation. Next, we derive, from the spectral properties obtained in the previous section, the structure of the matrix  $U^{ab}$ . The corresponding constraints allow for the existence of only  $p-2$  such permutation operators. This implies that there are  $p$  orthogonal, pairwise commuting measurement operators with their spectrum given by Eq. (B.8), namely  $M_a$  plus the  $p-2$  operators obtained by applying  $U^{ab}$  to  $M_a$  plus identity.

Due to the spectral condition, Eq. (B.8), all operators in  $\tilde{\mathcal{M}}$  are non-degenerate. This together with the assumption of commutativity implies that for each index  $k$  enumerating the eigenbasis of  $M_a$  there exists an index  $l$  enumerating the eigenbasis of  $M_b$  such that  $|\psi_k^a\rangle = |\psi_l^b\rangle$  and the mapping between  $k$  and  $l$  is bijective. That is to say that the eigenbases of  $M_a$  and  $M_b$  are the same up to reordering which means that certain eigenvectors can correspond to different eigenvalues. In this case, the change of basis  $U^{ab}$  between the eigenbases of  $M_a$  and  $M_b$ , defined by Eq. (B.11), is a permutation operator.

In the eigenbasis of  $M_a$ , the matrix elements of  $U^{ab}$  are either zero or one and the total number of one's is  $p$ .  $S^a(s)$  is also a permutation operator which shifts the columns of  $U^{ab}$  in this representation by  $s$  to the right. This means that for all  $s$ , the sum over  $k$  in Eq. (B.13) is a non-negative integer,

$$\sum_k |\langle \psi_k^a | S^a(s) U^{ab} | \psi_k^a \rangle|^2 = c_s. \quad (\text{B.14})$$

Since  $U^{ab}$  and  $S^a(s)$  are both permutation operators, so is their product,  $P^{ab}(s) = S^a(s)U^{ab}$ . Note that  $S^a(s=0) = \mathbb{1}_p$ , and  $c_0$  is given by the sum over the diagonal elements squared of  $U^{ab}$ . For  $s = 1$ , all columns of  $U^{ab}$  are shifted to the right by one, i.e. the first upper diagonal of  $U^{ab}$  becomes the diagonal of  $P^{ab}$ , and the sum over its elements squared yields  $c_1$ . In other words, each  $c_s$  corresponds to the sum over the diagonal of  $P^{ab}(s)$ , that is the  $s$ -th secondary diagonal of  $U^{ab}$ , and thus takes a value between 0 and  $p$ . Due to orthogonality of the operator basis, Eq. (B.13), the set of integers  $\{c_s\}_{s=0,\dots,p-1}$  has to fulfil the condition

$$\sum_{s=0}^{p-1} c_s e^{i \frac{2\pi s}{p}} = 0. \quad (\text{B.15})$$

Note that,  $\sum_{s=0}^{p-1} c_s = p$  since summing over all  $c_s$  corresponds to summing over all elements squared of  $P^{ab}(s)$ , or  $U^{ab}$ . According to Lemma B.1 for  $p$  prime no linear combination with non-negative integers  $c_s$  can exist that makes the sum go to zero except if  $c_s = 1$  for all  $s$ .

Since  $c_s$  corresponds to the sum over the  $s$ -th secondary diagonal of  $U^{ab}$ , we have thus restricted all possible matrices  $U^{ab}$  for a change of basis between the eigenbases of commuting measurement operators  $M_a, M_b \in \tilde{\mathcal{M}}$  to those that contain exactly one entry equal to one on each (secondary) diagonal with all other entries being zero. In addition, each row and each column of  $U^{ab}$  also contains exactly one entry equal to one with all other entries being zero since  $U^{ab}$  is a permutation operator.

We now show that under these constraints there exist  $p - 2$  distinct permutation operators  $U^{ab}$ , demonstrating first how one can construct  $p - 2$  such unitaries and then proving in a second step that these are indeed all unitaries that fulfil the given constraints. In order to construct the  $p - 2$  matrices  $U^{ab}$  for a change of basis, we reorder the eigenbases of  $M_a$  and  $M_b$  such that the main diagonal always contains one as its first entry for all  $b$ :  $(U^{ab})_{11} = 1$ ,  $(U^{ab})_{ii} = 0$  for  $i = 2, \dots, p$ . This reordering does not interfere with ordering the eigenbases of  $M_a$  and  $M_b$  in terms of the eigenvalues, Eq. (B.8), since  $M_a$  and  $M_b$  can be multiplied by  $e^{i \frac{2\pi t}{p}}$  for some  $t$  without changing the orthogonality condition. This multiplication performs exactly the shift in the eigenbases required to ensure  $(U^{ab})_{11} = 1$  for all  $b$ . In other words: The ordering of the eigenvalues determines the indexing of the eigenbasis of  $M_b$  while now in addition the global phase of  $M_b$  is fixed. Then, for  $p$  prime, a set of  $p - 2$  permutation operators that have on each of their diagonals exactly one entry equal to one with all others being zero and  $(U^{ab})_{11} = 1$  is given by

$$(U^{ab})_{ik} = \delta_{k, (i-1) \cdot b \oplus 1} \quad \text{with} \quad b = 2, \dots, p - 1. \quad (\text{B.16})$$

The construction that leads to Eq. (B.16) proceeds as follows: The first row is given by the assumption  $(U^{ab})_{11} = 1$  for all  $b$ . In the second row,  $(U^{ab})_{21}$  and  $(U^{ab})_{22}$  need to be zero due to the constraints of each column and the main diagonal containing exactly one entry equal to one. The smallest  $j$  for which  $(U^{ab})_{2j}$  can be non-zero is thus  $j = 3$ . Analogously, in the third row, the smallest entry that can be non-zero is  $j = 5$  (with  $j = 4$  being excluded by the condition on the first upper diagonal). This construction is similar to the movement of a knight on a chess board: one step down, two steps to the right. It is continued until the last row is reached to yield the first  $U^{ab}$  (with  $b$  set to 2). The second  $U^{ab}$  is obtained by choosing  $j = 4$  in the construction of the second row. This implies a modified movement of the knight with one step down,  $b = 3$  steps to the right. Once the right

boundary on the matrix is reached, the movement is simply continued by counting from the left, as implied by the modulo algebra in Eq. (B.16). For a  $p \times p$  matrix  $U^{ab}$ , there are  $p - 2$  distinct knight-type movements since in the construction of the second row,  $(U^{ab})_{21}$  and  $(U^{ab})_{22}$  are always fixed and one can choose at most  $j = p$ , i.e. move at most  $p - 1$  steps to the right. According to Lemma B.2, for  $p$  prime, the construction rule, Eq. (B.16), yields proper unitary permutation operators which have on each (secondary) diagonal only one entry equal to one. This holds only for prime  $d = p$ . For non-prime  $d$ , the above construction leads to a contradiction to the unitarity constraint of each column having exactly one entry equal to one with all others being zero.

When applied to  $M_a$ , the  $U^{ab}$  constructed according to Eq. (B.16) yield  $p - 2$  operators  $M_b$  that are orthogonal to  $M_a$ . We now show that Eq. (B.16) represents all the unitaries that fulfil the constraint of having exactly one entry equal to one on each (secondary) diagonal, i.e. there are exactly  $p$  commuting measurement operators (including identity). As a side result, we obtain that all  $M_b$  obtained from applying the  $U^{ab}$  to  $M_a$  are not only orthogonal to  $M_a$  but also to each other.

The fact that, for  $p$  prime, all permutation operators, that have on each of their diagonals exactly one entry equal to one with all other entries being zero and  $(U^{ab})_{11} = 1$ , are given by Eq. (B.16) and that there are thus  $p - 2$  such unitaries can be seen as follows: Since  $U^{ab}$  maps the eigenvectors of  $M_a$  onto the eigenvectors of  $M_b$ , it also corresponds to a mapping between the eigenvalues  $\lambda_k^a$  and  $\lambda_{k'}^b$ . The fact that we fixed  $(U^{ab})_{11} = 1$  together with Eq. (B.8) implies  $\lambda_0^a = \lambda_0^b = 1$ . The other eigenvalues are redistributed according to  $\lambda_k^b = e^{i\frac{2\pi}{p} \cdot k} \mapsto \lambda_{kb}^a = e^{i\frac{2\pi}{p} \cdot kb}$  where the product  $kb$  is to be understood modulo  $p$ . Since the eigenvalue  $\lambda_{kb}^a$  shows up in the spectral decomposition of the  $b$ -th power of  $M_a$ ,

$$(M_a)^b = \left( \sum_k e^{i\frac{2\pi}{p} k} |\psi_k^a\rangle \langle \psi_k^a| \right)^b = \sum_k e^{i\frac{2\pi}{p} kb} |\psi_k^a\rangle \langle \psi_k^a|, \quad (\text{B.17})$$

we find

$$M_b = (M_a)^b \quad \text{with} \quad b = 2, \dots, p - 1. \quad (\text{B.18})$$

Moreover,  $(M_a)^p = \mathbb{1}_p$  since  $kp = 1$  when interpreted modulo  $p$  for all  $k$ . Then all powers of  $M_a$  are orthonormal since, for all  $b$ ,

$$\text{Tr} \left[ M_a (M_a^\dagger)^b \right] = \text{Tr} \left[ M_a M_a^\dagger (M_a^\dagger)^{b-1} \right] = \text{Tr} \left[ (M_a^\dagger)^{b-1} \right] = \begin{cases} 1, & \text{if } b \bmod p = 1 \\ 0, & \text{otherwise} \end{cases}. \quad (\text{B.19})$$

The last step follows from the fact that  $M_a^{b-1}$  has the same spectrum as  $M_a$  and is consequently traceless, unless  $b - 1 = p$  where we obtain identity. This is evident from Eq. (B.17). Adjungation of the operator just returns the complex conjugated result for the trace. Since this result is real in either case, it is unaffected by adjungation. Finally, the maximal number of commuting, pairwise orthogonal unitaries  $M_a$  defined on a  $p$ -dimensional Hilbert space is  $p$ . This can be seen by considering their common eigenbasis  $\{|\psi_k\rangle\}_{k=1, \dots, p}$ . Any linear combination of the commuting, pairwise orthogonal unitaries  $M_a$  also has this eigenbasis. We can thus employ the common eigenbasis to construct a representation of any operator  $M$  with this eigenbasis,  $M = \sum_{k=0}^{p-1} \lambda_k |\psi_k\rangle \langle \psi_k|$ . This is a linear combination of  $p$  orthonormal operators  $|\psi_k\rangle \langle \psi_k|$  with coefficients corresponding to the eigenvalues of  $M$ . Consequently, no orthonormal basis of the space of operators with common eigenbasis to  $M_a$  can have more than  $p$  elements and as such the maximal number of commuting, pairwise orthogonal

unitaries  $M_a$  is  $p$ .

As a corollary, we obtain that the set  $\tilde{\mathcal{M}}_a = \{(M_a)^b\}_{b=1,\dots,p-1}$  with the spectrum of all elements given by Eq. (B.8) together with the identity forms an Abelian group of pairwise orthonormal operators with matrix multiplication as group operation.  $\tilde{\mathcal{M}}_a$  contains all the unitaries that share an eigenbasis with  $M_a$  while having the same spectrum as  $M_a$  and being pairwise orthogonal.

After constructing  $p$  commuting measurement operators from the spectral conditions and orthogonality, we now identify the remaining  $p^2 - p$  measurement operators that are required to complete the optimal operator basis. Since we have also shown above that there are only  $p$  commuting measurement operators, the remaining ones are necessarily non-commuting.

The complete set of measurement operators  $\tilde{\mathcal{M}}$  is obtained iteratively: That is, one chooses a starting point, i.e. an operator  $M_a$  with spectrum according to Eq. (B.8).  $M_a$  defines the commuting set  $\tilde{\mathcal{M}}_a$  with all operators in  $\tilde{\mathcal{M}}_a$  given by Eq. (B.18). Next one needs to find another matrix  $M_{a'}$  with the same spectrum, Eq. (B.8), but orthogonal to all  $M_a \in \tilde{\mathcal{M}}_a$ . By construction,  $M_{a'}$  does not share an eigenbasis with the  $M_a \in \tilde{\mathcal{M}}_a$ . Rather, it defines, according to Eq. (B.18), its own set of commuting operators,  $\tilde{\mathcal{M}}_{a'}$  which, together with the identity, forms another Abelian group. A constructive method to determine  $M_{a'}$  is obtained by exploiting mutual unbiasedness of the eigenbases of the sets  $\tilde{\mathcal{M}}_a$  for different  $a$ , as we show below. The step of identifying  $M_{a'}$  and its commuting set needs to be repeated until  $p + 1$  Abelian groups  $\tilde{\mathcal{M}}_a \cup \mathbb{1}_p$  have been found. The procedure of identifying  $p + 1$  sets of  $p$  commuting, pairwise orthogonal measurement operators yields, without double-counting the identity which is an element of all the Abelian groups,  $p^2$  orthogonal measurement operators, i.e. the complete operator basis  $\mathcal{M}$ .

Clearly, one cannot find more than  $p + 1$  Abelian groups of orthogonal operators since there exist only  $p^2$  orthogonal operators on a  $p$ -dimensional Hilbert space. Note that we know of the existence of at least one such set of Abelian groups – the generalised Pauli operator basis  $\mathcal{P}$  and its separation into mutually commuting subsets, cf. Sec. 4.3.

The existence of  $p + 1$  Abelian groups  $\tilde{\mathcal{M}}_a \cup \mathbb{1}_p$  of orthogonal measurement operators is in a one-to-one correspondence to the existence of  $p + 1$  mutually unbiased bases [84]. This is easily seen using the construction from above. The common eigenbasis of  $\tilde{\mathcal{M}}_a$ ,  $\{|\psi_k^a\rangle\}$ , can be used to construct an operator basis,

$$M_{au} = (M_a)^u = \sum_k e^{i\frac{2\pi}{p}uk} |\psi_k^a\rangle \langle \psi_k^a| .$$

Projectors can be defined in terms of the operator basis, that is,

$$P_n^a = |\psi_n^a\rangle \langle \psi_n^a| = \frac{1}{p} \sum_u e^{-i\frac{2\pi}{p}un} (M_a)^u .$$

Then,

$$|\langle \psi_n^a | \psi_{n'}^b \rangle|^2 = \text{Tr} \left[ P_n^a (P_{n'}^b)^\dagger \right] = \frac{1}{p^2} \sum_{uu'} e^{-i\frac{2\pi}{p}(un - u'n')} \text{Tr} \left[ M_{au} M_{bu'}^\dagger \right] .$$

If  $M_a$  and  $M_b$  are from different Abelian groups, only identity ( $u = u' = 0$ ) contributes due to orthogonality of all other measurement operators. In this case

$$|\langle \psi_n^a | \psi_{n'}^b \rangle|^2 = \frac{1}{p^2} \text{Tr} [\mathbb{1}_p] = \frac{1}{p} . \quad (\text{B.20})$$

If  $M_a$  and  $M_b$  are from the same set  $\tilde{\mathcal{M}}_a \cup \mathbb{1}_p$ , all  $u = u'$  contribute and as a result

$$|\langle \psi_n^a | \psi_{n'}^a \rangle|^2 = \frac{1}{p^2} \sum_u e^{-i\frac{2\pi}{p}u(n-n')} \text{Tr} [M_{au} M_{au}^\dagger] = \frac{1}{p} \sum_u e^{-i\frac{2\pi}{p}u(n-n')} = \delta_{nn'}.$$

### B.3 Optimal Measurement Bases and Efficiently Characterisable Unitaries

The findings from Secs. B.1 and B.2 allow us to construct the set of measurement operators as mentioned above. After identifying the first set  $\tilde{\mathcal{M}}_a$  of  $p$  commuting measurement operators by picking an  $M_a$  and employing Eq. (B.18), a new measurement operator  $M_{a'}$  is found by choosing its eigenvectors as a MUB with respect to the eigenbases of  $\tilde{\mathcal{M}}_a$  (in the subsequent steps of the iterative procedure, the eigenvectors have to be mutually unbiased with respect to all previously constructed sets). The eigenvectors of  $M_{a'}$  are assigned a spectrum analogously to Eq. (B.17), using Eq. (B.8). Thus  $M_{a'}$  and all of its powers form a commuting set with proper spectrum that is orthogonal to all matrices from  $\tilde{\mathcal{M}}_a$  (or, in the subsequent steps of the iterative procedure, to all previously constructed sets  $\tilde{\mathcal{M}}_a, \tilde{\mathcal{M}}_{a'}, \dots$ ). It is indeed possible to construct a complete basis of measurement operators with this method since the maximal number of  $p + 1$  MUB does exist for prime dimension  $p$ .

The identification of the eigenbases of the measurement operators with mutually unbiased bases allows us to determine which unitaries can be efficiently characterised with this operator basis. The candidate unitaries need to map any measurement operator onto another measurement operator from the set, modulo a phase corresponding to a  $p$ -th root of unity. Consider a specific measurement operator  $M$  from an optimal set  $\tilde{\mathcal{M}}^*$ .  $M$  is mapped by the candidate unitaries either to the same or to a different Abelian group in  $\tilde{\mathcal{M}}^*$ . Given the spectral decomposition of  $M$  in terms of its eigenbasis,  $\{|\psi_k^a\rangle\}$ , with eigenvalues  $\lambda_a$ , we can write

$$UMU^\dagger = \sum_a \lambda_a U |\psi_k^a\rangle \langle \psi_k^a| U^\dagger = \sum_a \lambda_a |U\psi_k^a\rangle \langle U\psi_k^a|, \quad (\text{B.21})$$

which must be equal to  $M'$  where  $M' \in \tilde{\mathcal{M}}^*$  by definition of  $U$ . Since the  $\{|\psi_k^a\rangle\}$  are orthonormal, so are the  $\{|U\psi_k^a\rangle\}$ ; hence they correspond to the eigenbasis of  $M'$ . Consequently, the set  $\{|U\psi_k^a\rangle\}$  must either be identical to the set  $\{|\psi_k^a\rangle\}$  modulo phase factors on the individual states or correspond to a basis which is mutually unbiased to  $\{|\psi_k^a\rangle\}$ . Therefore a unitary  $U$  is efficiently characterisable if and only if it keeps the partitioning of the  $p + 1$  mutually unbiased bases in a Hilbert space of prime dimension  $p$  intact.

## C Controllability for High-Frequency Amplitude Control on a Phase Qudit

In this section we will analyse the dynamical Lie algebra of the Hamiltonian

$$H = \sum_n \left[ \frac{1}{2} u_n |n\rangle \langle n-1| + \frac{1}{2} u_n^* |n-1\rangle \langle n| \right] \quad (\text{C.1})$$

for  $u_n$  purely imaginary, i.e. we want to find a basis of the Lie algebra spanned by the matrices

$$h_n = |n\rangle \langle n-1| - |n-1\rangle \langle n| \quad (\text{C.2})$$

and their commutators.

Since the notation would otherwise get very confusing in the following, we will keep the plus and minus signs inside kets, bras, and indices as a standard  $+$ , respectively  $-$ , while using the symbols  $\oplus$ , respectively  $\ominus$ , for the matrix operations between dyadic products.

We first calculate the commutators  $[h_m, h_n]$ ,

$$\begin{aligned} [h_n, h_m] &= |n\rangle \langle n-1| m\rangle \langle m-1| \ominus |n\rangle \langle n-1| m-1\rangle \langle m| \\ &\quad \ominus |n-1\rangle \langle n| m\rangle |m-1\rangle \oplus |n-1\rangle \langle n| m-1\rangle \langle m| \\ &\quad \ominus |m\rangle \langle m-1| n\rangle \langle n-1| \oplus |m\rangle \langle m-1| n-1\rangle \langle n| \\ &\quad \oplus |m-1\rangle \langle m| n\rangle \langle n-1| \ominus |m-1\rangle \langle m| n-1\rangle \langle n| \\ &= \delta_{n-1,m} |n\rangle \langle m-1| \ominus \delta_{n,m} |n\rangle \langle m| \ominus \delta_{n,m} |n-1\rangle \langle m-1| \oplus \delta_{n,m-1} |n-1\rangle \langle m| \\ &\quad \ominus \delta_{n,m-1} |m\rangle \langle n-1| \oplus \delta_{n,m} |m\rangle \langle n| \oplus \delta_{n,m} |m-1\rangle \langle n-1| \ominus \delta_{n-1,m} |m-1\rangle \langle n| \\ &= \delta_{n-1,m} (|n\rangle \langle m-1| \ominus |m-1\rangle \langle n|) \oplus \delta_{n,m-1} (|n-1\rangle \langle m| \ominus |m\rangle \langle n-1|) . \end{aligned}$$

Hence, the only nonvanishing commutators are of the form

$$[h_{n-1}, h_n] = |n-2\rangle \langle n| \oplus |n\rangle \langle n-2| \equiv h_n^{(2)} . \quad (\text{C.3})$$

Defining

$$h_n^{(j)} \equiv |n-j\rangle \langle n| \oplus |n\rangle \langle n-j| \quad (\text{C.4})$$

we can now calculate the remaining commutators,

$$\begin{aligned}
\left[ h_n^{(j)}, h_m^{(k)} \right] &= |n\rangle \langle n-j | m \rangle \langle m-k | \ominus |n\rangle \langle n-j | m-k \rangle \langle m| \\
&\quad \ominus |n-j\rangle \langle n | m \rangle |m-k\rangle \oplus |n-j\rangle \langle n | m-k \rangle \langle m| \\
&\quad \ominus |m\rangle \langle m-k | n \rangle \langle n-j | \oplus |m\rangle \langle m-k | n-j \rangle \langle n| \\
&\quad \oplus |m-k\rangle \langle m | n \rangle \langle n-j | \ominus |m-k\rangle \langle m | n-j \rangle \langle n| \\
&= \delta_{n-j,m} |n\rangle \langle m-j | \ominus \delta_{n-j,m-k} |n\rangle \langle m| \ominus \delta_{n,m} |n-j\rangle \langle m-k | \oplus \delta_{n,m-k} |n-j\rangle \langle m| \\
&\quad \ominus \delta_{n,m-k} |m\rangle \langle n-j | \oplus \delta_{n-j,m-k} |m\rangle \langle n| \oplus \delta_{n,m} |m-k\rangle \langle n-j | \ominus \delta_{n-j,m} |m-k\rangle \langle n| \\
&= \delta_{n-j,m} (|n\rangle \langle m-k | \ominus |m-k\rangle \langle n|) \oplus \delta_{n,m-k} (|n-j\rangle \langle m| \ominus |m\rangle \langle n-j |) \\
&\quad \ominus \delta_{n-j,m-k} (|n\rangle \langle m| \ominus |m\rangle \langle n|) \ominus \delta_{n,m} (|n-j\rangle \langle m-k | \ominus |m-k\rangle \langle n-j |) .
\end{aligned}$$

If  $n = m$  and  $j = k$ , then the commutator will vanish. Otherwise, since  $j \neq 0$ ,  $k \neq 0$  only at most one of the four summands will be non-zero. As a result, these commutators can be written in the form of a  $h_n^{(j)}$  for  $j \neq 0$ . The condition  $j \neq 0$  is due to the fact that any contribution that would lead to a  $|n\rangle \langle n|$  is immediately cancelled out with another term in the above expression. As a consequence, a basis of the Lie algebra is given by matrices of the form  $h_n^{(j)}$  in Eq. (C.4) for  $j \neq 0$ .



## References

- [1] A. Einstein and M. Born. *Albert Einstein Max Born, Briefwechsel 1916-1955* (Langen-Müller, 2005).
- [2] A. Einstein, B. Podolsky, and N. Rosen. *Can quantum-mechanical description of physical reality be considered complete?* Phys. Rev. **47**, 777 (1935).
- [3] J. S. Bell. *On the Einstein-Podolsky-Rosen paradox.* Physics **1**, 195 (1964).
- [4] A. Aspect, P. Grangier, and G. Roger. *Experimental realization of Einstein-Podolsky-Rosen-Bohm gedankenexperiment: A new violation of Bell's inequalities.* Phys. Rev. Lett. **49**, 91 (1982).
- [5] J. Yin, Y. Cao, H. L. Yong, J. G. Ren, H. Liang, S. K. Liao, F. Zhou, C. Liu, Y. P. Wu, G. S. Pan, L. Li, N. L. Liu, Q. Zhang, C. Z. Peng, and J. W. Pan. *Lower bound on the speed of nonlocal correlations without locality and measurement choice loopholes.* Phys. Rev. Lett. **110**, 260407 (2013).
- [6] M. A. Nielsen and I. L. Chuang. *Quantum Computation and Quantum Information* (Cambridge University Press, 2000).
- [7] A. I. Konnov and V. A. Krotov. *On global methods of successive improvement of controlled processes.* Aut. Remote Control **60**, 1428 (1999).
- [8] S. E. Sklarz and D. J. Tannor. *Loading a Bose-Einstein condensate onto an optical lattice: An application of optimal control theory to the nonlinear Schrödinger equation.* Phys. Rev. A **66**, 053619 (2002).
- [9] D. M. Reich, M. Ndong, and C. P. Koch. *Monotonically convergent optimization in quantum control using Krotov's method.* J. Chem. Phys. **136**, 104103 (2012).
- [10] T. F. Jordan, A. Shaji, and E. C. G. Sudarshan. *Dynamics of initially entangled open quantum systems.* Phys. Rev. A **70**, 052110 (2004).
- [11] H. A. Carteret, D. R. Terno, and K. Życzkowski. *Dynamics beyond completely positive maps: Some properties and applications.* Phys. Rev. A **77**, 042113 (2008).
- [12] M. D. Choi. *Completely positive linear maps on complex matrices.* Linear Algebra and its Applications **10**, 285 (1975).
- [13] J. de Pillis. *Linear transformations which preserve Hermitian and positive semidefinite operators.* Pacific Journal of Mathematics **23**, 129 (1967).
- [14] A. Jamiołkowski. *Linear transformations which preserve trace and positive semidefiniteness of operators.* Reports on Mathematical Physics **3**, 275 (1972).
- [15] J. M. Finn. *Classical Mechanics* (Jones & Bartlett Publishers, 2009).
- [16] N. D. Mermin. *Quantum mechanics vs local realism near the classical limit: A Bell inequality for spin  $s$ .* Phys. Rev. D **22**, 356 (1980).

- [17] J. W. Pan, D. Bouwmeester, M. Daniell, H. Weinfurter, and A. Zeilinger. *Experimental test of quantum nonlocality in three-photon greenberger-horne-zeilinger entanglement*. Nature **403**, 515 (2000).
- [18] W. Heisenberg. *The Physical Principles of the Quantum Theory* (Courier Dover Publications, 1949).
- [19] J. Cramer. *The transactional interpretation of quantum mechanics*. Rev. Mod. Phys. **58**, 647 (1986).
- [20] L. de Broglie. *La mécanique ondulatoire et la structure atomique de la matière et du rayonnement*. J. Phys. Radium **8**, 225 (1927).
- [21] D. Bohm. *A suggested interpretation of the quantum theory in terms of "hidden" variables. i*. Phys. Rev. **85**, 166 (1952).
- [22] D. Bohm. *A suggested interpretation of the quantum theory in terms of "hidden" variables. ii*. Phys. Rev. **85**, 180 (1952).
- [23] S. Weinberg. *Testing quantum mechanics*. Annals of Physics **194**, 336 (1989).
- [24] N. Gisin. *Weinberg's non-linear quantum mechanics and supraluminal communications*. Physics Letters A **143**, 1 (1990).
- [25] J. Polchinski. *Weinberg's nonlinear quantum mechanics and the Einstein-Podolsky-Rosen paradox*. Phys. Rev. Lett. **66**, 397 (1991).
- [26] D. S. Abrams and S. Lloyd. *Nonlinear quantum mechanics implies polynomial-time solution for NP-complete and #P problems*. Phys. Rev. Lett. **81**, 3992 (1998).
- [27] C. M. Caves, C. A. Fuchs, and R. Schack. *Unknown quantum states: The quantum de Finetti representation*. Journal of Mathematical Physics **43**, 4537 (2002).
- [28] D. Werner. *Funktionalanalysis* (Springer, 2007).
- [29] A. Grigorenko. *Geometry of projective Hilbert space*. Phys. Rev. A **46**, 7292 (1992).
- [30] G. Lüders. *Über die Zustandsänderung durch den Meßprozess*. Ann. Phys. **8**, 322 (1952).
- [31] W. Pauli. *Allgemeine Prinzipien der Wellenmechanik* (Springer, 1933). Volume XXIV, Part 1 of Handbuch der Physik.
- [32] J. V. Neumann. *Mathematical Foundations of Quantum Mechanics* (Princeton university press, 1955).
- [33] M. Brune, S. Haroche, J. M. Raimond, L. Davidovich, and N. Zagury. *Manipulation of photons in a cavity by dispersive atom-field coupling: Quantum-nondemolition measurements and generation of "Schrödinger cat" states*. Phys. Rev. A **45**, 5193 (1992).
- [34] L. Chirolli and G. Burkard. *Quantum nondemolition measurements of a qubit coupled to a harmonic oscillator*. Phys. Rev. B **80**, 184509 (2009).

- [35] A. Khrennikov. *Two versions of the projection postulate: From EPR argument to one-way quantum computing and teleportation*. Advances in Mathematical Physics (2010).
- [36] P. Busch, P. J. Lahti, and P. Mittelstaedt. *The quantum theory of measurement*. In: *The Quantum Theory of Measurement*, volume 2 of *Lecture Notes in Physics Monographs*, pp. 25–90 (Springer Berlin Heidelberg, 1996).
- [37] W. Nolting. *Grundkurs Theoretische Physik 5/1* (Springer, 2012).
- [38] H. P. Breuer and F. Petruccione. *The Theory of Open Quantum Systems* (Oxford University Press, Great Clarendon Street, 2002).
- [39] F. Töppel, A. Aiello, C. Marquardt, E. Giacobino, and G. Leuchs. *Classical entanglement in polarization metrology*. New J. Phys. **16**, 073019 (2014).
- [40] D. D'Alessandro. *Introduction to Quantum Control and Dynamics* (Chapman & Hall/CRC, 2007).
- [41] P. Pechukas. *Reduced dynamics need not be completely positive*. Phys. Rev. Lett. **73**, 1060 (1994).
- [42] Y. S. Weinstein, T. F. Havel, J. Emerson, N. Boulant, M. Saraceno, S. Lloyd, and D. G. Cory. *Quantum process tomography of the quantum Fourier transform*. The Journal of Chemical Physics **121**, 6117 (2004).
- [43] D. R. Terno. *Nonlinear operations in quantum-information theory*. Phys. Rev. A **59**, 3320 (1999).
- [44] M. Asorey, A. Kossakowski, G. Marmo, and E. C. G. Sudarshan. *Dynamical maps and density matrices*. Journal of Physics: Conference Series **196**, 012023 (2009).
- [45] W. F. Stinespring. *Positive functions on  $C^*$ -algebras*. Proceedings of the American Mathematical Society **6**, pp. 211 (1955).
- [46] K. Życzkowski and I. Bengtsson. *On duality between quantum maps and quantum states*. Open Systems & Information Dynamics **11**, 3 (2004).
- [47] T. F. Havel. *Robust procedures for converting among Lindblad, Kraus and matrix representations of quantum dynamical semigroups*. Journal of Mathematical Physics **44**, 534 (2003).
- [48] E. Andersson, J. D. Cresser, and M. J. W. Hall. *Finding the Kraus decomposition from a master equation and vice versa*. Journal of Modern Optics **54**, 1695 (2007).
- [49] M. Jiang, S. Luo, and S. Fu. *Channel-state duality*. Phys. Rev. A **87**, 022310 (2013).
- [50] W. Nolting. *Grundkurs Theoretische Physik 4* (Springer, 2005).
- [51] D. C. Marinescu. *Classical and Quantum Information* (Academic Press, 2011).
- [52] F. Hulpke, U. V. Poulsen, A. Sanpera, A. Sen(De), U. Sen, and M. Lewenstein. *Unitarity as preservation of entropy and entanglement in quantum systems*. Foundations of Physics **36**, 477 (2006).

- [53] D. M. Reich, G. Gualdi, and C. P. Koch. *Minimum number of input states required for quantum gate characterization*. Phys. Rev. A **88**, 042309 (2013).
- [54] A. Harrow, P. Hayden, and D. Leung. *Superdense coding of quantum states*. Phys. Rev. Lett. **92**, 187901 (2004).
- [55] P. Aliferis, D. Gottesman, and J. Preskill. *Quantum accuracy threshold for concatenated distance-3 codes*. Quant. Info. Comput. **6**, 97 (2006).
- [56] K. Vogel and H. Risken. *Determination of quasiprobability distributions in terms of probability distributions for the rotated quadrature phase*. Phys. Rev. A **40**, 2847 (1989).
- [57] I. L. Chuang and M. A. Nielsen. *Prescription for experimental determination of the dynamics of a quantum black box*. Journal of Modern Optics **44**, 2455 (1997).
- [58] J. F. Poyatos, J. I. Cirac, and P. Zoller. *Complete characterization of a quantum process: The two-bit quantum gate*. Phys. Rev. Lett. **78**, 390 (1997).
- [59] S. T. Flammia and Y. K. Liu. *Direct fidelity estimation from few Pauli measurements*. Phys. Rev. Lett. **106**, 230501 (2011).
- [60] M. P. da Silva, O. Landon-Cardinal, and D. Poulin. *Practical characterization of quantum devices without tomography*. Phys. Rev. Lett. **107**, 210404 (2011).
- [61] A. Shabani, R. L. Kosut, M. Mohseni, H. Rabitz, M. A. Broome, M. P. Almeida, A. Fedrizzi, and A. G. White. *Efficient measurement of quantum dynamics via compressive sensing*. Phys. Rev. Lett. **106**, 100401 (2011).
- [62] C. T. Schmiegelow, A. Bendersky, M. A. Larotonda, and J. P. Paz. *Selective and efficient quantum process tomography without ancilla*. Phys. Rev. Lett. **107**, 100502 (2011).
- [63] E. Magesan, J. M. Gambetta, and J. Emerson. *Scalable and robust randomized benchmarking of quantum processes*. Phys. Rev. Lett. **106**, 180504 (2011).
- [64] E. Magesan, J. M. Gambetta, and J. Emerson. *Characterizing quantum gates via randomized benchmarking*. Phys. Rev. A **85**, 042311 (2012).
- [65] C. C. López, A. Bendersky, J. P. Paz, and D. G. Cory. *Progress toward scalable tomography of quantum maps using twirling-based methods and information hierarchies*. Phys. Rev. A **81**, 062113 (2010).
- [66] M. Mohseni and A. T. Rezakhani. *Equation of motion for the process matrix: Hamiltonian identification and dynamical control of open quantum systems*. Phys. Rev. A **80**, 010101 (2009).
- [67] M. Cramer, M. B. Plenio, S. T. Flammia, R. Somma, D. Gross, S. D. Bartlett, O. Landon-Cardinal, D. Poulin, and Y. K. Liu. *Efficient quantum state tomography*. Nature Commun. **1**, 149 (2010).
- [68] S. T. Flammia, D. Gross, Y.-K. Liu, and J. Eisert. *Quantum tomography via compressed sensing: error bounds, sample complexity and efficient estimators*. New J. Phys. **14**, 095022 (2012).

- [69] L. Steffen, M. P. da Silva, A. Fedorov, M. Baur, and A. Wallraff. *Experimental Monte Carlo quantum process certification*. Phys. Rev. Lett. **108**, 260506 (2012).
- [70] C. T. Schmiegelow, M. A. Larotonda, and J. P. Paz. *Selective and efficient quantum process tomography with single photons*. Phys. Rev. Lett. **104**, 123601 (2010).
- [71] D. Gottesman. *Fault-tolerant quantum computation with higher-dimensional systems*. Chaos, Solitons & Fractals **10**, 1749 (1999).
- [72] P. O. Boykin, T. Mor, M. Pulver, V. Roychowdhury, and F. Vatan. *A new universal and fault-tolerant quantum basis*. Information Processing Letters **75**, 101 (2000).
- [73] D. Gottesman. *The Heisenberg representation of quantum computers*. In: S. P. Corney, R. Delbourgo, and P. D. Jarvis (editors), *Group22: Proceedings of the XXII International Colloquium on Group Theoretical Methods in Physics*, pp. 32–43 (International Press, Cambridge, MA, 1999).
- [74] D. M. Reich, G. Gualdi, and C. P. Koch. *Optimal strategies for estimating the average fidelity of quantum gates*. Phys. Rev. Lett. **111**, 200401 (2013).
- [75] G. Gualdi, D. Licht, D. M. Reich, and C. P. Koch. *Efficient Monte Carlo characterization of quantum operations for qudits*. Phys. Rev. A **90**, 032317 (2014).
- [76] D. M. Reich, G. Gualdi, and C. P. Koch. *Optimal qudit operator bases for efficient characterization of quantum gates*. Journal of Physics A: Mathematical and Theoretical **47**, 385305 (2014).
- [77] G. D’Ariano and P. Lo Presti. *Quantum tomography for measuring experimentally the matrix elements of an arbitrary quantum operation*. Phys. Rev. Lett. **86**, 4195 (2001).
- [78] J. O’Brien, G. Pryde, A. Gilchrist, D. James, N. Langford, T. Ralph, and A. White. *Quantum process tomography of a Controlled-NOT gate*. Phys. Rev. Lett. **93**, 080502 (2004).
- [79] D. James, P. Kwiat, W. Munro, and A. White. *Measurement of qubits*. Phys. Rev. A **64**, 052312 (2001).
- [80] S. Lorenzo, F. Plastina, and M. Paternostro. *Geometrical characterization of non-Markovianity*. Phys. Rev. A **88**, 020102 (2013).
- [81] R. Blume-Kohout. *Optimal, reliable estimation of quantum states*. New Journal of Physics **12**, 043034 (2010).
- [82] J. Lawrence, C. Brukner, and A. Zeilinger. *Mutually unbiased binary observable sets on  $n$  qubits*. Phys. Rev. A **65**, 032320 (2002).
- [83] D. Gottesman. *Stabilizer Codes and Quantum Error Correction*. Ph.D. thesis, California Institute of Technology (1997).
- [84] S. Bandyopadhyay, P. O. Boykin, V. Roychowdhury, and F. Vatan. *A new proof of the existence of mutually unbiased bases*. Algorithmica **34**, 512 (2002).

- [85] D. Gottesman and I. L. Chuang. *Demonstrating the viability of universal quantum computation using teleportation and single-qubit operations*. *Nature* **402**, 390 (1999).
- [86] D. Gottesman. *Theory of fault-tolerant quantum computation*. *Phys. Rev. A* **57**, 127 (1998).
- [87] J. Bermejo-Vega and M. Van Den Nest. *Classical simulations of abelian-group normalizer circuits with intermediate measurements*. *Quant. Info. Comput.* **14**, 0181 (2014).
- [88] R. Jozsa. *Fidelity for mixed quantum states*. *Journal of Modern Optics* **41**, 2315 (1994).
- [89] I. Bengtsson and K. Życzkowski. *Geometry of Quantum States: An Introduction to Quantum Entanglement* (Cambridge University Press, 2006).
- [90] K. Życzkowski and H. J. Sommers. *Average fidelity between random quantum states*. *Phys. Rev. A* **71**, 032313 (2005).
- [91] M. Horodecki, P. Horodecki, and R. Horodecki. *General teleportation channel, singlet fraction, and quasidistillation*. *Phys. Rev. A* **60**, 1888 (1999).
- [92] B. Rosgen and J. Watrous. *On the hardness of distinguishing mixed-state quantum computations*. In: *Proceedings of the 20th Annual IEEE Conference on Computational Complexity, CCC '05*, pp. 344–354 (IEEE Computer Society, Washington, DC, USA, 2005).
- [93] M. F. Sacchi. *Minimum error discrimination of Pauli channels*. *Journal of Optics B: Quantum and Semiclassical Optics* **7**, S333 (2005).
- [94] A. Gilchrist, N. Langford, and M. Nielsen. *Distance measures to compare real and ideal quantum processes*. *Phys. Rev. A* **71**, 062310 (2005).
- [95] C. Zhang. *Preparation of polarization-entangled mixed states of two photons*. *Phys. Rev. A* **69**, 014304 (2004).
- [96] J. A. Miszczak, Z. Puchała, and P. Gawron. *Quantum Information Package for Mathematica*. <http://zksi.iitis.pl/wiki/projects/mathematica-qi>.
- [97] F. Mezzadri. *How to generate random matrices from the classical compact groups*. *Notices of the AMS* **54**, 592 (2007).
- [98] J. Fiurášek and M. Sedláč. *Bounds on quantum process fidelity from minimum required number of quantum state fidelity measurements*. *Phys. Rev. A* **89**, 012323 (2014).
- [99] H. F. Hofmann. *Complementary classical fidelities as an efficient criterion for the evaluation of experimentally realized quantum operations*. *Phys. Rev. Lett.* **94**, 160504 (2005).
- [100] W. K. Wootters and B. D. Fields. *Optimal state-determination by mutually unbiased measurements*. *Ann. Phys.* **191**, 363 (1989).
- [101] A. Klappenecker and M. Rötteler. *Constructions of mutually unbiased bases*. In: G. L. Mullen, A. Poli, and H. Stichtenoth (editors), *Finite Fields and Applications*, volume 2948 of *Lecture Notes in Computer Science*, pp. 137–144 (Springer Berlin Heidelberg, 2004).
- [102] W. Hoeffding. *Probability inequalities for sums of bounded random variables*. *Journal of the American statistical association* **58**, 13 (1963).

- [103] C. Dankert, R. Cleve, J. Emerson, and E. Livine. *Exact and approximate unitary 2-designs and their application to fidelity estimation*. Phys. Rev. A **80**, 012304 (2009).
- [104] A. Ambainis and J. Emerson. *Quantum  $t$ -designs:  $t$ -wise independence in the quantum world*. In: *CCC '07. Twenty-Second Annual IEEE Conference on Computational Complexity*, pp. 129–140 (2007).
- [105] A. Bendersky, F. Pastawski, and J. P. Paz. *Selective and efficient quantum process tomography*. Phys. Rev. A **80**, 032116 (2009).
- [106] C. Spengler and B. Kraus. *Graph-state formalism for mutually unbiased bases*. Phys. Rev. A **88**, 052323 (2013).
- [107] A. Bendersky, F. Pastawski, and J. P. Paz. *Selective and efficient estimation of parameters for quantum process tomography*. Phys. Rev. Lett. **100**, 190403 (2008).
- [108] M. Neeley, M. Ansmann, R. C. Bialczak, M. Hofheinz, E. Lucero, A. D. O’Connell, D. Sank, H. Wang, J. Wenner, A. N. Cleland, M. R. Geller, and J. M. Martinis. *Emulation of a quantum spin with a superconducting phase qudit*. Science **325**, 722 (2009).
- [109] F. W. Strauch. *All-resonant control of superconducting resonators*. Phys. Rev. Lett. **109**, 210501 (2012).
- [110] G. Molina-Terriza, A. Vaziri, J. Řeháček, Z. Hradil, and A. Zeilinger. *Triggered qutrits for quantum communication protocols*. Phys. Rev. Lett. **92**, 167903 (2004).
- [111] S. Gröblacher, T. Jennewein, A. Vaziri, G. Weihs, and A. Zeilinger. *Experimental quantum cryptography with qutrits*. New J. Phys. **8**, 75 (2006).
- [112] T. C. Ralph, K. J. Resch, and A. Gilchrist. *Efficient Toffoli gates using qudits*. Phys. Rev. A **75**, 022313 (2007).
- [113] B. P. Lanyon, T. J. Weinhold, N. K. Langford, J. L. O’Brien, K. J. Resch, A. Gilchrist, and A. G. White. *Manipulating biphotonic qutrits*. Phys. Rev. Lett. **100**, 060504 (2008).
- [114] J. Lawrence. *Mutually unbiased bases and ternary operator sets for  $n$  qutrits*. Phys. Rev. A **70**, 012302 (2004).
- [115] T. Paterek. *Measurements on composite qudits*. Physics Letters A **367**, 57 (2007).
- [116] G. Lindblad. *On the generators of quantum dynamical semigroups*. Communications in Mathematical Physics **48**, 119 (1976).
- [117] V. Gorini, A. Kossakowski, and E. C. G. Sudarshan. *Completely positive dynamical semigroups of  $n$ -level systems*. Journal of Mathematical Physics **17**, 821 (1976).
- [118] P. Brumer and M. Shapiro. *Principles and Applications of the Quantum Control of Molecular Processes* (Wiley Interscience, 2003).
- [119] K. Bergmann, H. Theuer, and B. W. Shore. *Coherent population transfer among quantum states of atoms and molecules*. Rev. Mod. Phys. **70**, 1003 (1998).

- [120] S. A. Rice and M. Zhao. *Optical Control of Molecular Dynamics* (John Wiley & Sons, 2000).
- [121] A. Sørensen and K. Mølmer. *Quantum computation with ions in thermal motion*. Phys. Rev. Lett. **82**, 1971 (1999).
- [122] M. Wollenhaupt, V. Engel, and T. Baumert. *Femtosecond laser photoelectron spectroscopy on atoms and small molecules: Prototype studies in quantum control*. Ann. Rev. Phys. Chem. **56**, 25 (2005).
- [123] L. S. Pontryagin, V. G. Boltyanskii, R. V. Gamkrelidze, and E. F. Mishechenko. *The Mathematical Theory of Optimal Processes* (John Wiley & Sons, New York / London, 1962).
- [124] R. E. Bellman. *Dynamic Programming* (Princeton University Press, Princeton, NJ, 1957).
- [125] W. Zhu, J. Botina, and H. Rabitz. *Rapidly convergent iteration methods for quantum optimal control of population*. J. Chem. Phys. **108**, 1953 (1998).
- [126] N. Khaneja, T. Reiss, C. Kehlet, T. Schulte-Herbrüggen, and S. J. Glaser. *Optimal control of coupled spin dynamics: Design of NMR pulse sequences by gradient ascent algorithms*. Journal of Magnetic Resonance **172**, 296 (2005).
- [127] M. H. Goerz, D. M. Reich, and C. P. Koch. *Optimal control theory for a unitary operation under dissipative evolution*. New J. Phys. **16**, 055012 (2014).
- [128] M. H. Stone. *On one-parameter unitary groups in Hilbert space*. Annals of Mathematics **33**, pp. 643 (1932).
- [129] J. J. Sakurai and S. F. Tuan. *Modern Quantum Mechanics*, volume 1 (Addison-Wesley Reading, Massachusetts, 1985).
- [130] K. Kraus, A. Böhm, J. D. Dollard, and W. H. Wootters. *States, Effects, and Operations Fundamental Notions of Quantum Theory* (Springer Berlin Heidelberg, 1983).
- [131] S. M. Barnett and S. Stenholm. *Hazards of reservoir memory*. Phys. Rev. A **64**, 033808 (2001).
- [132] C. P. Koch, T. Klüner, and R. Kosloff. *A complete quantum description of an ultrafast pump-probe charge transfer event in condensed phase*. J. Chem. Phys. **116**, 7983 (2002).
- [133] C. P. Koch. *Quantum dissipative dynamics with a Surrogate Hamiltonian. The method and applications*. Dissertation, Humboldt Universität Berlin (2002).
- [134] C. P. Koch, T. Klüner, H. J. Freund, and R. Kosloff. *Femtosecond photodesorption of small molecules from surfaces: A theoretical investigation from first principles*. Phys. Rev. Lett. **90**, 117601 (2003).
- [135] J. Dalibard, Y. Castin, and K. Mølmer. *Wave-function approach to dissipative processes in quantum optics*. Phys. Rev. Lett. **68**, 580 (1992).
- [136] C. W. Gardiner, A. S. Parkins, and P. Zoller. *Wave-function quantum stochastic differential equations and quantum-jump simulation methods*. Phys. Rev. A **46**, 4363 (1992).
- [137] M. J. W. Hall, J. D. Cresser, L. Li, and E. Andersson. *Canonical form of master equations and characterization of non-Markovianity*. Phys. Rev. A **89**, 042120 (2014).

- [138] M. J. W. Hall. *Complete positivity for time-dependent qubit master equations*. Journal of Physics A: Mathematical and Theoretical **41**, 205302 (2008).
- [139] H. P. Breuer, E. M. Laine, and J. Piilo. *Measure for the degree of non-Markovian behavior of quantum processes in open systems*. Phys. Rev. Lett. **103**, 210401 (2009).
- [140] A. Rivas, S. F. Huelga, and M. B. Plenio. *Entanglement and non-Markovianity of quantum evolutions*. Phys. Rev. Lett. **105**, 050403 (2010).
- [141] S. Luo, S. Fu, and H. Song. *Quantifying non-Markovianity via correlations*. Phys. Rev. A **86**, 044101 (2012).
- [142] Z. He, C. Yao, Q. Wang, and J. Zou. *Measuring non-Markovianity based on local quantum uncertainty*. Phys. Rev. A **90**, 042101 (2014).
- [143] B. Bylicka, D. Chruściński, and S. Maniscalco. *Non-Markovianity and reservoir memory of quantum channels: a quantum information theory perspective*. Sci. Rep. **4**, 5720 (2014).
- [144] C. Addis, B. Bylicka, D. Chruściński, and S. Maniscalco. *Comparative study of non-Markovianity measures in exactly solvable one- and two-qubit models*. Phys. Rev. A **90**, 052103 (2014).
- [145] S. Machnes, U. Sander, S. J. Glaser, P. de Fouquières, A. Gruslys, S. Schirmer, and T. Schulte-Herbrüggen. *Comparing, optimizing, and benchmarking quantum-control algorithms in a unifying programming framework*. Phys. Rev. A **84**, 022305 (2011).
- [146] T. Caneva, T. Calarco, and S. Montangero. *Chopped random-basis quantum optimization*. Phys. Rev. A **84**, 022326 (2011).
- [147] D. M. Reich, J. P. Palao, and C. P. Koch. *Optimal control under spectral constraints: Enforcing multi-photon absorption pathways*. J. Mod. Opt. (2013).
- [148] G. Jäger, D. M. Reich, M. H. Goerz, C. P. Koch, and U. Hohenester. *Optimal quantum control of Bose-Einstein condensates in magnetic microtraps: Comparison of gradient-ascent-pulse-engineering and Krotov optimization schemes*. Phys. Rev. A **90**, 033628 (2014).
- [149] J. P. Palao, R. Kosloff, and C. P. Koch. *Protecting coherence in optimal control theory: State-dependent constraint approach*. Phys. Rev. A **77**, 063412 (2008).
- [150] J. P. Palao, D. M. Reich, and C. P. Koch. *Steering the optimization pathway in the control landscape using constraints*. Phys. Rev. A **88**, 053409 (2013).
- [151] Y. Ohtsuki. *Simulating quantum search algorithm using vibronic states of  $I_2$  manipulated by optimally designed gate pulses*. New J. Phys. **12**, 045002 (2010).
- [152] S. Kallush and R. Kosloff. *Quantum governor: Automatic quantum control and reduction of the influence of noise without measuring*. Phys. Rev. A **73**, 032324 (2006).
- [153] J. P. Palao and R. Kosloff. *Optimal control theory for unitary transformations*. Phys. Rev. A **68**, 062308 (2003).

- [154] J. Koch, T. M. Yu, J. Gambetta, A. A. Houck, D. I. Schuster, J. Majer, A. Blais, M. H. Devoret, S. M. Girvin, and R. J. Schoelkopf. *Charge-insensitive qubit design derived from the Cooper pair box*. Phys. Rev. A **76**, 042319 (2007).
- [155] A. Blais, J. Gambetta, A. Wallraff, D. I. Schuster, S. M. Girvin, M. H. Devoret, and R. J. Schoelkopf. *Quantum-information processing with circuit quantum electrodynamics*. Phys. Rev. A **75**, 032329 (2007).
- [156] M. D. Grace, J. Dominy, R. L. Kosut, C. Brif, and H. Rabitz. *Environment-invariant measure of distance between evolutions of an open quantum system*. New J. Phys. **12**, 015001 (2010).
- [157] D. A. Lidar and K. B. Whaley. *Decoherence-free subspaces and subsystems*. In: F. Benatti and R. Floreanini (editors), *Irreversible Quantum Dynamics*, volume 622 of *Lecture Notes in Physics*, pp. 83–120 (Springer Berlin Heidelberg, 2003).
- [158] D. P. DiVincenzo. *The physical implementation of quantum computation*. Fortschritte der Physik **48**, 771 (2000).
- [159] M. Viteau, A. Chotia, M. Allegrini, N. Bouloufa, O. Dulieu, D. Comparat, and P. Pillet. *Optical pumping and vibrational cooling of molecules*. Science **321**, 232 (2008).
- [160] D. Sofikitis, S. Weber, A. Fioretti, R. Horchani, M. Allegrini, B. Chatel, D. Comparat, and P. Pillet. *Molecular vibrational cooling by optical pumping with shaped femtosecond pulses*. New J. Phys. **11**, 055037 (2009).
- [161] J. F. Poyatos, J. I. Cirac, and P. Zoller. *Quantum reservoir engineering with laser cooled trapped ions*. Phys. Rev. Lett. **77**, 4728 (1996).
- [162] J. M. Raimond, M. Brune, and S. Haroche. *Manipulating quantum entanglement with atoms and photons in a cavity*. Rev. Mod. Phys. **73**, 565 (2001).
- [163] S. Haroche. *Nobel lecture: Controlling photons in a box and exploring the quantum to classical boundary*. Rev. Mod. Phys. **85**, 1083 (2013).
- [164] S. Haroche and J. M. Raimond. *Exploring the Quantum: Atoms, Cavities, and Photons* (Oxford University Press, USA, 2013).
- [165] C. K. Law and J. H. Eberly. *Arbitrary control of a quantum electromagnetic field*. Phys. Rev. Lett. **76**, 1055 (1996).
- [166] B. Mischuck and K. Mølmer. *Qudit quantum computation in the Jaynes-Cummings model*. Phys. Rev. A **87**, 022341 (2013).
- [167] S. Deléglise, I. Dotsenko, C. Sayrin, J. Bernu, M. Brune, J. M. Raimond, and S. Haroche. *Reconstruction of non-classical cavity field states with snapshots of their decoherence*. Nature **455**, 510 (2008).
- [168] D. M. Reich and C. P. Koch. *Cooling molecular vibrations with shaped laser pulses: Optimal control theory exploiting the timescale separation between coherent excitation and spontaneous emission*. New J. Phys. **15**, 125028 (2013).

- [169] A. Carvalho, P. Milman, R. de Matos Filho, and L. Davidovich. *Decoherence, pointer engineering, and quantum state protection*. Phys. Rev. Lett. **86**, 4988 (2001).
- [170] C. J. Myatt, B. E. King, Q. A. Turchette, C. A. Sackett, D. Kielpinski, W. M. Itano, C. Monroe, and D. J. Wineland. *Decoherence of quantum superpositions through coupling to engineered reservoirs*. Nature **403**, 269 (2000).
- [171] C. Arenz, C. Cormick, D. Vitali, and G. Morigi. *Generation of two-mode entangled states by quantum reservoir engineering*. Journal of Physics B: Atomic, Molecular and Optical Physics **46**, 224001 (2013).
- [172] C. Cohen-Tannoudji and D. Guéry-Odelin. *Advances in Atomic Physics* (World Scientific, Singapore, 2011).
- [173] A. Aspect, E. Arimondo, R. Kaiser, N. Vansteenkiste, and C. Cohen-Tannoudji. *Laser cooling below the one-photon recoil energy by velocity-selective coherent population trapping*. Phys. Rev. Lett. **61**, 826 (1988).
- [174] A. Bartana, R. Kosloff, and D. J. Tannor. *Laser cooling of molecular internal degrees of freedom by a series of shaped pulses*. J. Chem. Phys. **99**, 196 (1993).
- [175] A. Bartana, R. Kosloff, and D. J. Tannor. *Laser cooling of internal degrees of freedom. ii*. J. Chem. Phys. **106**, 1435 (1997).
- [176] A. Bartana, R. Kosloff, and D. J. Tannor. *Laser cooling of molecules by dynamically trapped states*. Chem. Phys. **267**, 195 (2001).
- [177] M. Viteau, A. Chotia, D. Sofikitis, M. Allegrini, N. Bouloufa, O. Dulieu, D. Comparat, and P. Pillet. *Broadband lasers to detect and cool the vibration of cold molecules*. Faraday Discuss. **142**, 257 (2009).
- [178] D. Sofikitis, A. Fioretti, S. Weber, R. Horchania, M. Pichler, X. Lia, M. Allegrini, B. Chatel, D. Comparat, and P. Pillet. *Vibrational cooling of cold molecules with optimised shaped pulses*. Mol. Phys. **108**, 795 (2010).
- [179] H. Lignier, A. Fioretti, R. Horchani, C. Drag, N. Bouloufa, M. Allegrini, O. Dulieu, L. Pruvost, P. Pillet, and D. Comparat. *Deeply bound cold caesium molecules formed after  $0_g^-$  resonant coupling*. Phys. Chem. Chem. Phys. **13**, 18910 (2011).
- [180] R. Horchani, H. Lignier, N. Bouloufa-Maafa, A. Fioretti, P. Pillet, and D. Comparat. *Triplet-singlet conversion by broadband optical pumping*. Phys. Rev. A **85**, 030502 (2012).
- [181] A. Wakim, P. Zabawa, M. Haruza, and N. P. Bigelow. *Luminorefrigeration: Vibrational cooling of NaCs*. Opt. Express **20**, 16083 (2012).
- [182] C. Y. Lien, S. R. Williams, and B. Odom. *Optical pulse-shaping for internal cooling of molecules*. Phys. Chem. Chem. Phys. **13**, 18825 (2011).
- [183] I. Manai, R. Horchani, H. Lignier, P. Pillet, D. Comparat, A. Fioretti, and M. Allegrini. *Rovibrational cooling of molecules by optical pumping*. Phys. Rev. Lett. **109**, 183001 (2012).

- [184] I. Manai, R. Horchani, M. Hamamda, A. Fioretti, M. Allegrini, H. Lignier, P. Pillet, and D. Comparat. *Laser cooling of rotation and vibration by optical pumping*. Mol. Phys. **111**, 1844 (2013).
- [185] F. Masnou-Seeuws and P. Pillet. *Formation of ultracold molecules ( $T \leq 200\mu K$ ) via photoassociation in a gas of laser-cooled atoms*. Adv. in At., Mol. and Opt. Phys. **47**, 53 (2001).
- [186] K. M. Jones, E. Tiesinga, P. D. Lett, and J. P. S. *Ultracold photoassociation spectroscopy: Long-range molecules and atomic scattering*. Rev. Mod. Phys. **78**, 483 (2006).
- [187] C. Amiot and O. Dulieu. *The  $Cs_2$  ground electronic state by Fourier transform spectroscopy: Dispersion coefficients*. J. Chem. Phys. **117**, 5155 (2002).
- [188] P. Staantum, A. Pashov, H. Knöckel, and E. Tiemann.  *$X^1\Sigma^+$  and  $a^3\Sigma^+$  states of  $LiCs$  studied by Fourier-transform spectroscopy*. Phys. Rev. A **75**, 042513 (2007).
- [189] U. Diemer, R. Duchowicz, M. Ertel, E. Mehdizadeh, and W. Demtröder. *Doppler-free polarization spectroscopy of the  $B^1\Pi_u$  state of  $Cs_2$* . Chem. Phys. Lett. **164**, 419 (1989).
- [190] A. Grochola, A. Pashov, J. Deiglmayr, M. Repp, E. Tiemann, R. Wester, and M. Weidemüller. *Photoassociation spectroscopy of the  $B^1\Pi$  state of  $LiCs$* . J. Chem. Phys. **131**, 054304 (2009).
- [191] R. Kosloff. *Time-dependent quantum-mechanical methods for molecular dynamics*. The Journal of Physical Chemistry **92**, 2087 (1988).
- [192] H. Tal-Ezer and R. Kosloff. *An accurate and efficient scheme for propagating the time dependent schrödinger equation*. J. Chem. Phys. **81**, 3967 (1984).
- [193] K. Rojan, D. M. Reich, I. Dotsenko, J. M. Raimond, C. P. Koch, and G. Morigi. *Arbitrary-quantum-state preparation of a harmonic oscillator via optimal control*. Phys. Rev. A **90**, 023824 (2014).
- [194] D. B. Uskov and R. H. Pratt. *Master equations for degenerate systems: Electron radiative cascade in a Coulomb potential*. Journal of Physics B: Atomic, Molecular and Optical Physics **37**, 4259 (2004).
- [195] R. Schmidt, A. Negretti, J. Ankerhold, T. Calarco, and J. T. Stockburger. *Optimal control of open quantum systems: Cooperative effects of driving and dissipation*. Phys. Rev. Lett. **107**, 130404 (2011).
- [196] F. F. Floether, P. de Fouquieres, and S. G. Schirmer. *Robust quantum gates for open systems via optimal control: Markovian versus non-Markovian dynamics*. New J. Phys. **14**, 073023 (2012).
- [197] G. Ithier, E. Collin, P. Joyez, P. Meeson, D. Vion, D. Esteve, F. Chiarello, A. Shnirman, Y. Makhlin, J. Schrieffer, and G. Schön. *Decoherence in a superconducting quantum bit circuit*. Phys. Rev. B **72**, 134519 (2005).
- [198] Y. M. Galperin, B. L. Altshuler, J. Bergli, and D. V. Shantsev. *Non-Gaussian low-frequency noise as a source of qubit decoherence*. Phys. Rev. Lett. **96**, 097009 (2006).

- [199] M. H. Devoret and R. J. Schoelkopf. *Superconducting circuits for quantum information: An outlook*. Science **339**, 1169 (2013).
- [200] E. Paladino, Y. M. Galperin, G. Falci, and B. L. Altshuler. *1/f noise: Implications for solid-state quantum information*. Rev. Mod. Phys. **86**, 361 (2014).
- [201] J. Lisenfeld, C. Müller, J. H. Cole, P. Bushev, A. Lukashenko, A. Shnirman, and A. V. Ustinov. *Rabi spectroscopy of a qubit-fluctuator system*. Phys. Rev. B **81**, 100511 (2010).
- [202] Y. Shalibo, Y. Rofe, D. Shwa, F. Zeides, M. Neeley, J. M. Martinis, and N. Katz. *Lifetime and coherence of two-level defects in a josephson junction*. Phys. Rev. Lett. **105**, 177001 (2010).
- [203] M. H. Devoret. *Quantum fluctuations in electrical circuits*. Les Houches, Session LXIII (1995).
- [204] Y. Shalibo. *Control and Measurement of Multi-Level States in the Josephson Phase Circuit*. Ph.D. thesis, Hebrew University of Jerusalem, Israel (2012).
- [205] H. Suchowski, Y. Silberberg, and D. B. Uskov. *Pythagorean coupling: Complete population transfer in a four-state system*. Phys. Rev. A **84**, 013414 (2011).
- [206] E. Svetitsky, H. Suchowski, R. Resh, Y. Shalibo, J. M. Martinis, and N. Katz. *Hidden two-qubit dynamics of a four-level josephson circuit*. Nature Commun. **5**, (2014).
- [207] Y. M. Galperin, B. L. Altshuler, and D. V. Shantsev. *Low-frequency noise as a source of dephasing of a qubit*. In: I. Lerner, B. Altshuler, and Y. Gefen (editors), *Fundamental Problems of Mesoscopic Physics*, volume 154 of *NATO Science Series II: Mathematics, Physics and Chemistry*, pp. 141–165 (Springer Netherlands, 2004).
- [208] Y. Galperin, B. Altshuler, J. Bergli, D. Shantsev, and V. Vinokur. *Non-Gaussian dephasing in flux qubits due to 1/f noise*. Phys. Rev. B **76**, 064531 (2007).
- [209] H. J. Wold, H. Brox, Y. M. Galperin, and J. Bergli. *Decoherence of a qubit due to either a quantum fluctuator, or classical telegraph noise*. Phys. Rev. B **86**, 205404 (2012).
- [210] C. Gardiner and P. Zoller. *Quantum Noise: A Handbook of Markovian and Non-Markovian Quantum Stochastic Methods with Applications to Quantum Optics*, volume 56 (Springer, 2004).
- [211] R. Karrlein and H. Grabert. *Exact time evolution and master equations for the damped harmonic oscillator*. Phys. Rev. E **55**, 153 (1997).
- [212] D. F. Walls and G. J. Milburn. *Quantum Optics* (Springer-Verlag, Berlin, 1994).
- [213] G. Burkard, R. Koch, and D. DiVincenzo. *Multilevel quantum description of decoherence in superconducting qubits*. Phys. Rev. B **69**, 064503 (2004).
- [214] G. Ashkenazi, R. Kosloff, S. Ruhman, and H. Tal-Ezer. *Newtonian propagation methods applied to the photodissociation dynamics of  $I_3^-$* . J. Chem. Phys. **103**, 10005 (1995).
- [215] T. Caneva, M. Murphy, T. Calarco, R. Fazio, S. Montangero, V. Giovannetti, and G. E. Santoro. *Optimal control at the quantum speed limit*. Phys. Rev. Lett. **103**, 240501 (2009).
- [216] H. S. Knowles, D. M. Kara, and M. Atatüre. *Observing bulk diamond spin coherence in high-purity nanodiamonds*. Nature Materials **13**, 21 (2014).

- [217] C. H. Baldwin, A. Kalev, and I. H. Deutsch. *Quantum process tomography of unitary and near-unitary maps*. Phys. Rev. A **90**, 012110 (2014).
- [218] R. Piziak and P. L. Odell. *Matrix Theory: From Generalized Inverses to Jordan Form*, volume 288 (CRC Press, 2007).
- [219] J. Todd. *Induced norms*. In: *Basic Numerical Mathematics*, volume 22 of *ISNM International Series of Numerical Mathematics*, pp. 19–28 (Birkhäuser Basel, 1977).
- [220] Z. Hong-Hao, Y. Wen-Bin, and L. Xue-Song. *Trace formulae of characteristic polynomial and Cayley-Hamilton's theorem, and applications to chiral perturbation theory and general relativity*. Communications in Theoretical Physics **49**, 801 (2008).
- [221] M. Manjunath, K. Mehlhorn, K. Panagiotou, and H. Sun. In: C. Demetrescu and M. M. Halldorsson (editors), *Proceedings of the 19th Annual European Symposium on Algorithms (ESA)*, volume 6942 of *Lecture Notes in Computer Science*, p. 677 (Springer, 2011).
- [222] S. T. Li, S. Oymak, and B. Hassibi. *Deterministic phase guarantees for robust recovery in incoherent dictionaries*. Proceedings of the 2012 IEEE International Conference on Acoustics, Speech and Signal Processing p. 3817 (2012).
- [223] T. Y. Lam and K. H. Leung. *On vanishing sums of roots of unity*. J. Algebra **224**, 91 (2000).

## List of Publications

1. M. M. Müller, **D. M. Reich**, M. Murphy, H. Yuan, J. Vala, K. B. Whaley, T. Calarco, and C. P. Koch. *Optimizing entangling quantum gates for physical systems.* Phys. Rev. A **84**, 042315 (2011).
2. **D. M. Reich**, M. Ndong, and C. P. Koch. *Monotonically convergent optimization in quantum control using Krotov's method.* J. Chem. Phys. **136**, 104103 (2012).
3. **D. M. Reich**, G. Gualdi, and C. P. Koch. *Minimum number of input states required for quantum gate characterization.* Phys. Rev. A **88**, 042309 (2013).
4. S. Amaran, R. Kosloff, M. Tomza, W. Skomorowski, F. Pawłowski, R. Moszynski, L. Rybak, L. Levin, Z. Amitay, J. M. Berglund, **D. M. Reich**, and C. P. Koch. *Femtosecond two-photon photoassociation of hot magnesium atoms: A quantum dynamical study using thermal random phase wavefunctions.* J. Chem. Phys. **139**, 164124 (2013).
5. J. P. Palao, **D. M. Reich**, and C. P. Koch. *Steering the optimization pathway in the control landscape using constraints.* Phys. Rev. A **88**, 053409 (2013).
6. **D. M. Reich**, G. Gualdi, and C. P. Koch. *Optimal strategies for estimating the average fidelity of quantum gates.* Phys. Rev. Lett. **111**, 200401 (2013).
7. **D. M. Reich** and C. P. Koch. *Cooling molecular vibrations with shaped laser pulses: Optimal control theory exploiting the timescale separation between coherent excitation and spontaneous emission.* New J. Phys. **15**, 125028 (2013).
8. **D. M. Reich**, J. P. Palao, and C. P. Koch. *Optimal control under spectral constraints: Enforcing multi-photon absorption pathways.* J. Mod. Opt. **61**, 822 (2014).
9. M. H. Goerz, **D. M. Reich**, and C. P. Koch. *Optimal control theory for a unitary operation under dissipative evolution.* New J. Phys. **16**, 055012 (2014).
10. K. Rojan, **D. M. Reich**, I. Dotsenko, J.-M. Raimond, C. P. Koch, and G. Morigi. *Arbitrary quantum-state preparation of a harmonic oscillator via optimal control.* Phys. Rev. A **90**, 023824 (2014).
11. **D. M. Reich**, G. Gualdi, and C. P. Koch. *Optimal qudit operator bases for efficient characterization of quantum gates.* J. Phys. A: Math. Theor. **47**, 385305 (2014).
12. G. Gualdi, D. Licht, **D. M. Reich**, and C. P. Koch. *Efficient Monte Carlo characterization of quantum operations for qudits.* Phys. Rev. A **90**, 032317 (2014).
13. G. Jäger, **D. M. Reich**, M. H. Goerz, C. P. Koch, U. Hohenester. *Optimal quantum control of Bose-Einstein condensates in magnetic microtraps: Comparison of GRAPE and Krotov optimization schemes.* Phys. Rev. A **90**, 033628 (2014).
14. **D. M. Reich**, N. Katz, and C. P. Koch. *Exploiting Non-Markovianity of the Environment for Quantum Control.* arXiv:1409.7497, submitted to Sci. Rep.



**Erklärung:**

Hiermit versichere ich, dass ich die vorliegende Dissertation selbstständig, ohne unerlaubte Hilfe Dritter angefertigt und andere als die in der Dissertation angegebenen Hilfsmittel nicht benutzt habe. Alle Stellen, die wörtlich oder sinngemäß aus veröffentlichten oder unveröffentlichten Schriften entnommen sind, habe ich als solche kenntlich gemacht. Dritte waren an der inhaltlich-materiellen Erstellung der Dissertation nicht beteiligt; insbesondere habe ich hierfür nicht die Hilfe eines Promotionsberaters in Anspruch genommen. Kein Teil dieser Arbeit ist in einem anderen Promotions- oder Habilitationsverfahren verwendet worden.

---

Ort, Datum

---

Unterschrift